Laboratory Medicine

March 2023 Vol 54 No 2 Pgs 113–224

labmedicine.com

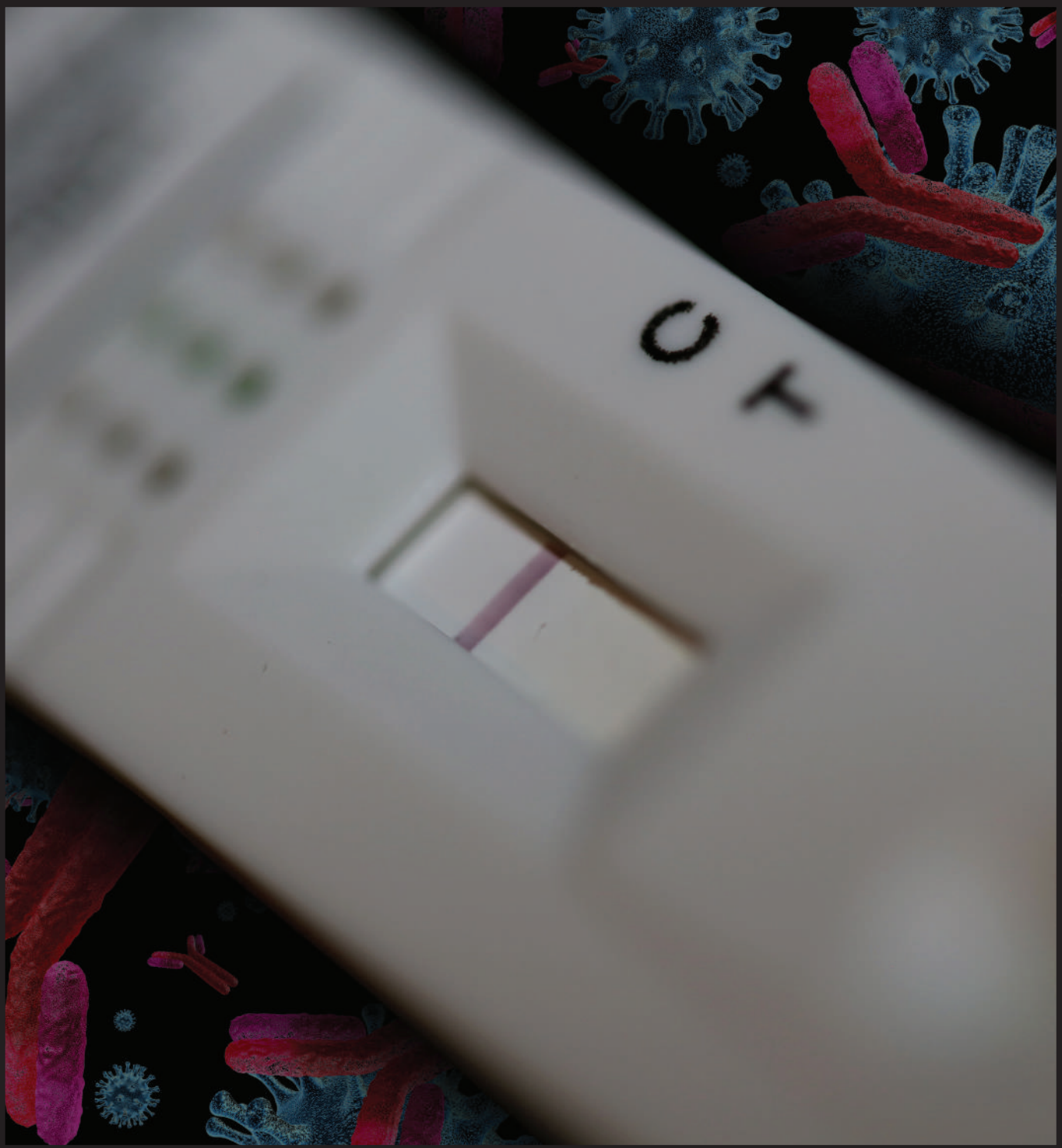

Laboratory Medicine (ISSN 0007-5027), is published 6 times per year (bimonthly). Periodicals Postage paid at Chicago, IL and additional mailing offices. POSTMASTER: Send address changes to *Laboratory Medicine*, Journals Customer Service Department, Oxford University Press, 4000 CentreGreen Way, Suite 310, Cary, NC 27513, USA.

SUBSCRIPTION INFORMATION: Annually for North America, $182 (electronic) or $241 (electronic and print); single issues for individuals are $32 and for institutions $71. Annually for Rest of World, £118/€167 (electronic) or £154/€220 (electronic and print); single issues for individuals are £21/€30 and for institutions £44/€63. All inquiries about subscriptions should be sent to Journals Customer Service Department, Oxford Journals, Great Clarendon Street, Oxford OX2 6DP, UK, Tel: +44 (0) 1865-35-3907, e-mail: jnls.cust.serv@oup.com. In the Americas, please contact Journals Customer Service Department, Oxford Journals, 4000 CentreGreen Way, Suite 310, Cary, NC 27513, USA. Tel: 800-852-7323 (toll-free in USA/Canada) or 919-677-0977, e-mail: jnlorders@oup.com.

MEMBERSHIP INFORMATION: The ASCP membership fees for pathologists are as follows: fellow membership is $399; fellow membership plus 1-year unlimited online CE is $529; 2-year fellow membership is $749; and 2-year fellow membership plus 2-year unlimited online CE is $1,009. The ASCP membership fees for laboratory professionals are as follows: newly certified membership is $59; annual membership is $119; annual membership plus 1-year unlimited online CE is $158; 3-year membership is $389. All inquiries about membership should be sent to American Society for Clinical Pathology, 33 West Monroe Street, Suite 1600, Chicago, IL 60603, Tel: 312-541-4999, e-mail: ascp@ascp.org.

CLAIMS: Publisher must be notified of claims within four months of dispatch/ order date (whichever is later). Subscriptions in the EEC may be subject to European VAT. Claims should be made to Laboratory Medicine, Journals Customer Service Department, Oxford University Press, 4000 CentreGreen Way, Suite 310, Cary, NC 27513, USA, Tel: 800-852-7323 (toll-free in USA/Canada) or 919-677-0977, e-mail: jnlorders@oup.com.

Laboratory Medicine is published bimonthly by Oxford University Press (OUP), on behalf of the ASCP, a not-for-profit corporation organized exclusively for educational, scientific, and charitable purposes. Devoted to the continuing education of laboratory professionals, *Laboratory Medicine* features articles on the scientific, technical, managerial, and educational aspects ofthe clinical laboratory. Publication of an article, column, or other item does not constitute an endorsement by the ASCP of the thoughts expressed or the techniques, organizations, or products described therein. *Laboratory Medicine* is indexed in the following: MEDLINE/PubMed, Science Citation Index, Current Contents—Clinical Medicine, and the Cumulative Index to Nursing and Allied Health Literature.

Printed in the USA

ASCP
Laboratory Medicine
33 West Monroe Street, Suite 1600
Chicago, IL 60603

T: 312-541-4999
F: 312-541-4750

LaboratoryMedicine

March 2023
Vol 54, No 2
Pgs 113-224

OVERVIEW

SPECIAL REPORT

SCIENCE

CASE STUDY

REVIEWER LIST

The following are online-only papers that are available as part of Issue 54(2) online.

ON THE COVER: One of the many consequences of the COVID-19 pandemic was the laboratory diagnostics industry refocusing its efforts on manufacturing point-of-care devices to test for the SARS-CoV-2 virus, and these devices are now ubiquitous. Although most rapid tests for the virus were granted waived status by the FDA, and therefore could be used at home, many testing sites were created in cities and communities to offer COVID-19 screening. In addition, many physician offices, assisted living facilities, pharmacies, and schools offered the service. Under CLIA, each of these sites was required to have a Certificate of Waiver (CoW) to perform the test. In this issue of *Laboratory Medicine*, Xia and Anderson, of the Centers for Disease Control and Prevention, report that first-time CoW applications more than doubled in 2020-2021 compared to 2018-2019 and suggest strategies for clinical testing in future public health emergencies.

OVERVIEW

Urinary Exosomes: A Promising Biomarker for Disease Diagnosis

Yizhao Wang, MD,[1] *and Man Zhang, MD*[1,2,3,*]

[1]Clinical Laboratory Medicine, Beijing Shijitan Hospital, Capital Medical University, Beijing Key Laboratory of Urinary Cellular Molecular Diagnostics, Beijing, China, [2]Clinical Laboratory Medicine, Peking University Ninth School of Clinical Medicine, Beijing, China, [3]Beijing Key Laboratory of Urinary Cellular Molecular Diagnostics, Beijing, China. *To whom correspondence should be addressed: zhangman@bjsjth.cn.

Keywords: biomarker, exosome, urinary proteomics, extracellular vesicle, multivesicular body, intraluminal vesicles

Abbreviations: ESCRT, endosomal sorting complex required for transport; TSG, tumor susceptibility gene; AQP, aquaporin; MMP-1, matrix metallopeptidase 1.

Laboratory Medicine 2023;54:115–125; https://doi.org/10.1093/labmed/lmac087

ABSTRACT

Exosomes are nanoscale vesicles derived from endocytosis, formed by fusion of multivesicular bodies with membranes and secreted into the extracellular matrix or body fluids. Many studies have shown that exosomes can be present in a variety of biological fluids, such as plasma, urine, saliva, amniotic fluid, ascites, and sweat, and most types of cells can secrete exosomes. Exosomes play an important role in many aspects of human development, including immunity, cardiovascular diseases, neurodegenerative diseases, and neoplasia. Urine can be an alternative to blood or tissue samples as a potential source of disease biomarkers because of its simple, noninvasive, sufficient, and stable characteristics. Therefore, urinary exosomes have valuable potential for early screening, monitoring disease progression, prognosis, and treatment. The method for isolating urinary exosomes has been perfected, and exosome proteomics is widely used. Therefore, we review the potential use of urinary exosomes for disease diagnosis and summarize the related literature.

Exosomes are nanosized vesicles released after the fusion of multivesicular bodies with the cell membrane. The first biochemist to describe exosomes was Rose Johnstone in the 1980s. Johnstone reported a lipid-encapsulated particle with a diameter of 30 to 100 nm, which was produced due to downregulation of a specific membrane receptor during reticulocyte maturation.[1] Since then, many exosome studies have been performed on bodily fluids, including blood, cerebrospinal fluid, urine, sweat, milk, synovial fluid, and pleural effusion.[2–6] The role of exosomes in cell-to-cell communication, immune regulation, and paracrine processes and the similarity of their contents to the cells of origin have aroused interest as potential sources of biomarkers.[7] Urinary exosomes combine the advantages of exosomes and urine to provide a new noninvasive method to obtain information about the physiological or pathophysiological state of cells. Thus, urinary exosomes have attracted increasing attention in recent years.

Urine is an ideal source of protein markers for the detection of urinary tract–related diseases. It contains proteins secreted from the prostate, bladder, and kidneys and is produced by the lysis of exfoliated cells.[8] Compared to blood, cerebrospinal fluid, ascites, pathological slices, and other samples, urine has unique advantages. Acquiring urine does not require the invasiveness of other liquid samples, avoids the infection risk of tissue biopsies, and allows continuous monitoring of the state of the body.[9] In addition, the separation of exosomes can be a good way to note the enrichment of low-abundance proteins in urine, which has pathophysiological significance, and may become a biomarker with high sensitivity and specificity. The study of urinary exosomal proteins can provide clinicians with a simple, safe, and accurate method for detecting disease progression and monitoring treatment.

This review will briefly describe the origin and discovery of exosomes, summarize and analyze the isolation methods and potential applications of urinary exosomes, comprehensively introduce the latest research on urinary exosomes, and, finally, provide ideas and insights for further research on urinary exosomes.

Formation and Characteristics of Urinary Exosomes

Formation of Urinary Exosomes

Exosomes are a special type of cell-derived vesicle that originate from endocytosis. Studies have shown that, besides exocytosis, endocytosis also plays a role in their secretion. A key part of multivesicular body formation is the endosome.[10] The endosomal membrane invades the organelle cavity to form intraluminal vesicles.[11] Late endosomes, also called multivesicular bodies, contain multiple intraluminal vesicles. In the classical endosomal pathway, late endosomes fuse with lysosomes, resulting in the degradation of their vesicle structures and proteins. Late endosomes can also fuse with the plasma membrane to release the contents of intraluminal vesicles into the extracellular space.[1] These released vesicles are called exosomes (**FIGURE 1**). Therefore, exosomes can be defined as intraluminal vesicles secreted by multivesicular

FIGURE 1. Exosome formation. Late endosomes derived from endosomal membrane invaginations, also known as multivesicular bodies (MVBs), contain multiple intraluminal vesicles (ILVs). MVBs that fuse with lysosomes undergo degradation of their vesicle structures and proteins. MVBs that fuse with the plasma membrane release their ILV contents into the extracellular space, and these released vesicles are called exosomes. ESCRT, endosomal sorting complex required for transport.

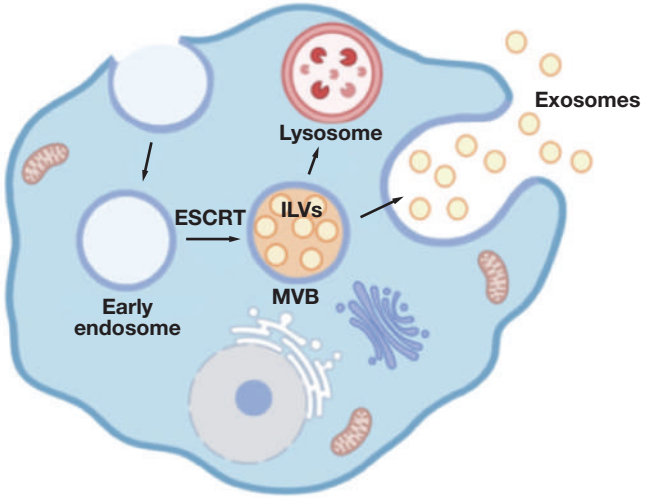

bodies. Two consecutive membrane invaginations lead to the outward orientation of the exosome lipid membrane, which is an important reason exosomes retain their original cellular characteristics.[1] Various types of cells can secrete exosomes into the interstitial space through endocytosis. Blood is filtered through the glomerulus to form urine, and urinary exosomes are vesicles that can pass through the glomerular filtration barrier.[12]

Intraluminal vesicle formation occurs through the endosomal sorting complex required for transport (ESCRT) and/or non-ESCRT-related mechanisms, such as the four-molecular cross-linked body family and membrane lipids.[13] The ESCRT system includes ESCRT-0, ESCRT-I, ESCRT-II, ESCRT-III, and VPS4-Vtal. Its main role is to promote the degradation of ubiquitinated membrane proteins.[14] The monoubiquitinated protein binds to the ESCRT-0 complex on the cytoplasmic surface of the endosomal membrane and recruits tumor susceptibility gene 101 (*TSG-101*) during assembly of the ESCRT-I complex, resulting in the recruitment of the endosomal membrane to deform and form an initial bud.[15] With the recruitment of ESCRT-III, the neck of the formed vesicle is restricted, forming a ring structure and shrinking, causing the initial bud to be sheared, releasing intraluminal vesicles. VPS4-Vtal participates in the formation of intraluminal vesicles by hydrolyzing adenosine triphosphate to provide energy for ESCRT-III depolymerization and the establishment of its cyclic form.[15]

Characteristics of Urinary Exosomes

Extracellular vesicles are a group of heterogeneous membrane vesicles. According to their biological origin, morphology, and physical and chemical characteristics, they can be divided into apoptotic bodies, microvesicles, and exosomes.[16] Apoptotic bodies are produced in the late stage of cell death and contain nuclear content, organelles, and cytoplasm. Their diameter varies from 800 to 5000 nm and their density overlaps with exosomes (1.16–1.28 g/mL).[17,18] Microvesicles originate from the plasma membrane, bud directly outward on the plasma membrane, and detach from the cell to form microvesicles, with diameters ranging from 50 to 1000 nm and densities ranging from 1.16 to 1.19 g/mL.[19] Exosomes are vesicles with a diameter of approximately 30 to 150 nm with a lipid bilayer membrane structure. They are cup-shaped, determined via transmission electron microscopy, and have a sedimentation coefficient of 1.10 to 1.21 g/mL in a sucrose gradient.[20,21] They also contain characteristic proteins, such as CD9 and CD63, which are essential for their secretion.[22] Exosomes are rich in cholesterol and sphingolipids, intracellular nucleic acid components, and contain complete membrane proteins, especially glycoproteins, peripheral membrane proteins, cytoplasmic proteins, and nuclear proteins.[23–25] The new generation of mass spectrometry has identified around 3000 urinary exosomal proteins, including membrane transport components, membrane transport, and cytoskeleton proteins.[26] These proteins originate from different parts of the genitourinary system, including glomeruli, renal tubules, prostate gland, and bladder.[27]

History and Discovery of Urinary Exosomes

History of Urinary Exosomes

In 1983, Pan and Johnstone[28] published a paper stating that they had discovered a vesicle with a diameter of approximately 30 to 150 nm in the supernatant of cultured sheep red blood cells, which they believed was a nonfunctional cellular component. However, follow-up studies indicated the vesicle body could participate in physiological processes by carrying biological substances, such as genes and proteins, between cells for "information transmission."[1,29–31] Researchers then suggested that exosomes may be used for cell communication.[23,32] In 1987, Johnstone et al[1] named this vesicle body "exosome." Valadi et al[23] and Lotvall et al[33] showed that exosomes contain messenger RNAs and microRNAs that can be captured by other cells. Today, there is a better understanding of the composition and function of exosomes. Exosomes have successfully attracted the interest of scientific researchers as potential biomarkers because they are considered nonfunctional waste disposal bags that play a vital role in cell-to-cell communication.

In 2004, Pisitkun et al[34] discovered human urinary exosomes for the first time and demonstrated the potential to use urinary exosomes as biomarkers. The membrane protein aquaporin 2 (*AQP2*) and other apical plasma membrane proteins of the renal tubular segment can be detected in urine. It is speculated these apical plasma membrane proteins are secreted into urine during exosome formation. The proteomic results show that the sorting complexes ESCRT-I, ESCRT-II, ESCRT-III, VPS4-Vtal, and Alix are necessary for the formation of multivesicular bodies.[34] This evidence suggests that intraluminal vesicles (exosomes) are formed by the fusion of multivesicular bodies with the plasma membrane and are released into urine.

Discovery of Urinary Exosomes

Existing Research on Urinary Exosomes

Although the specific mechanism of the action of urinary exosomes in the body needs to be further explored, they undoubtedly play an important role in a variety of physiological and pathological processes, with unique exocrine advantages. Current research shows that urinary

exosomes are related to immune responses,[13,35] viral pathogenicity,[36] pregnancy,[37] cardiovascular disease,[38] central nervous system–related diseases,[39] and cancer.[40] Some exosome-derived proteins or nucleic acid molecules exhibit the potential for candidate biomarkers (**TABLE 1**). Cancer formation is affected by many factors, including genetic, physical, chemical, and biotic factors.[41–43] Urinary exosomes play a key role in tumor development, growth, apoptosis, immune response, and chemotherapy resistance.[44] Cancer cells usually produce more exosomes than normal cells, and exosomes extracted from cancer cells have a powerful ability to alter local and distant microenvironments. Exosomes can regulate intercellular communication between tumor cells and the normal stroma, tumor-associated fibroblasts, and local immune cells in the tumor microenvironment.

Studies have shown that primary ovarian tumors release exosomes outside the cell to prepare a distant tumor microenvironment to accelerate metastasis and invasion.[45] Research on the relationship between urinary exosomes and the pathological state of diseases involves various contents of urinary exosomes. MicroRNA profiles in the urine of patients with urothelial bladder carcinoma have been analyzed and identified. Urinary exosomes were first extracted by ultracentrifugation and 7 microRNAs (miR-200c, miR-93, miR-940, miRlet7b, miR-191, miR-21, and miR-15a) were significantly elevated in the urine of patients with bladder cancer, and their expression levels were correlated with the developmental stage of the disease.[46] Chu et al[47] investigated the potential of sex steroid hormones in urinary exosomes as biomarkers for predicting prostate cancer. They found 7 sex steroid hormones that could distinguish not only those with prostate cancer from healthy controls but also those with mild and severe prostate cancer. Renal fibrosis is the final stage of most chronic kidney diseases and results in a progressive and irreversible decline in kidney function. Lupus nephritis has always been 1 of the main causes of death in patients with systemic lupus erythematosus, and for lupus nephritis, early detection of fibrosis is important.[48] Urinary exosomal miRNAs analysis can serve as a potential multimarker phenotypic tool to identify early fibrosis. The researchers found that miR-21, miR-150, and miR-29 were differentially expressed in urinary exosomes from patients with lupus nephritis and correlated with chronic scores on renal biopsies. High-grade fibrosis is characterized by marked upregulation and downregulation of miR-21, miR-150, and miR-29c. Also, the miR-29c/miR-150/miR-21 combination panel can predict end-stage renal disease progression.[49] Moreover, diabetic nephropathy is the most common cause of end-stage renal disease, and the current marker albumin has many shortcomings, including slow response, unpredictable prognosis, and limited sensitivity. Therefore, some studies have explored new markers of diabetic nephropathy and found that urinary exosomal regucalcin can be used for the early diagnosis and progress monitoring of diabetic nephropathy.[50]

Clinical Application

Urinary Exosomes and Diagnostic Biomarkers.—Urinary exosomes contain a variety of proteins, nucleic acids, and lipids, which exist in many or even in all body fluids. In addition, urinary exosomes can be used for disease diagnosis. Many studies have shown that the molecular components of urinary exosomes, especially proteins and microRNAs, have great potential as new biomarkers for clinical diagnosis.[51,52] For example, the highly enriched tetraspanins in exosomes are a family of scaffold membrane proteins, and the exosomal marker CD9 is a member of this protein family. Previous studies have indicated that CD9

TABLE 1. Exosomes as Candidate Biomarkers[a]

Biomarkers Candidate	Source	Disease	Methodologies	ClinicalTrials.gov Identifier	Reference
CUEDC2	Exosomal mRNAs in cerebrospinal fluid	Amyotrophic lateral sclerosis	Size-exclusion method	None	2
miR-21, miR-141, miR-200a, miR-200c, miR-200b, miR-203, miR-205, and miR-214	Exosomes from serum	Ovarian cancer	Immunoaffinity chromatography	None	24
miR-1246	Exosomes from serum, tissue, and cell	Esophageal squamous cell carcinoma	Ultracentrifugation	NCT00190554	25
BPGM, CANX, PRL, CDH5, and *ART3*	Urinary exosomes	Nephronophthisis-related ciliopathies	Ultrafiltration and immunoaffinity chromatography	None	26
Bkv-miR-B1-5p, bkv-miR-B1-5p/miR-1	Urinary exosomes	BK virus nephropathy	Immunoaffinity chromatography	None	36
miR-21, miR-29a, and miR-590-3p	Urinary exosomes	Intrahepatic cholestasis of pregnancy	Immunoaffinity chromatography	None	37
SNAP23 and calbindin	Urinary exosomes	Parkinson disease	Ultracentrifugation	NCT01860118	39
miR-29c	Urinary exosomes	Renal interstitial fibrosis	Precipitation	None	48
miR-21 and *MMP*/CD63	Urinary exosomes	Breast cancer	Immunoaffinity chromatography	NCT00190489	57
PCA3 and *ERG*	Urinary exosomes	Prostate cancer		NCT04720599	121
T790M	Exosomes from plasma	Non–small cell lung cancer		NCT02702856	6,122

[a]*Summarizes the exosome-derived biomarkers involved in this review.*

in urinary exosomes may be a marker for the differential diagnosis of urothelial tract infection and asymptomatic bacteriuria. The levels of CD9 in urinary exosomes were higher in patients with urothelial tract infection than in patients with asymptomatic bacteriuria. Urothelial tract infection is treated differently from asymptomatic bacteriuria, and asymptomatic bacteriuria does not require antimicrobial agent treatment. However, the difference between the 2 is only distinguished by clinical symptoms. Therefore, some patients with asymptomatic bacteriuria are misdiagnosed as having urinary tract infections and are treated with antibiotics. Inappropriate use of antibiotics has resulted in overuse of antibiotics and decreased costs.[53] Noninvasive urine collection, exosome extraction, and analysis of the protein content analysis have potential applications in diagnosis, especially for urinary system diseases.

Besides proteins, other substances in exosomes can be used as diagnostic markers. In 2007, Valadi et al[23] discovered that exosomes contain RNA, and research on exosomal RNAs, especially microRNAs, as diagnostic biomarkers has gradually become popular. Studies have shown that exosomal microRNAs are not degraded in an RNase-dependent manner[24,52,54]; therefore, they can be stably detected in circulating plasma and urine, which suggests that they are ideal biomarkers for clinical diagnosis. In 2016, Samsonov et al[55] reported that miR-574-3p, miR-141-5p, and miR-21-5p levels are powerful diagnostic markers for prostate cancer. Likewise, Magayr et al[56] reported that miR-192-5p, miR-194-5p, miR-30a-5p, miR-30d-5p, and miR-30e-5p detected in urinary exosomes, mouse kidney tissue, and human kidney tissue of polycystic kidney disease were significantly downregulated in cystic kidney tissue. All 5 miRNAs were significantly associated with baseline estimated glomerular filtration rate and ultrasound-determined mean kidney length and improved the diagnostic performance of mean kidney length on the disease progression rate. The miR-21 in serum and tissue is a valuable biomarker for breast cancer diagnosis, progression, and treatment. Ando et al[57] detected the expression of MiR-21 and MMP-1/CD63 in urinary exosomes by quantitative reverse transcriptase–polymerase chain reaction and Western blot analysis. The sensitivity and specificity of miR-21 in patients with breast cancer without metastasis were 71% and 78%, respectively, and the sensitivity and specificity of combined MMP-1/CD63 expression were 95% and 79%, respectively. Thus, miR-21 and MMP-1/CD63 may be helpful markers for breast cancer screening.

Urinary Exosomes and Drug Therapy.—Besides research on pathogenic mechanisms, the medicinal value of exosomes is constantly being explored. Exosomes comprise cell membranes with a variety of adhesion proteins on their surfaces and can be used exclusively for communication between cells. This provides a unique method for delivering various therapeutic drugs to target cells.[39] Because exosomes can provide the advantages of drug delivery and nanotechnology, based on biomembrane fusion, researchers are focusing on developing treatments using exosomes. Through fat-soluble membrane fusion, exosomal carriers can shuttle between different cells, easily pass through the cell membrane, and transport their cargo in a biologically active form. It is noteworthy that exosomes have the inherent ability to cross biological barriers and can even penetrate the blood–brain barrier,[58] considered the most difficult to penetrate. In some existing studies, drug delivery vehicles for applying exosomes in the delivery of low-molecular-weight drugs in vivo have been successfully constructed. For example, exosomes containing the anti-inflammatory small molecule curcumin protect mice from lipopolysaccharide-induced brain inflammation.[59,60] Exosomes or exosome-like vesicles packed with chemotherapeutic drugs, such as doxorubicin, enter tumor tissue cells and inhibit tumor growth in mice.[61,62] Even more gratifying is that they have fewer side effects than general chemotherapeutic drugs. In addition, given that exosomes contain a variety of nucleic acids,[63] Alvarez-Erviti et al[64] pioneered a method for nucleic acid transfer to electroporate small interfering RNA into dendritic cell-derived exosomes. Following this method, other researchers have successfully loaded exosomes carrying microRNAs into breast cancer cells expressing epidermal growth factor receptor.[65] The development of drug therapy with urinary exosomes has limitations. However, some studies have found that the injection of exosomes of urine-derived stem cells into the tail vein of rats may prevent diabetes-induced kidney damage by reducing urinary microalbumin excretion and preventing the apoptosis of podocyte and tubular epithelial cells in diabetic rats.[66] Drug-loaded exosomes are a promising next-generation drug delivery system because of their nanoscale size, lack of cytotoxicity, high drug-loading capacity, and low immunogenicity. Future research should focus on the production of many exosomal carriers with high load capacity characteristics.

Technology of Exosome Research

Separation

Exosomes can be separated from conditioned cell culture media or body fluids via differential centrifugation, centrifugal filtration, immunoaffinity, size-exclusion chromatography or polymer precipitation, and microfluidic technology.[67] Each separation method has different advantages but also limitations. Different methods require different sample pretreatment methods and produce exosome-enriched samples of different purities and qualities. Herein, we introduce commonly used urine exosome separation methods (**FIGURE 2**).

The urine proteome contains many highly abundant proteins filtered from the plasma and proteins produced by renal tubular cells.[68] The presence of these high-abundance proteins complicates the detection of relatively low-abundance proteins. However, low-abundance proteins may have special pathophysiological significance. Excluding high-abundance proteins in the urine such as Tamm-Horsfall protein and albumin, proteins in urinary exosomes account for only 3% of total urine protein content.[69] Urinary exosomes (99.96%) originate from the kidneys, urothelial cells, and the male reproductive tract.[70] Isolation of exosomes reduces the complexity of urine proteomes. Because of their membranous vesicle structure, the stability of the contained molecules is high, which can reflect the physiological and pathological functions of secretory cells. Exosomes can also reduce the interference of high-abundance proteins in whole urine samples, and during their formation, various components go through a selective enrichment process, which prevents the dilution effect that causes markers with low concentrations to be undetectable. To some extent, exosome detection can improve the sensitivity of detecting meaningful proteins in urine.[71] Therefore, urinary exosomes are ideal for studying diseases, especially those of the genitourinary system. There is no recognized uniform separation method or gold standard.[72] Many researchers have focused on exosome separation and extraction as well as methodological comparison and optimization. Here, we briefly introduce several main extraction methods in current scientific research.

FIGURE 2. Exosome separation method. 1, The ultracentrifugation uses centrifugal force to separate substances of different densities by centrifugation for over 10 hours. 2, The sucrose density gradient method uses the difference in sedimentation coefficient between different particles and combines centrifugation to separate extracellular vesicles. PBS, phosphate-buffered saline. 3, The ultrafiltration is a polyethersulfone nanomembrane filter designed according to the size of the vesicles, and the vesicles are retained in the supernatant by a certain centrifugal force. 4, The precipitation method is based on the hydrophilicity of some polymers. Polymers such as polyethylene glycol dehydrate the exosomes and aggregate them. Finally, the aggregates can be precipitated to obtain exosomes under low-speed centrifugation. 5, Magnetic beads coated with specific antibodies are incubated with exosomes fluid, then exosomes-beads are collected by centrifugation, and the magnetic beads are eluted to obtain exosomes. 6, Size-exclusion chromatography: Different components in the suspension pass through the solid-phase molecular sieve at different speeds, the flow of macromolecules is fast, and the flow of small molecules is slow (created in Biorender, https://biorender.com).

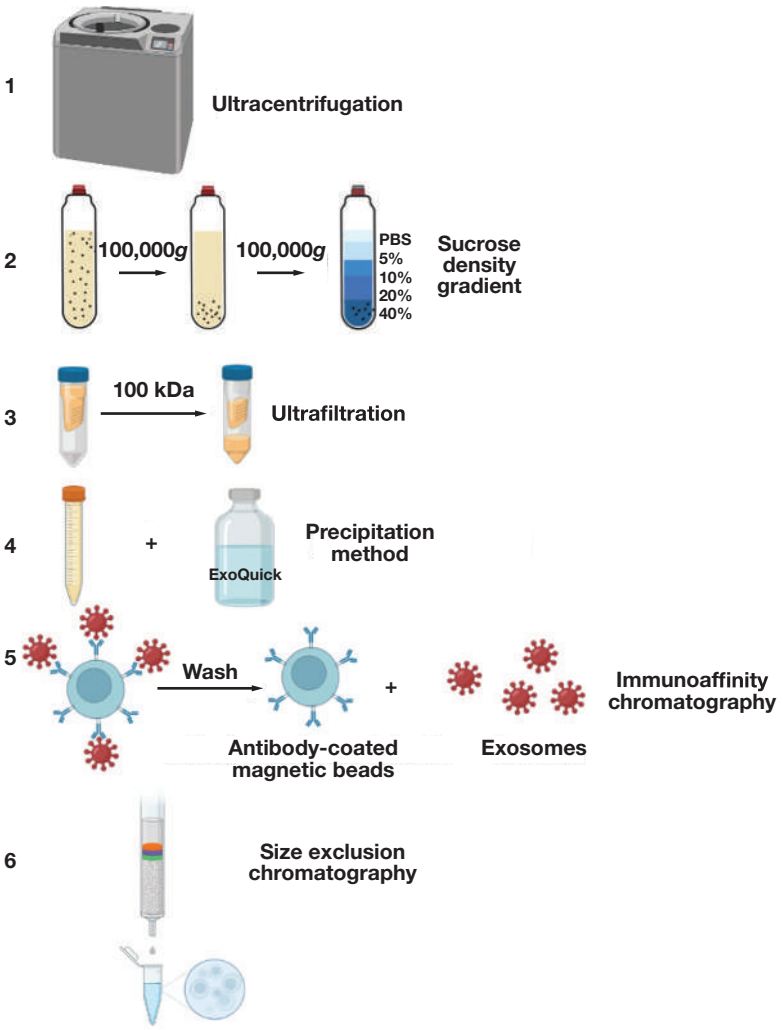

Ultracentrifugation

Ultracentrifugation has always been the most common method for separating extracellular vesicles from urine. It uses centrifugal force to separate substances with different densities. This method is suitable for large volumes of samples. Ultracentrifugation is a simple procedure. However, it is time-consuming and prone to contamination, resulting in unstable recovery. In addition, it requires expensive equipment and is not widely used in the clinic. More importantly, long-term high-speed centrifugation can destroy the exosome structure.[70] Therefore, this method requires further improvement.

This method first requires the centrifugation of the sample at a low centrifugal force (approximately 3,000*g*) for 15–20 min to remove cells and debris. Then a centrifugal force of 10,000*g* was applied and extracellular vesicles in urine finally precipitate at 100,000*g* or more (eg, 200,000*g*).[73–75] Although most studies use the term exosomes to refer to extracellular vesicles, some studies revealed that the largest vesicles after ultracentrifugation at 200,000*g* are 300 nm in diameter. As much as 40% of urinary extracellular vesicles is retained in the supernatant, and precipitate obtained via ultracentrifugation contains a variety of mixtures.[76,77]

Sucrose Density Gradient Method

The density of exosomes is 1.16 to 1.28 g/mL. The sucrose density gradient method uses the difference in sedimentation coefficients between

different particles. Under the action of a specific centrifugal force, the particles settle at a certain speed. However, the sucrose gradient lacks sufficient resolution to separate extracellular vesicles.[78] It is necessary to combine ultracentrifugation with the sucrose density gradient method to remove nonvesicular substances and then extract exosomes through gradient density concentration. This method can compensate for the problem of soluble nonspecific proteins remaining after ultracentrifugation. It is suitable for proteomics and microRNA analysis but it has a low resolution, takes a long time, and requires expensive equipment.[79]

Ultrafiltration

Ultrafiltration is another method for separating exosomes according to their size. Usually, a polyethersulfone nanomembrane filter with a molecular cutoff of 100 kDa is used to remove large and small protein molecules. This method is suitable for samples with larger volumes. Ultrafiltration does not require special equipment and is simple and fast. The efficiency of exosome separation in ultrafiltration is as high as that of ultracentrifugation.[80–82] However, nanomembranes adsorb extracellular vesicles and proteins containing AQP2 and TSG101. Even if the Laemmli buffer containing dithiothreitol is used to recover extracellular vesicles from the nanomembrane, this buffer will interfere with downstream experiments and is not conducive to mass spectrometry.[83,84]

Precipitation

Over 40 years ago, it was discovered that polyethylene glycol could be used as a precipitation reagent to separate viruses, showing good results.[85] Because exosomes and viruses have similar sizes, structures, and material compositions, Rider et al[86] proposed a polyethylene glycol-based method for exosome separation and purification. Polyethylene glycol has once again come to the forefront as a method of separating exosomes, and it is the most commonly used precipitation reagent. Due to its strong hydrophilicity, polyethylene glycol will "snatch" water molecules around the exosomes in solution. The dehydrated exosomes aggregate, and finally, the aggregates can be precipitated by low-speed centrifugation.

There are commercial kits available for exosome extraction using polyethylene glycol solutions. The most common kits are the ExoQuick and ExoQuick-TC kits from System Biosciences and Life Technologies, respectively. The kits are simple to operate, do not require special equipment, and have a high recovery rate. However, the extract inevitably contains a large amount of lipoprotein and RNA complexes, the purity is poor, and the polymer is difficult to remove, which affects downstream analysis and is expensive. Therefore, this method is not suitable for large-scale sample processing. Some researchers believe that using polymers to precipitate exosomes is "hijacking" water molecules, which reduces the solubility of exosomes, because enriched exosomes are often accompanied by polymers that are difficult to remove. Therefore, electron microscopy of exosomes is more difficult.[87,88] However, this method is worthy of further research and support, and commercial polymer precipitation kits must be further optimized and improved.

Immunoaffinity Chromatography

Immunoaffinity chromatography is a separation method that uses the highly specific affinity between antigens and antibodies existing in organisms and is mainly used for the separation and purification of biological macromolecules. Exosomes extracted using this method have high purity. However, the method is time-consuming and inefficient, not suitable for large-scale analysis, and easily affected by pH and salt concentration, which is not conducive to downstream experiments.[89] Some studies have reported that the immunoaffinity method can purify exosomes, and antibody-coated magnetic beads can specifically adsorb proteins enriched on the surface of exosomes. In 2011, Taylor et al[90] isolated exosomes from ascites of subjects with stage III ovarian serous adenocarcinoma. Magnetic beads coated with specific antibodies were mixed with ascites and incubated at room temperature. Subsequently, Prunotto et al[91] and Zhang et al[92] successfully used the same method to isolate exosomes from the urine of healthy individuals and performed mass spectrometry. Notably, exosomes obtained via adsorption must be thoroughly cleaned before mass spectrometry analysis. However, the removal efficiency of protein extraction reagents rarely reaches 100%, which may interfere with subsequent mass spectrometry.

Size-Exclusion Method

Size-exclusion chromatography uses the molecular sieve theory to separate proteins based on their molecular size. The main advantage of this method is that it does not require centrifugal force, thus ensuring the integrity of exosomes.[88]

Multiple experimental results have shown that the protein abundance of exosomes obtained via the size-exclusion method was higher than that obtained via ultra-high-speed centrifugation. Ultracentrifugation combined with the size-exclusion method can recover 400 times more exosomes from cord blood mononuclear cell culture media than ultracentrifugation.[93] Similarly, studies on urine revealed that urinary exosomes extracted using the size-exclusion method have higher purity and are superior to ultracentrifugation in recovering extracellular particles and proteins.[94] During ultracentrifugation, some exosomes are broken, and precipitation is insufficient.

In recent years, researchers have used size-exclusion kits to extract exosomes. Size-exclusion chromatography is superior to traditional ultracentrifugation in terms of time, operation, scalability, and exosome yield,[95] and isolated exosomes are relatively pure and perfect. Moreover, this method is reproducible, scalable, inexpensive, and does not require special equipment or user expertise. Therefore, it is an effective method for urinary exosome separation.[96] At the 2020 National Conference on Extracellular Vesicles, the combination of size-exclusion and ultrafiltration methods was widely recognized and supported.

Emerging Methods

Optimizing exosome extraction methods is challenging, and many exosome extraction methods have emerged. Examples include gold-loaded ferric oxide nanocubes based on immunochromatography,[97] asymmetric flow field-flow separation methods based on particle size,[98,99] and EXODUS.[100] Asymmetric flow field-flow separation methods have also been developed for different particle sizes, but their cumbersome processing procedures limit their throughput.[101,102] A recently discovered technology named EXODUS has the advantages of convenience, stability, speed, and high quality, and is the optimal extraction method for exosomes, but its processing ability must be verified using more data.[100]

The extraction methods based on the physical properties and composition of exosomes can yield different qualities of exosomes. Although ultracentrifugation is effective for the separation of extracellular vesicles in urine, this technique is time-consuming, labor-intensive, and requires expensive equipment. However, these are not conducive

to clinical translation. Ultrafiltration and precipitation methods incorporate impurities that are not conducive to downstream experiments. Although immunoaffinity chromatography is highly pure, it has low efficiency and is not suitable for the extraction of many exosomes from urine samples. Size-exclusion chromatography does not require ultracentrifugation, and the simple operation can obtain intact high-purity exosomes. Therefore, size-exclusion chromatography is the most suitable method for the extraction of urinary exosomes.

Verification

Exosomes are characterized by their size, protein content, and lipid content. According to their different characteristics, researchers have developed various techniques to characterize exosomes. Common detection techniques include fluorescence microscopy, Western blotting, and flow cytometry to detect protein markers on the membrane surface. As technology advances, nanoparticle tracking analysis, dynamic light scattering, mass spectrometry, and a variety of precision microscopy techniques are gradually being applied.[103] The International Association of Extracellular Vesicles recommends that exosome characterization of exosomes be verified by the presence of exosome-related surface markers and the absence of proteins not related to exosomes. According to documentation provided by the International Association of Extracellular Vesicles, exosome surface markers include CD9, CD63, CD81 (corresponding to the proteins Alix, flotillin 1, and tetraspanin), TSG101, integrin, and cell adhesion molecule. Exosomes contain high concentrations of cholesterol and most of the fatty acids they enclose are saturated or monounsaturated, mainly sphingomyelin and hexosylceramide, whereas phosphatidylcholine and phosphatidylethanolamine account for a small proportion.[104] This difference in the lipid composition ratio may be the reason for lateral separation into exosomes during multivesicular body formation.

Proteomics

In recent years, an increasing number of studies have demonstrated the role of exosomes in the transmission of information between cells.[105–107] Compared to soluble molecules, their lipid bilayer structure makes them effective carriers for "long-distance" signal transmission.[52] The advent of proteomics has greatly affected protein research methodology and promoted the ability to obtain protein-related information in both basic and clinical research.[108] Urine biomarkers have become a research hotspot in recent years due to their comprehensive advantages. Various mass spectrometry techniques,[75] including 2-dimensional polyacrylamide electrophoresis, surface-enhanced laser desorption/ionization time-of-flight mass spectrometry, liquid chromatography tandem mass spectrometry, and capillary electrophoresis mass spectrometry, have been applied to urine proteomic analysis and are expected to provide patients with true precision medicine. Through high-throughput omics research, urinary exosomes have become a potential source of biomarkers. Urine is formed by the kidneys filtering the blood and is discharged through the ureter and bladder. In addition, prostate secretions are discharged into the urine through the prostate catheter.[74] Thus, exosomes secreted by urothelial cells may contain a variety of molecular markers of urinary tract diseases.

Hogan et al[109] used the sucrose density gradient method combined with ultracentrifugation to perform density ultracentrifugation to separate urinary exosomes from volunteers. Using 1-dimensional liquid chromatography tandem mass spectrometry, 552 proteins were identified. In the same year, Pisitkun et al[34] were the first to use ultracentrifugation to separate urinary exosomes. Through enzyme digestion, gel electrophoresis, and liquid chromatography tandem mass spectrometry, 295 urinary exosomal proteins were identified, 14 of which were related to kidney disease and 7 related to hypertension. In 2012, Wang et al[110] used ultracentrifugation to separate urinary exosomes. A total of 3280 proteins were identified in 9 urine samples, 31% of which overlapped. In 2019, researchers used mass spectrometry to determine the protein content of exosomes in the urine of 15 patients with medullary sponge kidneys and 15 patients with autosomal dominant polycystic kidney disease.[111] The researchers performed weighted gene coexpression network analysis and used enzyme-linked immunosorbent assay to verify the proteomic data. The results showed that 2950 proteins were isolated, 1579 of which were specific exosomal proteins of medullary sponge kidneys and 183 were specific exosomal proteins of autosomal dominant polycystic kidney disease. There is an increasing amount of research on the role of exosomes in disease.

Besides research on healthy individuals, more data are available related to disease. In 2011, Moon et al[112] used ultracentrifugation to separate urinary exosomes from patients with early stage immunoglobulin A nephropathy and thin basement membrane nephropathy. The results showed that 31 proteins were upregulated in the immunoglobulin A nephropathy group and 52 in the thin basement membrane nephropathy group. The 4 main differential proteins were verified via Western blotting, and it was found that ceruloplasmin could effectively distinguish immunoglobulin A nephropathy from thin basement membrane nephropathy. Raimondo et al[113] used ultracentrifugation to isolate urinary exosomes from the urine of patients with renal cell carcinoma. After removing the Tamm-Horsfall protein, the remaining bands were digested and analyzed via 1-dimensional liquid chromatography tandem mass spectrometry. A total of 261 and 186 proteins were identified in the urinary exosomes of healthy individuals and subjects with kidney cancer, respectively, and most proteins were membrane proteins. Until now, there have been no similar studies. Research methods have become more advanced, and the content has become more in-depth.

Besides urinary system diseases, high-throughput detection using proteomics has also identified potential markers in the urinary exosomes of patients with nonurinary system diseases, including hypertension, stomach cancer, lung cancer, pancreatic cancer, mesothelioma, liver cancer, cervical cancer, and ovarian cancer, which is important.[114–120] For urinary system tumors, blood and urine samples can be analyzed relatively minimally or even noninvasively. Helped by high-throughput proteomic analysis, the bioburden and function of exosomes can be better understood, which will help provide new insights into the complex changes in cancer and reveal potential therapeutic targets, driving the development of personalized medicine.

Conclusions

Urinary exosomes are promising noninvasive and easily accessible biological materials that can be used for biomarker discovery. High-throughput and high-sensitivity omics methods have emerged in recent years. These methods have improved our understanding of diseased urinary extracellular vesicles and promoted a large-scale and in-depth analysis of urinary exosomal proteins. Proteomics studies based on urinary exosomes have revealed potential biomarkers, most of which

focus on urogenital diseases, whereas the potential of urinary exosome biomarkers for other types of disease needs to be further investigated.

Despite progress, many questions regarding the role of urinary exosomes remain unanswered. For example, the methodological differences in urinary exosomes in various laboratories are not conducive to horizontal comparison and more in-depth research. Standard operating procedures are required for the selection, collection, preparation, storage, and transportation of urine samples. To improve the efficiency of scientific research, scientists should reach a consensus and conduct further standardization and unification. Second, there are differences in urinary proteomics within and between individuals. In different populations, diet, mental state, exercise, environmental factors, and genetic background vary for each person. Therefore, the variation in the proteome of urinary exosome levels requires further investigation. Future studies should use more optimized uniform extraction methods to conduct large-scale studies in well-defined patient populations. Only by isolating exosomes with clinically applicable and reproducible methods and obtaining more convincing and reliable conclusions can they be transformed and applied in the clinic.

REFERENCES

1. Johnstone RM, Adam M, Hammond JR, et al. Vesicle formation during reticulocyte maturation. Association of plasma membrane activities with released vesicles (exosomes). *J Biol Chem.* 1987;262:9412–9420.
2. Otake K, Kamiguchi H, Hirozane Y. Identification of biomarkers for amyotrophic lateral sclerosis by comprehensive analysis of exosomal mRNAs in human cerebrospinal fluid. *BMC Med Genomics.* 2019;12:7. doi:10.1186/s12920-019-0473-z.
3. Riau AK, Ong HS, Yam GHF, et al. Sustained delivery system for stem cell-derived exosomes. *Front Pharmacol.* 2019;10:1368. doi:10.3389/fphar.2019.01368.
4. Chen W, Chen X, Qian Y, et al. Lipidomic profiling of human milk derived exosomes and their emerging roles in the prevention of necrotizing enterocolitis. *Mol Nutr Food Res.* 2021;65:e2000845. doi:10.1002/mnfr.202000845.
5. Song JE, Kim JS, Shin JH, et al. Role of synovial exosomes in osteoclast differentiation in inflammatory arthritis. *Cells.* 2021;10:120. doi:10.3390/cells10010120.
6. Kim Y, Shin S, Lee KA. Exosome-based detection of EGFR T790M in plasma and pleural fluid of prospectively enrolled non-small cell lung cancer patients after first-line tyrosine kinase inhibitor therapy. *Cancer Cell Int.* 2021;21:50. doi:10.1186/s12935-021-01761-x.
7. Pegtel DM, Gould SJ. Exosomes. *Annu Rev Biochem.* 2019;88:487–514. doi:10.1146/annurev-biochem-013118-111902.
8. Jing J, Gao Y. Urine biomarkers in the early stages of diseases: current status and perspective. *Discov Med.* 2018;25:57–65.
9. Yoshioka Y, Konishi Y, Kosaka N, et al. Comparative marker analysis of extracellular vesicles in different human cancer types. *J Extracell Vesicles.* 2013;2.
10. Sotelo JR, Porter KR. An electron microscope study of the rat ovum. *J Biophys Biochem Cytol.* 1959;5:327–342. doi:10.1083/jcb.5.2.327.
11. Katzmann DJ, Babst M, Emr SD. Ubiquitin-dependent sorting into the multivesicular body pathway requires the function of a conserved endosomal protein sorting complex, ESCRT-I. *Cell.* 2001;106:145–155. doi:10.1016/s0092-8674(01)00434-2.
12. Erdbrügger U, Blijdorp CJ, Bijnsdorp IV, et al. Urinary extracellular vesicles: a position paper by the Urine Task Force of the International Society for Extracellular Vesicles. *J Extracell Vesicles.* 2021;10:e12093. doi:10.1002/jev2.12093.
13. Hiemstra TF, Charles PD, Gracia T, et al. Human urinary exosomes as innate immune effectors. *J Am Soc Nephrol.* 2014;25:2017–2027. doi:10.1681/ASN.2013101066.
14. Katzmann DJ, Odorizzi G, Emr SD. Receptor downregulation and multivesicular-body sorting. *Nat Rev Mol Cell Biol.* 2002;3:893–905. doi:10.1038/nrm973.
15. Juan T, Fürthauer M. Biogenesis and function of ESCRT-dependent extracellular vesicles. *Semin Cell Dev Biol.* 2018;74:66–77. doi:10.1016/j.semcdb.2017.08.022.
16. Jadli AS, Ballasy N, Edalat P, et al. Inside(sight) of tiny communicator: exosome biogenesis, secretion, and uptake. *Mol Cell Biochem.* 2020;467:77–94. doi:10.1007/s11010-020-03703-z.
17. Turturici G, Tinnirello R, Sconzo G, et al. Extracellular membrane vesicles as a mechanism of cell-to-cell communication: advantages and disadvantages. *Am J Physiol Cell Physiol.* 2014;306:C621–C633. doi:10.1152/ajpcell.00228.2013.
18. Poon IK, Lucas CD, Rossi AG, et al. Apoptotic cell clearance: basic biology and therapeutic potential. *Nat Rev Immunol.* 2014;14:166–180. doi:10.1038/nri3607.
19. Shao H, Im H, Castro CM, et al. New technologies for analysis of extracellular vesicles. *Chem Rev.* 2018;118:1917–1950. doi:10.1021/acs.chemrev.7b00534.
20. Simpson RJ, Jensen SS, Lim JW. Proteomic profiling of exosomes: current perspectives. *Proteomics.* 2008;8:4083–4099. doi:10.1002/pmic.200800109.
21. Graner MW, Alzate O, Dechkovskaia AM, et al. Proteomic and immunologic analyses of brain tumor exosomes. *FASEB J.* 2009;23:1541–1557. doi:10.1096/fj.08-122184.
22. Andaloussi S EL, Mäger I, Breakefield XO, et al. Extracellular vesicles: biology and emerging therapeutic opportunities. *Nat Rev Drug Discov.* 2013;12:347–357.
23. Valadi H, Ekström K, Bossios A, et al. Exosome-mediated transfer of mRNAs and microRNAs is a novel mechanism of genetic exchange between cells. *Nat Cell Biol.* 2007;9:654–659. doi:10.1038/ncb1596.
24. Taylor DD, Gercel-Taylor C. MicroRNA signatures of tumor-derived exosomes as diagnostic biomarkers of ovarian cancer. *Gynecol Oncol.* 2008;110:13–21. doi:10.1016/j.ygyno.2008.04.033.
25. Takeshita N, Hoshino I, Mori M, et al. Serum microRNA expression profile: miR-1246 as a novel diagnostic and prognostic biomarker for oesophageal squamous cell carcinoma. *Br J Cancer.* 2013;108:644–652. doi:10.1038/bjc.2013.8.
26. Stokman MF, Bijnsdorp IV, Schelfhorst T, et al. Changes in the urinary extracellular vesicle proteome are associated with nephronophthisis-related ciliopathies. *J Proteomics.* 2019;192:27–36.
27. Street JM, Koritzinsky EH, Glispie DM, et al. Urine exosomes: an emerging trove of biomarkers. *Adv Clin Chem.* 2017;78:103–122. doi:10.1016/bs.acc.2016.07.003.
28. Pan BT, Johnstone RM. Fate of the transferrin receptor during maturation of sheep reticulocytes *in vitro*: selective externalization of the receptor. *Cell.* 1983;33:967–978. doi:10.1016/0092-8674(83)90040-5.
29. Kassis S, Lauter CJ, Stojanov M, et al. Exfoliation of the beta-adrenergic receptor and the regulatory components of adenylate cyclase by cultured rat glioma C6 cells. *Biochim Biophys Acta.* 1986;886:474–482. doi:10.1016/0167-4889(86)90184-9.
30. Pyne NJ, Anderson N, Lavan BE, et al. Specific antibodies and the selective inhibitor ICI 118233 demonstrate that the hormonally stimulated "dense-vesicle" and peripheral-plasma-membrane cyclic AMP phosphodiesterases display distinct tissue distributions in the rat. *Biochem J.* 1987;248:897–901. doi:10.1042/bj2480897.
31. Schwartz Z, Amir D, Weinberg H, et al. Extracellular matrix vesicle distribution in primary mineralization two weeks after injury to rat tibial bone (ultrastructural tissue morphometry). *Eur J Cell Biol.* 1987;45:97–101.
32. Raposo G, Nijman HW, Stoorvogel W, et al. B lymphocytes secrete antigen-presenting vesicles. *J Exp Med.* 1996;183:1161–1172. doi:10.1084/jem.183.3.1161.
33. Lotvall J, Valadi H. Cell to cell signalling via exosomes through esRNA. *Cell Adh Migr.* 2007;1:156–158. doi:10.4161/cam.1.3.5114.

34. Pisitkun T, Shen RF, Knepper MA. Identification and proteomic profiling of exosomes in human urine. *Proc Natl Acad Sci USA.* 2004;101:13368–13373. doi:10.1073/pnas.0403453101.
35. Patras KA, Ha AD, Rooholfada E, et al. Augmentation of urinary lactoferrin enhances host innate immune clearance of uropathogenic Escherichia coli. *J Innate Immun.* 2019;11:481–495. doi:10.1159/000499342.
36. Kim MH, Lee YH, Seo JW, et al. Urinary exosomal viral microRNA as a marker of BK virus nephropathy in kidney transplant recipients. *PLoS One.* 2017;12:e0190068. doi:10.1371/journal.pone.0190068.
37. Jiang PY, Zhu XJ, Jiang RA, et al. MicroRNAs derived from urinary exosomes act as novel biomarkers in the diagnosis of intrahepatic cholestasis of pregnancy. *Am J Transl Res.* 2019;11:6249–6261.
38. Agudiez M, Martinez PJ, Martin-Lorenzo M, et al. Analysis of urinary exosomal metabolites identifies cardiovascular risk signatures with added value to urine analysis. *BMC Biol.* 2020;18:192. doi:10.1186/s12915-020-00924-y.
39. Wang S, Kojima K, Mobley JA, et al. Proteomic analysis of urinary extracellular vesicles reveal biomarkers for neurologic disease. *EBioMedicine.* 2019;45:351–361. doi:10.1016/j.ebiom.2019.06.021.
40. Yang C, Wu S, Mou Z, et al. Exosome-derived circTRPS1 promotes malignant phenotype and CD8+ T cell exhaustion in bladder cancer microenvironments. *Mol Ther.* 2022;30:1054–1070. doi:10.1016/j.ymthe.2022.01.022.
41. Khan S, Zakariah M, Rolfo C, et al. Prediction of mycoplasma hominis proteins targeting in mitochondria and cytoplasm of host cells and their implication in prostate cancer etiology. *Oncotarget.* 2017;8:30830–30843. doi:10.18632/oncotarget.8306.
42. Wang Y, Imran A, Shami A, et al. Decipher the *Helicobacter pylori* protein targeting in the nucleus of host cell and their implications in gallbladder cancer: an insilico approach. *J Cancer.* 2021;12:7214–7222.
43. Harris CC, Mulvihill JJ, Thorgeirsson SS, et al. Individual differences in cancer susceptibility. *Ann Intern Med.* 1980;92:809–825.
44. Zhu Q, Cheng L, Deng C, et al. The genetic source tracking of human urinary exosomes. *Proc Natl Acad Sci USA.* 2021;118(43):e2108876118.
45. Feng W, Dean DC, Hornicek FJ, et al. Exosomes promote premetastatic niche formation in ovarian cancer. *Mol Cancer.* 2019;18:124.
46. Long JD, Sullivan TB, Humphrey J, et al. A non-invasive miRNA based assay to detect bladder cancer in cell-free urine. *Am J Transl Res.* 2015;7:2500–2509.
47. Chu L, Shu X, Huang Y, Chu T, Ge M, Lu Q. Sex steroid hormones in urinary exosomes as biomarkers for the prediction of prostate cancer. *Clin Chim Acta.* 2022;531:389–398.
48. Chun-Yan L, Zi-Yi Z, Tian-Lin Y, et al. Liquid biopsy biomarkers of renal interstitial fibrosis based on urinary exosome. *Exp Mol Pathol.* 2018;105:223–228.
49. Solé C, Moliné T, Vidal M, et al. An exosomal urinary miRNA signature for early diagnosis of renal fibrosis in lupus nephritis. *Cells.* 2019;8:773.
50. Zubiri I, Posada-Ayala M, Benito-Martin A, et al. Kidney tissue proteomics reveals regucalcin downregulation in response to diabetic nephropathy with reflection in urinary exosomes. *Transl Res.* 2015;166:474–484.
51. Vitorino R, Ferreira R, Guedes S, et al. What can urinary exosomes tell us? *Cell Mol Life Sci.* 2021;78:3265–3283.
52. Mitchell PS, Parkin RK, Kroh EM, et al. Circulating microRNAs as stable blood-based markers for cancer detection. *Proc Natl Acad Sci USA.* 2008;105:10513–10518.
53. Mizutani K, Kawakami K, Horie K, et al. Urinary exosome as a potential biomarker for urinary tract infection. *Cell Microbiol.* 2019;21:e13020.
54. Kumar S, Vijayan M, Bhatti JS, et al. MicroRNAs as peripheral biomarkers in aging and age-related diseases. *Prog Mol Biol Transl Sci.* 2017;146:47–94.
55. Samsonov R, Shtam T, Burdakov V, et al. Lectin-induced agglutination method of urinary exosomes isolation followed by mi-RNA analysis: application for prostate cancer diagnostic. *Prostate.* 2016;76:68–79.
56. Magayr TA, Song X, Streets AJ, et al. Global microRNA profiling in human urinary exosomes reveals novel disease biomarkers and cellular pathways for autosomal dominant polycystic kidney disease. *Kidney Int.* 2020;98:420–435.
57. Ando W, Kikuchi K, Uematsu T, et al. Novel breast cancer screening: combined expression of miR-21 and MMP-1 in urinary exosomes detects 95% of breast cancer without metastasis. *Sci Rep.* 2019;9:13595.
58. Joshi BS, Zuhorn IS. Heparan sulfate proteoglycan-mediated dynamin-dependent transport of neural stem cell exosomes in an in vitro blood-brain barrier model. *Eur J Neurosci.* 2021;53:706–719.
59. Sun D, Zhuang X, Xiang X, et al. A novel nanoparticle drug delivery system: the anti-inflammatory activity of curcumin is enhanced when encapsulated in exosomes. *Mol Ther.* 2010;18:1606–1614.
60. Zhuang X, Xiang X, Grizzle W, et al. Treatment of brain inflammatory diseases by delivering exosome encapsulated anti-inflammatory drugs from the nasal region to the brain. *Mol Ther.* 2011;19:1769–1779.
61. Jang SC, Kim OY, Yoon CM, et al. Bioinspired exosome-mimetic nanovesicles for targeted delivery of chemotherapeutics to malignant tumors. *ACS Nano.* 2013;7:7698–7710.
62. Tian Y, Li S, Song J, et al. A doxorubicin delivery platform using engineered natural membrane vesicle exosomes for targeted tumor therapy. *Biomaterials.* 2014;35:2383–2390.
63. Théry C, Ostrowski M, Segura E. Membrane vesicles as conveyors of immune responses. *Nat Rev Immunol.* 2009;9:581–593.
64. Alvarez-Erviti L, Seow Y, Yin H, et al. Delivery of siRNA to the mouse brain by systemic injection of targeted exosomes. *Nat Biotechnol.* 2011;29:341–345.
65. Ohno S, Takanashi M, Sudo K, et al. Systemically injected exosomes targeted to EGFR deliver antitumor microRNA to breast cancer cells. *Mol Ther.* 2013;21:185–191.
66. Jiang ZZ, Liu YM, Niu X, et al. Exosomes secreted by human urine-derived stem cells could prevent kidney complications from type I diabetes in rats. *Stem Cell Res Ther.* 2016;7:24.
67. Witwer KW, Buzás EI, Bemis LT, et al. Standardization of sample collection, isolation and analysis methods in extracellular vesicle research. *J Extracell Vesicles.* 2013;2.
68. Dhondt B, Van Deun J, Vermaerke S, et al. Urinary extracellular vesicle biomarkers in urological cancers: from discovery towards clinical implementation. *Int J Biochem Cell Biol.* 2018;99:236–256.
69. Zhou H, Yuen PS, Pisitkun T, et al. Collection, storage, preservation, and normalization of human urinary exosomes for biomarker discovery. *Kidney Int.* 2006;69:1471–1476.
70. Svenningsen P, Sabaratnam R, Jensen BL. Urinary extracellular vesicles: origin, role as intercellular messengers and biomarkers; efficient sorting and potential treatment options. *Acta Physiol (Oxf).* 2020;228:e13346.
71. Wang D, Sun W. Urinary extracellular microvesicles: isolation methods and prospects for urinary proteome. *Proteomics.* 2014;14:1922–1932.
72. Lötvall J, Hill AF, Hochberg F, et al. Minimal experimental requirements for definition of extracellular vesicles and their functions: a position statement from the International Society for Extracellular Vesicles. *J Extracell Vesicles.* 2014;3:26913.
73. Linxweiler J, Junker K. Extracellular vesicles in urological malignancies: an update. *Nat Rev Urol.* 2020;17:11–27.
74. Dhondt B, Geeurickx E, Tulkens J, et al. Unravelling the proteomic landscape of extracellular vesicles in prostate cancer by density-based fractionation of urine. *J Extracell Vesicles.* 2020;9:1736935.
75. Bandu R, Oh JW, Kim KP. Mass spectrometry-based proteome profiling of extracellular vesicles and their roles in cancer biology. *Exp Mol Med.* 2019;51:1–10.

76. Musante L, Saraswat M, Ravidà A, et al. Recovery of urinary nanovesicles from ultracentrifugation supernatants. *Nephrol Dial Transplant.* 2013;28:1425–1433.
77. Rood IM, Deegens JK, Merchant ML, et al. Comparison of three methods for isolation of urinary microvesicles to identify biomarkers of nephrotic syndrome. *Kidney Int.* 2010;78:810–816.
78. Bobrie A, Colombo M, Krumeich S, et al. Diverse subpopulations of vesicles secreted by different intracellular mechanisms are present in exosome preparations obtained by differential ultracentrifugation. *J Extracell Vesicles.* 2012;1.
79. Gheinani AH, Vögeli M, Baumgartner U, et al. Improved isolation strategies to increase the yield and purity of human urinary exosomes for biomarker discovery. *Sci Rep.* 2018;8:3945.
80. He L, Zhu D, Wang J, et al. A highly efficient method for isolating urinary exosomes. *Int J Mol Med.* 2019;43:83–90.
81. Yang M, Liu X, Luo Q, et al. An efficient method to isolate lemon derived extracellular vesicles for gastric cancer therapy. *J Nanobiotechnology.* 2020;18:100.
82. Barreiro K, Dwivedi OP, Leparc G, et al. Comparison of urinary extracellular vesicle isolation methods for transcriptomic biomarker research in diabetic kidney disease. *J Extracell Vesicles.* 2020;10:e12038.
83. Miranda KC, Bond DT, McKee M, et al. Nucleic acids within urinary exosomes/microvesicles are potential biomarkers for renal disease. *Kidney Int.* 2010;78:191–199.
84. Musante L, Tataruch-Weinert D, Kerjaschki D, et al. Residual urinary extracellular vesicles in ultracentrifugation supernatants after hydrostatic filtration dialysis enrichment. *J Extracell Vesicles.* 2017;6:1267896.
85. Yamamoto KR, Alberts BM, Benzinger R, et al. Rapid bacteriophage sedimentation in the presence of polyethylene glycol and its application to large-scale virus purification. *Virology.* 1970;40:734–744.
86. Rider MA, Hurwitz SN, Meckes DG Jr. ExtraPEG: a polyethylene glycol-based method for enrichment of extracellular vesicles. *Sci Rep.* 2016;6:23978.
87. Patel GK, Khan MA, Zubair H, et al. Comparative analysis of exosome isolation methods using culture supernatant for optimum yield, purity and downstream applications. *Sci Rep.* 2019;9:5335.
88. Zeringer E, Barta T, Li M, et al. Strategies for isolation of exosomes. *Cold Spring Harb Protoc.* 2015;2015:319–323.
89. Greening DW, Xu R, Ji H, et al. A protocol for exosome isolation and characterization: evaluation of ultracentrifugation, density-gradient separation, and immunoaffinity capture methods. *Methods Mol Biol.* 2015;1295:179–209.
90. Taylor DD, Zacharias W, Gercel-Taylor C. Exosome isolation for proteomic analyses and RNA profiling. *Methods Mol Biol.* 2011;728:235–246.
91. Prunotto M, Farina A, Lane L, et al. Proteomic analysis of podocyte exosome-enriched fraction from normal human urine. *J Proteomics.* 2013;82:193–229.
92. Zhang N, Sun N, Deng C. Rapid isolation and proteome analysis of urinary exosome based on double interactions of Fe3O4@TiO2-DNA aptamer. *Talanta.* 2021;221:121571.
93. Cardoso RMS, Rodrigues SC, Gomes CF, et al. Development of an optimized and scalable method for isolation of umbilical cord blood-derived small extracellular vesicles for future clinical use. *Stem Cells Transl Med.* 2021;10:910–921.
94. Guan S, Yu H, Yan G, et al. Characterization of urinary exosomes purified with size exclusion chromatography and ultracentrifugation. *J Proteome Res.* 2020;19:2217–2225.
95. Jain R, Randev S, Kumar P, et al. Acute kidney injury and encephalopathy in a child: diethylene glycol poisoning. *Indian J Pediatr.* 2021;88:194–195.
96. Sidhom K, Obi PO, Saleem A. A review of exosomal isolation methods: is size exclusion chromatography the best option? *Int J Mol Sci .* 2020;21.
97. Boriachek K, Masud MK, Palma C, et al. Avoiding pre-isolation step in exosome analysis: direct isolation and sensitive detection of exosomes using gold-loaded nanoporous ferric oxide nanozymes. *Anal Chem.* 2019;91:3827–3834.
98. Zhang H, Lyden D. Asymmetric-flow field-flow fractionation technology for exomere and small extracellular vesicle separation and characterization. *Nat Protoc.* 2019;14:1027–1053.
99. Kotoucek J, Hezova R, Vrablikova A, et al. Characterization and purification of pentameric chimeric protein particles using asymmetric flow field-flow fractionation coupled with multiple detectors. *Anal Bioanal Chem.* 2021;413:3749–3761.
100. Chen Y, Zhu Q, Cheng L, et al. Exosome detection via the ultrafast-isolation system: EXODUS. *Nat Methods.* 2021;18:212–218.
101. Wang Y, Cuss CW, Shotyk W. Application of asymmetric flow field-flow fractionation to the study of aquatic systems: coupled methods, challenges, and future needs. *J Chromatogr A.* 2020;1632:461600.
102. Singh K, Nalabotala R, Koo KM, et al. Separation of distinct exosome subpopulations: isolation and characterization approaches and their associated challenges. *Analyst.* 2021;146:3731–3749.
103. Van der Pol E, Coumans FA, Grootemaat AE, et al. Particle size distribution of exosomes and microvesicles determined by transmission electron microscopy, flow cytometry, nanoparticle tracking analysis, and resistive pulse sensing. *J Thromb Haemost.* 2014;12:1182–1192.
104. Aalberts M, van Dissel-Emiliani FM, van Adrichem NP, et al. Identification of distinct populations of prostasomes that differentially express prostate stem cell antigen, annexin A1, and GLIPR2 in humans. *Biol Reprod.* 2012;86:82.
105. Zhang H, Wang L, Li C, et al. Exosome-induced regulation in inflammatory bowel disease. *Front Immunol.* 2019;10:1464.
106. Wan M, Ning B, Spiegel S, et al. Tumor-derived exosomes (TDEs): how to avoid the sting in the tail. *Med Res Rev.* 2020;40:385–412.
107. Jan AT, Rahman S, Khan S, et al. Biology, pathophysiological role, and clinical implications of exosomes: a critical appraisal. *Cells.* 2019;8.
108. Nawaz M, Camussi G, Valadi H, et al. The emerging role of extracellular vesicles as biomarkers for urogenital cancers. *Nat Rev Urol.* 2014;11:688–701.
109. Hogan MC, Manganelli L, Woollard JR, et al. Characterization of PKD protein-positive exosome-like vesicles. *J Am Soc Nephrol.* 2009;20:278–288.
110. Wang Z, Hill S, Luther JM, et al. Proteomic analysis of urine exosomes by multidimensional protein identification technology (MudPIT). *Proteomics.* 2012;12:329–338.
111. Bruschi M, Granata S, Santucci L, et al. Proteomic analysis of urinary microvesicles and exosomes in medullary sponge kidney disease and autosomal dominant polycystic kidney disease. *Clin J Am Soc Nephrol.* 2019;14:834–843.
112. Moon PG, Lee JE, You S, et al. Proteomic analysis of urinary exosomes from patients of early IgA nephropathy and thin basement membrane nephropathy. *Proteomics.* 2011;11:2459–2475.
113. Raimondo F, Morosi L, Corbetta S, et al. Differential protein profiling of renal cell carcinoma urinary exosomes. *Mol Biosyst.* 2013;9:1220–1233.
114. Gonzalez-Calero L, Martínez PJ, Martin-Lorenzo M, et al. Urinary exosomes reveal protein signatures in hypertensive patients with albuminuria. *Oncotarget.* 2017;8:44217–44231.
115. Erozenci LA, Böttger F, Bijnsdorp IV, et al. Urinary exosomal proteins as (pan-)cancer biomarkers: insights from the proteome. *FEBS Lett.* 2019;593:1580–1597.
116. Humphries JM, Penno MA, Weiland F, et al. Identification and validation of novel candidate protein biomarkers for the detection of human gastric cancer. *Biochim Biophys Acta.* 2014;1844:1051–1058.

117. Zhang C, Leng W, Sun C, et al. Urine proteome profiling predicts lung cancer from control cases and other tumors. *EBiomedicine.* 2018;30:120–128.

118. Radon TP, Massat NJ, Jones R, et al. Identification of a three-biomarker panel in urine for early detection of pancreatic adenocarcinoma. *Clin Cancer Res.* 2015;21:3512–3521.

119. Mundt F, Johansson HJ, Forshed J, et al. Proteome screening of pleural effusions identifies galectin 1 as a diagnostic biomarker and highlights several prognostic biomarkers for malignant mesothelioma. *Mol Cell Proteomics.* 2014;13:701–715.

120. Zhao Y, Li Y, Liu W, et al. Identification of noninvasive diagnostic biomarkers for hepatocellular carcinoma by urinary proteomics. *J Proteomics.* 2020;225:103780.

121. Donovan MJ, Noerholm M, Bentink S, et al. A molecular signature of PCA3 and ERG exosomal RNA from non-DRE urine is predictive of initial prostate biopsy result. *Prostate Cancer Prostatic Dis.* 2015;18:370–375.

122. Castellanos-Rizaldos E, Grimm DG, Tadigotla V, et al. Exosome-based detection of EGFR T790M in plasma from non-small cell lung cancer patients. *Clin Cancer Res.* 2018;24:2944–2950.

SPECIAL REPORT

Increases in CLIA-Waived Testing Sites Since the Start of the COVID-19 Pandemic

Yang Xia, PhD,[1,*] *Nancy Anderson, MMSc*[1]

[1]Division of Laboratory Systems, Center for Surveillance, Epidemiology, and Laboratory Services, Centers for Disease Control and Prevention, Atlanta, GA, USA. *To whom correspondence should be addressed: yax1@cdc.gov.

Keywords: COVID-19, CLIA laboratory, certificate of waiver, laboratory facility type, test volume, public health emergency

Abbreviations: CoW, Certificate of Waiver; CLIA, Clinical Laboratory Improvement Amendments of 1988; QIES, Quality Improvement and Evaluation System

Laboratory Medicine 2023;54:126–129; https://doi.org/10.1093/labmed/lmac154

ABSTRACT

The number of testing sites receiving their first Certificate of Waiver (CoW) under the Clinical Laboratory Improvement Amendments of 1988 (CLIA) increased significantly after the start of the COVID-19 pandemic. We compared the first-time CoWs in 2020–2021 to those in 2018–2019. The total number of first-time CoWs during 2020–2021 was more than twice what it was in 2018–2019, corresponding to population testing needs during the COVID-19 pandemic, especially in assisted living facility, pharmacy, physician office, and school/student health service settings. This study highlighted the need to strengthen clinical testing strategies to be better prepared for future public health emergencies.

Materials and Methods

Data on Clinical Laboratory Improvement Amendments of 1988 (CLIA)-certified laboratories were obtained from the Quality Improvement and Evaluation System (QIES), which is maintained by the Centers for Medicare & Medicaid Services. Each laboratory has a unique identification number and certificate effective date, which were used to identify the first Certificate of Waiver (CoW) issued during the period of investigation. Pre-COVID-19 CoW data from January 2018 to December 2019 were compared with January 2020 to December 2021, during COVID-19. Facility types in QIES include assisted living facility, pharmacy, school/student health service, physician office, and others. First-time CoW issued monthly (including CLIA-exempt states New York and Washington) were analyzed for each selected facility type. All computational work was conducted in SAS (version 9.4, SAS Institute, Cary, NC).

Results

The number of first-time CoWs increased 73% from 2019 to 2020 (12,796 vs 22,105) and 39% from 2020 to 2021 (22,105 vs 30,599) (**FIGURE 1A**). The total number of first-time CoWs during 2020 to 2021 was more than twice what it had been in 2018 to 2019 (52,704 vs 25,872, **FIGURE 2**). **FIGURE 2** demonstrates a dramatic rise of first-time CoWs in each facility category for 2020 to 2021, compared with 2018 to 2019. The increases ranged from 20% in physician offices (12,215 vs 10,128) to more than a ten-fold increase in assisted living facility/home health agency/intermediate care facility (5352 vs 446). Assisted living facility, pharmacy, physician office, and school/student health service categories had a pronounced increase during 2020 to 2021 compared with 2018 to 2019 (**FIGURE 3**). Pharmacies responded to the pandemic early, with first-time CoWs rising significantly from April to June 2020. First-time CoWs held by assisted living facilities and school/student health services peaked in October 2020 and November 2020, respectively. The total test volume (not limited to COVID testing) reported by all first-time CoWs increased from 29 million in 2019 to 94 million in 2020 and to 204 million in 2021 (216% and 118% increase, respectively, **FIGURE 1B**).

Discussion

We found that first-time CoWs in nearly all types of testing sites increased during the first 2 years of the COVID-19 pandemic compared with the 2-year period prior to the pandemic. By contrast, the pattern of incremental increase of first-time CoWs by month varied among several selected facility types. Pharmacy not only had the largest increase in first-time testing sites but also responded the soonest at the onset of the pandemic in 2020 and performed the majority of COVID-19 testing for local communities.[1] After an elevated percentage of COVID-19–associated mortality occurred in long-term care facilities during March to May 2020,[2] assisted living facilities reached the highest number of first-time CoWs by October 2020. School/student health services had increased numbers of first-time CoWs from November 2020 to January 2021 and an even higher rise in the autumn of 2021, correlating with efforts to sustain in-person instruction and extracurricular activities.[3] Early COVID-19 testing was associated with reduced mortality and improved pandemic control.[4] Our results demonstrated that increased numbers of first-time CoWs correlated with population testing needs during the COVID-19 pandemic. To improve the current CLIA laboratory

FIGURE 1. Number of first-time CoW testing sites (A) and test volume (B) 2014–2021.

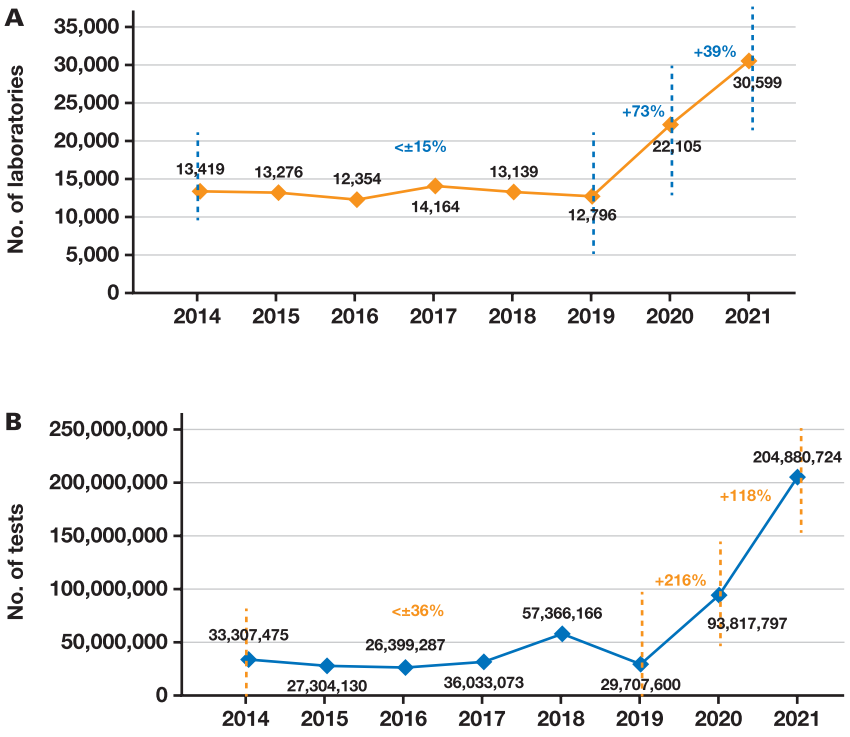

FIGURE 2. Distribution of first-time CoW facilities before 2018–2019 and during 2020–2021 in the COVID-19 pandemic.

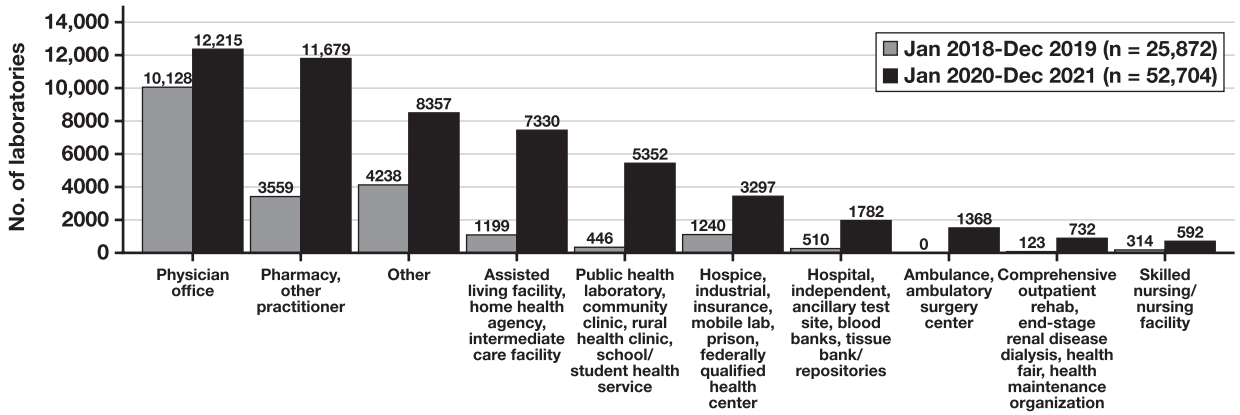

infrastructure so that it can better handle the urgent need for increased testing, strategies that enable existing laboratories to ramp up testing capacity when needed will be essential. This could potentially decrease instances of falsified or inaccurate testing as reportedly occurred in some pop-up COVID-19 testing locations.[5] This study helps shed light on the need to strengthen clinical testing strategies to be better prepared for future public health emergencies.

Acknowledgments

The findings and conclusions in this report are those of the authors and do not necessarily represent the views of the Centers for Disease Control and Prevention. Use of trade names and commercial sources is for identification only and does not constitute endorsement by the United States Department of Health and Human Services or the Centers for Disease Control and Prevention.

FIGURE 3. Number of first-time CoW testing sites by selected facility type before 2018–2019 and during 2020–2021 in the COVID-19 pandemic. A, Assisted living facilities. B, Pharmacy. C, Physician office. D, School/student health service.

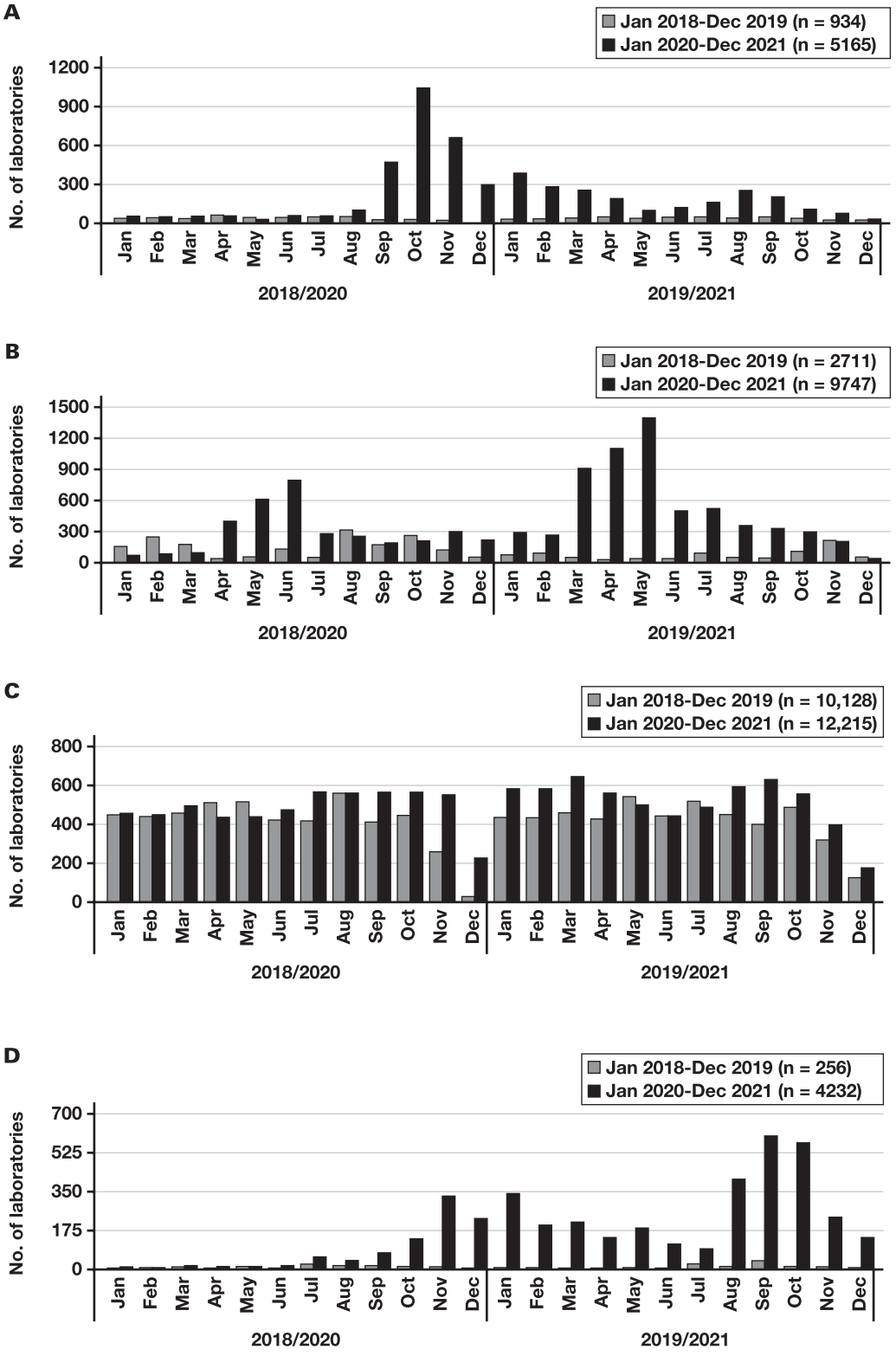

Conflict of Interest Disclosure

The authors have nothing to disclose.

REFERENCES

1. Miller MF, Shi M, Motsinger-Reif A, Weinberg CR, Miller JD, Nichols E. Community-based testing sites for Sars-Cov-2 — United States, March 2020–November 2021. *MMWR Morb Mortal Wkly Rep.* 2021;70(49):1706–1711. PMID: 34882655. doi:10.15585/mmwr.mm7049a3.
2. Telford CT, Onwubiko U, Holland D, et al. Preventing COVID-19 outbreaks in long-term care facilities through preemptive testing of residents and staff members - Fulton County, Georgia, March–May 2020. *MMWR Morb Mortal Wkly Rep*. 2020;69(37):1296–1299. PMID: 32941413. doi: 10.15585/mmwr.mm6937a4.
3. Lanier WA, Babitz KD, Collingwood A, et al. COVID-19 Testing to sustain in-person instruction and extracurricular activities in high schools - Utah, November 2020–March 2021. *MMWR Morb Mortal Wkly Rep.* 2021;70(21):785–791. PMID: 34043614. doi:10.15585/mmwr.mm7021e2.
4. Kannoth S, Kandula S, Shaman J. The association between early country-level COVID-19 testing capacity and later COVID-19 mortality outcomes. *Influenza Other Respir Viruses.* 2022;16(1):56–62. doi:10.1111/irv.12906.
5. Federal inspectors allege Covid testing firm didn't put patients' names on specimens. https://www.nbcnews.com/health/health-news/federal-inspectors-allege-covid-testing-firm-didnt-put-patient-names-s-rcna12822. Accessed October 19, 2022.

SCIENCE

Combination of Circulating Cell-Free DNA and Positron Emission Tomography to Distinguish Non–Small Cell Lung Cancer from Tuberculosis

Wenqiang Zheng,[1,a] Bin Quan,[2] Guangjian Gao,[1] Puhong Zhang,[3] and Lizhu Huang[4,a,]*

[1]Department of Nuclear Medicine, First Affiliated Hospital of Wannan Medical College, Wuhu, China, [2]Department of Infectious Diseases, First Affiliated Hospital of Wannan Medical College, Wuhu, China, [3]Department of Clinical Laboratory, Second Affiliated Hospital of Wannan Medical College, Wuhu, China, [4]Department of Clinical Laboratory, First Affiliated Hospital of Wannan Medical College, Wuhu, China. *To whom correspondence should be addressed: hlz-8718@163.com. [a]First authors.

Keywords: circulating cell-free DNA, metabolic tumor burden, non–small cell lung cancer, tuberculosis, glucose transporter 1

Abbreviations: NSCLC, non–small cell lung cancer; cfDNA, circulating cell-free DNA; PET/CT, positron emission tomography-computed tomography; GLU1, glucose transporter 1; FasL, factor-related apoptosis ligand; SUV-Maxa, maximum standardized uptake value; AUC, area under the curve; siRNA, small interfering RNA

Laboratory Medicine 2023;54:130–141; https://doi.org/10.1093/labmed/lmac085

ABSTRACT

Objective: Non–small cell lung cancer (NSCLC) holds high metabolic tumor burden and circulating cell-free DNA (cfDNA) levels, and the relationship between metabolic tumor burden and cfDNA in NSCLC and the underlying mechanism of their interaction therein remain poorly characterized. Our aim was to evaluate the clinical value of cfDNA and metabolic tumor burden by positron emission tomography-computed tomography (PET/CT) for NSCLC differential diagnosis from tuberculosis in patients with solitary pulmonary nodules.

Methods: Metabolic tumor burden values in humans (subjects with NSCLC, subjects with tuberculosis, and healthy control subjects) and relevant mouse models were detected by preoperative 18F-fluorodeoxyglucose PET (18F-FDG PET/CT) and [3H]-2-deoxy-DG uptake, respectively. The cfDNA levels were detected by quantifying serum cfDNA fragments from the *ALU* (115 bp) gene using reverse transcription–polymerase chain reaction. RNA sequence was performed to determine the underlying target genes and knocked down or inhibited the target genes in vivo and in vitro to determine the mechanism therein.

Results: Metabolic tumor burden correlated with serum cfDNA levels in NSCLC subjects but not in tuberculosis subjects or healthy controls. Mouse models showed a similar phenomenon. In addition, the RNA sequence showed that glucose transporter 1 (GLU1), factor-related apoptosis ligand (FasL), caspase 8, and caspase 3 were significantly increased in NSCLC mouse tumors compared with those in tuberculosis mouse masses. Inhibiting the metabolic tumor burden by blocking or knocking down GLU1 markedly reduced the expression of FasL, the phosphorylation of caspase 8/caspase 3, and serum cfDNA levels/apoptosis percentage in vivo and in vitro. Furthermore, the use of a combination of cfDNA and metabolic tumor burden allowed better ability to distinguish NSCLC subjects from those with tuberculosis or healthy controls than either method used alone.

Conclusion: Metabolic tumor burden promotes the formation of circulating cfDNA through GLU1-mediated apoptosis in NSCLC, and the combination of cfDNA and metabolic tumor burden could be valuable for distinguishing NSCLC from tuberculosis.

Lung cancer remains the most common cancer worldwide and is a leading cause of death due to its high morbidity and mortality.[1] Persons diagnosed with non–small cell lung cancer (NSCLC) account for approximately 85% of all lung cancer diagnoses.[1] The majority of NSCLC cases are diagnosed at late stages (stage III or IV) and have systemic tumor metastasis with 5-year survival rates of <5%, owing to the difficulty of early distinction of NSCLC from other lung masses such as occur in tuberculosis.[2,3] Tuberculosis, a common infectious respiratory disease caused by mycobacteria, infects one-third of the world's population and often radiologically manifests similar to NSCLC.[2,4] In tuberculosis epidemic regions, it is observed that the presence of tuberculosis has resulted in 58% to 92% of false-positive diagnoses of early NSCLC, and it is also listed as one of the major false-positive diagnoses of malignant lymph nodes.[5,6] Therefore, there is increased demand for new noninvasive diagnostic options.

Circulating cell-free DNA (cfDNA) refers to extracellular DNA present in peripheral blood, which is mainly derived from tumor DNA fragments by necrotic or apoptotic tumor cells with tumor-epigenetic changes.[7,8] The activation of the caspase 8/caspase 3 pathway, causing apoptosis through promoting poly (ADP-ribose) polymerase-induced cleavage of DNA, is recognized as the best biochemical hallmark of apoptosis.[9,10] Moreover, the size of the cfDNA released from dead lung cancer cells varies between small fragments of 70 to 200 base pairs and large fragments of about 21 kb and is longer than that of nonneoplastic DNA.[11] The cfDNA quantification is a new diagnostic option for cancer because it allows simple, noninvasive access to genetic material detectable in plasma and serum by sensitive molecular biology techniques.[12] Our previous research demonstrated that the levels of cfDNA in patients with early NSCLC are obviously higher than that in patients with tuberculosis.[13] Moreover, cfDNA could be used as an indicator for differentiation of early NSCLC from tuberculosis.[13] Unfortunately, the sensitivity and specificity of cfDNA to differentiate early NSCLC from tuberculosis has not been satisfactory.[13]

The use of PET/CT scans with 18F-FDG (a glucose analogue) is recommended for multiple types of tumor diagnosis due to high sensitivity.[14,15] The metabolic tumor burden is described as the maximum standardized uptake value (SUV-Max[a]) of the primary tumor depending on the rate of 18F-FDG uptake by the tumor.[16,17] Currently, PET/CT is a good procedure for the diagnosis of NSCLC patients because it has the capability of identifying lesions that would pass unnoticed in CT, preventing or reducing unnecessary operations.[18,19] However, PET/CT shows low specificity for differential diagnosis of early NSCLC from tuberculosis because the tuberculosis site also presents an elevated level of glucose consumption.[20,21] Of note, a larger prospective, interventional study demonstrated that the combination of cancer blood testing with PET/CT was feasible to screen for multicancer and guide intervention.[22]

The aim of this study is to evaluate the potential clinical value of the combination of cfDNA and metabolic tumor burden by PET/CT as an auxiliary tool for early NSCLC differential diagnosis from tuberculosis in patients with solitary pulmonary nodules. Also, NSCLC and tuberculosis mouse models were used to verify the correlation of cfDNA and metabolic tumor burden. Finally, gene silencing and inhibitor in vivo and in vitro are performed to elucidate the specific mechanism.

Materials and Methods

Subjects

All subjects were recruited from the First and the Second Affiliated Hospital of Wannan Medical College. This study was conducted in accordance with the Declaration of Helsinki and the ethical rules of good clinical practice, and the protocol was approved (201805432GH) by the Ethics Committee of the First Affiliated Hospital of Wannan Medical College. All subjects provided written informed consent. All participants with early stage NSCLC and those with tuberculosis were diagnosed by pathology through PET/CT-guided biopsy or CT-guided biopsy with World Health Organization criteria.[23,24] All NSCLC cases were divided into 2 subtypes: adenocarcinoma and squamous carcinoma (**TABLE 1**). All subjects were first diagnosed without any previous antituberculosis or antitumor treatment. Meanwhile, cfDNA detection and PET/CT imaging were performed during the same period. Participants were assigned to 1 of 3 groups: healthy controls (n = 150), tuberculosis (n = 151), and NSCLC (n = 143) groups.

Inclusion criteria of disease group included (1) lung cancer and tuberculosis that meet the relevant diagnostic criteria and were confirmed by histopathology and comorbidities of lung cancer and tuberculosis such as hypertension, diabetes, asthma, and chronic obstructive pulmonary disease could be included; and (2) the participant had detailed medical record information. The inclusion criteria for volunteers for control were healthy as confirmed by a health checkup with no history of related diseases. Exclusion criteria for disease and volunteer groups were (1) the existence of other metabolic diseases, blood diseases, other cancer, other lung disease, severe cardiovascular, cerebrovascular, or urinary system diseases, liver and kidney dysfunction; (2) HIV and other infectious diseases; (3) no definite diagnosis; and (4) pregnancy or lactation. All subjects met the inclusion criteria and were aged between 18 and 80 years. All blood samples were taken under fasting conditions and the obtained serum was immediately stored at −80°C.

Animals

Male BALB/c nude mice (age 5–6 weeks) were purchased from Slac Laboratory Animal. All animal experiments were in accordance with the Laboratory Animal Guidelines for Ethical Review of Animal Welfare (GB/T 35892–2018, China) and approved by the Laboratory Animal Ethics Committee of Wannan Medical College. Mice were randomly placed into 1 of 7 groups: control group (n = 8), tuberculosis group (n = 8), NSCLC group (n = 8); NSCLC + 0.9% saline (NS) group (n = 8), NSCLC + WZB117 group (n = 8), NSCLC + anti–FasL group (n = 8), or the NSCLC + Z-IETD-FMK group (n = 8). The mouse model of NSCLC was achieved by the injection of human non–small cell lung cancer cell line A549 cells (1×10^6, 50 μL) or NCI–H460 (1×10^6, 50 μL) via the tail vein. After 30 days, the mice were anesthetized and serum and lung tissues were collected.[25] A tuberculosis model was created by the injection of mycobacterium tuberculosis (1×10^6 cfu, 50 μL) via the tail vein. The serum and lung tissues were obtained for detection after 7 days.[26] Mice in NSCLC + WZB117 group, NSCLC + anti–FasL group, and NSCLC + Z-IETD-FMK group received an injection of WZB117 (1 mg/kg), anti–FasL antibody (1 μg/mice), Z-IETD-FMK (3 mg/kg), or an equivalent volume of NS, respectively, via the caudal vein 1 time 3 days before tissue collection.

Cells

A549 and NCI–H460 cells were cultured in Dulbecco's modified eagle medium containing 10% fetal bovine serum with 5% CO_2. Cells were allocated into 1 of 4 groups: an NS-siRNA group (n = 6), GLU1-siRNA group (n = 6), FasL-siRNA group (n = 6), or a Z-IETD-FMK group (n = 6). The small interfering RNA (siRNA) were used to silence the *GLU1* or *FasL* gene in A549 and NCI–H460 cells as reported.[27,28] The rate of cell apoptosis was detected by using Annexin V and PI staining.

Materials

Mycobacterium tuberculosis (ATCC:27294, 1×10^6 cfu/mg) was purchased from ATCC. Glu 1 inhibitor (WZB117) and caspase 3 and caspase 8 common inhibitor (Z-IETD-FMK) were obtained from MedChemExpress. Anti-Glu 1, anti-caspase 3 antibody, anti-caspase 8 antibody, and anti–FasL antibody were obtained from Abcam. The [3H]-2-deoxy-D-glucose was obtained from Perkin Elmer Life Sciences, and the rate of [3H]-2-deoxy-D-glucose uptake was measured according to the manufacturer's instructions.

TABLE 1. Correlation between Clinical Characteristics and Plasma cfDNA or SUV-Max[a]

	n	cfDNA	K-Wχ^2/Z	*P*	SUV_Max[a]	K-Wχ^2/Z	*P*
Healthy control							
Age (y)							
≤65	119	9.58 (5.06, 12.54)	0.991	.319	1.88 (1.14, 2.55)	0.501	.479
>65	31	10.01 (7.15, 17.75)			1.94 (0.89, 2.71)		
Sex (n)							
Male	116	9.82 (6.48, 12.53)	−0.608	.543	1.90 (1.09, 2.41)	0.514	.607
Female	34	7.14 (3.52, 17.62)			2.14 (.79, 3.41)		
Tuberculosis							
Age (y)			−0.102	.918		−1.448	.148
≤65	117	14.59 (11.34, 17.91)			2.53 (1.69, 3.12)		
>65	34	14.62 (6.30, 26.99)			2.10 (1.42, 3.25)		
Sex (n)			−0.311	.755		−0.270	.787
Male	114	14.50 (9.14, 18.78)			2.43 (1.52, 2.99)		
Female	37	14.66 (9.73, 18.94)			2.23 (1.46, 5.15)		
Early NSCLC							
Age (y)			−1.636	.102		−2.182	**.029**
≤65	113	18.64 (14.45, 23.64)			3.53 (2.86, 4.72)		
>65	36	27.90 (6.68, 41.91)			7.19 (2.04, 8.94)		
Sex (n)			–	.267		−1.157	.247
Male	114	19.05 (11.17, 26.12)			3.81 (2.28, 5.33)		
Female	35	20.29 (14.29, 35.03)			4.05 (3.00, 8.30)		
Pathological type			−3.682	**<.001**		−4.080	**<.001**
Adenocarcinoma	76	20.93 (16.89, 36.23)			4.36 (3.47, 8.05)		
Squamous carcinoma	73	17.37 (8.82, 22.81)			3.01 (1.57, 4.22)		

cfDNA, cell-free DNA; NSCLC, non–small cell lung cancer; SUV-Max[a], the maximum standardized uptake value.

Blood Collection and DNA Isolation

Blood collection and DNA isolation were described in our previous report.[13] Serum samples of 2 mL were collected into EDTA-2K containing tubes. The cell-free serum was stored at −80°C. Total DNA was extracted from 400 μL serum by using a QIAamp DNA Blood Mini Kit (Qiagen). Only the absorbance of the extracted DNA, which was measured by the NanoDrop ND-1000 nucleic acid quantifier (A 260/280 nm) at a ratio of 1.6:1.8 samples, was usable.

Measurement of Serum cfDNA Levels

The quantization of human and mouse serum DNA fragments was detected by quantitative real-time PCR, as in our previous report,[13,29] by amplifying and quantifying shorter (115 bp) fragments from abundant genomic ALU115 repeats. Sequences of ALU115 primers were forward CCTGAGGTCAGGAGTTCGAG and reverse CCCGAGTAGCTGGGATTACA. Both calibrators and samples were analyzed in triplicate.[13]

Western Blotting

For Western blots, lung tumor tissue and tuberculosis tissue were collected and lysed in chilled radio immunoprecipitation assay buffer diluted in phosphate-buffered saline and phosphatase inhibitor for 30 minutes on ice. Ten μg of protein were loaded for sodium dodecyl sulfate polyacrylamide gel electrophoresis and standard Western blotting procedures. The following primary antibodies and dilutions were used: GLU1 (1:1000); FasL (1:2000); and caspase 3 (1:1000), caspase 8 (1:1000).

PET/CT Scan

The PET/CT scans were acquired using an integrated PET/CT system (Siemens). Images were acquired 1 hour after the administration of 18F-FDG. The PET scan was reconstructed by filtered back-projection and ordered-subset expectation-maximization, with data from the CT scan used for attenuation correction. The SUV-Max[a] of a tumor was calculated according to standard formulas. Results were assessed by a nuclear medicine specialist.[20]

RNA Isolation, Microarray Analysis, and Data Analysis

The RNA from lung tumor tissue and tuberculosis tissue were isolated with the RNeasy Mini Kit (Qiagen) in accordance with the manufacturer's instructions for microarray analysis. Triplicate RNA samples were obtained for each test, and cDNA microarray analysis was performed twice for each RNA sample. Based on KEGG Mapper (https://www.kegg.jp/kegg/tool/map_pathway2.html), the fold changes were analyzed by filtering the data set with $P \leq .05$ and signal-to-noise ratio ≥2.0 for screening out differently expressed genes.

Statistical Analysis

Continuous variables were normally distributed by Kolmogorov-Smirnov test and provided as mean ± SD. Overall comparisons were performed with 1-way analysis of variance, and multiple comparisons between the 2 groups were derived from the least significant difference *t*-test. Categorical variables were expressed as percentages. Differences in percentages of variables were determined by χ^2

TABLE 2. Comparison of Clinical Characteristics among Early NSCLC, Tuberculosis, and Healthy Controls

	Healthy Control (n = 150)	Tuberculosis (n = 151)	NSCLC (n = 149)	*P*
Age (y)	59.92 ± 8.33	59.27 ± 9.70	60.08 ± 9.94	.734
Gender				.932
Male	116 (77.33%)	114 (75.5%)	114 (76.51%)	
Female	34 (22.67%)	37 (24.5%)	35 (23.49%)	
Smoking status				**<.001**
Current	45 (30%)	47 (31.13%)	65 (43.62%)	
Former	40 (26.67%)	59 (39.07%)	55 (36.91%)	
Never	65 (43.33%)	45 (29.8%)	29 (19.46%)	
Tobacco exposure (y)	30.23 ± 9.12	36.78 ± 12.97	42.65 ± 16.94	**<.001**
Comorbidities				
Hypertension	55 (36.67%)	54 (35.76%)	60 (40.27%)	.696
Diabetes	15 (10%)	12 (7.95%)	18 (12.08%)	.491
Asthma	7	9 (5.96%)	12 (4.03%)	.473

NSCLC, non-small cell lung cancer

test. Categorical variables were abnormally distributed and shown as median (quartile) [M (P25, P75)]. Differences in serum cfDNA concentrations and the integrity and SUV-Max[a] among participants with NSCLC, tuberculosis, and healthy controls were analyzed by using the Kruskal-Wallis test. Multiple comparisons between 2 groups were derived from the Mann-Whitney *U* test. Relationships between cfDNA and SUV-Max[a] were examined using Pearson linear regression analysis. The receiver operating characteristic (ROC) analysis was carried out to determine the area under the curve (AUC), sensitivity and specificity. Statistical analysis was performed by using the SPSS statistical package version 16.0. Statistically significance was established at $P < .05$.

Results

General Conditions

There were 143 participants with early NSCLC, 151 participants with tuberculosis, and 150 healthy controls in this study. Characteristics of patient groups are shown in **TABLE 2** and **TABLE 3**. There were no statistical differences in gender, age, and comorbidities among the 3 groups ($P = .929$ and $P = .573$, respectively, **TABLE 2**). Nevertheless, early NSCLC patients showed higher smoking rate (current: 43.62%, former: 36.91%, never: 19.46%) and tobacco exposure (42.65 ± 16.94 years) than healthy controls (current: 30%, former: 26.67%, never: 43.33%, $P < .001$; 30.23 ± 9.12 years, $P < .001$) and tuberculosis patients (current: 31.13%, former: 39.07%, never: 29.8%, $P = .039$; 36.78 ± 12.97 years, $P < .001$, **TABLE 2**)

The cfDNA and SUV-Max[a] Were Increased in Early NSCLC Patients

Serum levels of cfDNA [19.78(11.52, 28.36) ng/μL] and SUV-Max[a] [3.99 (2.33, 5.71)] were significantly higher in patients with early NSCLC than those in healthy controls (9.75 [5.27, 13.65] ng/μL, $P < .001$, **FIGURE 1B**; 1.93 [1.05, 2.59], $P < .001$, **FIGURE 1C**, respectively) and those in patients with tuberculosis 914.58 [9.149, 18.74] ng/μL, $P < .001$, **FIGURE 1B**; 2.41 [1.50, 3.12], $P < .001$, **FIGURE 1C**, respectively).

TABLE 3. Stage and Grade of Early NSCLC

	Early NSCLC n (%)
Stage	149 (100)
0	3 (2)
IA	43 (28.8)
IB	32 (21.4)
II A	41 (27.5)
II B	30 (20.1)
Grade	149 (100)
Well differentiated	13 (2)
Moderately differentiated	55 (36.9)
Poorly differentiated	63 (42.3)
Undifferentiated	20 (13.4)

cfDNA Levels Were Associated with SUV-Max[a] in Early NSCLC Patients

In healthy controls and subjects with tuberculosis, no statistical association was found between SUV-Max[a] and age ($P = .319$ and $P = .102$, respectively); in contrast, statistical association was found in early NSCLC patients ($P = .029$, **TABLE 1**). In addition, adenocarcinoma of early NSCLC subjects showed higher cfDNA and SUV-Max[a] than those with squamous carcinoma 920.93 [16.89, 36.23] ng/μL vs 17.37 [8.82, 22.81] ng/μL, $P < .001$; 4.36 [3.47, 8.05] vs 3.01 [1.57, 4.22], $P < .001$, respectively). Similarly, cfDNA and SUV-Max[a] had a significant negative correlation in healthy controls ($r = 0.163$, $P = .045$, **FIGURE 1D**). These 2 values had a significant positive correlation in patients with tuberculosis ($r = 0.226$, $P = .005$, **FIGURE 1E**). However, patients with early NSCLC exhibited a strongly significant positive correlation ($r = 0.841$, $P < .001$, **FIGURE 1F**).

Combining cfDNA and SUV-Max[a] to Distinguish Early NSCLC from Healthy Controls

The ROC curve analysis showed that the combination of cfDNA and SUV-Max[a] (AUC = 0.982, $P < .001$, cut-off values = 0.22, sensitivity = 94.5%, specificity = 92.7%) displayed higher efficacy to distinguish early NSCLC

FIGURE 1. The combination of circulating cell-free DNA (cfDNA) and metabolic tumor burden displayed better ability to distinguish early non–small cell lung cancer (NSCLC) patients from tuberculosis. A, The metabolic tumor burden was described with the SUV-Max[a] of the primary tumor, measured by positron emission tomography-computed tomography (PET/CT). Early NSCLC and tuberculosis (arrows) were diagnosed by pathology through PET/CT-guided biopsy or CT-guided biopsy. B, Serum cfDNA levels in healthy controls, subjects with tuberculosis, and subjects with early NSCLC. C, The metabolic tumor burden (maximum standardized uptake value [SUV-Max[a]]) in healthy controls, subjects with tuberculosis, and early NSCLC subjects. D, The correlation of cfDNA and SUV-Max[a] in healthy controls (r = 0.163; P = .045). E, The correlation of cfDNA and SUV-Max[a] in tuberculosis subjects (r = 0.226; P = .005). F, The correlation of cfDNA and SUV-Max[a] in subjects with early NSCLC (r = 0.841; P = .001). G, Receiver operating characteristic (ROC) curve analysis to distinguish early NSCLC from healthy controls by serum cfDNA levels, SUV-Max[a], or the combination of cfDNA and SUV-Max[a]. H, ROC curve analysis to distinguish early NSCLC from tuberculosis by serum cfDNA levels, SUV-Max[a], or the combination of cfDNA and SUV-Max[a]. Values represent means (quartile) (M [P25, P75]). AUC, area under the curve.

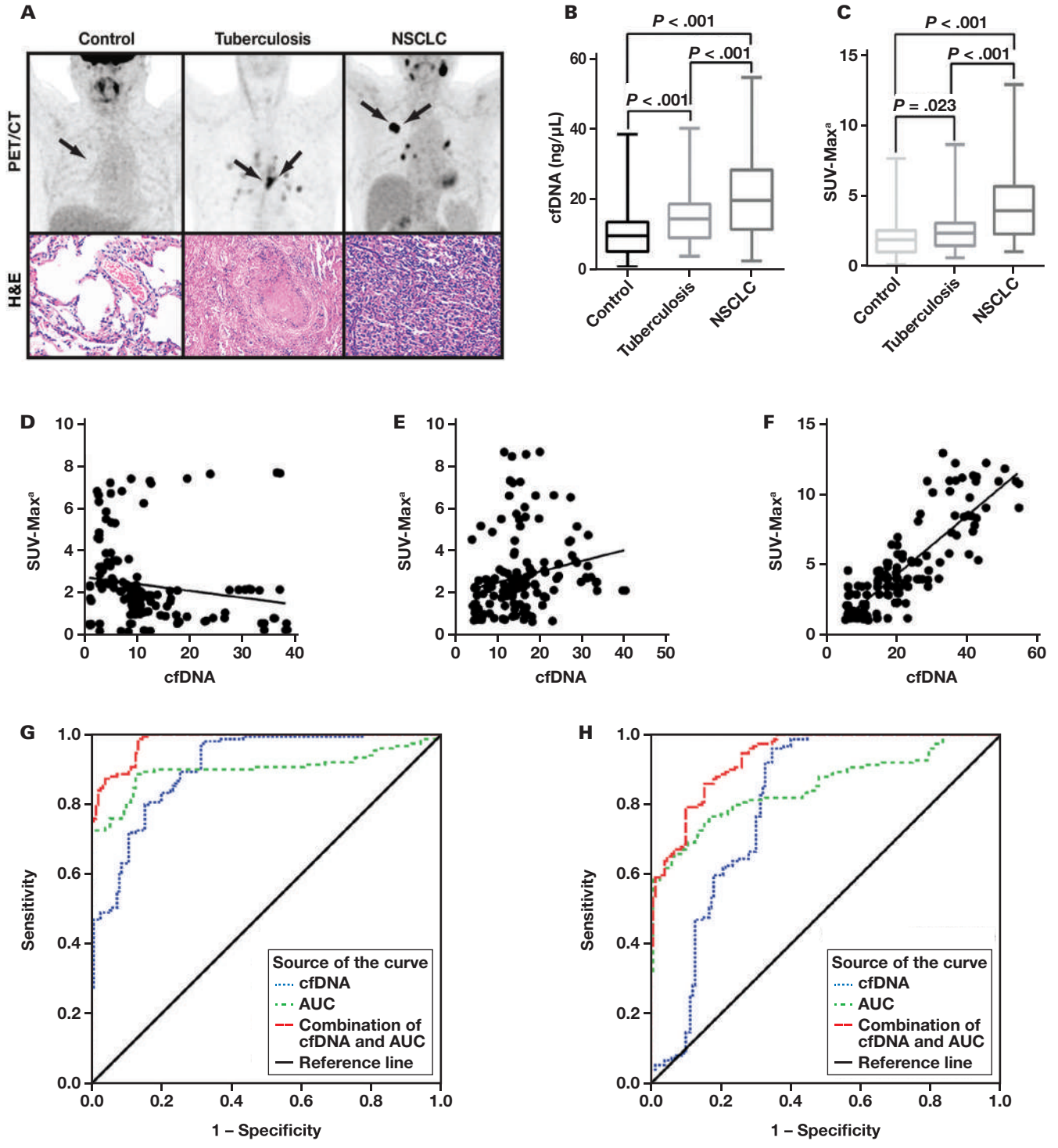

TABLE 4. Combining cfDNA and SUV Max[a] to Distinguish Early NSCLC from Healthy Controls

	AUC [ROC]	Cut-off Value	Sensitivity (%)	Specificity (%)	95% CI	*P*
cfDNA	0.907	20.25	98.0	67.3	0.875–0.939	<.001
SUV Max[a]	0.901	7.67	80.6	94.3	0.860–0.941	<.001
Combination of cfDNA and AUC-Max[a]	0.982	0.22	94.5	92.7	0.971–0.992	<.001

AUC, area under the curve; cfDNA, cell-free DNA; NSCLC, non–small cell lung cancer; SUV Max[a], maximum standardized uptake value.

TABLE 5. Combining cfDNA and SUV Max[a] to Distinguish Early NSCLC from Tuberculosis

	AUC [ROC]	Cut-off Value	Sensitivity (%)	Specificity (%)	95% CI	*P*
cfDNA	0.804	16.83	96	65.3	0.751-0.857	<.001
SUV-Max[a]	0.851	3.51	67.1	93.7	0.807-0.896	<.001
Combination of cfDNA and AUC-Max[a]	0.935	0.46	91.9	90.1	0.910-0.960	<.001

AUC, area under the curve; cfDNA,cell-free DNA; NSCLC, non-small cell lung cancer; SUV-Max[a], the maximum standardized uptake value.

from healthy controls than each measure alone (AUC = 0. 907, $P < .001$, cut-off values = 20.25, sensitivity = 98.0%, specificity = 67.3% and AUC = 0.901, $P < .001$, cut-off values = 7.67, sensitivity = 80.6%, specificity = 94.3%, respectively, **FIGURE 1G**, **TABLE 4**).

Combining cfDNA and SUV-Max[a] to Distinguish Early NSCLC from Tuberculosis

The ROC curve analysis showed that the combination of cfDNA and SUV-Max[a] (AUC = 0.935, $P < .001$, cut-off values = 0.46, sensitivity = 91.9%, specificity = 90.1%) also displayed better ability to distinguish early NSCLC from tuberculosis than each measure alone (AUC = 0.804, $P < .001$, cut-off values = 16.83, sensitivity = 96%, specificity = 65.3% and AUC = 0.851, $P < .001$, cut-off values = 3.51, sensitivity = 67.1%, specificity = 93.7%; respectively, **FIGURE 1H**, **TABLE 5**).

The cfDNA Was Associated with [3H]-2-Deoxy-DG Uptake in NSCLC Mouse Model

To investigate the specific mechanism of the relationship between cfDNA and SUV-Max[a], 2 NSCLC mouse models (A549 and NCI-H460) and the tuberculosis mouse model were used. Metabolic tumor burden was measured by the value of SUV-Max[a] in PET/CT, which depended on the rate of contrast agent (18F-FDG) uptake by the tumor.[16,17] Therefore, the rate of [3H]-2-deoxy-DG uptake was measured to show the metabolic tumor burden in lung tumors in the NSCLC mouse model. We found that the A549 NSCLC group and NCI–H460 NSCLC group both had a higher rate of [3H]-2-deoxy-DG uptake than those in the control group and in the tuberculosis group (**FIGURE 2B**), similar to humans. Moreover, the NSCLC group also showed higher cfDNA levels than those in the control group and tuberculosis group (**FIGURE 2A**). Similarly, there is also no correlation of cfDNA and the rate of [3H]-2-deoxy-DG uptake in the control group (**FIGURE 2C**) and the tuberculosis group (**FIGURE 2D**). However, the NSCLC group showed obvious association of cfDNA level and [3H]-2-deoxy-DG uptake (**FIGURE 2E**, **FIGURE 2F**).

GLU1/FasL/Caspase 8/Caspase 3 Were Upregulated in Lung Tumor Tissue of NSCLC Mouse Model

To further study the specific mechanism of glucose uptake of lung tumor interacting with serum cfDNA, RNA microarray analysis was performed. GLU1, FasL, caspase 8, and caspase 3 genes were significantly upregulated in lung tumors of the A549/NCI–H460 NSCLC group compared with those in the tuberculosis group (**FIGURE 2G**). Also, Western blotting also showed that GLU1, FasL, cleaved-caspase 8, and cleaved-caspase 3 were significantly increased, whereas pro-caspase 8 and pro-caspase 3 were decreased in the A549/NCI–H460 NSCLC group compared with those in the tuberculosis group (**FIGURE 2H-2I**).

GLU1 Promoted the [3H]-2-Deoxy-DG Uptake in NSCLC Mouse Model

To investigate whether [3H]-2-deoxy-DG uptake relies on GLU1, the GLU 1 inhibitor (WZB117) was used. The increased [3H]-2-deoxy-DG uptake was reversed by WZB117, indicating that the upregulated GLU1 promoted the [3H]-2-deoxy-DG uptake in A549/NCI–H460 NSCLC (**FIGURE 3C**, **FIGURE 3G**).

GLU1 Increased cfDNA Levels by FasL/Caspase 8/Caspase 3 Pathway In Vivo

To explore whether the apoptosis-induced cfDNA was mediated through GLU1/FasL/caspase 8/caspase 3 pathways, GLU 1 inhibitor (WZB117), anti–FasL antibody, and caspase 8 and caspase 3 inhibitor (Z-IETD-FMK) were used in vivo. We found that GLU1 increased the expression of cleaved-caspase 3 through increasing FasL and cleaved-caspase 8 expression in lung tumors of A549/NCI–H460 NSCLC mice (**FIGURE 3A**, **3D**, **3E**, **3H**), indicating that the GLU1/FasL/caspase 8/caspase 3 pathway was activated in NSCLC to promote apoptosis. Moreover, the increased serum cfDNA was reversed by WZB117, anti–FasL antibody, and Z-IETD-FMK (**FIGURE 3B**, **3F**), indicating that GLU1 increased cfDNA levels by FasL/caspase 8/caspase 3 pathways in vivo.

GLU1 Promoted Apoptosis by FasL/Caspase 8/Caspase 3 Pathway In Vitro

In vitro experiments also demonstrated similar results in A549 and NCI–H460 cell lines. Knocking down *GLU1* and *FasL* genes by siRNA and inhibited caspase 8/caspase 3 activities could significantly reduce apoptosis, indicating that GLU1 promotes apoptosis by the FasL/caspase 8/caspase 3 pathway in vitro (**FIGURE 4A-4F**).

Discussion

This study found that the serum levels of cfDNA and metabolic tumor burden (SUV-Max[a] and [3H]-2-deoxy-DG uptake) in human subjects and a mouse model of NSCLC were significantly higher than those in healthy controls and subjects with tuberculosis. In addition, the

FIGURE 2. Serum circulating cell-free DNA (cfDNA) level was correlated with [3H]-2-deoxy-DG uptake and GLU1/FasL/caspase 8/caspase 3 were upregulated in non–small cell lung cancer (NSCLC) mouse model. A, Serum cfDNA levels in control mouse model, tuberculosis mouse model, and NSCLC mouse model. B, The metabolic tumor burden ([3H]-2-deoxy-DG uptake). C, The correlation of cfDNA and [3H]-2-deoxy-DG uptake in controls ($r = 0.055$; $P = .893$). D, The correlation of cfDNA and [3H]-2-deoxy-DG uptake in tuberculosis mouse model ($r = 0.459$; $P = .251$). E, The correlation of cfDNA and [3H]-2-deoxy-DG uptake in A549 NSCLC mouse model ($r = 0.896$; $P = .003$). F, The correlation of cfDNA and [3H]-2-deoxy-DG uptake in NCI–H460 NSCLC mouse model ($r = 0.774$; $P = .023$). G, RNA microarray analysis was performed to investigate the differential gene between the NSCLC mouse model and the tuberculosis mouse model. H and J, GLUT1, FasL, pro-caspase 8, cleaved caspase 8, pro-caspase 3, and cleaved caspase 3 expression was evaluated using Western blotting in the tuberculosis mouse model and A549 NSCLC mouse model. I and K, GLUT1, FasL, pro-caspase 8, cleaved caspase 8, pro-caspase 3, and cleaved caspase 3 expression were evaluated using Western blotting in a tuberculosis mouse model and NCI–H460 NSCLC mouse model. Values represent mean ± SD, n = 8 per group.

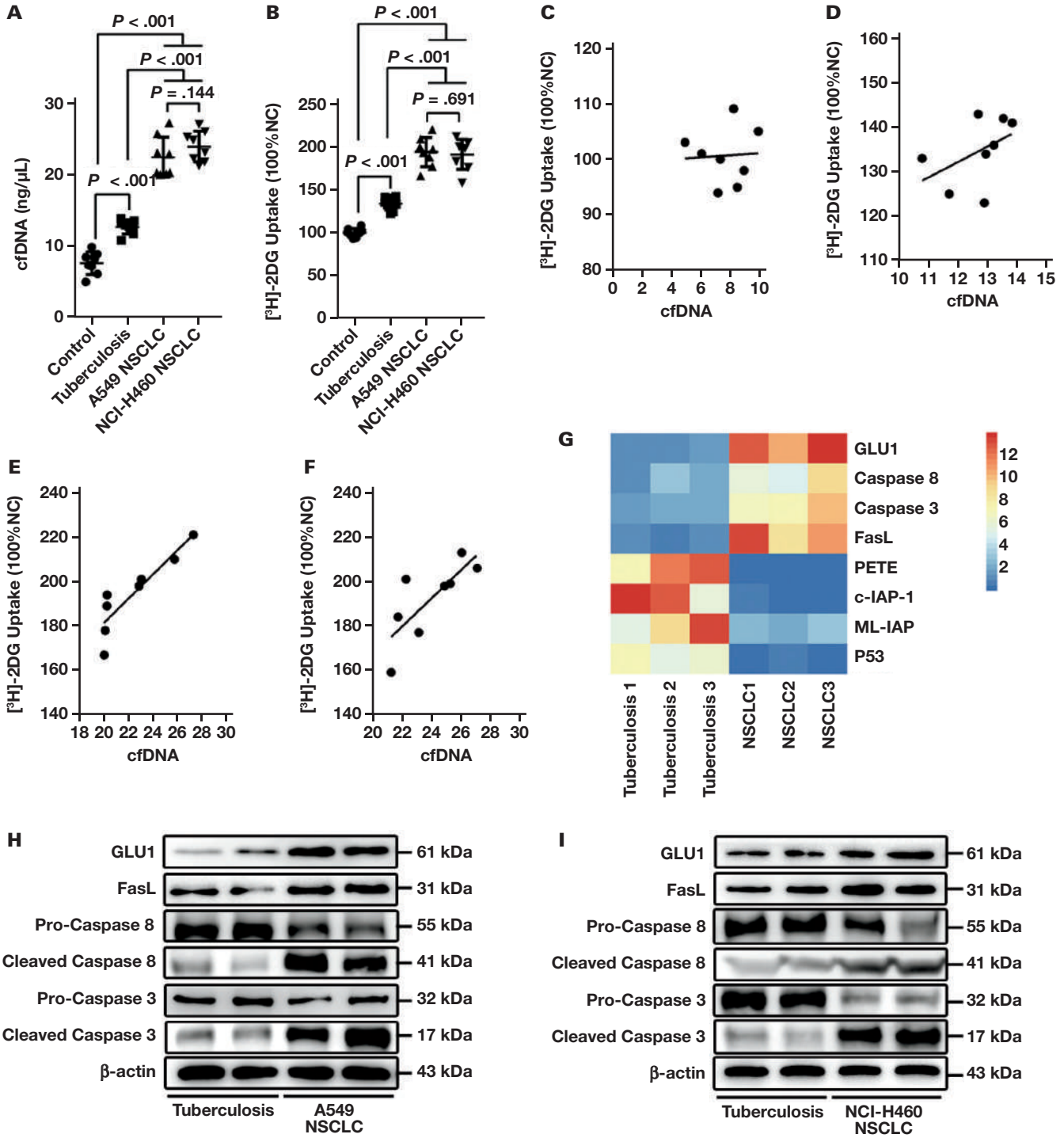

FIGURE 2. (CONT)

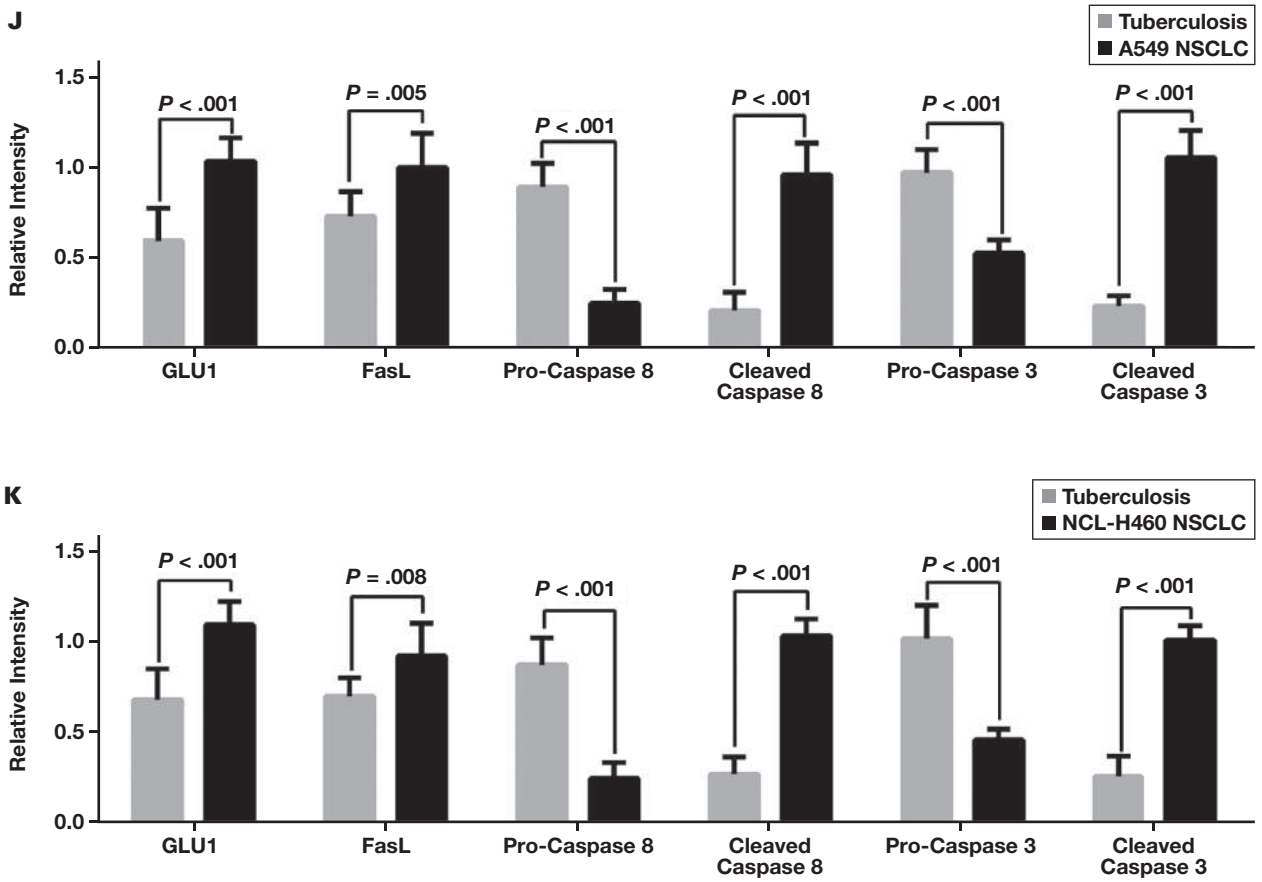

cfDNA levels were positively associated with metabolic tumor burden in NSCLC patients and the mouse model. Moreover, the combination of cfDNA and metabolic tumor burden displayed better ability to distinguish early NSCLC patients from tuberculosis patients than use of one alone. Mechanistically, upregulated GLU1 in tumor tissue promoted apoptosis-induced cfDNA elevation through FasL/caspase 8/caspase 3 pathways. Meanwhile, upregulated GLU1 also promoted the uptake of glucose of tumors to increase metabolic tumor burden in NSCLC.

Several reports have demonstrated higher levels of cfDNA in the serum of subjects with lung cancer compared with healthy controls, indicating it as a potential diagnostic biomarker.[13,30,31] In this study, both early NSCLC patients and the mouse model displayed higher levels of cfDNA than those in healthy controls, indicating that cfDNA could be used as a potential diagnostic biomarker for early NSCLC detection. In addition, our present research also demonstrated that the cfDNA levels increased in early NSCLC patients and the mouse model compared with those in subjects with tuberculosis and the mouse model, suggesting that cfDNA is a potential diagnostic biomarker to distinguish early NSCLC from tuberculosis, as shown in our previous report.[13] Unfortunately, the sensitivity and specificity of cfDNA to distinguish early NSCLC from tuberculosis were not satisfactory; therefore, it was necessary to seek a new approach to improve the efficiency of the differential diagnosis.

The 18F-FDG PET/CT was a valuable new imaging modality for diagnosis and differential diagnosis of NSCLC.[32,33] The PET/CT parameters (ie, SUV-Max[a]) could provide useful data on tumor metabolism. For instance, in the SUV-Max[a], the value of a single voxel with the highest radiotracer (18F-FDG) concentrations within the tumor was an indicator of the metabolic tumor burden.[16,17] This study found a significant correlation between the cfDNA and the metabolic tumor burden in subjects with tuberculosis vs an insignificant correlation in the tuberculosis mouse model. The possible rationale for this difference may result from the differences in severity and/or stage of tuberculosis in the subjects and/or the dosage of *Mycobacterium tuberculosis* used for making a tuberculosis model. This research also found that SUV-Max[a] was increased in early NSCLC patients compared with that in healthy controls and subjects with tuberculosis and could be used for the diagnosis and the differential diagnosis of early NSCLC, as shown in a previous report.[6] Of note, although SUV-Max[a] was useful and might be a surrogate marker of the metabolic tumor burden, it was affected by many factors and was highly sensitive to noise.[34,35] A previous study has demonstrated that SUV-Max[a] had low sensitivity for distinguishing early NSCLC from tuberculosis.[20] Our study also revealed this result, indicating that a combined approach to improve the differential diagnosis rate of early NSCLC from tuberculosis was required.

This study has several limitations. This study only used 2 A549 NSCLC and NCI–H460 NSCLC mouse models, whereas other available NSCLC mouse models may exhibit a different rate of [3H]-2-deoxy-DG uptake in comparison to the tuberculosis mouse model and control mouse model. Also, the sample size is small and would benefit by being larger.

FIGURE 3. GLU1 increased circulating cell-free DNA (cfDNA) levels by FasL/caspase 8/caspase 3 pathway and promoted the [3H]-2-deoxy-DG uptake in vivo. Glu 1 Inhibitor (WZB117), anti–FasL antibody, caspase 3 and caspase 8 common inhibitor (Z-IETD-FMK) were injected into A549 non–small cell lung cancer (NSCLC) mouse model (A and D) or NCI–H460 NSCLC mouse model (E and H) via the caudal vein 1 time 3 days before tissue collection to elucidate the specific signal pathway. GLUT1, FasL, pro-caspase 8, cleaved caspase 8, pro-caspase 3, and cleaved caspase 3 expression was evaluated using Western blotting. Increased serum cfDNA levels were reversed by anti–FasL antibody and Z-IETD-FMK in A549 NSCLC mouse model (B) or NCI–H460 NSCLC mouse model (F). The increased [3H]-2-deoxy-DG uptake was reversed by WZB117 in A549 NSCLC mouse model (C) or NCI–H460 NSCLC mouse model (G). Values represent mean ± SD, n = 8 per group.

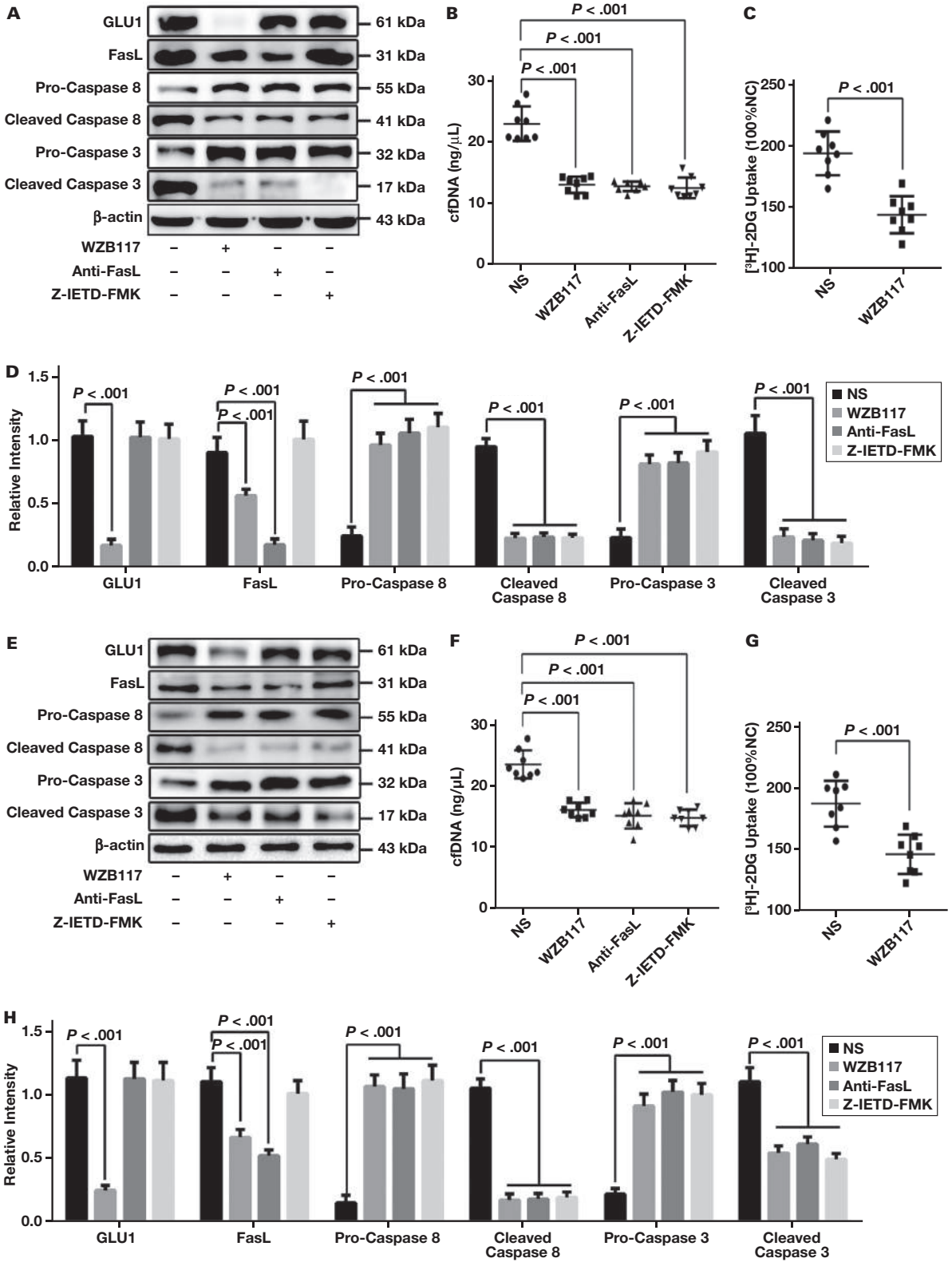

FIGURE 4. GLU1 promoted apoptosis by FasL/caspase 8/caspase 3 pathway in vitro. The GLU1 or FasL genes were knocked down by siRNA and the activation of caspase 3 and caspase 8 was blocked by Z-IETD-FMK. GLUT1, FasL, pro-caspase 8, cleaved caspase 8, pro-caspase 3, and cleaved caspase 3 expression was evaluated by Western blotting in A549 cells (A and C) and NCI–H460 cells (D and F). Apoptosis percent of A549 cell (B) and NCI–H460 cell (E) at the 24th hour. Values represent mean ± SD, n = 6 per group.

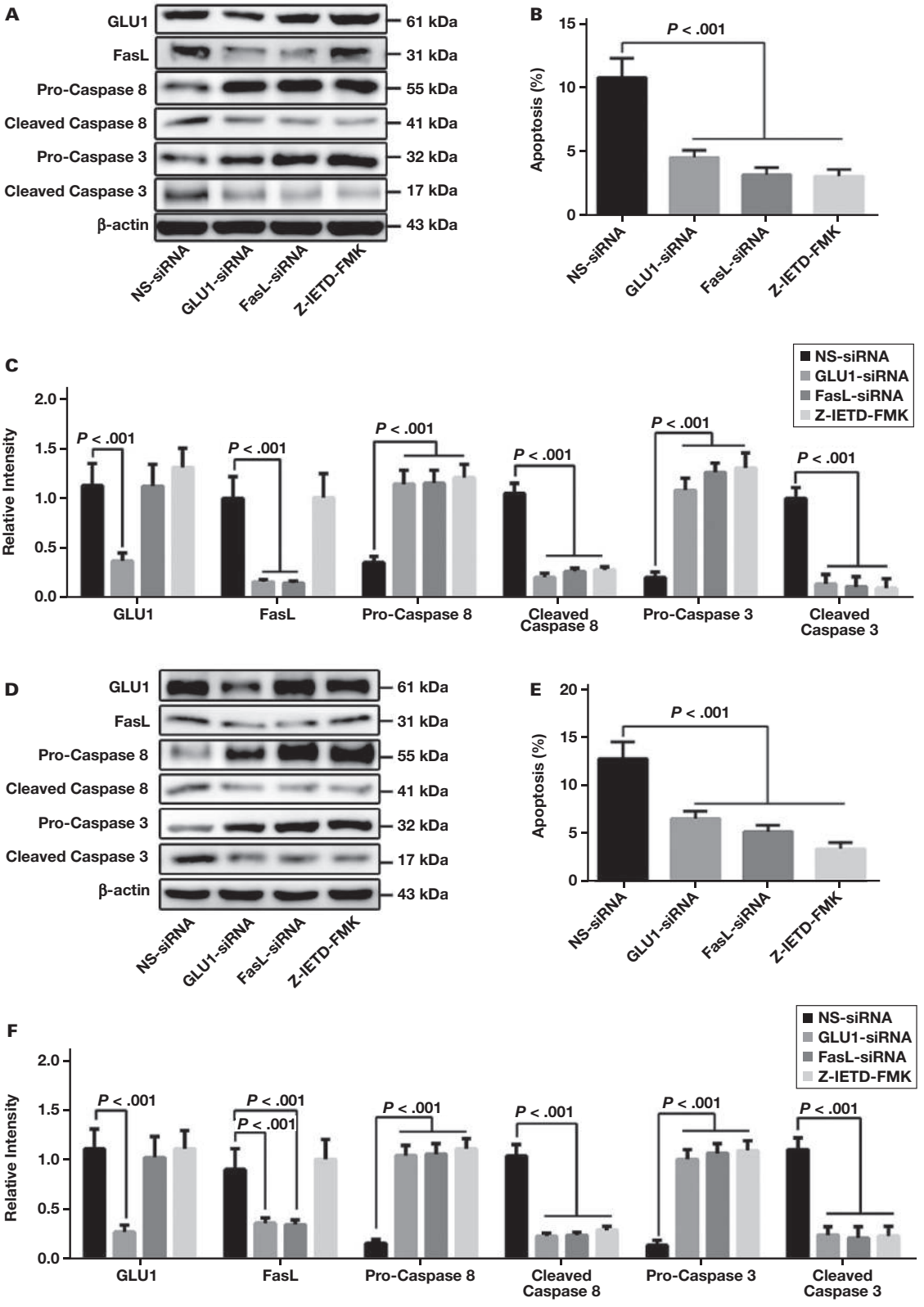

Recently, a larger prospective, interventional study demonstrated that the combination of blood testing with PET/CT could be used to screen for lung cancer.[22] Therefore, the combination of cfDNA and metabolic tumor burden was performed to distinguish early NSCLC from tuberculosis. Intriguingly, ROC curve analysis showed that the combination of cfDNA and SUV-Max[a] displayed better ability to distinguish early NSCLC from tuberculosis than use of either alone. Furthermore, patients with early NSCLC, rather than healthy controls or patients with tuberculosis, showed an obvious positive correlation of cfDNA and SUV-Max[a]. This association also was shown in the NSCLC mouse model, rather than the control or the tuberculosis mouse models, indicating that there may be a connection, to a certain degree, between the metabolism of cfDNA and tumor burden.

Tumor cells adapt to hypoxic conditions by controlling the expression of many endogenous glycolysis-related transporters and enzymes, such as GLU1, which play a pivotal role in the mechanisms of cellular metabolism.[36,37] Although several studies have reported a correlation between GLU1 expression and SUV-Max[a] in NSCLC subjects,[17,38] none have verified this relationship in an animal model. This research found that the expression of GLU1 mRNA and protein was also increased markedly in 2 NSCLC mouse models, similar to NSCLC patients; moreover, the increased glucose uptake in tumor cells was reversed by a GLU1-specific inhibitor, indicating that upregulated GLU1 increased metabolic tumor burden (SUV-Max[a]) by promoting glucose uptake in NSCLC.

Deregulation in apoptotic cell death machinery is a hallmark of cancer, and apoptosis alteration was responsible for the tumor burden, development, and progression.[9,10] Circulating cfDNAs were mainly derived from tumor DNA fragments by apoptotic tumor cells, whereas apoptosis was stimulated by the activation of caspases 8 and caspases 3.[7,8] Our study found that upregulated GLU1 increased the expression of cleaved-caspase 8 and cleaved-caspase 3 through upregulating FasL to promote apoptosis in vivo and in vitro. Moreover, increased serum cfDNA levels were reversed by GLU1-specific inhibitor, anti–FasL antibody, and caspase 8 and caspase 3 common inhibitor, indicating that the increased serum cfDNA depended on the GLU1/ FasL/caspase 8/caspase 3 pathway in NSCLC.

In conclusion, this study demonstrated that serum levels of cfDNA and metabolic tumor burden in human subjects and mouse models of NSCLC were significantly increased above those in healthy controls and subjects with tuberculosis. Moreover, serum cfDNA levels were correlated with metabolic tumor burden in early NSCLC. In addition, the combination of cfDNA and metabolic tumor burden displayed better ability to distinguish early NSCLC in subjects from those with tuberculosis than either alone. Mechanistically, upregulated GLU1 increased the serum levels of cfDNA by FasL/caspase 8/caspase 3 pathways and promoted the uptake of glucose to increase the metabolic tumor burden in NSCLC.

Acknowledgment

We acknowledge the contributions of study participants. The manuscript has been stored on a preprint server (Research Square) as a preprint (https://www.researchsquare.com/article/rs-54830/v2; doi is 10.21203/rs.3.rs-54830/v2). This article contains several revisions from the preprint.

Funding

This study was supported by grants from the Natural Science Research Project of Anhui Colleges and Universities (KJ2016A737), scientific research projects for middle-aged and young scientists of Wannan Medical College (WK2020F34).

REFERENCES

1. Siegel RL, Miller KD. Cancer statistics. *CA Cancer J Clin.* 2020. 2020;70(1):7–30.
2. Reck M, Rabe KF. Precision diagnosis and treatment for advanced non-small-cell lung cancer. *N Engl J Med.* 2017;377(9):849–861. doi:10.1056/NEJMra1703413.
3. Lai RS, Lee SS, Ting YM, et al. Diagnostic value of transbronchial lung biopsy under fluoroscopic guidance in solitary pulmonary nodule in an endemic area of tuberculosis. *Respir Med.* 1996;90(3):139–143.
4. Schrager LK, Vekemens J, Drager N, Lewinsohn DM, Olesen, OF. The status of tuberculosis vaccine development. *Lancet Infect Dis.* 2020;20(3):e28–e37. doi:10.1016/S1473-3099(19)30625-5.
5. Shim SS, Lee KS, Kim BT, et al. Non-small cell lung cancer: prospective comparison of integrated FDG PET/CT and CT alone for preoperative staging. *Radiology.* 2005;236(3):1011–1019. doi:10.1148/radiol.2363041310.
6. Kang F, Wang S, Tian F, et al. Comparing the diagnostic potential of 68Ga-alfatide II and 18F-FDG in differentiating between non-small cell lung cancer and tuberculosis. *J Nucl Med.* 2016;57(5):672–677.
7. Chabon JJ, Hamilton EG. Integrating genomic features for non-invasive early lung cancer detection. *Nature*. 2020;580(7802):245–251.
8. De Mattos-Arruda L, Mayor R, Ng CKY, et al. Cerebrospinal fluid-derived circulating tumour DNA better represents the genomic alterations of brain tumours than plasma. *Nat Commun.* 2015;6:8839. doi:10.1038/ncomms9839.
9. Bock FJ, Tait SWG. Mitochondria as multifaceted regulators of cell death. *Nat Rev Mol Cell Biol*. 2020;21(2):85–100.
10. Singh R, Letai A, Sarosiek, K. Regulation of apoptosis in health and disease: the balancing act of BCL-2 family proteins. *Nat Rev Mol Cell Biol.* 2019;20(3):175–193. doi:10.1038/s41580-018-0089-8.
11. Esposito A, Criscitiello C, Trapani D, Curigliano, G. The emerging role of "liquid biopsies," circulating tumor cells, and circulating cell-free tumor DNA in lung cancer diagnosis and identification of resistance mutations. *Curr Oncol Rep.* 2017;19(1):1. doi:10.1007/s11912-017-0564-y.
12. Heitzer E, Auinger L, Speicher MR. Cell-free DNA and apoptosis: how dead cells inform about the living. *Trends Mol Med.* 2020;26(5):519–528.
13. Leng S, Zheng J, Jin Y, et al. Plasma cell-free DNA level and its integrity as biomarkers to distinguish non-small cell lung cancer from tuberculosis. *Clin Chim Acta;* 2018;477:160–165. doi:10.1016/j.cca.2017.11.003.
14. Creff G, Devillers A, Depeursinge A, et al. Evaluation of the prognostic value of FDG PET/CT parameters for patients with surgically treated head and neck cancer: a systematic review. *JAMA Otolaryngol Head Neck Surg.* 2020;146(5):471–479.
15. De Leyn P, Dooms C, Kuzdzal J, et al. Revised ESTS guidelines for preoperative mediastinal lymph node staging for non-small-cell lung cancer. *Eur J Cardiothorac Surg.* 2014;45(5):787–798.
16. Na F, Wang J, Li C, et al. Primary tumor standardized uptake value measured on F18-Fluorodeoxyglucose positron emission tomography is of prediction value for survival and local control in non-small-cell lung cancer receiving radiotherapy: meta-analysis. *J Thorac Oncol.* 2014;9(6):834–842.
17. Koh YW, Lee SJ, Park SY. Differential expression and prognostic significance of GLUT1 according to histologic type of non-small-cell lung cancer and its association with volume-dependent parameters. *Lung Cancer.* 2017;104:31–37.
18. Vella M, Meyer CS, Zhang N, et al. Association of receipt of positron emission tomography-computed tomography with non-small cell lung cancer mortality in the Veterans Affairs Health Care System.

JAMA Netw Open. 2019;2(11):e1915828. doi:10.1001/jamanetworkopen.2019.15828.

19. Pacilio M, Lauri C, Prosperi D, Petitti A, Signore, A. New SPECT and PET radiopharmaceuticals for imaging inflammatory diseases: a meta-analysis of the last 10 years. *Semin Nucl Med.* 2018;48(3):261–276. doi:10.1053/j.semnuclmed.2017.12.004.
20. Werutsky G, Hochhegger B, Lopes de Figueiredo Pinto JA, et al. PET/CT has low specificity for mediastinal staging of non-small-cell lung cancer in an endemic area for tuberculosis: a diagnostic test study (LACOG 0114). *BMC Cancer.* 2019;19(1):5. doi:10.1186/s12885-018-5233-5.
21. Werutsky G, Hochhegger B, Lopes de Figueiredo Pinto JS, et al. PET/CT has low specificity for mediastinal staging of non-small-cell lung cancer in an endemic area for tuberculosis: a diagnostic test study (LACOG 0114). *BMC Cancer.* 2019;19(1):5.
22. Lennon AM, Buchanan AH, Kinde I, et al. Feasibility of blood testing combined with PET/CT to screen for cancer and guide intervention. *Science.* 2020;369(6499), undefined. doi:10.1126/science.abb9601.
23. Zumla A, George A, Sharma V, Herbert RH, Oxley A, Oliver M. The WHO 2014 global tuberculosis report--further to go. *Lancet Glob Health.* 2015;3(1):e10–e12. doi:10.1016/S2214-109X(14)70361-4.
24. Travis WD, Brambilla E, Nicholson AG, et al. The 2015 World Health Organization classification of lung tumors: impact of genetic, clinical and radiologic advances since the 2004 classification. *J Thorac Oncol.* 2015;10(9):1243–1260.
25. Zhang X, Liu Y, Peng X, et al. Influence of the vaccinating density of A549 cells on tumorigenesis and distant organ metastasis in a lung cancer mice model. *Cell Mol Biol (Noisy-le-Grand).* 2018;64(6):53–57.
26. Vilcheze C, Kim J, Jacobs WR Jr. Vitamin C potentiates the killing of mycobacterium tuberculosis by the first-line tuberculosis drugs isoniazid and rifampin in mice. *Antimicrob Agents Chemother.* 2018;62(3):e02165-17. doi:10.1128/AAC.02165-17.
27. Yi Y, Kim HJ, Zheng M, et al. Glucose-linked sub-50-nm unimer polyion complex-assembled gold nanoparticles for targeted siRNA delivery to glucose transporter 1-overexpressing breast cancer stem-like cells. *J Control Release.* 2019;295:268–277.
28. Zhang C, Gao F, Teng F, Zhang M. Fas/FasL complex promotes proliferation and migration of brain endothelial cells via FADD-FLIP-TRAF-NF-κB pathway. *Cell Biochem Biophys.* 2015;71(3):1319–1323.
29. Alekseeva LA, Sen'kova AV, Zenkova MA, Mironova NL. Targeting circulating SINEs and LINEs with DNase I provides metastases inhibition in experimental tumor models. *Mol Ther Nucleic Acids.* 2020;20:50–61.
30. Zheng H, Wu X, Yin J, et al. Clinical applications of liquid biopsies for early lung cancer detection. *Am J Cancer Res.* 2019;9(12):2567–2579.
31. Koldby KM, Mortensen MB, Detlefsen S, et al. Tumor-specific genetic aberrations in cell-free DNA of gastroesophageal cancer patients. *J Gastroenterol.* 2019;54(2):108–121.
32. Kirienko M, Padovano B, Serafini G, et al. CT, [F]FDG-PET/CT and clinical findings before and during early Covid-19 onset in a patient affected by vascular tumour. *Eur J Nucl Med Mol Imaging.* 2020;47(7):1769–1770.
33. Vansteenkiste J, Fischer BM, Dooms C, et al. Positron-emission tomography in prognostic and therapeutic assessment of lung cancer: systematic review. *Lancet Oncol.* 2004;5(9):531–540.
34. Park SY, Cho A, Yu WS, et al. Prognostic value of total lesion glycolysis by 18F-FDG PET/CT in surgically resected stage IA non-small cell lung cancer. *J Nucl Med.* 2015;56(1):45–49.
35. Hyun SH, Ahn HK, Kim H, et al. Volume-based assessment by (18) F-FDG PET/CT predicts survival in patients with stage III non-small-cell lung cancer. *Eur J Nucl Med Mol Imaging.* 2014;41(1):50–58. doi:10.1007/s00259-013-2530-8.
36. Wang J, Yu J, Zhang Y, et al. Glucose transporter inhibitor-conjugated insulin mitigates hypoglycemia. *Proc Natl Acad Sci USA.* 2019;116(22):10744–10748. doi:10.1073/pnas.1901967116.
37. Rosell R, Bivona TG, Karachaliou, N. Genetics and biomarkers in personalisation of lung cancer treatment. *Lancet.* 2013;382(9893):720–731. doi:10.1016/S0140-6736(13)61715-8.
38. Kaira K, Serizawa M, Koh Y, et al. Biological significance of 18F-FDG uptake on PET in patients with non-small-cell lung cancer. *Lung Cancer.* 2014;83(2):197–204. doi:10.1016/j.lungcan.2013.11.025.

Analysis of the Relationship between Bladder Cancer Gene Mutation and Clinical Prognosis by High-Throughput Sequencing

Xiaohang Li, MS,[1] Jie Liu, MS,[1] An'an Li, MS,[1] Xin Liu, MS,[1] Yuesong Miao, MS,[1] and Zhiyong Wang, MS[1,]*

[1]Department of Urology, Affiliated Hospital of Chengde Medical University, Chengde, China. *To whom correspondence should be addressed: prof_wangzy@163.com.

Keywords: bladder cancer, gene, high-throughput sequencing, mutation

Abbreviations: OS, overall survival; NMIBC, non-muscle invasive bladder cancer; MIBC, muscle invasive bladder cancer; SNV, single nucleotide variant; InDel, insertion deletion; CNV, copy number variation; PFS, progression-free survival; BCG, bacillus Calmette-Guérin.

Laboratory Medicine 2023;54:142–152; https://doi.org/10.1093/labmed/lmac083

ABSTRACT

Objective: Bladder cancer is one of the most common malignant tumors in urology in China. The analysis of gene mutation in bladder cancer and its relationship with clinical characteristics and prognosis will provide a basis for accurate treatment of bladder cancer. The aim of this study was to analyze the mutations and functional regions of bladder cancer–related genes based on high-throughput sequencing, and to explore the relationship between mutations and clinicopathological features, as well as its prognosis and clinical implication.

Methods: From April 2020 to October 2020, a total of 47 patients with bladder cancer in the Department of Urology, Affiliated Hospital of Chengde Medical College were studied. Gene sequencing was performed using Nextseq CN500 System, a high-throughput sequencing platform. The results of gene detection were described, and the relationship and clinical value of high frequency mutated genes with clinicopathological features and prognosis were systematically analyzed.

Results: A total of 29 mutation genes, 61 exons, and 95 mutation sites were identified in this study. The frequencies of *TP53*, *FGFR3*, *PIK3CA*, *ERBB2*, *MUC4*, and *KRAS* mutation are relatively high, accounting for 59.92 % of the total mutation frequency. The *TP53* was significantly associated with muscle invasive bladder cancer, T2 stage, and progression-free survival, while *FGFR3* was significantly associated with non-muscle invasive bladder cancer and T1 stage.

Conclusion: High-throughput sequencing technology provides a successful approach for detecting bladder cancer gene mutations. The *TP53*, *FGFR3*, *PIK3CA*, *ERBB2*, *MUC4*, and *KRAS* genes have high mutation frequencies in bladder cancer patients. The *TP53*, *FGFR3* and *PIK3CA* genes may play a predictive role in the prognosis of bladder cancer, which may hold certain guiding significance for in-depth study of the pathogenesis of bladder cancer and the development of targeted therapies.

Bladder cancer is one of the most common malignancies in urology in China.[1] According to Global Cancer Statistics data,[2–5] the incidence of bladder cancer worldwide was 7.2/100,000 in 2018 (11.0/100,000 men, 2.4/100,000 women) and 7.4/100,000 in 2020 (11.2/100,000 men, 1.7/100,000 women). In China, the incidence of bladder cancer in men was 8.8/100,000 in 2018 and 8.9/100,000 in 2020, with an increasing trend year by year. The incidence of bladder cancer in women is outside the top 10, and the incidence of bladder cancer in men is about 3 to 4 times higher than in women. With the improvement of clinical examination technology, early detection and treatment of bladder cancer can be achieved in the clinic. Along with improved surgical technology, surgical methods, and postoperative bladder perfusion chemotherapy, urine screening evaluation has an important role clinically in monitoring the recurrence of bladder cancer.[6] The 5-year overall survival (OS) rate of persons with non-muscle invasive bladder cancer (NMIBC) is about 90%.[7–9] Approximately 15% to 20% of NMIBC progressed to MIBC and carcinoma in situ and high-grade papillary tumors were more likely to progress to MIBC than low-grade papillary tumors.[10,11] The 5-year OS rate of MIBC patients is about 60% to 70%.[8,12] Despite radical cystectomy and pelvic lymph node dissection, about 50% of patients eventually developed renal, liver, intra-abdominal and retroperitoneal metastasis due to diffuse micrometastasis.[13,14] Moreover, postoperative intravesical treatment was ineffective for 30% to 50% of patients, or relapse occurred within 5 years after treatment.[15] Genetic heterogeneity may lead to differential responsiveness of individuals with bladder cancer to conventional treatment. Thus, it is of great clinical

significance to find effective biomarkers to develop molecularly targeted therapies for bladder cancer. High-throughput sequencing technology is one of the technologies to guide targeted therapy of bladder cancer. High-throughput sequencing technology can be used for synthesis and sequencing and detects multigene, multisite mutation, fusion genes, gene copy number variation, and other changes. In this study, we used high-throughput sequencing technology to detect gene mutations in 47 bladder cancer specimens, and further analyzed their relationship with clinical characteristics to provide new insights into therapeutic targeting in future bladder cancer treatment.

Materials and Methods

Recruitment of Research Participants

From April 2020 to October 2020, surgical pathology specimens of 32 males and 15 females with bladder cancer were collected in the Department of Urology, Affiliated Hospital of Chengde Medical College. The minimum age was 25 years and the maximum was 89 years, with an average age of 63 ± 11.85. Inclusion criteria included (1) age >18 years old with no gender requirement, (2) no other types of tumor, (3) postoperative pathological diagnosis of bladder cancer, and (4) voluntarily accepted gene sequencing and signed informed consent, which was finally approved by the ethics committee. Those who do not meet the above standards and individuals with cardiopulmonary insufficiency who could not tolerate surgery were excluded. This study met the requirements of the World Medical Association's Declaration of Helsinki. The approval number is CYFYLL2021097.

Bladder cancer includes urothelial carcinoma (transitional cell carcinoma), squamous cell carcinoma, and adenocarcinoma, followed by the less common small cell carcinoma, mixed carcinoma, carcinosarcoma, and metastatic carcinoma. Bladder urothelial carcinoma is the most common, accounting for more than 90% of bladder cancers. All 47 cases of bladder cancer in this study were diagnosed as urothelial carcinoma. In this article, "bladder cancer" refers specifically to urothelial carcinoma of the bladder. Through detailed medical history, 47 bladder cancer patients in this study denied a history of workplace exposure (aromatic amines, rubber, leather, textiles, paints, etc), exposure to toxic or radioactive substances, chronic bladder irritation and infection, personal history, genetic and family history of bladder or other urothelial cancers, etc. Specific clinical data are shown in **TABLE 1**.

TABLE 1. Clinical Data of 47 Subjects with Bladder Cancer

Clinicopathological Features	No. (%)
Sex	
M	32 (68.09)
F	15 (31.91)
Age, y	
>60	32 (68.09)
≤60	15 (31.91)
Smoker	
Y	28 (59.57)
N	19 (40.43)
Classification	
NMIBC	23 (48.94)
MIBC	24 (51.06)
T stage	
Ta	5 (10.64)
T1	18 (38.30)
T2a	2 (4.26)
T2b	20 (42.54)
T4	2 (4.26)
N stage	
NX	1 (2.13)
N0	45 (95.74)
N3	1 (2.13)
M stage	
M0	46 (97.87)
M1	1 (2.13)

MIBC, muscle invasive bladder cancer; NMIBC, non-muscle invasive bladder cancer.

Research Methods

After paraffin embedding, the pathological tissues of participants with bladder cancer were subjected to gene detection using the high-throughput sequencing platform Illumina Nextseq CN500 System. Pathological classification of bladder cancer was determined by a pathologist. The excess paraffin was removed using the dewaxing solution, and the genomic DNA was released using RNAase free water, uracil N-glycosylase buffer, and proteinase K. Genomic DNA was reversibly adsorbed by the silica gel membrane column. After removing protein, lipid, and polysaccharide impurities by protease digestion and washing with rinse solution, genomic DNA was obtained by elution of the purified liquid. The customized bladder cancer–related genes were captured and enriched by the probe capture method. The genomic DNA was fragmented by the Covaris ultrasonic interrupter and purified using a AMPure XP beads kit. The fragmentation effect was confirmed by an Agilent 2100 bioanalyzer, and the main peak was 150–200 base pairs. After terminal repair, connection, and purification, the library was prepared by polymerase chain reaction and hybridized with the "xGen Lockdown probe." DNA sequencing was performed using a NextseqTM CN500 System. Target region capture high-throughput sequencing was applied to all exons of 94 genes, and 4 mutation types of tumor genes, including point mutation (single nucleotide variant [SNV]), insertion deletion (InDel), fusion, and copy number variation (CNV), were detected.

Follow-up Survey

Time of surgery was considered as point zero of follow-up for all subjects. All patients received conventional chemotherapy after surgery. The combination of regular outpatient follow-up and telephone follow-up was adopted. Patients with bladder cancer were followed up once every 1 to 3 months within 1 year after operation, and once every 3 to 6 months from the second year. The follow-up content included B ultrasound, computed tomography, and cystoscopy. The end point of follow-up of all patients was February 28, 2022. Recurrence refers to when clinical, imaging, and cystoscopy indicated recurrence of bladder tumors, and distant metastasis refers to when clinical and imaging examination showed evidence of disease at a distant site. Histopathological diagnosis was the gold standard for subjects with suspected recurrence or metastasis. Progression-free survival (PFS) refers to the time from the first day after surgery to the first recurrence or metastasis, and OS refers to

the time from the first day after surgery to death or the last follow-up. The criteria for excluding subjects from follow-up included death from other diseases and missing interviews and other events. The time unit is in months.

Statistical Methods

SPSS 23.0 statistical software was used to analyze the relationship between mutant genes and clinical characteristics by χ^2 test or Fisher's precise probability method, and the count data were expressed as composition ratio and incidence rate. The OS and PFS were analyzed by Kaplan-Meier curve and log-rank test. Multivariate Cox proportional risk regression model was used to analyze univariate and multivariate factors affecting the prognosis of bladder cancer. $P < .05$ indicates that the difference was statistically significant.

Results

High-Throughput Sequencing Results of Gene Mutations in Study Subjects

In this study, all exons and more than 2000 gene loci of 94 genes in postoperative pathological specimens of 47 patients with bladder cancer were subjected to high-throughput sequencing. A total of 29 mutation genes, 61 exons, and 95 gene mutation sites were identified. In the 47 bladder cancer specimens, 31 had ≥2 gene mutations, 15 had a single gene mutation, and 1 had no gene mutation. Detected genetic alterations included 116 SNV cases, 7 InDel cases, 4 fusion cases, 2 CNV cases, and 4 complex cases. Among them, the mutation frequency of *TP53* gene was 23.31% (31/133), the mutation frequency of *FGFR3* gene was 17.29% (23/133), the mutation frequency of *PIK3CA* gene was 14.29% (19/133), the mutation frequencies of *ERBB2* and *MUC4* genes each was 5.26% (7/133), and the mutation frequency of *KRAS* gene was 4.51% (6/133). The mutation frequency of *TP53* gene in MIBC was 33.33% (27/81), *FGFR3* gene mutation frequency was 6.17% (5/81), and *PIK3CA* gene mutation frequency was 9.88% (8/81). The specific gene mutation analysis is shown in **FIGURE 1** and **TABLE 2**.

Mutations in *TP53, FGFR3, PIK3CA, ERBB2, MUC4* and *KRAS* Genes Detected by High-Throughput Sequencing

In *TP53*, a total of 7 exons were detected with gene mutations, of which 1 gene site of exon 2 had point mutation, with a mutation frequency of 1.16%. Four gene sites of exon 4 had point mutations, with a maximum mutation frequency of 56.47%. Six gene sites of exon 5 had point mutations, with a maximum mutation frequency of 85.65%. Five gene sites of exon 6 had point mutations, with a maximum mutation frequency of 64.09%. Four gene sites of exon 7 and exon 8 had point mutations, with a maximum mutation frequency of 16.36% and 35.03%, respectively. One gene site of exon 9 had a point mutation, with a mutation frequency of 46.13%. The variation sites are located at positions P72, Y163, N239, G245, E285, R280, and Q331 in the p53 protein.

A total of 3 exons of point mutations and insertion deletions, as well as the *FGFR3-TACC3* translocations, were detected in *FGFR3*. Two gene sites in exon 7 had point mutations, and the maximum mutation frequency was 84.05%. Three gene loci in exon 9 had point mutations and insertion deletions, and the maximum mutation frequency was 89.11%. One gene locus in exon 14 had point mutations, and the mutation frequency was 2.94%. A total of 4 fusion mutations of *FGFR3-TACC3* were detected, and the maximum mutation frequency was 47.22%. The variation sites are located at positions R248, S249, G370, Y373, and K403 in the FGFR3 protein.

A total of 9 exon mutations were detected by *PIK3CA*, all of which were point mutations. One gene mutation was detected in exons 2, 4, 8, 11, 15 and 21, and the mutation frequencies were 5.88%, 1.79%, 1.21%, 1.29%, 42.31% and 31.97%, respectively. The mutations are found at position N345, E542, E545, and H1047 in the *PIK3CA* protein. Four gene mutations were detected at exon 10, with the maximum mutation frequency of 53.40%. The mutations are found at position E542K, E545K, D549N, and Q546R. Two gene mutations were detected in exon 5 and exon 14, and the maximum mutation frequencies were 30.00% and 20.19%, respectively. The mutations are found at position N345K, N345Y, E707K, and E726K.

A total of 4 exon point mutations and 2 *ERBB2* gene CNVs were detected in *ERBB2*. Among them, exon 8, 19, and 20 were point mutations at 1 gene locus, and the mutation frequencies were 47.11%, 65.84%, and 43.91%, respectively. Two gene loci in exon 17 were point mutations, and the maximum mutation frequency was 69.24%. Four gene loci in exon 2 of *MUC4* gene were mutated, and the maximum mutation frequency was 8.86%.

A total of 2 exons were detected in *KRAS*. Point mutation and insertion deletion occurred in 3 gene loci of exon 2, with the maximum mutation frequency of 50.91%. Point mutation occurred in 1 gene locus of exon 4, with the mutation frequency of 38.52%. The mutation results are shown in **TABLE 3**.

Relationship between Clinical Features of Subjects and Mutation Frequency of *TP53, FGFR3, PIK3CA, ERBB2, MUC4,* and *KRAS* Detected by High-Throughput Sequencing

The mutation frequency of the *TP53* gene in MIBC was high, and the difference was statistically significant ($\chi^2 = 16.045$, $P = .000$). The mutation frequency of *FGFR3* in NMIBC was high, and the difference was statistically significant ($\chi^2 = 11.284$, $P = .001$). The *TP53* and *FGFR3* genes were associated with the clinical T stage: *TP53* mutation frequency in bladder cancer T2b stage was higher and the difference was statistically significant ($\chi^2 = 21.433$, $P = .000$). The *FGFR3* gene had a high mutation frequency in the T1 stage of bladder cancer and the difference was statistically significant ($\chi^2 = 12.566$, $P = .014$). The *TP53*, *FGFR3*, *PIK3CA*, *ERBB2*, *MUC4* and *KRAS* genes had no statistical difference in age, sex, and smoking history ($P > .05$), as shown in **TABLE 4**.

Recurrence and Metastasis

Recurrence and metastasis were found in 16 of the 47 study subjects, and 2 of the 16 died of recurrence and metastasis. Of these 16, 11 had muscle invasive bladder cancer and 5 had noninvasive bladder cancer. According to TNM staging, there were 1 TaN0M0, 4 T1N0M0, 2 T2aN0M0, 7 T2bN0M0, 1 T4N0M0, and 1 T4N3M1. There were 10 subjects with *TP53*(+) that showed mutations in exons 4, 5, 6, 7, 8, and 9. In 6 subjects with *FGFR3*(+), mutations appeared in exons 7 and 9. In 3 subjects with *PIK3CA*(+), mutations appeared in exons 2 and 10. In 3 subjects with *ERBB2*(+), mutations appeared in exons 8, 17 and 19. In 2 patients with *MUC4*(+), mutations appeared in exon 2; there were no subjects with *KRAS*(+). There was a significant correlation between

FIGURE 1. **Tissue gene mutation map of 47 subjects with bladder cancer. Each line represents a patient, each column represents the type of gene mutation.**

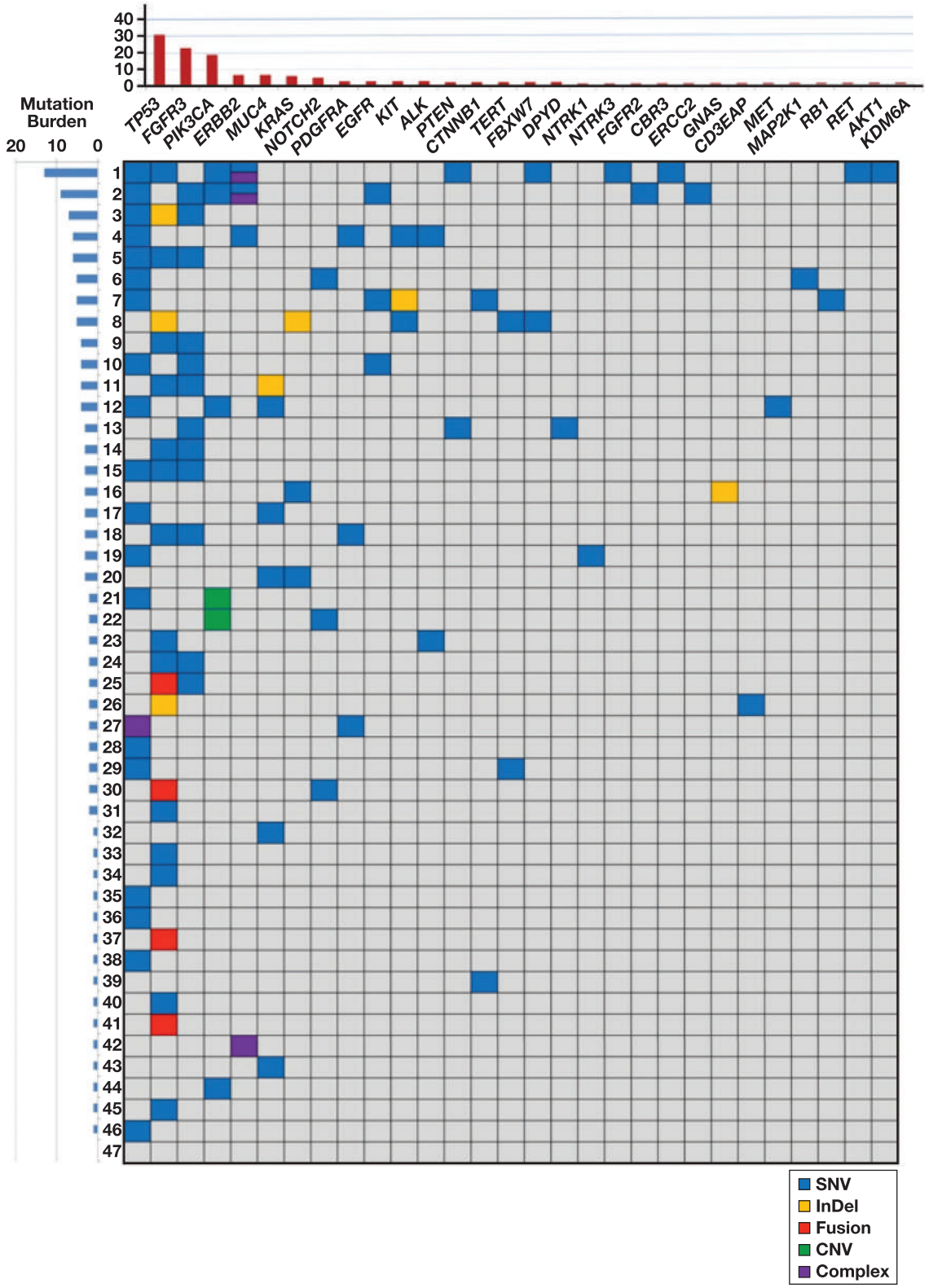

the TP53 gene mutation and recurrence and metastasis of bladder cancer (χ^2 = 3.948, P = .047). However, other gene mutations were not significantly correlated with recurrence and metastasis of bladder cancer (P > .05).

Survival Analysis

A total of 47 subjects diagnosed with bladder cancer were followed up after surgery, of whom 16 had recurrence and metastasis; 2 of the 16 died due to recurrence and metastasis. By February 28, 2022, the shortest

TABLE 2. High-Throughput Sequencing of Pathological Specimens from Study Subjects

Gene	No. (%)	Pathology Type	
		NMIBC	MIBC
		No. (%)	No. (%)
TP53	31 (23.31)	4 (7.69)	27 (33.33)
FGFR3	23 (17.29)	18 (34.62)	5 (6.17)
PIK3CA	19 (14.29)	11 (21.15)	8 (9.88)
ERBB2	7 (5.26)	2 (3.85)	5 (6.17)
MUC4	7 (5.26)	0 (0.00)	7 (8.64)
KRAS	6 (4.51)	4 (7.69)	2 (2.47)
NOTCH2	5 (3.76)	3 (5.77)	2 (2.47)
PDGFRA	3 (2.26)	1 (1.92)	2 (2.47)
EGFR	3 (2.26)	1 (1.92)	2 (2.47)
KIT	3 (2.26)	0 (0.00)	3 (3.70)
ALK	3 (2.26)	1 (1.92)	2 (2.47)
PTEN	2 (1.50)	0 (0.00)	2 (2.47)
CTNNB1	2 (1.50)	1 (1.92)	1 (1.23)
TERT	2 (1.50)	1 (1.92)	1 (1.23)
FBXW7	2 (1.50)	1 (1.92)	1 (1.23)
DPYD	2 (1.50)	1 (1.92)	1 (1.23)
NTRK1	1 (0.75)	1 (1.92)	0 (0.00)
NTRK3	1 (0.75)	0 (0.00)	1 (1.23)
FGFR2	1 (0.75)	0 (0.00)	1 (1.23)
CBR3	1 (0.75)	0 (0.00)	1 (1.23)
ERCC2	1 (0.75)	0 (0.00)	1 (1.23)
GNAS	1 (0.75)	0 (0.00)	1 (1.23)
CD3EAP	1 (0.75)	0 (0.00)	1 (1.23)
MET	1 (0.75)	1 (1.92)	0 (0.00)
MAP2K1	1 (0.75)	1 (1.92)	0 (0.00)
RB1	1 (0.75)	0 (0.00)	1 (1.23)
RET	1 (0.75)	0 (0.00)	1 (1.23)
AKT1	1 (0.75)	0 (0.00)	1 (1.23)
KDM6A	1 (0.75)	0 (0.00)	1 (1.23)

MIBC, muscle invasive bladder cancer; NMIBC, non-muscle invasive bladder cancer.

follow-up time was 6 months, the longest was 23 months, and the median follow-up time was 21 months. The shortest and longest PFS were 3 months and 23+ months, and the median PFS was 19+ months. The shortest and longest OS were 6 months and 23+ months, and the median OS was 21+ months.

The median PFS of *TP53*(+) group was 18.5 months, which was shorter than that of the *TP53*(–) group (19 months); the median PFS of the *FGFR3*(+) group was 19.43 months, which was longer than that of the *FGFR3*(–) group (18.5 months), and the median PFS of the *PIK3CA*(+) group was 19.25 months, which was longer than that of the *PIK3CA*(–) group (18.88 months). The median PFS of the *ERBB2*(+) group was 18 months, which was shorter than the 19.27 months for *ERBB2*(–). The median PFS of the *KRAS*(+) group was 20.5 months, which was longer than the 18.67 months for *KRAS*(–). However, no significant difference was found in OS between these genes, and no significant difference was found in PFS and OS between the *MUC4* positive group and the negative group.

Kaplan-Meier analysis showed that the PFS of the *TP53*(–) group was significantly better than that of the *TP53*(+) group, and the log-rank test confirmed the correlation between *TP53* and PFS ($P < .05$). There was a significant correlation between T stage and PFS ($P < .05$), and PFS decreased with the progression of the tumor stage. The association of other genes and factors with PFS was not proved, but the Kaplan-Meier survival curve showed that the PFS of the *FGFR3*(+) group was better than that of the *FGFR3*(–) group, and the PFS of those with NMIBC was better than those with MIBC, as shown in **FIGURE 2**. Since 2 out of 47 bladder cancer patients died of bladder cancer, no significant correlation between genes or elements and OS was found in the study of OS.

Cox Regression Analysis of PFS and OS

Cox proportional risk model univariate analysis of factors affecting postoperative PFS in study subjects showed that positive *TP53* gene and T stage of bladder cancer were correlated with PFS ($P < .05$), as shown in

TABLE 3. Mutations in *TP53*, *FGFR3*, *PIK3CA*, *ERBB2*, *MUC4*, and *KRAS* Genes Detected by High-Throughput Sequencing in Study Subjects

Mutant Functional Area	Mutation Frequency (%)	Gene Locus Mutations	Type of Mutation	No. (%)
TP53				
exon 2	1.16	1	SNV	1 (3.23)
exon 4	56.47	4	SNV	5 (16.13)
exon 5	85.65	6	SNV	7 (22.58)
exon 6	64.09	5	SNV	5 (16.13)
exon 7	16.36	4	SNV; Complex	6 (19.35)
exon 8	35.03	4	SNV	5 (16.13)
exon 9	46.13	1	SNV	2 (6.45)
FGFR3				
exon 7	84.05	2	SNV	8 (34.78)
exon 9	89.11	3	SNV; InDel	10 (43.48)
exon 14	2.94	1	SNV	1 (4.35)
FGFR3-TACC3	47.22		Fusion	4 (17.39)
PIK3CA				
exon 2	5.88	1	SNV	1 (5.26)
exon 4	1.79	1	SNV	1 (5.26)
exon 5	30.00	2	SNV	2 (10.53)
exon 8	1.21	1	SNV	1 (5.26)
exon 10	53.40	4	SNV	8 (42.11)
exon 11	1.29	1	SNV	1 (5.26)
exon 14	20.19	2	SNV	2 (10.53)
exon 15	42.31	1	SNV	1 (5.26)
exon 21	31.97	1	SNV	2 (10.53)
ERBB2				
exon 8	47.11	1	SNV	1 (14.29)
exon 17	69.24	2	SNV	2 (28.57)
exon 19	65.84	1	SNV	1 (14.29)
exon 20	43.91	1	SNV	1 (14.29)
ERBB2			CNV	2 (28.57)
MUC4				
exon 2	8.86	4	SNV; Complex	7 (100.00)
KRAS				
exon 2	50.91	3	SNV; InDel	5 (83.33)
exon 4	38.52	1	SNV	1 (16.67)

CNV, copy number variation; InDel, insertion deletion; SNV, single nucleotide variant.

TABLE 5. In the multivariate analysis of Cox proportional risk model, no other factors were found to be associated with PFS except T stage of bladder cancer. The Cox proportional risk model was used to analyze univariate and multivariate factors affecting postoperative OS in bladder cancer patients, but no relevant genes and factors were found.

Discussion

At present, the diagnosis and treatment of bladder cancer mainly rely on the comprehensive results of imaging, cystoscopy, and pathology. Surgery combined with postoperative intravesical chemotherapy has become the standard for the treatment of bladder cancer. However, for patients with the same clinical stage and pathological type of bladder cancer, the effect and prognosis after the same treatment are quite different.[16] There may be patients with local recurrence or recurrence and distant lymph node metastasis after surgery or chemotherapy, indicating that the diagnosis and conventional treatment of bladder cancer is still difficult to treat effectively. Further understanding of molecular biology and the genetics of bladder cancer has improved the diagnosis and treatment of local and advanced diseases. Although intravesical bacillus Calmette–Guérin (BCG) injection remains the main treatment for high-risk NMIBC, treatment options for muscle-invasive and advanced diseases have been extended to include immune checkpoint inhibition, targeted therapy, and antibody

TABLE 4. Relationship Between Different Clinical Features of Study Subjects and the Mutation Frequency of *TP53*, *FGFR3*, *PIK3CA*, *ERBB2*, *MUC4* and *KRAS* Detected by High-Throughput Sequencing

Factors	No.	*TP53*				*FGFR3*				*PIK3CA*			
		Positive	Negative	χ^2	*P*	Positive	Negative	χ^2	*P*	Positive	Negative	χ^2	*P*
Age (y)				2.275	.132			0.667	.414			0.231	.631
>60	32	16	16			13	19			7	25		
≤60	15	4	11			8	7			5	10		
Sex				1.047	.306			0.195	.659			0	1
Male	32	12	20			15	17			8	24		
Female	15	8	7			6	9			4	11		
Smoker				1.325	.250			0.793	.373			0.057	.811
Yes	28	10	18			14	14			8	20		
No	19	10	9			7	12			4	15		
Pathological type				16.045	.000			11.284	.001			2.027	.154
Muscle invasive bladder cancer	24	17	7			5	19			4	20		
Non-muscle invasive bladder cancer	23	3	20			16	7			8	15		
T stage				21.433	.000			12.566	.014			3.463	.484
Ta	5	0	5			3	2			1	4		
T1	18	3	15			13	5			7	11		
T2a	2	0	2			1	1			0	2		
T2b	20	15	5			4	16			4	16		
T4	2	2	0			0	2			0	2		
Factors	**No.**	***ERBB2***				***MUC4***				***KRAS***			
		Positive	Negative	χ^2	*P*	Positive	Negative	χ^2	*P*	Positive	Negative	χ^2	*P*
Age (y)				0.151	.697			0	1			0	1
>60	32	5	27			3	29			4	28		
≤60	15	1	14			1	14			2	13		
Sex				0.151	.697			0.758	.384			2.209	.137
Male	32	5	27			4	28			2	30		
Female	15	1	14			0	15			4	11		
Smoker				0	1			0.016	.901			0.916	.339
Yes	28	4	24			3	25			2	26		
No	19	2	17			1	18			4	15		
Pathological type				0.145	.703			2.323	.127			0.243	.622
Muscle invasive bladder cancer	24	4	20			4	20			2	22		
Non-muscle invasive bladder cancer	23	2	21			0	23			4	19		
T stage				2.301	.681			5.902	.207			1.204	.877
Ta	5	0	5			0	5			1	4		
T1	18	2	16			0	18			3	15		
T2a	2	0	2			0	2			0	2		
T2b	20	4	16			4	16			2	18		
T4	2	0	2			0	2			0	2		

drug conjugates.[17,18] In recent years, erdafitinib has been approved for platinum-resistant and advanced bladder cancer treatment,[19] and it is the first oral effective *FGFR* antagonist approved by the Food and Drug Administration (2019) for the treatment of urothelial carcinoma.[20] In the future, on the basis of these latest achievements, efforts will be made to provide new treatments earlier in the disease progression by optimizing the sequencing and combination of approved treatments, improved patient selection, and determination of new therapeutic targets.[19–21] So far, a variety of targeted drugs for bladder cancer treatment are still in the clinical research stage. In this study, the latest high-throughput sequencing technology was used to conduct in-depth analysis of bladder cancer genes and their exon mutation sites, providing a reliable experimental basis for the molecular mechanism and targeted therapy of clinical bladder cancer. Compared with traditional sequencing technology, high-throughput sequencing technology adopts the principle of simultaneous synthesis and sequencing, and parallel sequencing reactions are carried out for hundreds of thousands to millions of DNA molecules. Then, the original image data

FIGURE 2. **Kaplan-Meier survival curve of genes and factors affecting postoperative progression-free survival (PFS) in study subjects.**

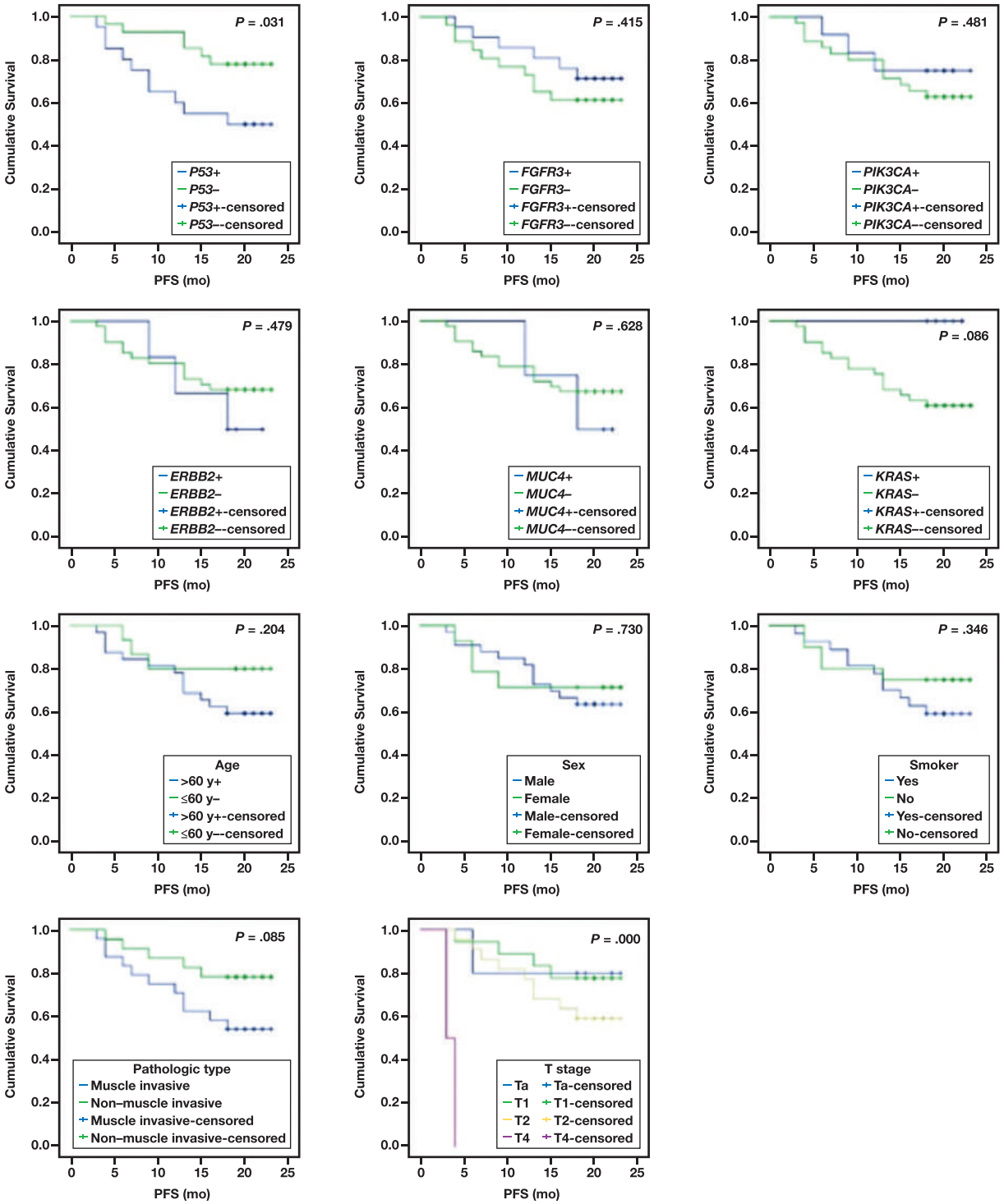

or electrochemical signals obtained by bioinformatics analysis are used to obtain the nucleic acid sequence of bladder cancer patients and the changes of multigene, multisite mutation, fusion genes, and gene CNV, which have unique advantages for studying the pathogenesis of bladder cancer and targeted drug therapy.

High-throughput sequencing of more than 2000 gene loci and all exons of 94 genes was performed on the pathological specimens of 47 bladder cancer patients included in this study. A total of 29 mutation genes, 61 exons, and 95 gene mutation loci were detected. Among them, *TP53*, *FGFR3*, *PIK3CA*, *ERBB2*, *MUC4*, and *KRAS* gene mutation frequency is higher, accounting for 59.92% of the total mutation frequency. This result is highly consistent with the research results of Wang et al[22] on potential targets for bladder cancer sequencing. In this study, the exons and gene loci of 6 genes with high mutation

TABLE 5. Single Factor Analysis of Cox Proportional Hazard Regression (HR) Model Affecting Postoperative Progression-Free Survival of Study Subjects

Factors	HR (95% CI)	*P* Value
Sex (male/female)	1.217 (0.392–3.777)	.734
Age (≤60 y vs >60 y)	2.189 (0.623–7.686)	.221
Smoker (yes/no)	1.644 (0.571–4.735)	.357
Pathological type (muscle invasive/ non-muscle invasive)	2.429 (0.843–6.997)	.100
T stage		.003
Ta	0.017 (0.001–0.260)	.003
T1	0.018 (0.018–0.153)	.000
T2	0.036 (0.005–0.267)	.001
TP53 (positive/negative)	2.863 (1.037–7.900)	.042
FGFR3 (positive/negative)	0.661 (0.240–1.821)	.424
PIK3CA (positive/negative)	0.643 (0.183–2.256)	.490
ERBB2 (positive/negative)	1.559 (0.444–5.480)	.488
MUC4 (positive/negative)	1.433 (0.325–6.308)	.634
KRAS (positive/negative)	0.038 (0.000–14.476)	.282

frequency were analyzed. The sequencing results showed that the mutation frequency of *TP53* gene was the highest, and the exons and mutation sites were the most detected. Mutations in the *TP53* gene affect half of human cancers, resulting in impaired regulation of multiple cellular functions, including cell cycle progression and cell death in response to gene toxic stress. Through over 40 years of high-quality research, both loss- and gain-of-function activities of mutant p53 proteins have been shown to play an important role in promoting tumorigenesis in various tissues. A total of 3 exons of point mutations and insertion deletions and fusion mutations of *FGFR3-TACC3* were detected in the *FGFR3* gene. The FGFR3 protein is one of the members of the fibroblast growth factor receptor (FGFR) family. At present, four types of FGFRs have been identified, namely *FGFR1*, *FGFR2*, *FGFR3*, and *FGFR4*. The *FGFR3* binds to acidic and basic fibroblast growth factor and plays an important role in bone development and maintenance. A total of 9 exon mutations were detected by *PIK3CA*, all of which are point mutations widely found in human cancers. Studies have shown that *PIK3CA* gene mutation often increases the catalytic activity of its protein product, resulting in enhanced downstream signals and carcinogenic changes in cells. A total of 4 exon point mutations and 2 gene copy number variations were detected in *ERBB2*. The *HER2* is a membrane receptor encoded by proto-oncogene erbB-2, which belongs to the human epidermal growth factor receptor (*EGFR/ERBB*) family. The *ERBB2* mutation can cause abnormal activation of *HER2*, through gene amplification, mutation (such as point mutation, small insertion, duplication, and deletion mutation), and fusion. Moreover, *ERBB2*'s extracellular domains and somatic mutations in the kinase domain can aberrantly induce *HER2* dimerization with its receptors, initiating tumor-forming signaling pathways. The 4 gene loci in exon 2 of *MUC4* gene were mutated, and the maximum mutation frequency was 8.86%. MUC4 is a type of dry molecular weight glycosylated protein secreted by epithelial cells, which is mainly expressed on the surface of epithelial cells of human lumen organs. The *MUC4* is associated with the occurrence and development of various human tumors and has been used as a diagnostic basis for lung cancer and esophageal squamous cell carcinoma. Our work showed that *MUC4* gene mutations are present in bladder cancer patients, raising the possibility that mutant MUC4 protein may be involved in the biology of bladder cancer. A total of 2 exons were detected by *KRAS*. *KRAS* activates the activity of phosphokinase by binding to GTP, and further activates the downstream proteins. The activated downstream signaling pathways include the MAPK and PI3K/AKT pathways. The *KRAS* gene belongs to the RAS family of oncogenes, which are commonly mutated in human cancers, leading to aberrant activation of cell growth. In 1 patient's gene sequencing data, distinct gene mutations could either occur in different exons of the same gene or in the same exon of the gene. We identified *TP53*, *FGFR3*, *PIK3CA*, *ERBB2*, *MUC4*, and *KRAS* gene mutations that show significant alterations in their functional regions. Notably, 31 of the 47 subjects in our study carried 2 or more mutation genes, and most of them are concentrated in *TP53*, *FGFR3*, *PIK3CA*, *ERBB2*, *MUC4*, and *KRAS*, indirectly suggesting that the mutation of these genes might be biologically related to the occurrence of bladder cancer. Four fusion mutations of the *FGFR3-TACC3* gene were detected in the 47 subjects and the mutation frequency was 8.51%, accounting for 17.39% of the total number of *FGFR3* gene mutations. Consistent with this, other studies have also reported that the prevalence of *FGFR3-TACC3* mutations in bladder cancer is 2% to 3%,[23–25] indicating that the resulting fusion protein may play an important role in the occurrence and development of bladder cancer. In this study, TNM staging analysis was performed on 47 patients with bladder cancer, according to the 2017 UICC standard.[26] Tis, Ta, and T1 stages of bladder cancer are collectively referred to as NMIBC, whereas bladder cancer above T2 stage is collectively referred to as MIBC. Since only 2 patients had lymphatic metastasis and 1 had distant metastasis (which invades the whole bladder and can be seen in the peritoneal cavity, retroperitoneal multiple enlarged lymph nodes), N staging and M staging were not included in this analysis. The age, sex, smoking history, pathological type, T stage, and gene mutation of 47 subjects with bladder cancer were compared and analyzed. The results showed that *TP53* gene mutations mostly frequently occur in MIBC specimens, while the mutation frequency of *FGFR3* appears to be higher in NMIBC. The clinical T stage data further showed that the mutation frequency of the *TP53* gene was higher at the T2b stage, and the mutation frequency of the *FGFR3* gene was higher in the T1 stage. This is consistent with the findings of Wu et al[27] and van Rhijn et al,[28] emphasizing the potential significance of *TP53* and *FGFR3* mutations in bladder cancer

progression and drug selection. In addition, the studies of Wang et al,[29] Tan et al,[30] and Kaur et al[31] have confirmed that the differential expression of *PIK3CA*, *ERBB2*, *MUC4*, and *KRAS* genes plays an important role in the process of bladder cancer development. As potential therapeutic targets, they may have important guiding significance for the targeted treatment of bladder cancer. Finally, we found no statistical difference in *TP53*, *FGFR3*, *PIK3CA*, *ERBB2*, *MUC4* and *KRAS* mutation frequencies in age, sex, and smoking history. Smoking is the strongest risk factor for bladder cancer, accounting for 59.57% of all cases; it has been reported that smoking could increase the recurrence risk of bladder cancer and damage the therapeutic effect of BCG.[32,33] Therefore, the exact impact of smoking on gene mutations still remains to be investigated by large sample studies. With the exception of mutations in *NTRK1*, *MET*, and *MAP2K1* genes which were only found in NMIBC, other mutation genes detected in this study appear in MIBC; the relationship between these genes and bladder cancer needs a larger sample of clinical data and experiments to verify.

Analysis of gene mutations in 16 subjects with recurrent and metastatic bladder cancer showed that exon 2 of *TP53*, exon 14 of *FGFR3*, exons 4, 5, 8, 11, 14, 15, and 21 of *PIK3CA*, exon 20 of *ERBB2*, and exons 2 and 4 of the *KRAS* gene did not appear in the recurrence and metastasis cases. Whether these exons are not involved in the recurrence and metastasis of bladder cancer needs to be verified by clinical statistics and basic studies with larger samples. The significant correlation between *TP53* gene and the recurrence and metastasis of bladder cancer further indicates that *TP53* gene plays an important role in the occurrence and development of bladder cancer.

There are many factors affecting postoperative survival of bladder cancer patients, but the use of gene mutation as a predictor of postoperative survival of bladder cancer patients remains controversial. In this study, 47 patients with bladder cancer were followed up for 23 months. The log-rank test confirmed the correlation between the *TP53* gene and PFS. The Kaplan-Meier survival curve showed that PFS in the positive *TP53* gene group was worse than that in the negative *TP53* gene group. Cox proportional risk model univariate analysis also confirmed that positive *TP53* gene was a risk factor affecting the prognosis of bladder cancer patients. The *TP53* gene mutation increases the risk function of bladder cancer. Although there is no significant correlation between muscle invasion and postoperative PFS for subjects with bladder cancer by log-rank test, Kaplan-Meier survival curves of the 2 factors show the curve trends are very similar. Moreover, the χ^2 test also confirmed the significant correlation between the *TP53* gene mutation and MIBC. The study of Nassar et al[34] also confirmed that the overall survival of patients with mutated *TP53* in MIBC was shorter than that of wild-type *TP53*. Braicu et al[35] also confirmed that wild-type *TP53* had a higher survival rate compared with mutant *TP53*. Log-rank test confirmed that the T stage was a factor affecting postoperative PFS of bladder cancer subjects, and patients with bladder cancer above the T2 stage also had worse PFS than those in the Ta and T1 stages, which was also significantly correlated with *TP53* gene mutation. These findings suggest that the high expression of *TP53* gene is related to the aggressive characteristics and poor prognosis of tumors, which is indicated in the findings of Chen et al.[36] The log-rank test showed no significant correlation between *FGFR3* and *PIK3CA* genes and PFS in subjects with bladder cancer. Cox proportional risk model univariate analysis also confirmed that *FGFR3* and *PIK3CA* gene mutations are not risk factors affecting the prognosis of bladder cancer. However, the Kaplan-Meier survival curve showed that the PFS of the *FGFR3* and *PIK3CA* gene positive group was better than that of the negative group, and the trend of the survival curve was similar to that of NMBIC. The χ^2 test also confirmed the correlation between *FGFR3* and NMIBC at the Ta and T1 stages. This suggest that *FGFR3* and *PIK3CA* gene mutations are more common in low-grade and low-stage bladder cancer, and that *FGFR3* gene positivity may predict a better prognosis for bladder cancer, which is roughly consistent with the results of the study of Kim et al.[37] However, Geelvink et al[38] argued that FGFR3 mutations did not predict the risk of tumor recurrence and progression. Although *PIK3CA* gene mutations show different prognosis in different tumors, in bladder cancer combined survival analysis with *FGFR3* is required. Analysis of *TP53* and *FGFR3* shows that they are mutually exclusive mutations, which is consistent with the study by Apollo et al.[39] Other genes may not show sufficient mutation numbers due to the influence of sample size. No significant correlation was found in the log-rank test, they could not be regarded as independent risk factors in univariate analysis of the Cox proportional risk model, and no difference in survival status was observed in Kaplan-Meier survival curve for these other genes.

In summary, high-throughput sequencing technology can be used to detect multiple gene mutations in bladder cancer. The *TP53*, *FGFR3*, *PIK3CA*, *ERBB2*, *MUC4*, and *KRAS* genes have high mutation rates in bladder cancer. Of these, *TP53*, *FGFR3*, and *PIK3CA* may predict the prognosis of bladder cancer, which has potential guiding significance for the pathogenesis of bladder cancer.

REFERENCES

1. Huang W, Kong L, Xie Z, et al. *2019 edition of Chinese Guidelines for Diagnosis and Treatment of Urology and Male Diseases*.
2. Bray F, Ferlay J, Soerjomataram I, et al. Global cancer statistics 2018: GLOBOCAN estimates of incidence and mortality worldwide for 36 cancers in 185 countries. *CA Cancer J Clin.* 2018;68(6):394–424. doi:10.3322/caac.21492.
3. Ning W, Shuo L, Lei Y, et al. Interpretation on the report of global cancer statistics 2018. *J Multidiscip Cancer Manage.* 2019;5(01):87–97.
4. Sung H, Ferlay J, Siegel RL, et al. Global cancer statistics 2020: GLOBOCAN estimates of incidence and mortality worldwide for 36 cancers in 185 countries. *CA Cancer J Clin.* 2021;71(3):209–249. doi:10.3322/caac.21660.
5. Zongchao L, Zhexuan L, Yang Z, et al. Interpretation on the report of Global Cancer Statistics 2020. *J Multidiscip Cancer Manage.* 2021;7(02):1–14.
6. Tran L, Xiao JF, Agarwal N, Duex JE, Theodorescu D. Advances in bladder cancer biology and therapy. *Nat Rev Cancer.* 2021;21(2):104–121.
7. Torre LA, Bray F, Siegel RL, Ferlay J, Lortet-Tieulent J, Jemal A. Global cancer statistics, 2012. *CA Cancer J Clin.* 2015;65:87–108. doi:10.3322/caac.21262.
8. Edge SB, Byrd DR, Compton CC, Fritz AG, Greene FL, Trotti A, eds. *AJCC Cancer Staging Manual*. Vol 7. New York, NY: Springer; 2010.
9. Magers MJ, Lopez-Beltran A, Montironi R, Williamson SR, Kaimakliotis HZ, Cheng L. Staging of bladder cancer. *Histopathology*. 2019;74:112–134.
10. Dinney CP, McConkey DJ, Millikan RE, et al Focus on bladder cancer. *Cancer Cell.* 2004;6:111–116. doi:10.1016/j.ccr.2004.08.002.
11. Knowles MA, Hurst CD. Molecular biology of bladder cancer: new insights into pathogenesis and clinical diversity. *Nat Rev Cancer.* 2015;15:25–41. doi:10.1038/nrc3817.

12. Siegel RL, Miller KD, Jemal A. Cancer statistics, 2018. *CA Cancer J Clin.* 2018;68:7–30. doi:10.3322/caac.21442.
13. Stein JP, Lieskovsky G, Cote R, et al. Radical cystectomy in the treatment of invasive bladder cancer: long-term results in 1,054 patients. *J Clin Oncol.* 2001;19:666–675. doi:10.1200/JCO.2001.19.3.666.
14. Yafi FA, Aprikian AG, Chin JL, et al Contemporary outcomes of 2287 patients with bladder cancer who were treated with radical cystectomy: a Canadian multicentre experience. *BJU Int.* 2011;108:539–545. doi:10.1111/j.1464-410X.2010.09912.x.
15. Zahoor H, Mir MC, Barata PC, et al. Phase II trial of continuous treatment with sunitinib in patients with high-risk (BCG-refractory) non-muscle invasive bladder cancer. *Invest New Drugs.* 2019;37(6):1231–1238. doi:10.1007/s10637-018-00716-w.
16. Su H, Jiang H, Tao T, et al. Hope and challenge: precision medicine in bladder cancer. *Cancer Med.* 2019;8(4):1806–1816. doi:10.1002/cam4.1979.
17. Lenis AT, Lec PM, Chamie K, Mshs MD. Bladder cancer: a review. *JAMA.* 2020;324(19):1980–1991. doi:10.1001/jama.2020.17598.
18. Facchini G, Cavaliere C, Romis L, et al. Advanced/metastatic bladder cancer: current status and future directions. *Eur Rev Med Pharmacol Sci.* 2020;24(22):11536–11552.
19. Patel VG, Oh WK, Galsky M. Treatment of muscle-invasive and advanced bladder cancer in 2020. *CA Cancer J Clin.* 2020;70(5):404–423. doi:10.3322/caac.21631.
20. Hanna KS. Erdafitinib to treat urothelial carcinoma. *Drugs Today.* 2019;55(8):495–501.
21. Osterman CK, Milowsky MI. New and emerging therapies in the management of bladder cancer. *F1000Res.* 2020;9:1146F1000 Faculty Rev-1146. doi: 10.12688/f1000research.26841.1
22. Wang T, Liu Z, Wang X, et al. Identification of potential therapeutic targets in urothelial bladder carcinoma of Chinese population by targeted next-generation sequencing. *Cancer Biol Ther.* 2020;21(8):709–716.
23. Robertson AG, Kim J, Al-Ahmadie H, et al. Comprehensive molecular characterization of muscle-invasive bladder cancer. *Cell.* 2018;174(4):1033.
24. Cancer Genome Atlas Research Network. Comprehensive molecular characterization of urothelial bladder carcinoma. *Nature.* 2014;507(7492):315–322.
25. Helsten T, Elkin S, Arthur E, Tomson BN, Carter J, Kurzrock R. The FGFR landscape in cancer: analysis of 4,853 tumors by next-generation sequencing. *Clin Cancer Res.* 2016;22(1):259.
26. Brierley JD, et al. *TNM Classification of Malignant Tumours*. 8th ed. John Wiley and Sons; 2017.
27. Wu G, Wang F, Li K, et al. Significance of TP53 mutation in bladder cancer disease progression and drug selection. *PeerJ.* 2019;7:e8261. doi:10.7717/peerj.8261.
28. van Rhijn BWG, Mertens LS, Mayr R, et al. Zuiverloon TCM. *FGFR3* mutation status and *FGFR3* expression in a large bladder cancer cohort treated by radical cystectomy: implications for anti-*FGFR3* treatment? *Eur Urol.* 2020;78(5):682–687.
29. Wang Z, Shang J, Li Z, et al. *PIK3CA* is regulated by CUX1, promotes cell growth and metastasis in bladder cancer via activating epithelial-mesenchymal transition. *Front Oncol.* 2020;10:536072.
30. Tan TZ, Rouanne M, Tan KT, Huang RY, Thiery JP. Molecular subtypes of urothelial bladder cancer: results from a meta-cohort analysis of 2411 tumors. *Eur Urol.* 2019;75(3):423–432.
31. Kaur S, Momi N, Chakraborty S, et al. Altered expression of transmembrane mucins, MUC1 and MUC4, in bladder cancer: pathological implications in diagnosis. *PLoS One.* 2014;9(3):e92742.
32. Rozanec JJ, Secin FP. Epidemiology, etiology and prevention of bladder cancer [in Spanish]. *Arch Esp Urol.* 2020;73(10):872–878.
33. Mori K, Mostafaei H, Abufaraj M, Yang L, Egawa S, Shariat SF. Smoking and bladder cancer: review of the recent literature. *Curr Opin Urol.* 2020;30(5):720–725.
34. Nassar AH, Umeton R, Kim J, et al. Mutational analysis of 472 urothelial carcinoma across grades and anatomic sites. *Clin Cancer Res.* 2019;25:2458–2470.
35. Braicu C, Buiga R, Cojocneanu R, et al. Connecting the dots between different networks: miRNAs associated with bladder cancer risk and progression. *J Exp Clin Cancer Res.* 2019;38(1):433.
36. Chen L, Liu Y, Zhang Q, et al. p53/PCDH17/Beclin-1 proteins as prognostic predictors for urinary bladder cancer. *J Cancer.* 2019;10:6207–6216.
37. Kim YS, Kim K, Kwon GY, Lee SJ, Park SH. Fibroblast growth factor receptor 3 (FGFR3) aberrations in muscle-invasive urothelial carcinoma. *BMC Urol.* 2018;18(1):68.
38. Geelvink M, Babmorad A, Maurer A, et al. Diagnostic and prognostic implications of FGFR3high/Ki67high papillary bladder cancers. *Int J Mol Sci.* 2018;19(9):2548.
39. Apollo A, Ortenzi V, Scatena C, et al. Molecular characterization of low grade and high grade bladder cancer. *PLoS One.* 2019;14(1):e0210635.

Total Analytical Error and Measurement Uncertainty for Analytical Performance Evaluation and Determination of Gray Zones of Glucose Critical Value Limits

Canan Karadağ, MD[*], *and Nafi Demirel, MSc*

Consultant on Biochemistry, Eskişehir, Turkey. *To whom correspondence should be addressed: canankaradag@outlook.com.

Keywords: total analytical error, measurement uncertainty, ISO/TS 20914, analytical performance, critical values, gray zone, glucose

Abbreviations: TAE, total analytical error; MU, measurement uncertainty; AP, analytical performance; APS, AP specifications; GUM, Guide to the Expression of Uncertainty in Measurement; ISO, International Organization for Standardization; CRM, certified reference material; ATE-TMH, acceptable total error limit of the Turkish Ministry of Health; EFLM, European Federation of Clinical Chemistry and Laboratory Medicine; EQA, external quality assessment; IQC, internal quality control; EuBIVAS, European Biological Variation Study; CLIA, Clinical Laboratory Improvement Amendments.

Laboratory Medicine 2023;54:153–159; https://doi.org/10.1093/labmed/lmac077

ABSTRACT

Objective: Total analytical error (TAE) and measurement uncertainty (MU) are important approaches to evaluating and improving the quality of measurement procedures. This study evaluates glucose analytical performance (AP) according to TAE and MU and calculates gray zones of glucose critical value limits.

Methods: Using TAE and MU values, AP was evaluated according to 5 different analytical performance specifications (APS) and the gray zones of critical value limits were calculated. The number of patients in these zones was compared.

Results: TAE was higher than MU at all 3 levels. The AP for the low glucose level was poor. The number of patients in the gray zones was statistically higher in the TAE groups than in the MU groups ($P < .05$).

Conclusion: TAE and MU values can be used to evaluate the AP of glucose measurement as well as to evaluate the compliance of patient results with decision limits by creating gray zones.

As a scientific assumption, every measurement result includes some errors. In 1974, Westgard et al[1] used the total analytical error (TAE) to define the error in clinical laboratory results. Almost 20 years after the TAE approach, the famous guide GUM (*Guide to the Expression of Uncertainty in Measurement*) was published by ISO (International Organization for Standardization) and 6 collaborating organizations to define and estimate measurement uncertainty (MU).[2] According to the GUM: "Error is an idealized concept and errors cannot be exactly known." Contrary to the MU approach, TAE assumes that the true value of a measurement result can be known, and the error of the result can be calculated by a simple equation that sums the absolute value of systematic error and a multiple of random error.[1]

Due to its simplicity and more understandable calculation, the TAE approach has a huge impact on clinical chemistry, especially in the United States. The US Food and Drug Administration refers to the Clinical and Laboratory Standards Institute guideline based on the TAE approach for clinical laboratory tests.[3] On the other hand, MU-based calculations are applied especially as a requirement of ISO 15189.[4] The standard does not clarify how to determine MU in practice but uses the terms and definitions of ISO/IEC Guide 99, *International Vocabulary of Metrology*,[5] and gives the GUM[2] in the bibliography list. Ultimately, an ISO standard ISO/TS 20914 was published as a practical guide for estimating MU in clinical laboratories.[6] Unlike the complex mathematical models of the GUM based on the "bottom-up" approach, this technical standard offers more practical solutions to estimate MU, which is known as the "top-down" approach.

Although TAE and MU values are used for analytical performance (AP) evaluation in many laboratories, they have not been applied to the evaluation of the compliance of patient results with decision limits. The ISO/TS 20914 gives examples of applying MU to patient result interpretation.[6] Using 1 of these examples, this study proposes to call this uncertain region around the critical value limit the "gray zone".

This study clarifies the difference between TAE and MU approaches to glucose measurement and evaluates their suitability against some AP specifications (APS). To assess the significance of the difference between the 2 approaches, the gray zones of the glucose critical value limits are calculated using the TAE and MU values, and the number of patients in these zones is compared. In addition, this study is important as it is the

first study in the literature to compare the MU value calculated according to ISO/TS 20914 with TAE.

Materials and Methods

The Public Health Laboratory (PHL, Kayseri, Turkey) has been accredited to ISO 17025 since 2016, including more than 40 parameters of chemical and microbiological analysis of water. Since it is necessary to estimate the MU values of clinical measurements within the scope of ISO 15189 accreditation studies, after the ISO/TS 20914 was published, MU estimations were revised according to this guide.[6] On the other hand, TAE calculation is requested from clinical laboratories in Turkey within the scope of the circular of the Ministry of Health.[7]

Glucose measurements spanning 1 year at approximately 500 samples per day were performed on 2 identical Architect c16000 (Abbott Laboratories) biochemistry auto analyzers using calibrators and reagents from the same manufacturer. Third-party commutable quality control materials (Tecnopath Multichem S Plus, ref 08P88: level 1, level 2, level 3) with a total of 3 different concentrations, 2 of which correspond to glucose critical value limits were assayed at least 2 levels on each day. External quality control was performed monthly by human-based samples (RIQAS, Randox Laboratories).

Measurement Uncertainty of Glucose According to ISO/TS 20914

According to ISO/TS 20914(6), in the case where a measurement procedure does not exhibit medically significant bias, does not require an in-house calibrator correction factor, and is monitored according to external quality assessment (EQA) peer group reports, ISO/TS 20914 proposes a top-down approach that uses internal quality control (IQC) data of the measurement procedure and uncertainty information of the calibrator regarding higher-order elements of the calibration hierarchy. The uncertainty of the bias correction factor does not apply in these cases.

The uncertainty of any bias corrections, u_{bias}, should be included: $u(y) = \sqrt{(u^2_{RW} + u^2_{cal} + u_{bias}{}^2)}$. In this situation, ISO/TS 20914 states that certified reference material (CRM) should be used to estimate u_{bias}, which is calculated by the uncertainty of CRM from certificate, u_{ref}, and standard deviation of replicate measurements of CRM.[6]

In this study, the performance of glucose measurement was within specification according to the last 10 EQA peer group reports. Standard MU of glucose, $u_{glucose}$, was calculated by Equation 1 (**TABLE 1**). The uncertainty of the end-user calibrator, u_{cal}, was provided by the manufacturer (Abbott Laboratories) and calibrator was defined as traceable to NIST-SRM 965.

The long term imprecision of glucose measurement, u_{RW}, was determined retrospectively by using the results of a 1-year period for each level of the third-party, commutable IQC materials with a total of 3 different concentrations, 2 of which correspond to glucose critical value limits (Tecnopath Multichem S Plus, ref 08P88: level 1, level 2, level 3). Two different lots of IQC materials were used during this period. According to ISO/TS 20914(6), the u_{RW} of these 2 different lots can be combined with Equation 2 (**TABLE 1**).

Since 2 identical Architect c16000 biochemistry auto analyzers (Abbott Laboratories) were used, u_{lot1} and u_{lot2} were named $u_{pooled\ 1}$ and $u_{pooled2}$, which means that the results of instrument A and instrument B were combined with Equation 3 (**TABLE 1**) according to the worked example A.4 from ISO/TS 20914(6). In this equation, $u^2_{(A,B)}$ is the variance of the 2 mean values among the 2 auto analyzers, and $u^2_{RW\ (A,B)}$ is the pooled average imprecision variance of the 2 instruments for each level.

TAE According to the Westgard Method

TAE was calculated with the "% TAE = (k*%CV) + % Bias" formula, which is detailed in Equation 4 (**TABLE 2**). The %CV is equal to $\%u_{RW}$ for each level of IQC from **TABLE 1**.

%Bias was calculated by using 10 EQA peer group reports with Equation 5.

Equation 5 is

$$\frac{1}{n}\sum_{i=1}^{n}\left[\frac{laboratory\ result - mean\ of\ peer\ group * 100}{mean\ of\ peer\ group}\right]$$

AP Evaluation

AP of glucose for TAE and MU (**TABLE 3**) was evaluated according to acceptable total error limit of the Turkish Ministry of Health (ATE-TMH)[7] Clinical Laboratory Improvement Amendments (CLIA),[8] European Biological Variation Study (EuBIVAS) (specifications based on biological variation),[9] and Guideline of the German Medical Association on Quality Assurance in Medical Laboratory Examinations (Rili-BAEK).[10] Standard MU of glucose was evaluated according to MU targets of the European Federation of Clinical Chemistry and Laboratory Medicine (EFLM).[11]

Critical Value Limits

Critical value limits were determined according to the circular of the Ministry of Health[12] that defines a low critical value limit as ≤50 mg/dL (2.78 mmol/L) and a high critical value limit of ≥400 mg/dL (22.2 mmol/L) for patients >4 weeks.

Gray Zones of Glucose Critical Value Limits

In ISO/TS 20914(6), an example is given in Annex B explaining how to apply MU to determine whether a measured value exceeds a clinical decision limit with a 95% confidence level. Similar to this example, Equation 6 (**TABLE 4**) is used to calculate the confidence limit with a coverage factor of 1.65 for a one-sided 95% level of confidence. A confidence limit is added to the clinical decision limit to decide whether the result is higher than the clinical decision limit with a 95% confidence level, and vice versa for the lower decision limit.

Equation 7 was used to calculate the confidence limit of the TAE method and details are given in **TABLE 4**.

Using the confidence limits, recalculated critical value limits are shown in **TABLE 4**, and according to these limits, gray zones are given in **TABLE 5**.

Statistical Analysis

Jamovi (v.1.6, the Jamovi Project, Sydney, Australia) was used for statistical analysis. The results of patients reported as critical values in the last year were analyzed retrospectively to determine whether there was a statistically significant difference between the 2 methods in terms of the number of patients in the gray zones with the McNemar test.

Results

MU of glucose for each level is detailed in **TABLE 1**. TAE of each level is given in **TABLE 2**. TAE values were higher than $\%U_{glucose}$ in each level.

TABLE 1. Measurement Uncertainty Estimation According to ISO/TS 20914

Component (Analyte)	Glucose in Serum					
Measurand	Amount of glucose concentration in serum					
Measurement method	Enzymatic photometric (hexokinase)					
Measurement procedure	Abbott c16000 chemistry analyzer, Abbott glucose reagent, MCC calibrator, Technopath IQC materials					
Measurement unit	mg/dL					
Calibrator traceability	NIST-SRM 965					
Calibrator uncertainty (%U_{cal})	2.683%, k = 2 (95% confidence)					
Bias	Not medically significant according to EQA peer group reports					
IQC matrix	Human serum					
	Level 1		Level 2		Level 3	
IQC LOT 1	Data collection: 6/20/2016–12/30/2016					
Instrument	A	B	A	B	A	B
n	63	63	127	128	69	70
Mean (mg/dL)	49.5	49.7	126[b]	127[b]	281[b]	285[b]
Mean (mmol/L)[a]	2.75	2.76	7	7.1	15.6	15.8
SD (mg/dL)	1.85	1.31	2.92	3.06	8.28	7.9
SD (mmol/L)	0.10	0.07	0.16	0.17	0.46	0.44
$u_{pooled\ 1}$ Equation 3 = $u_{pooled1}$ = $\sqrt{(u^2(A,B) + u^2_{RW}(A,B))}$	$\bar{x}_{(A,B)} = (49.5 + 49.7)/2 = 49.6$ $u(A,B) = SD_{(A,B)} = 0.1414\ u_{RW}$ $(A,B) = \sqrt{((1.85^2 + 1.31^2)/2)} = 1.6029$ $u_{pooled1} = \sqrt{(0.1414^2 + 1.6029^2)} = 1.6091$		$\bar{x}_{(A,B)} = (127 + 128)/2 = 127.5$ $u(A,B) = SD_{(A,B)} = 0.7071\ u_{RW}$ $(A,B) = \sqrt{[(2.92^2 + 3.06^2)/2]} = 2.9908$ $u_{pooled1} = \sqrt{(0.7071^2 + 2.9908^2)} = 3.0733$		$\bar{x}_{(A,B)} = (281 + 285)/2 = 283$ $u_{(A,B)} = SD_{(A,B)} = 2.8284\ u_{RW}(A,B) = \sqrt{((8.28^2 + 7.9^2)/2)} = 8.0922\ u_{pooled1} = \sqrt{(2.8287^2 + 8.0922^2)} = 8.5723$	
IQC LOT 2	Data collection: 1/2/2017–6/30/2017					
Instrument	A	B	A	B	A	B
n	69	69	125	125	64	63
Mean (mg/L)	48.6	48.3	123	124	292	294
Mean (mmol/L)	2.7	2.68	6.83	6.89	16.2	16.3
SD (mg/dL)	1.69	1.18	3.84	2.91	7.68	6.59
SD (mmol/L)	0.09	0.07	0.21	0.16	0.43	0.37
$u_{pooled\ 2}$ Equation 3 $= u_{pooled2} = \sqrt{(u^2(A,B) + u^2_{RW}(A,B))}$	$\bar{x}_{(A,B)} = (48.6 + 48.3)/2 = 48.45$ $u(A,B) = SD_{(A,B)} = 0.2121\ u_{RW}$ $(A,B) = \sqrt{((1.69^2 + 1.18^2)/2)} = 1.45$ $75\ u_{pooled2} = \sqrt{(u^2(A,B) + u^2_{RW}(A,B))} = \sqrt{(0.2121^2 + 1.4575^2)} = 1.4728$		$\bar{x}_{(A,B)} = (123 + 124)/2 = 123.5$ $u(A,B) = SD_{(A,B)} = 0.7071\ u_{RW}$ $(A,B) = \sqrt{((3.84^2 + 2.91^2)/2)} = 3.40$ $69\ u_{pooled2} = \sqrt{(u^2(A,B) + u^2_{RW}(A,B))} = \sqrt{(0.7071^2 + 3.4069^2)} = 3.4795$		$\bar{x}_{(A,B)} = (292 + 294)/2 = 293$ $u_{(A,B)} = SD_{(A,B)} = 1.4142\ u_{RW}$ $(A,B) = \sqrt{((7.68^2 + 6.59^2)/2)} = 7.15$ $58\ u_{pooled2} = \sqrt{(u^2(A,B) + u^2_{RW}(A,B))} = \sqrt{(1.4142^2 + 7.1558^2)} = 7.2942$	
$u_{RW(Lot1,Lot2)}$ Equation 2 = $\sqrt{((u_{pooled1}{}^2 + u_{pooled2}{}^2)/2)}$	$\sqrt{(1.6091^2 + 1.4728^2)/2} = 1.5425$		$\sqrt{(3.0733^2 + 3.4795^2)/2} = 3.2827$		$\sqrt{(8.5723^2 + 7.2942^2)/2} = 7.9589$	
$\%u_{RW}$	u RW(Lot1,Lot2)/ $\bar{x}$(Lot1,Lot2)*100 = 1.5425/ ((46.6 + 48.45)/2) = 3.1463%		u RW(Lot1,Lot2)/ $\bar{x}$(Lot1,Lot2)*100 = 3.2827/ ((127.5 + 123.5)/2) = 2.6157%		u RW(Lot1,Lot2)/ $\bar{x}$(Lot1,Lot2)*100 = 7.9589/ ((283 + 293)/2) = 2.7635%	
$\%u_{cal}$	$\%U_{cal}/2 = 2.683\%/2 = 1.3415\%$		$\%U_{cal}/2\ 2.683\%/2 = 1.3415\%$		$\%U_{cal}/2\ 2.683\%/2 = 1.3415\%$	
% $u_{glucose}$ Equation 1 = $\sqrt{(\%u_{cal}{}^2 + \%u_{RW}{}^2)}$	$= \sqrt{(1.3415^2 + 3.1463^2)} = \%3.4205 = 3.4\%$		$= \sqrt{(1.3415^2 + 2.6157^2)} = \%2.9396 = 2.9\%$		$= \sqrt{(1.3415^2 + 2.7635^2)} = \%3.0719 = 3.1\%$	
% $U_{glucose}$ K = 2 (≈95 % confidence)	$\%U_{glucose}*2 = 3.4*2 = 6.8\%$		$\%U_{glucose}*2 = 2.9*2 = 5.8\%$		$\%U_{glucose}*2 = 3.1*2 = 6.2\%$	

IQC, internal quality control.
[a]Converted to mmol/L where possible, as measurements are made in mg/dL.
[b]Numbers of instruments A and B are close to each other, so the weighted formula is not applied.

The AP assessment of glucose using TAE and MU values is given in **TABLE 3**. According to the EuBIVAS, the MU of levels 2 and 3 were at the desirable level, whereas the others were at the minimum level. TAE of level 1 was out of the CLIA limit. Standard MUs (%u) for levels 1 and 3 were out of the minimum limit of EFLM-MU.

Critical value limits according to a 95% level of confidence are given in **TABLE 4**. For patients with low critical values (n = 131, **TABLE 5**), there was a statistically significant difference ($\chi^2 = 7$, $P = .008$) between the number of patients in the gray zone of TAE (n = 27) and ISO/TS 20914 (n = 22).

For patients with high critical value (n = 202, **TABLE 5**), there was a statistically significant difference ($\chi^2 = 6$, $P = .014$) between the number of patients in the gray zone of TAE (n = 33), and ISO/TS 20914 (n = 26).

TABLE 2. MU (Expanded Relative Uncertainty) and TAE Values

	Equation	Level 1	Level 2	Level 3
%MU (according to ISO/TS 20914)	$\%u_{glucose} = \sqrt{(\%u_{cal}^2 + \%u_{RW}^2)}$ ($\%u_{RW}$ for each level and $\%u_{cal}$ from Table 1)	$\%u_{glucose} = \sqrt{(1.3415^2 + 3.1463^2)} = 3.4205\% = 3.4\%$	$\%u_{glucose} = \sqrt{(1.3415^2 + 2.6157)} = 2.9396\% = 2.9\%$	$\%u_{glucose} = \sqrt{(1.3415^2 + 2.7635^2)} = 3.0719\% = 3.1\%$
	$\%U_{glucose} = \%u_{glucose}$*2k = 2(≈95 % confidence)	3.4*2 = 6.8%	2.9*2 = 5.8%	3.1*2 = 6.2%
%TAE [Equation 4]	TAE = (k*%CV) + %Bias [%CV is equal to $\%u_{RW}$ for each level from Table 1 and %u bias according to Equation 5. k = 2 (≈95 % confidence)]	(2*3.1463%) + 2.187% = 8.4%	(2*2.6157%) + 2.1879% = 7.4%	(2*2.7635%) + 2.1879% = 7.7%

MU, measurement uncertainty; TAE, total analytical error.

TABLE 3. The AP Assessment of Glucose Using TAE and MU Values

	Values	ATE-TMH	CLIA	Rili-BAEK	EuBİVAS	EFLM-MU
%MU level 1	6.8%	11%	8%	11%	Minimum, 9.5%	NA
%MU level 2	5.8%	11%	8%	11%	Desirable, 6.5%	NA
%MU level 3	6.2%	11%	8%	11%	Desirable, 6.5%	NA
%u level 1	3.4%	NA	NA	NA	NA	Minimum, 3%[a]
%u level 2	2.9%	NA	NA	NA	NA	Minimum, 3%
%u level 3	3.1%	NA	NA	NA	NA	Minimum, 3%[a]
%TAE level 1	8.4%	11%	8%[a]	11%	Minimum, 9.5%	NA
%TAE level 2	7.4%	11%	8%	11%	Minimum, 9.5%	NA
%TAE level 3	7.7%	11%	8%	11%	Minimum, 9.5%	NA

AP, analytical performance; ATE-TMH, acceptable total error limit of the Turkish Ministry of Health; CLIA, Clinical Laboratory Improvement Amendments; EFLM, European Federation of Clinical Chemistry and Laboratory Medicine; EuBIVAS, European Biological Variation Study; MU, measurement uncertainty; NA, not applicable; Rili-BAEK, Guideline of the German Medical Association on Quality Assurance in Medical Laboratory Examinations; TAE, total analytical error.
[a]*Outside the target limit.*

TABLE 4. Confidence Limits of Critical Value Limits

	Critical Value Limit	Critical Value Limit for 95% Confidence (with MU of ISO/TS 20914)	Critical Value Limit for 95% Confidence (with TAE)
Critical value limit for low serum glucose, mg/dL (mmol/L)[a]	≤50 (2.78)	Equation 6: 1.65*(%u glucose*critical limit)/100	Equation 7: = (1.65 *$\%CV_{glucose}$) + (%Bias)
		50-(1.65*($\%u_{glucose}$*critical limit)/100) = 50-(1.65*(3.4*50)/100) = 50-2.805 = 47.195 = 47 (k = 1.65 for one-sided 95% confidence and $\%u_{glucose}$ for level 1 is 3.4% according to ISO/TS 20914)	50 - [(1.65*($\%CV_{glucose}$*critical limit)/100) + (%Bias*critical limit/100)] = 50-[(1.65*(3.1*50)/100) + (2.2*50/100)} = 50-3.6575 = 46.3425 = 46 (k = 1.65 for one-sided 95% confidence and $\%CV_{glucose}$ for Level 1 is 3.1% and %Bias is 2.2% according to TAE)
		≤47 (2.61)	≤46(2.55)
Critical value limit for high serum glucose, mg/dL (mmol/L)[a]	≥400 (22.2)	Equation 6: 1.65*(%u glucose*critical limit)/100	Equation 7: = (1.65 *$\%CV_{glucose}$) + (%Bias)
		400 + (1.65*($\%u_{glucose}$*critical limit)/100) = 400 + (1.65*(3.1*400)/100) = 400 + 20.46 = 420.46 = 420 (k = 1.65 for one-sided 95% confidence and $\%u_{glucose}$ for level 3 is 3.1% according to ISO/TS20914)	400 + [(1.65*($\%CV_{glucose}$*critical limit)/100) + (%Bias*critical limit/100)] = 400+ [(1.65*(2.8*400)/100) + (2.2*400/100)} = 400 + 27,28 = 427 28 = 427 (k = 1.65 for one-sided 95% confidence and $\%CV_{glucose}$ for level 3 is 2.8% and %Bias is 2.2% according to TAE)
		≥420 (23.3)	≥427 (23.7)

MU, measurement uncertainty; TAE, total analytical error.
[a] *Converted to mmol/L where possible, as measurements are made in mg/dL.*

Discussion

TAE and MU values are used to evaluate the reliability of medical laboratory results. This evaluation must determine the APS. In this study, the TAE and MU of glucose measurement are compared according to 5 different APS, and different performance results were obtained. This situation can be explained by the models defined by

TABLE 5. Gray Zones of Glucose Critical Value Limits and Patient Numbers

	No. of Patients with Low Critical Value	Gray Zone for Low Critical Value (mg/dL)	Gray Zone for Low Critical Value (mmol/L)	No. of Patients in the Gray Zone of Low Critical Value (Percentage of Patients in the Low Gray Zone)	No. of Patients with High Critical Value (Percentage of Patients in the Gray Zone)	Gray Zone for High Critical Value (mg/dL)	Gray Zone for High Critical Value (mmol/L)	No. of Patients in Gray Zone for High Critical Value (Percentage of Patients in the High Gray Zone)
Critical value limit	131	—		—	202	—		—
MU of ISO/TS 20914	109	48–50	2.7–2.8	22 (17%)	176	400–420	22.2–23.3	26 (13%)
TAE	102	47–50	2.6–2.8	29 (22%)	169	400–427	22.2–23.7	33 (16%)

MU, measurement uncertainty; TAE, total analytical error.

the EFLM for analytical performance specifications.[13] Outcome-based MU targets are based on model 1, in which test performance is determined by the impact of clinical outcomes. For this study, it was the most difficult target to achieve because minimum performance is achieved only for level 2. EuBIVAS targets are based on model 2, determined according to biological variation, and are more accessible than model 1 because TAE and MU values were mostly at the minimum level in this study. Rili-BAEK, CLIA, and ATE-TMH targets of glucose were determined according to model 3, which is based on the state of the art principle that represents the highest technically achievable analytical performance, and they were the most suitable targets achieved in terms of this study.

Therefore, the acceptability of the AP of a test varies with the APS applied and whether the TAE or MU value is used. Compliance with the local authority is of priority, and the TAE value in this study is suitable according to the ATE-TMH limit. However, PHL calculates the MU as required by ISO 15189, but no national or international target value has been determined for MU. The ISO/TS 20914 states that[6] "estimating the uncertainty of the results produced is of very limited value unless it can be compared with the allowable MU based on the quality of results required for medical use," and it suggests that the target values for MU should be established as maximum allowable MU and that the upper limit of allowable MU should be based on models defined at the Milan conference and described above.[13]

Braga and Panteghini[11] proposed that target MU values should be determined according to model 1 for glucose; they determined the target standard MU value as a minimum of 3% and a desirable 2% for glucose and stated that the calibrator uncertainty should be at most one-third of the total MU budget. In this case, the calibrator uncertainty should be no more than 0.7% for the desirable level and 1% for the minimum level. Since the standard MU value of the calibrator used in this study is 1.34%, these targets do not seem achievable, and the target standard MU could not be achieved at the minimum level in this study. The target MU defined by Braga and Panteghini is important as being the first target value published on this subject, but there is a need for more laboratories to share their calculations according to ISO/TS 20914 for the attainability of these targets.

An issue that contradicts MU is that TAE adds the bias to a multiple of CV as a constant value. According to the GUM, if only the significance of the bias is statistically demonstrated and cannot be corrected, then it can be added as a constant value to the expanded MU.[2] In contrast, the TAE approach uses the bias from EQA data, and the bias calculation approach amplifies the contribution of bias to TAE by removing the inherent directionality of bias and assumes that the bias now becomes a distribution equally contributing in both directions around the measured result. Due to this difference in approach, TAE values in this study were found to be higher than MU values at all 3 levels.

This study is the first to compare the TAE value of a measurement procedure with the MU value calculated according to ISO/TS 20914, and more work is needed to explain the difference. Two studies in the literature compared the TAE and MU values; both calculated MU according to the Nordtest guideline, and they found the MU value higher than the TAE value.[14,15] However, both of them made the bias calculation based on the EQA data as described in the Nordtest guideline. Unlike the Nordtest guide, ISO/TS 20914 has no recommendations or examples of using EQA data in terms of MU. Therefore, the bias calculation of Nordtest based on the EQA data, similar to the TAE, may lead to a higher MU value. The MU of ISO/TS 20914 used in this study is lower than the TAE value since it does not contain a component based on EQA data.

Another important result of this study is the poor performance of level 1, because the TAE value for level 1 is outside the CLIA target. The MU value is at the minimum level for EuBIVAS, and it is outside the EFLM-MU target. On the other hand, if the 3 levels are evaluated together instead of separately, the performance would be sufficient, as the total TAE value would be below 8%. Since ISO/TS 20914 recommends MU calculations to be made at different concentrations, 3 different levels of MU and TAE calculations are made in this study. It would be more accurate to evaluate the reliability of low critical values according to the low-level measurement performance of glucose, as this study did.

According to the results of this study, if PHL uses the TAE value to evaluate the patient results in the gray zone of critical value limits, it may generate more questionable results, as the number of patients in the gray zone will be higher compared to MU. Whether this statistically significant difference is important from the clinician's point of view and will lead to a change in the treatment process can be clarified by collaborative studies with clinicians. Although some think that this information will only confuse the clinician,[16,17] some suggest methods for sharing this information.[18,19] Considering that a laboratory result does not mean an absolute value and has a probability of distribution, it can be difficult to explain this issue to clinicians. Even laboratory experts have not yet fully resolved the difference between TAE and MU assumptions. In fact, according to a survey, most of them declared that they only calculate MU as a requirement of accreditation and do not know how to use it routinely.[20] As this study and some authors suggest,[18,21] the gray zones of clinical decision limits can be calculated and shared with clinicians.

An issue to discuss here is whether the gray zone limits should be calculated as two-sided or one-sided, or in the positive or negative direction if one-sided. In this study, critical value limits were recalculated according to the example of ISO/TS 20914 in Annex B with Equation 5.[6] Of course,

the reverse of these limits may also be possible. For example, it could be argued that glucose of 53 mg/dL (2.94 mmol/L) has a nonzero probability of having a true value of <50 mg/dL (2.78 mmol/L). The clinician may even prefer to be on the safe side. Collaborative studies between laboratory professionals and clinicians are important to decide which choice of limits is more suitable for patient care. However, due to the retrospective nature of this study, it was necessary to use the calculation suggested by ISO/TS 20914, since the number of patients falling into the gray zones was compared to the critical values reported in the past. It is worth noting that ISO/TS 20914 only gives 2 examples of applying MU values for test result interpretation, and that may not be enough. Although the ISO/TS 20914 standard seems to be subject to criticism due to some of its shortcomings and flaws,[22] it will undoubtedly become an even more important standard for clinical laboratories thanks to its reference in the new version of ISO 15189,[23] which will be published soon. It is extremely important for the quality and standardization of clinical laboratories that ISO/TS 20914 both brings standardization to MU estimation and emphasizes the need to establish MU target values. In addition it creates an important awareness of the application of metrological traceability.[6] The draft version of ISO 15189[23] says that "MU information shall be made available to laboratory users on request." However, there is a need for guidance on how laboratories can take MU values into account, especially when assessing compliance with regulatory limits such as ethanol and addictive substance analysis.

As a limitation of this study, all glucose results were from outpatients. If inpatient results are included, the number of patient results in the gray zones may give more valuable information about the effect of TAE and MU on results around the decision limits. There is no consensus on how to name critical values and what their limits should be in the clinical laboratory, so collaborative studies with clinicians are very important.[24,25] Those studies may also demonstrate the real impact of TAE and MU implementations on clinical decisions and patient care.[26]

Consequently, the TAE and MU approaches can be used to evaluate the AP of clinical laboratory tests. However, the acceptability of the AP of a test varies with the APS applied and whether the TAE or MU value is used. It is extremely important to define achievable MU target values for the adoption of ISO/TS 20914, which is important for standardizing and facilitating MU calculations, by laboratories. TAE and MU values should not only be used to evaluate AP but also to contribute to clinical decision-making. Using the TAE and MU values, it can be easy to define the uncertain regions around the decision limits as gray zones. Since in the formula of TAE the bias value is added as a constant value to the imprecision, it may cause a larger gray zone than the MU value of ISO/TS 20914. This increases the number of questionable patient results for TAE. Whether this situation will make a significant difference in terms of medical diagnosis and treatment should be clarified by collaborative studies with clinicians. It will not be of any use in terms of patient care to discuss the differences between TAE and MU values only among laboratory professionals.

REFERENCES

1. Westgard JO, Carey RN, Wold S. Criteria for judging precision and accuracy in method development and evaluation. *Clin Chem.* 1974;20:825–833.
2. JCGM. Evaluation of measurement data—guide to the expression of uncertainty in measurement. *JCGM*100:2008. GUM 1995 with minor corrections. Available at: https://www.bipm.org/documents/20126/2071204/JCGM_100_2008_E.pdf/cb0ef43f-baa5-11cf-3f85-4dcd86f77bd6. Accessed January 2022.
3. CLSI. Evaluation of total analytical error for quantitative clinical laboratory measurement procedures. *CLSI EP21-A*. 2nd ed. Wayne, PA: Clinical and Laboratory Standards Institute; 2016.
4. International Organization for Standardization. ISO 15189:2012. *Medical Laboratories—Requirements for Quality and Competence*. Geneva, Switzerland: International Standardization Organization; 2012.
5. JCGM. *International Vocabulary of Metrology—Basic and General Concepts and Associated Terms (VIM 3): Bureau International des Poids et Mesures*. 3rd ed. 2012. Available at: https://www.bipm.org/en/search?p_p_id=search_portlet&p_p_lifecycle=2&p_p_state=normal&p_p_mode=view&p_p_resource_id=%2Fdownload%2Fpublication&p_p_cacheability=cacheLevelPage&_search_portlet_dlFileId=41373499. Accessed April 2022.
6. International Organization for Standardization. ISO/TS 20914. *Medical Laboratories—Practical Guidance for the Estimation of Measurement Uncertainty*. Geneva, Switzerland: International Standardization Organization; 2019.
7. İzin Verilen Toplam Hata Sınırları. T.C.Sağlık Baknlığı Sağlık Hizmetleri Genel Müdürlüğü. 2016. Available at https://tetkikteshis.saglik.gov.tr/Eklenti/2581/0/genelge-201618izin-verilen-toplam-hata-sinirlaripdf.pdf. Accessed April 2022.
8. Clinical Laboratory Improvement Amendments of 1988 (CLIA). Proficiency testing regulations related to analytes and acceptable performance. *Fed Reg.* 2019;84:1536–1567.
9. Aarsand AK, Fernandez-Calle P, Webster C, et al. The EFLM Biological Variation Database. https://biologicalvariation.eu/. Accessed March 2022.
10. Revision of the "Guideline of the German Medical Association on Quality Assurance in Medical Laboratory Examinations – Rili-BAEK" (unauthorized translation). *Laboratoriums Medizin.* 2015;39(1):26–69. https://doi.org/10.1515/labmed-2014-0046
11. Braga F, Panteghini M. Performance specifications for measurement uncertainty of common biochemical measurands according to Milan models. *Clin Chem Lab Med.* 2021;59:1362–1368.
12. *Karar Sınırı (Eşik Değer), Kritik Değer (Panik Değer) ve Ölçüm Birimlerinin Harmonizasyonu Prosedürü*. Tetkik ve Teşhis Hizmetleri Dairesi Başkanlığı, T.C. Sağlık Bakanlığı. 2018. Available at https://shgmlabdb.saglik.gov.tr/TR-53826. Accessed April 2022.
13. Ceriotti F, Fernandez-Calle P, Klee GG, et al. Criteria for assigning laboratory measurands to models for analytical performance specifications defined in the 1st EFLM Strategic Conference. *Clin Chem Lab Med.* 2017;55:189–194.
14. Keleş M. Evaluation of the clinical chemistry tests analytical performance by using different models and specifications. *Turk J Biochem.* 2020;45:11–18.
15. Balık AR, Güçel F. Evaluation of 20 clinical chemistry and 12 immunoassay analytes in terms of total analytical error and measurement uncertainty. *Scand J Clin Lab Invest.* 2021;81:517–522. doi:10.1080/00365513.2021.1955294.
16. Westgard JO. Useful measures and models for analytical quality management in medical laboratories. *Clin Chem Lab Med.* 2016;54:223–233. doi:10.1515/cclm-2015-0710.
17. Westgard JO. Managing quality vs. measuring uncertainty in the medical laboratory. *Clin Chem Lab Med.* 2010;48:31–40. doi:10.1515/CCLM.2010.024.
18. Oosterhius WP, Bayat H, Ambruster D, et al. The use of error and uncertainty methods in the medical laboratory. *Clin Chem Lab Med.* 2017;55:225–230.
19. Plebani M, Sciacovelli L, Bernardi D, Aita A. Antonelli G, Padoan A. What information on measurement uncertainty should be communicated to clinicians, and how? *Clin Biochem.* 2018;57:18–22. doi:10.1016/j.clinbiochem.2018.01.017.
20. Westgard SA. Rhetoric versus reality? Laboratory surveys show actual practice differs considerably from proposed models and mandated calculations. *Clin Lab Med.* 2017;37:35–45. doi:10.1016/j.cll.2016.09.004.
21. Lazzati JM, Zaidman V, Maceiras M, Belgorosky A, Chaler E. The use of a "gray zone" considering measurement uncertainty in

pharmacological tests: the serum growth hormone stimulation test as an example. *Clin Chem Lab Med.* 2016;54:349–351.

22. Farrance I, Frenkel R, Badrick T. ISO/TS 20914:2019—a critical commentary. *Clin Chem Lab Med.* 2020;58:1182–1190. doi:10.1515/cclm-2019-1209.
23. ISO/DIS 15189 Medical laboratories—requirements for quality and competence. Available at https://www.iso.org/standard/76677.html. Accessed May 2022.
24. White G, Campbell C, Horvath A. Is this a critical, panic, alarm, urgent, or markedly abnormal result? *Clin Chem.* 2014;60:1569–1570.
25. Campbell CA, Georgiou A, Westbrook JI, Horv AR. What alert thresholds should be used to identify critical risk results: a systematic review of the evidence. *Clin Chem.* 2017;63:1541–1543.
26. Smith AF, Shinkins B, Hall PS, Hulme CT, Messenger MP. Toward a framework for outcome-based analytical performance specifications: a methodology review of indirect methods for evaluating the impact of measurement uncertainty on clinical outcomes. *Clin Chem.* 2019;65:1363–1374. doi:10.1373/clinchem.2018.300954.

Dysregulation of Long Noncoding RNA *NEAT1/miR-199a-5/BiP* Axis in Patients with Diabetic Neuropathy

Seyedeh Sara Hassani, MSc,[1,2] Negin Karamali, MSc,[1,2] Misagh Rajabinejad, PhD,[3,4] Donya Ashjari, MSc,[1,2] Leila Afshar Hezarkhani, MD,[5] Ali Gorgin Karaji, PhD,[2] Farhad Salari, PhD,[2] Alireza Rezaiemanesh, PhD[2,]*

[1]Student Research Committee, School of Medicine, Kermanshah University of Medical Sciences, Kermanshah, Iran, [2]Department of Immunology, School of Medicine, Kermanshah University of Medical Sciences, Kermanshah, Iran, [3]Student Research Committee, School of Medicine, Mazandaran University of Medical Sciences, Sari, Iran, [4]Department of Immunology, School of Medicine, Mazandaran University of Medical Sciences, Sari, Iran, [5]Department of Neurology, School of Medicine, Farabi Hospital, Kermanshah University of Medical Sciences, Kermanshah, Iran. *To whom correspondence should be addressed: alireza.rezaiemanesh@kums.ac.ir.

Keywords: diabetic neuropathy, endoplasmic reticulum stress, inflammation, *NEAT1*, *BiP*, *miR-199a-5*

Abbreviations: T2DM, type 2 diabetes mellitus; DN, diabetic neuropathy; ER, endoplasmic reticulum; AGEs, advanced glycation end products; RAGE, receptor for AGEs; NADPH, nicotinamide adenine dinucleotide phosphate; Nox, NADPH oxidase; UPR, unfolded protein response; *BiP*, binding immunoglobulin protein; lncRNA, long noncoding RNA; miRNA, microRNA; UTR, untranslated region; EMG, electromyography; NCV, nerve conduction velocity; PBMCs, peripheral blood mononuclear cells; cDNA, complementary DNA; ROC, receiver operating characteristic curve; AUC, area under the ROC curve; FBS, fasting blood sugar; HbA1C, hemoglobin A1c; GRP78, glucose-regulated protein 78; RT-qPCR, reverse transcription-quantitative polymerase chain reaction; ATG, autophagy-related gene; GLUT, glucose transporter.

Laboratory Medicine 2023;54:160–165; https://doi.org/10.1093/labmed/lmac082

ABSTRACT

Objective: Diabetic neuropathy (DN) is a type of nerve damage and the most common complication of diabetes. Regarding the association between endoplasmic reticulum (ER) stress with the pathogenesis of neuropathy, this study aims to examine binding immunoglobulin protein (*BiP*) gene expression and long noncoding RNA nuclear enriched abundant transcript 1 (*NEAT1*), *miR-199a-5* as its regulator in the peripheral blood of DN patients compared to diabetic patients without neuropathy.

Methods: Peripheral blood samples were obtained from DN (n = 20) patients and diabetic patients without neuropathy (non-DN) (n = 20). After RNA extraction from peripheral blood mononuclear cells, reverse transcription-quantitative polymerase chain reaction was performed to evaluate RNA expression.

Results: The results showed that the expression level of *NEAT1* and *BiP* genes in the DN group increased significantly compared to the non-DN group. Also, the expression level of *miR-199a-5p* in the DN group was significantly downregulated.

Conclusion: As a result, the axis of *NEAT1*, *miR-199a-5p*, and *BiP* may have a role in the DN pathogenesis.

Type 2 diabetes mellitus (T2DM) is a metabolic disorder, and its prevalence has increased dramatically in recent decades.[1] Neuropathy is the most common chronic complication of T2DM, associated with pain, loss of sensation, and dysfunction in peripheral and autonomic nerves that affect up to 50% of patients with T2DM.[2,3] Types of diabetic neuropathy are classified into 3 general categories: (1) diffuse neuropathy, including distal symmetric polyneuropathy and diabetic autonomic neuropathies; (2) mononeuropathy; and (3) radiculopathy.[4] Increasing the prevalence of T2DM with its inappropriate control increases diabetic neuropathy (DN).[5] In general, T2DM occurs due to insulin resistance or impaired insulin secretion from pancreatic β-cells.[6] Hyperglycemia activates the pathways of advanced glycation end products, polyol, hexosamine, and protein kinase C pathways, leading to oxidative stress, gene expression disturbances, inflammation, and neuronal dysfunction. The oxidative stress induced by hyperglycemia disrupts protein folding and increases misfolded proteins and consequently endoplasmic reticulum (ER) stress. In the other hand, advanced glycation end products (AGEs) interact with receptor for AGEs (RAGE) and activates nicotinamide adenine dinucleotide phosphate (NADPH) oxidase (Nox2/4) at ER and cell membranes. Nox activation also leads to ER stress.[7,8] Studies have shown that ER stress is involved in insulin resistance and reduces pancreatic β-cells mass.[9–11] This ER stress occurs in oxidative damage conditions, calcium or glucose homeostasis disruption, and unfolded/misfolded proteins accumulation.[12] Following the accumulation of unfolded/misfolded proteins and ER stress, unfolded protein response (UPR) is activated to improve ER stress by reducing the arrival of new proteins into the ER lumen and

increasing the number of ER chaperones for the degradation of irreversibly misfolded proteins. If UPR fails, apoptosis occurs.[12–14] UPR signaling is associated with the production of large amounts of proinflammatory cytokines by activating inflammatory pathways such as nuclear factor, mitogen-activated protein kinase (p38MAPK), and C-Jun N-terminal kinase signaling. Thus, ER stress strongly affects cell signaling and plays a vital role in neurodegenerative diseases.[10] Three transmembrane ER stress sensors are required to activate UPR, including inositol-requiring protein 1, activating transcription factor, and PKR-like ER kinase. By the accumulation of unfolded protein in the ER lumen and UPR stimulation, BiP (immunoglobulin heavy chain binding protein, also known as glucose-regulated protein 78 [GRP78] and heat shock protein 5 [HSPA5]) dissociated from ER stress sensors, leading to the subsequent activation.[15] Then, BiP helps with folding correction or preventing the transfer of unfolded/misfolded proteins by binding to these proteins. Therefore, there is a high expression of *BiP* in UPR to maintain ER homeostasis and prevent apoptosis in ER stress.[16,17] Various studies have shown that polymorphisms in *BiP* are correlated with different diseases, including hepatocellular carcinoma, gastric cancer, and colorectal cancer.[18,19] Some reports refer to the role of *BiP* polymorphism in the pathogenesis of DN.[20] Also, studies on diabetic model animals have shown that ER stress can induce apoptosis in the spinal cord and sciatic nerve and affect signal transduction.[21] Considering the importance of the BiP protein, studying its regulatory mechanisms can play an essential role in clarifying the pathogenesis of DN and the development of its therapies.

Long noncoding RNAs (lncRNA) are nonprotein-coding transcripts over 200 nucleotides in length and potential microRNA (miRNA) sponges that regulate gene expression.[22] Nuclear enriched abundant transcript 1 (*NEAT1*) is an lncRNA with evidence of its possible role in DN pathogenesis.[23–25] This lncRNA is located on chromosome 11q13.1 and regulates several pathways associated with neurodegeneration, including inflammation and neuronal apoptosis in the absence of cellular oxygen or glucose.[25] Studies have shown that miRNA, as another ncRNA, can directly target the 3 prime untranslatable regions (3'-UTR) of the mRNA sequence and thus reduce gene expression, such as the *miR-199a-5*, which targets the *BiP* gene.[26] Based on previous reports and in silico evaluation and for determining the role of the lncRNA *NEAT1*, *miR-199a-5*, *BiP* axis in DN pathogenesis, we evaluated the gene expression of each ncRNA and their target gene in the peripheral blood mononuclear cells of DN patients.

Methods

Participants

In this study, whole blood samples (5 mL) were obtained from 20 DN patients and 20 non-DN patients as the control group referred to Farabi Clinic and Taleghani Hospital, Kermanshah, Iran. T2DM was determined according to the Report of the Expert Committee on the Diagnosis and Classification of Diabetes Mellitus.[23,27] The diagnosis of diabetic neuropathy was based on the clinical finding. Neuropathy complication in patients was confirmed by electromyography (EMG) and nerve conduction velocity (NCV) tests and confirmed by a neurologist. NCV/ EMG tests are an essential diagnostic tool in peripheral neuropathy.[26] Nerve conduction studies are considered to be the gold standard for the diagnosis of diabetic peripheral neuropathy.[27] The demographic characteristics of participants are shown in **TABLE 1**. Patients with diabetes were matched in age, sex, and type of medications in both groups. Samples are taken from nonsmoking patients based on their history. After collecting blood, the total RNA extraction was performed immediately.

The study was conducted with the support of the Ethics Committee of the Kermanshah University of Medical Sciences (IR.KUMS.REC.1399.250). Written informed consent was obtained from all participants.

Bioinformatics Analysis

According to TargetScan, miRanda, miRTarBase, and miRDB databases, miRNAs targeting *BiP* were intensely screened, and the *miR-199a-5* was selected because of the highest correlation score. Lncrnadb, NONCODE, and StarBase databases were also used to determine the lncRNA related to miR-199a-5p. We used the DIANA algorithm to check the interaction score between lnc*NEAT1* and *hsa-miR-199a-5*. The GeneCards database was used to examine the expression of genes in the peripheral blood mononuclear cells as well.

TABLE 1. Baseline Characteristics and Clinical Presentations of Subjects

Variables	Groups	
	Diabetic Neuropathy Patients (n = 20)	Diabetes without Neuropathy Patients (n = 20)
Age (y) (mean ± SEM)	58.20 ± 1.44	57.60 ± 1.83
Sex (male/female)	12 (60%)/8 (40%)	6 (30%)/14 (70%)
Duration of diabetes (y)	13.92 ± 0.9[b]	8.35 ± 0.82
Drugs		
Gabapentin	+	–
Nortriptyline	+	–
Insulin	–	–
Lab tests (mean ± SEM)		
FBS (mg/dL)	238.95 ± 19.3[b]	155.27 ± 13.29
HbA1c (%)[a]	9.35 ± 0.44 (n = 19)[c]	7.97 ± 0.34 (n = 13)
Cholesterol (mg/dL)	166.33 ± 11.43	166.60 ± 8.85

FBS, fasting blood sugar; HbA1c, hemoglobin A1c; SEM, standard error of the mean.
[a]*Data from HbA1c: 19 patients with diabetic neuropathy and 13 diabetic patients were available.*
[b]$P < .001$.
[c]$P < .05$.

RNA Extraction and cDNA Synthesis

Total RNA was extracted from the peripheral blood mononuclear cells (PBMCs) using the NORGEN Biotek Total RNA Purification Kit (Norgen Biotek) according to the kit protocol. The quality of extracted RNA and concentration was measured using a Nanodrop device (Nanodrop 2000 Spectrophotometer ThermoScientific). Complementary DNA (cDNA) synthesis for mRNA was performed using the nRT-ROSET Kit (ROJETechnologies). Also, the miRCURY LNA RT Kit (Qiagen) was used for miRNA cDNA synthesis.

Quantitative Real-Time Polymerase Chain Reaction

Measurement of the lncRNA expression and target gene was performed using SYBER green Premix (Ampliqon) by the real-time polymerase chain reaction (RT-PCR) technique (LighCycler 96 instrument, Roche Applied Science), and miRCURY LNA SYBR Green PCR Kit (ID:339345) was used for microRNA expression. The quantitative (q)RT-PCR primers are shown in **TABLE 2**, and the miRNA primer was ordered from QIAGEN. U6 small nuclear RNA and 18s ribosomal RNA were used as the internal control to normalize gene and ncRNA expression. The melting curve was analyzed to evaluate the specificity of the qRT-PCR product. qRT-PCR was performed in duplicate for all samples.

Statistics

The obtained data were analyzed using Excel and GraphPad Prism software version 8 (GraphPad Software). Mann-Whitney *U* test was used for nonparametric and unpair variables to compare data between 2 groups. The receiver operating characteristic (ROC) curve and area under the curve (AUC) were evaluated to check the specificity and sensitivity of the genes expression as biomarkers for DN patients compared to controls. In general, $P < .05$ was considered as significant. The $2^{-\Delta\Delta CT}$ formula was used to calculate the relative expression of gene and ncRNAs, as described by Pfaffel.[28]

Results

Demographic Data and Laboratory Findings

As shown in **TABLE 1**, demographic information and laboratory test results were examined between the DN and non-DN groups. Duration of diabetes, fasting blood sugar (FBS; $P < .001$), and hemoglobin A1c (HbA1c; $P < .05$) were significantly higher in DN patients compared to the non-DN group, but there was no significant difference in their serum cholesterol levels.

TABLE 2. Primer Sets and Their Specifications Used in Quantitative Real-Time PCR

Type of Genes	Gene Name	Sequences
Target genes	*NEAT1*	F: 5′-GCCAGTGTGAGTCCTAGCATTG-3′
		R: 5′-ACTTCCTCCTCCTAAGCCTCTG-3′
	BiP	F: 5′-GGGAAAGAAGGTTACCCATGC-3′
		R: 5′-TCTTTGGTTGCTTGGCGTTG-3′
Reference genes	*18s rRNA*	F: 5′-GTAACCCGTTGAACCCCATT-3′
		R: 5′-CCATCCAATCGGTAGTAGCG-3′
	U6 snRNA	F: 5′-CTCGCTTCGGCAGCACA-3′
		R: 5′-AACGTTCACGAATTTGCGT-3′

Gene Expression Levels

Analysis of qPCR data showed that lncRNA *NEAT1* and *BiP* expression levels were significantly higher in the DN group than in the non-DN group, respectively (fold change = 2.76, $P = .01$, **FIGURE 1A**) (fold change = 2.29, $P = .01$, **FIGURE 1C**). Also, the expression level of *miR-199a-5* was significantly lower in the DN group than the control group (fold change = 0.44, $P = .04$, **FIGURE 1B**)

ROC Curve Analysis

AUC for lncRNA *NEAT1* was 0.7 (good diagnostic accuracy, $P = .01$, 95% CI = 0.5616–0.8809) and the optimum cutoff point of lnc*NEAT1* was 1.15 (80% sensitivity and 60% specificity). For *miR-199a-5*, the AUC value was 0.7 ($P = .04$, 95% CI = 0.5516–0.9651) and the optimum cutoff point was 0.66 (sensitivity 66% and specificity 70%), and for *BiP* the AUC value was 0.8 ($P = .01$, 95% CI = 0.6191–0.9920) and its optimum cutoff point was 1.7 (75% sensitivity and 77% specificity) (**FIGURE 2**).

Discussion

The regulatory axis of lnc*NEAT1*, *miR-199a-5*, and *BiP* gene expression in the PBMCs of patients with DN compared to type 2 diabetic patients without neuropathy were measured in this study. DN is a complication with a significant increase in immune cells and their infiltration into the diabetic nerves and activation of macrophages, dendritic cells (DCs), and T cells, including CD8+ cells. Immune cells are involved in the pathogenesis of DN; in addition to developing inflammation and oxidative stress, they trigger immune responses and ultimately damage peripheral nerves.[29,30] Studies have shown that *NEAT1* is associated with NOD-like receptor family pyrin domain containing 3, NLR family CARD domain containing 4 (NLRC4), and absent in melanoma 2 (AIM2) inflammasome, leading to the induction of pyroptosis in hypoxic conditions. It can increase the expression of inflammatory cytokines and chemokines (such as IL6 and C-X-C motif chemokine ligand 10 [CXCL10]) in hyperglycemia. This lncRNA can also play a role in regulating neuronal apoptosis.[31–33] Therefore, in our study, lnc*NEAT1* expression was increased significantly in DN patients compared to the control group, probably due to the role of *NEAT1* in the pathogenesis of the inflammatory process and neuronal destruction. Our findings showed that the expression of *miR-199a-5* in DN patients was significantly lower than in the control group (**FIGURE 1**).

In previous studies, *miR-199a* was defined as a potential autophagy suppressor in cardiomyocytes, and *BiP* was identified as a direct target of *miR-199a* in this process.[34] A study in 2018 by Li et al[35] on diabetic patients showed that *miR-199a-5* expression was increased and autophagy-related gene 14 (ATG14) was decreased, which resulted in a reduction in autophagy in the liver. The knockdown of *miR-199a-5* decreased insulin-dependent phosphorylation of insulin receptor β (IRβ), AKT, and glycogen synthase kinase-3 (GSK3) in vitro. This study suggested the biological role of *miR-199a-5* in regulating hepatocyte insulin sensitivity through the regulation of ATG14-mediated autophagy.[35] High levels of *miR-199a* were observed in the plasma of patients with T2DM in a study by Yan et al[36] in 2014. They also showed that *miR-199a* could play a role in insulin resistance by targeting glucose transporter 4 (GLUT4) in L6 cells.[36] According to our results, the *BiP* gene expression in DN patients was significantly higher than that of the control group. Induction of ER stress and accumulation of unfolded proteins are involved in the pathogenesis of neurodegenerative

FIGURE 1. Comparison of expression levels of the studied genes in patient and control groups. A, Gene expression of lnc*NEAT1* in neuropathic patients was significantly increased compared to the control group. B, The level of expression of *miR-199a-5* in neuropathic patients decreased significantly compared to the diabetic group without neuropathy (C) and the expression of the *BiP* gene in neuropathic patients compared to the control group showed a significant increase. DN, diabetic neuropathy; T2DM, type 2 diabetes mellitis.

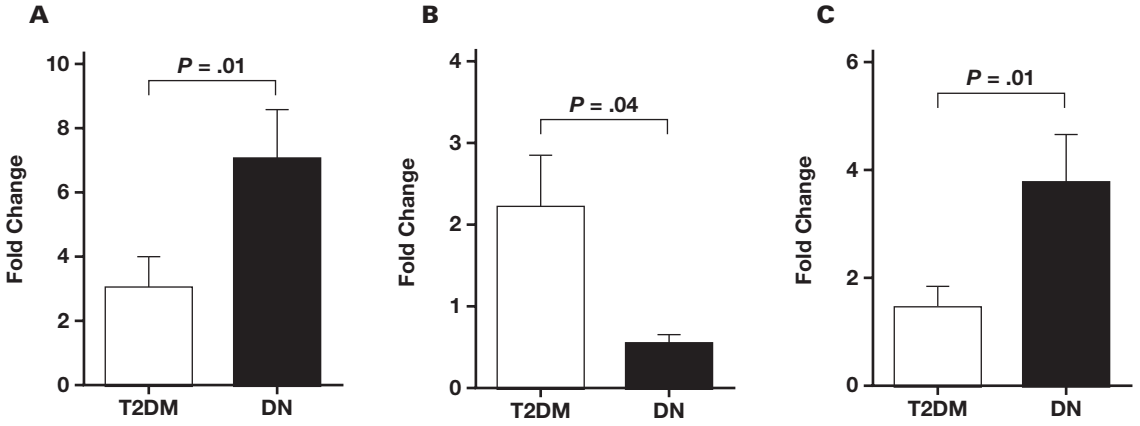

FIGURE 2. Receiver operating characteristic curve and area under the curve (AUC) for expression of *NEAT1* (AUC = 0.7; 95% CI = 0.5616–0.8809; *P* = .01) (A), *miR-199a-5* (AUC = 0.7; 95% CI = 0.5516–0.9651; *P* = .04) (B), and *BiP* gene (AUC = 0.8; 95% CI = 0.6191–0.9920; *P* = .01) (C).

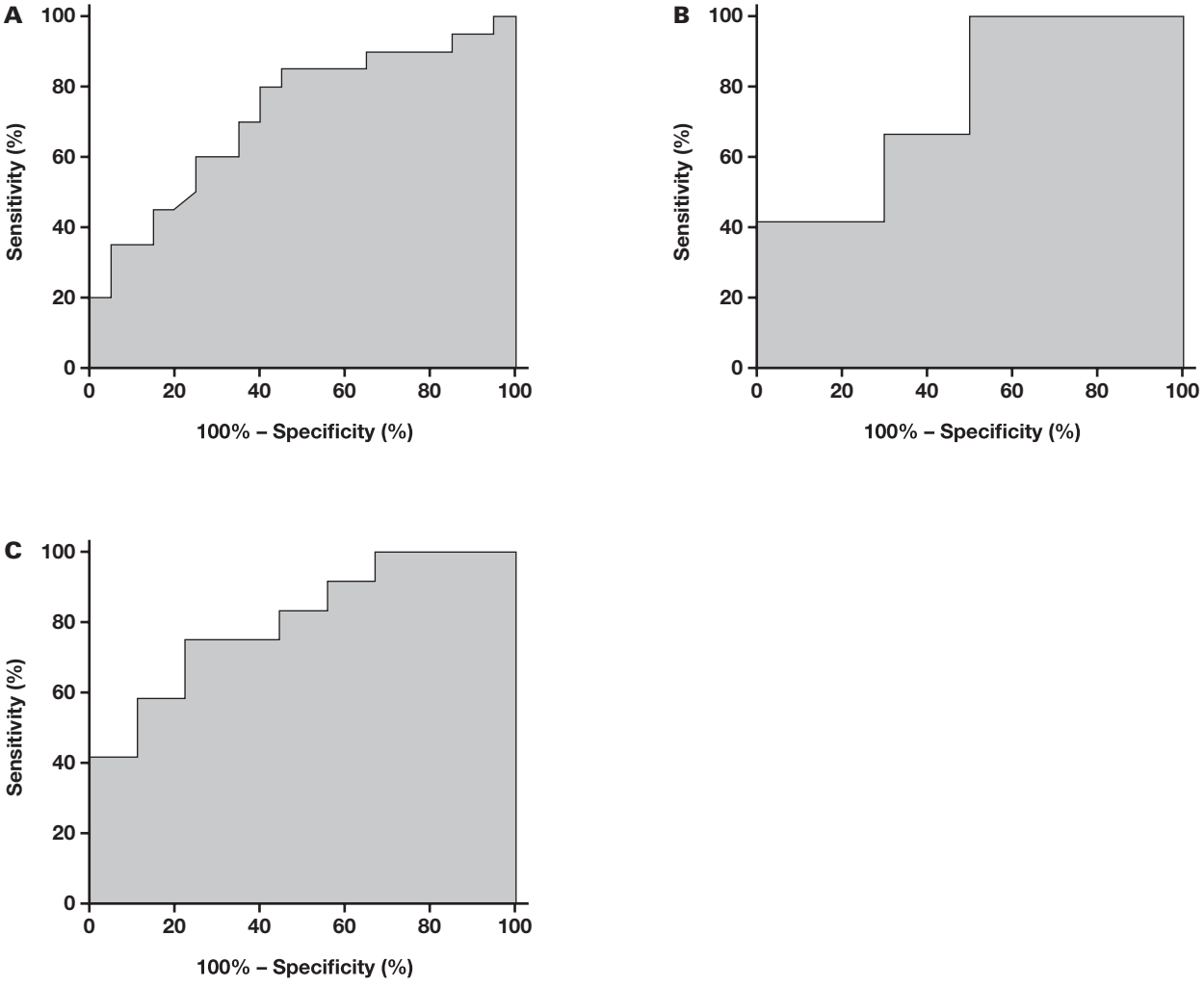

diseases such as Parkinson, Alzheimer, and neuropathy disease.[37] The *BiP* has been mentioned in different studies as a therapeutic target for neurodegenerative diseases.[38] Gorbatyuk et al[39] in 2012 showed that increased BiP expression levels were associated with decreased ER stress mediators, apoptosis, and α-synuclein neurotoxicity and resulted in survival tyrosine hydroxylase-positive nigral cells. Thus, BiP molecular chaperone has a neuroprotective role against alpha-synuclein in degenerative neuronal diseases such as Parkinson disease.[39] Considering the role of ER stress and BiP in the pathogenesis of neurodegenerative diseases mentioned in the previous studies, it can be concluded that increased *BiP* gene expression can be associated with ER stress induced by hyperglycemia. The final goal of UPR activation is to reduce cellular stress and restore homeostasis by decreasing protein translation, synthesis of molecular chaperones such as BiP, and activating ER-associated protein degradation that is responsible for the destruction of translocated proteins in the proteasome. The activation of autophagy after ER stress protects the cell from death; however, in conditions of continuous stimulation and prolonged stress of the ER, the autophagy pathway and the response pathway of unfolded proteins lead to apoptosis.[40]

According to the association of lnc*NEAT1* and *miR-199a-5* based on bioinformatics tools and previous studies,[34] the inhibitory role of *NEAT1* on *miR-199a-5* is defined.[41] In our research, increasing *NEAT1* expression along with reduced *miR-199a-5* expression was probably related to the inhibitory effect of lnc*NEAT1* in DN patients. Also, one of the inhibitory targets of *miR-199a-5* is the mRNA of the *BiP* gene.[26] Decreased expression of *miR-199a-5* in DN patients probably leads to an increase in *BiP* gene expression due to reducing its inhibitory effect on the target gene. Increased *BiP* expression may indicate activation of ER stress and UPR mediators involved in the pathogenesis of DN, which acts as a stimulant of neuronal dysfunction and apoptosis of Langerhans β-cells under chronic cellular stress.

In general, considering the changes in the expression of lnc*NEAT1*/*miR-199a-5*/*BiP* regulatory axis in DN patients, it can be expected that positive effects will be observed by targeting this pathway in improving patients. In the future, further clinical and preclinical research on the regulatory impact of this axis in the pathogenesis of DN will be necessary.

Conclusion

In summary, our study indicated that *NEAT1* and *BiP* were upregulated whereas *miR-199a-5* was downregulated in DN patients compared with the T2DM control group. Considering the inflammatory and neurodegenerative effects of *NEAT1* and *BiP* on the nervous system, it can be concluded that the disturbance in this axis may associate with activation of ER stress mediators and UPR that act as stimuli for β-Langerhans cells dysfunction and their apoptosis in chronic cellular stress. One of the limitations in this study was the small sample size, limiting other data analysis. Further studies with more samples are suggested in the future to determine the role of this axis in the pathogenesis of DN and to identify it as a therapeutic goal or gene therapy.

Acknowledgments

We thank all the patients and medical staff who generously contributed to this study.

Ethical Statement

The protocol of the study was endorsed by the ethical committee of Kermanshah University of Medical Sciences (ethical code: IR.KUMS.REC.1399.250) for the use of human participants. All study subjects signed informed consent before sampling. All research was performed in accordance with relevant guidelines and regulations of Kermanshah University of Medical Sciences.

Funding

This research has been supported by grants from Kermanshah University of Medical Sciences (KUMS grant No. 990342).

REFERENCES

1. Cho NH, Shaw JE, Karuranga S, et al. IDF Diabetes Atlas: global estimates of diabetes prevalence for 2017 and projections for 2045. *Diabetes Res Clin Pract.* 2018;138:271–281. doi:10.1016/j.diabres.2018.02.023.
2. Tesfaye S, Boulton A. *Diabetic Neuropathy (Oxford Diabetes Library).* Oxford, UK: Oxford University Press; 2011.
3. Boulton AJM. Management of diabetic peripheral neuropathy. *Clin Diabetes.* 2005;23(1):9.
4. Pop-Busui R, Boulton AJ, Feldman EL, et al. Diabetic neuropathy: a position statement by the American Diabetes Association. *Diabetes Care.* 2017;40(1):136–154. doi:10.2337/dc16-2042.
5. Gries FA, Cameron NE, Low PA, Ziegler D. eds. *Textbook of Diabetic Neuropathy*. Stuttgart, Germany: Thieme; 2003.
6. Kahn SE, Hull RL, Utzschneider KM. Mechanisms linking obesity to insulin resistance and type 2 diabetes. *Nature.* 2006;444(7121):840–846. doi:10.1038/nature05482.
7. Edwards JL, Vincent AM, Cheng HT, Feldman EL. Diabetic neuropathy: mechanisms to management. *Pharmacol Therapeut.* 2008;120(1):1–34. doi:10.1016/j.pharmthera.2008.05.005.
8. Pathomthongtaweechai N, Chutipongtanate S. AGE/RAGE signaling-mediated endoplasmic reticulum stress and future prospects in non-coding RNA therapeutics for diabetic nephropathy. *Biomed Pharmacother.* 2020;131:110655.
9. Eizirik DL, Cardozo AK, Cnop M. The role for endoplasmic reticulum stress in diabetes mellitus. *Endocr Rev.* 2008;29(1):42–61. doi:10.1210/er.2007-0015.
10. O'Brien PD, Hinder LM, Sakowski SA, Feldman EL. ER stress in diabetic peripheral neuropathy: a new therapeutic target. *Antiox Redox Signal*. 2014;21(4):621–33. doi:10.1089/ars.2013.5807.
11. Prentki M, Nolan CJ. Islet beta cell failure in type 2 diabetes. *J Clin Invest.* 2006;116(7):1802–1812. doi:10.1172/JCI29103.
12. Ron D, Walter P. Signal integration in the endoplasmic reticulum unfolded protein response. *Nat Rev Mol Cell Biol.* 2007;8(7):519–529. doi:10.1038/nrm2199.
13. Cross M, Smith E, Hoy D, et al. The global burden of rheumatoid arthritis: estimates from the Global Burden of Disease 2010 study. *Ann Rheum Dis.* 2014;73(7):1316–1322. doi:10.1136/annrheumdis-2013-204627.
14. Lupachyk S, Watcho P, Stavniichuk R, Shevalye H, Obrosova IG. Endoplasmic reticulum stress plays a key role in the pathogenesis of diabetic peripheral neuropathy. *Diabetes.* 2013;62(3):944–952. doi:10.2337/db12-0716.
15. Back SH, Kaufman RJ. Endoplasmic reticulum stress and type 2 diabetes. *Annu Rev Biochem.* 2012;81:767–793. doi:10.1146/annurev-biochem-072909-095555.
16. Gething MJ, Sambrook J. Protein folding in the cell. *Nature.* 1992;355(6355):33–45. doi:10.1038/355033a0.
17. Zhang XY, Yang SM, Zhang HP, et al. Endoplasmic reticulum stress mediates the arsenic trioxide-induced apoptosis in

human hepatocellular carcinoma cells. *Int J Biochem Cell Biol.* Nov 2015;68:158–165. doi:10.1016/j.biocel.2015.09.009.

18. Zhu X, Zhang J, Fan W, et al. The rs391957 variant cis-regulating oncogene GRP78 expression contributes to the risk of hepatocellular carcinoma. *Carcinogenesis.* 2013;34(6):1273–1280. doi:10.1093/carcin/bgt061.
19. Winder T, Bohanes P, Zhang W, et al. GRP78 promoter polymorphism rs391957 as potential predictor for clinical outcome in gastric and colorectal cancer patients. *Ann Oncol.* 2011;22(11):2431–2439.
20. Jia Y, Tong Y, Min L. Significance of functional GRP78 polymorphisms in predicting the onset of type 2 diabetic peripheral neuropathy in Chinese population. *Neurol Res.* 2015;37(8):683–687. doi:10.1179/1743132815Y.0000000054.
21. Pan H, Huang H, Zhang L, Ma S, Yang H. Wang H. "Adjusting internal organs and dredging channel" electroacupuncture treatment prevents the development of diabetic peripheral neuropathy by downregulating glucose-related protein 78 (GRP78) and caspase-12 in streptozotocin-diabetic rats. *J Diabetes.* 2019;11(12):928–937. doi:10.1111/1753-0407.12916.
22. Moore JB, Uchida S. Functional characterization of long noncoding RNAs. *Curr Opin Cardiol.* 2020;35(3):199–206. doi:10.1097/HCO.0000000000000725.
23. Asadi G, Rezaei Varmaziar F, Karimi M, et al. Determination of the transcriptional level of long non-coding RNA NEAT-1, downstream target microRNAs, and genes targeted by microRNAs in diabetic neuropathy patients. *Immunol Lett.* 2021;232:20–26. doi:10.1016/j.imlet.2021.01.007.
24. Zhan JF, Huang HW, Huang C, Hu LL, Xu WW. Long non-coding RNA NEAT1 regulates pyroptosis in diabetic nephropathy via mediating the miR-34c/NLRP3 axis. *Kidney Blood Press Res.* 2020;45(4):589–602. doi:10.1159/000508372.
25. An H, Williams N, Shelkovnikova T. NEAT1 and paraspeckles in neurodegenerative diseases: A missing lnc found? *Noncoding RNA Res.* 2018;11(01):3.
26. Su SF, Chang YW, Andreu-Vieyra C, et al. miR-30d, miR-181a and miR-199a-5p cooperatively suppress the endoplasmic reticulum chaperone and signaling regulator GRP78 in cancer. *Oncogene.* 2013;32(39):4694–4701. doi:10.1038/onc.2012.483.
27. Report of the Expert Committee on the Diagnosis and Classification of Diabetes Mellitus. *Diabetes Care.* 2003;26(suppl 1):S5–S20.
28. Pfaffl M, WA. new mathematical model for relative quantification in real-time RT–PCR. *Nucleic Acids Res.* 2001;29(9):e45–e45.
29. O'Brien JA, McGuire HM, Shinko D, et al. T lymphocyte and monocyte subsets are dysregulated in type 1 diabetes patients with peripheral neuropathic pain. *Brain Behav Immun Health.* 2021;15:100283.
30. Younger D, Rosoklija G, Hays A, Trojaborg W, Latov N. Diabetic peripheral neuropathy: a clinicopathologic and immunohistochemical analysis of sural nerve biopsies. *Muscle Nerve.* 1996;19(6):722–727.
31. An H, Williams NG, Shelkovnikova TA. NEAT1 and paraspeckles in neurodegenerative diseases: a missing lnc found? *Noncoding RNA Res.* 2018;3(4):243–252. doi:10.1016/j.ncrna.2018.11.003.
32. Spreafico M, Grillo B, Rusconi F, Battaglioli E, Venturin M. Multiple layers of CDK5R1 regulation in Alzheimer's disease implicate long non-coding RNAs. *Int J Mol Sci .* 2018;19(7):2022. doi:10.3390/ijms19072022.
33. Zhang P, Cao L, Zhou R, Yang X, Wu M. The lncRNA Neat1 promotes activation of inflammasomes in macrophages. *Nat Commun.* 2019;10(1):1495. doi:10.1038/s41467-019-09482-6.
34. Chen L, Wang F-Y, Zeng Z-Y, et al. MicroRNA-199a acts as a potential suppressor of cardiomyocyte autophagy through targeting Hspa5. *Oncotarget.* 2017;8(38):63825–63834. doi:10.18632/oncotarget.19133.
35. Li B, Wu X, Chen H, et al. miR199a-5p inhibits hepatic insulin sensitivity via suppression of ATG14-mediated autophagy. *Cell Death Dis.* 2018;9(3):1–15.
36. Yan S-T, Li C-L, Tian H, et al. miR-199a is overexpressed in plasma of type 2 diabetes patients which contributes to type 2 diabetes by targeting GLUT4. *Mol Cell Biochem.* 2014;397(1-2):45–51. doi:10.1007/s11010-014-2170-8.
37. Enogieru AB, Omoruyi SI, Hiss DC, Ekpo OE. GRP78/BIP/HSPA5 as a therapeutic target in models of Parkinson's disease: a mini review. *Adv Pharmacol Sci.* 2019;2019:1–11. doi:10.1155/2019/2706783.
38. Gorbatyuk MS, Gorbatyuk OS. The molecular chaperone GRP78/BiP as a therapeutic target for neurodegenerative disorders: a mini review. *J Genet Syndr Gene Ther.* 2013;4(2).
39. Gorbatyuk MS, Shabashvili A, Chen W, et al. Glucose regulated protein 78 diminishes α-synuclein neurotoxicity in a rat model of Parkinson disease. *Mol Ther.* 2012;20(7):1327–1337. doi:10.1038/mt.2012.28.
40. Mokaram P, Dastghaib S, Siri M, Rezayi S. Evaluation of endoplasmic reticulum stress mechanism and unfold protein response signaling in cancer. *Sadra Med J*. 2018;6(4):317–330.
41. Zhang Q, Cheng Q, Xia M, Huang X, He X, Liao J. Hypoxia-induced lncRNA-NEAT1 sustains the growth of hepatocellular carcinoma via regulation of miR-199a-3p/UCK2. *Front Oncol.* 2020;10:998. doi:10.3389/fonc.2020.00998.

Elevated Kynurenine Levels in Patients with Primary Sjögren's Syndrome

Hakan Apaydın, MD,[1,] Cemile Koca Bicer, MD,[2] Emine Feyza Yurt, MD,[2] Muhittin Abdulkadir Serdar, MD,[3] İsmail Dogan, MD,[4] and Sukran Erten, MD[4]*

[1]Department of Rheumatology, Ankara City Hospital, Ankara, Turkey, [2]Department of Biochemistry, Ankara City Hospital, Ankara Yıldırım Beyazıt University, Ankara, Turkey, [3]Department of Biochemistry, Acıbadem University, İstanbul, Turkey, [4]Department of Rheumatology, Ankara City Hospital, Ankara Yıldırım Beyazıt University, Ankara, Turkey. *To whom correspondence should be addressed: drhakanapaydin@gmail.com.

Keywords: autoimmune, connective tissue disease, IDO, kynurenine, Sjögren's syndrome, tryptophan

Abbreviations: Trp, tryptophan; pSS, primary Sjögren's syndrome; Kyn, kynurenine; sSS, secondary SS; RA, rheumatoid arthritis; SLE, systemic lupus erythematosus; IDO, indoleamine 2,3-dioxygenase; EULAR, European League Against Rheumatism; ESSDAI, EULAR Sjögren's Syndrome Disease Activity Index; ESSPRI, EULAR SS Patient Reported Index; LC-MS/MS, liquid chromatography with tandem mass spectrometry; SSc, systemic sclerosis; CRP, C-reactive protein; KP, kynurenine pathway; AS, ankylosing spondylitis.

Laboratory Medicine 2023;54:166–172; https://doi.org/10.1093/labmed/lmac084

ABSTRACT

Objective: We aimed to investigate the plasma levels of tryptophan (Trp) and its metabolites in patients with primary Sjögren's syndrome (pSS).

Methods: The study included 34 pSS patients and 42 healthy individuals, and serum Trp and kynurenine (Kyn) concentrations were measured by liquid chromatography with tandem mass spectrometry. Trp degradation was predicted using the ratio of Kyn and Trp concentrations (Kyn/Trp).

Results: In our study, the mean serum Trp concentration was found to be considerably lower in the pSS group than in the control group ($P = .001$). The levels of Kyn ($P = .019$) and the Kyn/Trp ratio ($P < .001$) were significantly higher in the pSS group than in the control group. The Kyn/Trp ratio was negatively correlated with C-reactive protein ($r = -0.369$, $P = .032$).

Conclusion: We found that Kyn pathway metabolism was altered in patients with pSS. This suggests that Trp metabolism may be closely linked to the disease pathogenesis of pSS.

Primary Sjögren's syndrome (pSS) is a chronic systemic autoimmune illness characterized by salivary and lacrimal gland involvement, resulting in keratoconjunctivitis sicca and xerostomia, as well as various extraglandular signs such as severe fatigue, vasculitis, and multiorgan involvement.[1] Secondary Sjögren's syndrome (sSS), which occurs as a result of other autoimmune illnesses, is distinguished from pSS[2]; sSS is commonly found in connective tissue diseases such as rheumatoid arthritis (RA) and systemic lupus erythematosus (SLE), and it is less commonly found in multiple sclerosis, autoimmune hepatitis, and thyroiditis.[3] Sjögren's syndrome predominantly affects women, and the incidence of the disease ranges from 3 to 11 cases per 100,000 population,[4,5] with a prevalence ranging from 0.01% to 0.72%.[6]

pSS is a disease whose etiology is not yet fully understood, as in most autoimmune diseases, where genetic, epigenetic, and environmental factors are hypothesized to play into the pathogenesis of the disease. pSS has a complicated pathophysiology that is multifaceted and linked to a number of genetic, immunological, environmental, and hormonal risk factors.[7] The disease course can be divided into several phases due to its complexity: an initiation phase triggered by exogenous and endogenous causes, dysregulation of salivary gland epithelial cells, immune system activation, and chronic inflammation stimulated by B cell hyperactivity.[8] Both innate and acquired immunity play a role in the pathogenesis of pSS, each constituting a multistep process that leads to illness onset and persistence. Persistent B-cell activation and the proliferation of Th1 and Th17 cells contribute to the progression of the disease.[9] Nevertheless, the exhaustive mechanism of disease progression in the salivary and lacrimal glands is still unknown.[10]

Serotonin and kynurenines (Kyn) are the indispensable amino acid tryptophan (Trp) metabolites, and the Kyn pathway is the main pathway of Trp metabolism, responsible for approximately 90% of its catabolism. The rate-limiting enzyme in this Trp catabolism pathway is indoleamine 2,3-dioxygenase (IDO), which converts Trp to Kyn.[11] It is thought that the catabolism of Trp via Kyn plays an important immunosuppressive role.[12,13] It has been found that blood Trp concentrations are decreased in RA patients,[14] various cancers,[15] and other autoimmune diseases such as antineutrophil cytoplasmic antibody-associated vasculitis.[16] The IDO expression is induced by immune mediators, particularly interferon.[17] Although IDO expression is usually quite low, it can be significantly upregulated in response to infection and inflammation.[18] The Kyn pathway produces an immunosuppressive effect by simultaneously activating Treg cells and decreasing effector T cell responses.[19] The IDO

plays a substantial role in sustaining peripheral immunological tolerance.[20] Increased Kyn concentration is common in many diseases, such as RA,[21] SLE,[22] and Huntington disease.[23] Also, Kyn and its metabolites are biologically active. For instance, in the immune system, Kyn and its metabolites play a role in suppressing the immune system.[13] Recently, there has been increasing interest in the role of Kyn in the regulation and maintenance of immune homeostasis. However, the precise role of IDO and the regulatory Kyn pathway in autoimmunity remains unclear.

In this study, we investigated levels of Trp and its metabolites in the Kyn pathway in patients with pSS and in healthy controls. Also, through the relationship between Trp metabolites, laboratory parameters, and disease activity was evaluated in patients with pSS.

Materials and Methods

Patients

This study was conducted in Ankara Yıldırım Beyazıt University Medical Faculty Atatürk Training and Research Hospital and Ankara City Hospital. Thirty-four pSS patients who were diagnosed according to the 2016 classification criteria of the American College of Rheumatology/European League Against Rheumatism (EULAR)[24] and 42 healthy volunteers were recruited into the study. The EULAR Sjögren's Syndrome Disease Activity Index (ESSDAI)[25] and the EULAR SS Patient Reported Index (ESSPRI)[26] were used to assess disease activity. Healthy subjects who did not have an autoimmune condition and malignancy were included as controls. At the time of enrollment, all study participants were checked to ensure that they were free of symptoms of underlying viral infections. The study was approved by the ethics committee decision of Ankara Yıldırım Beyazıt University Medical Faculty Local Ethics Committee and written informed consent was obtained from all subjects.

Analysis and Determination of Tryptophan and Kynurenine Concentrations

Following the approval of the ethics committee, peripheral venous blood samples from all individuals included in the study under fasting (12 hours) were taken into tubes for blood testing. Plasma and serum samples were obtained by centrifugation for 10 minutes at 3000*g* and were stored at −80°C until day of analysis. Parameters were measured on the same day.

Trp and Kyn were measured in plasma samples using liquid chromatography–tandem mass spectrometry (LC-MS/MS) as previously described.[27] Trp degradation was determined using the ratio of Kyn and Trp concentrations. This ratio shows IDO enzyme activity.[28] The Kyn/Trp ratio was calculated in μmol/mmol.

Statistical Analysis

Continuous variables showing normal distribution were analyzed by Kolmogorov-Smirnov test. Independent samples *t*-test and Mann-Whitney *U* test were performed to evaluate whether there was a statistically significant difference between patient and control groups. Correlations between groups were evaluated by Spearman rank correlation analysis. Statistical results of parametric and nonparametric variables are expressed as mean ± standard deviation and median (interquartile range [IQR]), respectively. Statistical analyses were performed using the SPSS version 21.0 package program, and $P < .05$ was accepted as statistically significant.

Results

The study comprised a total of 34 pSS patients and 42 healthy controls. The patient and control groups are similar with regard to age, gender, body mass index, smoking, and comorbidity. Characteristics of patients with pSS and controls are reported in **TABLE 1**.

TABLE 1. Characteristics of Patients with Primary Sjögren's Syndrome and Controls[a]

Characteristics	Sjögren's Syndrome (n = 34)	Control (n = 42)	*P*
Age (y), mean ± SD (minimum–maximum)	53 ± 11 (25–71)	54 ± 11 (27–67)	.612[b]
BMI (kg/m^2), mean ± SD (minimum–maximum)	29 ± 4 (23–41)	28 ± 3 (20–35)	.513[b]
Sex	32 (94.1)	39 (92.9)	.601[c]
Female			
Male	2 (5.9)	3 (7.1)	
Smoking	28 (82.4)	36 (85.7)	.737[d]
None	1 (2.9)	2 (4.8)	
Ex-smoker	5 (14.7)	4 (9.5)	
Active			
DM	3 (8.8)	3 (7.1)	.556[c]
HT	10 (29.4)	13 (31.0)	.884[d]
CAD	4 (11.8)	6 (14.3)	.511[c]
CKD	1 (2.9)	2 (4.8)	.580[c]
COPD	1 (2.9)	2 (4.8)	1.000[c]
IBD	1 (2.9)	2 (4.8)	1.000[c]

BMI, body mass index; CAD, coronary artery disease; CKD, chronic kidney disease; COPD, chronic obstructive pulmonary disease; DM, diabetes mellitus; HT, Hashimoto thyroiditis; IBD, inflammatory bowel disease.
[a]*Data are given as No. (%) unless indicated otherwise.*
[b]*Independent* t *test.*
[c]*Fisher exact test.*
[d]*Pearson's* χ^2 *test.*

Median (IQR) duration of disease was 84 (30–120) months. The most common clinical findings were keratoconjunctivitis sicca (n = 34, 100%), xerostomia (n = 33, 97.1%), an abnormal Schirmer's test (n = 26, 76.5%), positive minor salivary gland biopsy (n = 28, 82.4%), synovitis (n = 23, 67.6%), fibromyalgia (n = 15, 44.1%), and fatigue (n = 26, 76.5%). Most of the patient results showed antinuclear antibody (ANA) positivity (n = 27, 79.4%) followed by anti-SS-A/Ro positivity (n = 20, 58.8%) and rheumatoid factor positivity (n = 25, 75%). The majority of patients were receiving hydroxychloroquine treatment (n = 30, 88.2%) followed by prednisolone treatment (n = 13, 38.2%). Clinical characteristics of the patients with pSS are shown in **TABLE 2**.

When the groups were compared in terms of Kyn pathway results, there were significant differences between Kyn (P = .019), Trp (P = .001), and the Kyn/Trp ratio (P < .001) between the patient and control groups. Level of Kyn and Kyn/Trp ratio was significantly higher in the pSS group whereas tryptophan was significantly lower (**TABLE 3**).

Trp concentration was positively correlated with albumin (r = 0.384, P = .025) and hemoglobin (P = .396, r = 0.020). Kyn/Trp ratio was negatively correlated with C-reactive protein (CRP) (r = –0.369, P = .032). Correlations between Kyn pathway results and clinical parameters in patients with pSS is reported in **TABLE 4**. In the results of linear regression analysis, hemoglobin explained 15% of Trp concentration (R^2 = 0.15, F = 6.018, P = .020). Also, glucose explained 15% of Kyn concentration (R^2 = 0.15, F = 5.869, P = .021) (**TABLE 5**).

No significant relation was found between the Kyn pathway and the presence of fibromyalgia, SS-A positivity and SS-A negativity, or prednisolone use in patients with pSS (P > .05) (**TABLE 6**).

TABLE 2. Clinical Characteristics of Patients with Sjögren's Syndrome

Characteristic (n = 34)	Result
Duration of disease, mo, median (IQR)	84 (30–120)
Disease activity scores, median (IQR)	
ESSDAI	2 (2–4)
Doctor global assessment	4 (3–4)
Patient global assessment	5 (3–6)
ESSPRI	4 (3–4)
Dryness	4 (3-5)
Fatigue	4 (3-5)
Pain	4 (3-5)
Clinical findings, No. (%)	
Ocular symptom	34 (100)
Oral symptom	33 (97.1)
Schirmer test right	26 (76.5)
Schirmer test left	26 (76.5)
Minor salivary gland biopsy	28 (82.4)
Synovitis	23 (67.6)
Leukopenia	4 (11.8)
Interstitial lung disease	1 (2.9)
Fibromyalgia	15 (44.1)
Fatigue	26 (76.5)
Laboratory signs, mean (SD) (95% CI)	
WBC	6319 (2209) (5548–7089)
HGB	12.8 (1.4) (12.3–13.3)
PLT	258,324 (73,422) (232,705–283,941)
Glucose	89 (12) (84.9–93.6)
Creatinine, median (IQR)	1 (1–1)
AST, median (IQR)	22 (15–24)
ALT, median (IQR)	19 (15–21)
ALP, median (IQR)	72 (47–80)
GGT, median (IQR)	16 (11–20)
Albumin, mean (SD) (%95 CI)	44 (3) (43.3–45.4)
Total protein, mean (SD) (%95 CI)	73 (5) (71.1–74.7)
Sedimentation, median (IQR)	17 (5–19)
CRP, median (IQR)	3 (1–5)
Serological findings, No. (%)	
ANA positivity	27 (79.4)
RF positivity	25 (73.5)
Anti-CCP positivity	4 (11.8)
SS-A positivity	20 (58.8)
SS-B positivity	6 (17.6)
Treatment	
Prednisolone, No. (%)	13 (38.2)
Prednisolone dose, mg/d, median (IQR)	4 (2–4)
Hydroxychloroquine, No. (%)	30 (88.2)
Methotrexate, No. (%)	6 (18.2)
Azathioprin, No. (%)	1 (2.9)

ALT, alanine transaminase; ALP, alkaline phosphatase; AST, aspartate aminotransferase; CCP, cyclic citrullinated peptide; ESSDAI, EULAR Sjögren's Syndrome Disease Activity Index; ESSPRI, EULAR Sjögren's Syndrome Patient Reported Index; GGT, gamma-glutamyl transferase; HGB, hemoglobin; IQR, interquartile range; PLT, platelets.

Discussion

In this study, we report higher levels of the Trp metabolite Kyn and an increased Kyn/Trp ratio in patients with pSS compared with controls. We found that levels of Trp were lower in pSS as measured by LC-MS/MS. Although Trp was negatively correlated with the physician global assessment, a positive correlation was observed with hemoglobin and albumin. The Kyn/Trp ratio showed a negative correlation with CRP. No significant relationship was found between the Kyn pathway metabolites and fibromyalgia, SS-A positivity, or prednisolone use in patients with pSS.

Trp, the rarest indispensable amino acid, is a precursor for protein synthesis and the manufacture of many chemicals involved in basic biological processes. The Kyn pathway metabolizes the vast majority of Trp (90%), with the serotonin pathway converting the remaining 1% to serotonin and melatonin.[29,30] The IDO expression is upregulated locally and systemically in numerous tissues by immune activation and inflammation, and IDO reduces the concentration of Trp in the milieu of inflammatory cells.[31,32] The IDO activity can inhibit a potentially harmful autoimmune response, induce peripheral tolerance, and minimize chronic immunological activation in T cells, which are particularly susceptible to Trp depletion.[33,34] Overexpression of IDO has been observed in patients with SLE, pSS, and sepsis.[35] Serum Trp levels are higher in healthy women than in women diagnosed with pSS. However, patients with pSS have higher Kyn levels and a higher Kyn/Trp ratio than healthy women and patients with non-SS sicca. The same findings were made in men with pSS, indicating that the IDO enzyme activity in the kynurenine pathway (KP) is enhanced.[34,36] In the metabolic profile comparison of SLE with pSS and systemic sclerosis (SSc), decreased levels of

2023;54:166–172 | https://doi.org/10.1093/labmed/lmac084

TABLE 3. Comparison of the Kynurenine Pathway Results of Patients with Sjögren's Syndrome and Controls

	Sjögren's Syndrome (n = 34), Median (IQR)	Control Group (n = 42), Median (IQR)	P[a]
Kynurenine (ng/mL)	485 (378–601)	386 (356–496)	**.019**
Tryptophan (ng/mL)	10,660 (9160–12,282)	12,258 (11,442–14,711)	**.001**
Kynurenine/tryptophan ratio (%)	4 (3–6)	3 (3–4)	**<.001**

[a]*Mann-Whitney* U *test.*

TABLE 4. Correlation between Kynurenine Pathway Results and Clinical Parameters in Patients with Primary Sjögren's Syndrome[a]

	Kynurenine, *r*	Tryptophan, *r*	Kynurenine/Tryptophan Ratio, *r*
Age	0	0	–0.08
BMI	–0.05	0.04	–0.11
Duration of disease	0.08	–0.06	0.05
Prednisolone dose	–0.08	0.1	–0.18
Laboratory signs			
WBC	0.13	–0.03	0.1
HGB	0.04	**0.39**[b]	–0.28
PLT	–0.24	0.01	–0.26
Glucose	**–0.39**[b]	0.02	–0.28
Creatinine	–0.17	–0.08	–0.03
AST	–0.07	0.17	–0.22
ALT	–0.17	0.19	–0.24
ALP	0.26	–0.05	0.08
GGT	0.1	0.28	–0.19
Albumin	–0.19	**0.38**[b]	–0.28
Total protein	–0.15	0.04	–0.19
Sedimentation	0.08	-0.16	0
CRP	–0.16	0.19	**–0.37**[b]
Disease activity scores			
ESSDAI	–0.29	0.07	–0.21
Doctor global assessment	–0.3	0.11	–0.26
Patient global assessment	–0.25	0.1	-0.19
ESSPRI	–0.23	0.11	–0.17
Dryness	–0.09	0.17	–0.11
Fatigue	–0.28	0.07	–0.17
Pain	–0.21	0.15	–0.24

ALP, alkaline phosphatase; ALT, alanine transaminase; AST, aspartate aminotransferase; BMI, body mass index; CCP, cyclic citrullinated peptide; CRP, C-reactive protein; ESSDAI, EULAR Sjögren's Syndrome Disease Activity Index; ESSPRI, EULAR Sjögren's Syndrome Patient Reported Index; GGT, gamma-glutamyl transferase; HGB, hemoglobin; PLT, platelets.
[a]*Spearman's correlation coefficients* (r) *above |0.3| are highlighted in bold.*
[b]P < *.05.*

tryptophan were seen in SLE patients compared to control groups.[37] In studies conducted on the role of IDO and Trp catabolism in RA in humans, it has been shown that Trp levels decrease and Kyn levels increase in a patient's sera.[21,38] When compared to healthy controls, persons with RA were shown to have lower Trp levels and greater Kyn levels.[14,39,40] These findings were verified in a mouse model of collagen-induced arthritis, where activation of the Trp pathway was revealed to be critical during the arthritis induction and resolution phases.[41] Similar to the literature, in this study we found that Kyn levels were higher, Kyn/Trp ratio increased, and Trp levels were lower in patients with pSS compared to the control group.

Increased IDO serum activity has previously been defined in patients with pSS and was associated with disease severity.[35] Patients with RA show a distribution of Trp metabolites in serum characterized by a high ratio of Kyn/Trp. In persons with RA, decreased Trp and increased Kyn have been linked to disease activity and clinical symptoms.[14,42] The IDO activity was increased in patients with SLE in a cross-sectional study.[43] Patients with active disease (SLE disease activity index ≥6) showed lower Trp levels than controls, but IDO levels of patients with SLE in remission were not different from those in controls. Trp metabolites Kyn and quinolinic acid were higher in patients with SLE compared to controls.[43] In a study evaluating serum levels of Kyn pathway

TABLE 5. Regression Analysis Results for Kynurenine and Tryptophan[a]

	Kynurenine				Tryptophan			
	Constant	B	*t*	*P*	Constant	B	*t*	*P*
Glucose	833.1	−3.9	−2.4	**<.001**	NA	NA	NA	NA
Hemoglobin	NA	NA	NA	NA	-397.6	866.2	2.4	**.02**

NA, not applicable.
[a]*Linear regression analysis.* P < *.05 is highlighted in bold.*

TABLE 6. Comparison of the Kynurenine Pathway Results for Fibromyalgia, SS-A, and Prednisolone in Patients with Sjögren's Syndrome

	Tryptophan (ng/mL), Median (IQR)	Kynurenine (ng/mL), Median (IQR)	Kynurenine/Tryptophan ratio (%), Median (IQR)
Control group (n = 42)	12,258 (11,442–14,711)	386 (356–496)	3 (3–4)
Patients with Sjögren's syndrome			
Fibromyalgia (n = 15)	10,609 (8527–18,319)	478 (317–611)	4 (3–6)
Nonfibromyalgia (n = 19)	10,839 (6842–13,934)	509 (315–670)	5 (3–14)
P value	.456	.456	.206
SS-A positivity (n = 20)	10,429 (6842–12,662)	447 (349–643)	5 (3–9)
SS-A negativity (n = 14)	11,656 (8516–18,319)	521 (301–615)	4 (3–8)
P value	.107	.675	.248
Prednisolone user (n = 21)	10,401 (8516–18,319)	500 (315–643)	4 (3–7)
Non-prednisolone user (n = 13)	10,712 (7058–13,424)	478 (317–625)	4 (3–9)
P value	.535	.986	.468

metabolites in patients with ankylosing spondylitis (AS), serum Trp, Kyn, and 3-hydroxykynurenine levels were found to be remarkably lower in both AS groups compared to the control group, whereas Kyn, quinolinic acid, CRP, erythrocyte sedimentation rate (ESR), and interleukin-6 levels were found to be higher. Conventional treatment and anti-tumor necrosis factor-α treatment were found to be effective in reducing the Kyn/Trp ratio and CRP levels.[44] In our study, there was no correlation between serum Trp, Kyn, and the Kyn/Trp ratio and ESSDAI and ESSPRI disease activity scores in patients with pSS.

Anti-Ro (SS-A) and anti-La (SS-B) autoantibodies were shown to be more frequently positive in patients with polyneuropathy in a study.[45] Trp levels were significantly lower in SSc patients compared to healthy controls according to a recent study.[46] Patients with anti-RNA-polymerase III positivity were shown to have lower Trp levels and higher Kyn levels than patients with anti-centromere and anti-topoisomerase positivity, and autoantibody profile was also found to be considerably correlated with Kyn and Trp levels.[46] Taken together, these findings imply that the higher activity of the KP may be associated with clinical and laboratory manifestations of systemic inflammation.[35,36,45] Although those investigations show a link between neurological or laboratory results and Kyn metabolites, the cause-and-effect link between KP metabolites and these manifestations is yet unknown. Furthermore, the expression of IDO, which metabolizes tryptophan, is known to be upregulated by glucocorticoids.[47] Higher levels of Kyn have also been linked to a decreased percentage of people taking corticosteroids, but not to the frequency of neurological symptoms in pSS patients.[35,36] In our study, although Trp levels were lower in prednisolone users and SS-A positive patients, no statistically significant difference was observed. In addition, no difference was observed between Kyn and Kyn/Trp ratios. This may be related to the small size of the patient population in our cohort.

Trp metabolism through the Kyn pathway has been identified as a central fatigue mechanism.[48,49] In pSS, the interferon-γ-inducible-Kyn pathway could have a role in the neurological symptoms, fatigue, and chronic pain.[45] Since the kynurenine pathway is responsible for the metabolism of around 95% of plasma-free Trp, any change in its activity in response to inflammation is likely to have a disproportionate impact on other Trp or nonkynurenine product pathways. The fact that increased Trp metabolism to kynurenines reduces Trp availability for conversion to 5-HT (serotonin), tryptamine, and melatonin is usually neglected.[50] In a study, a link was made between fibromyalgia and other psychological symptoms such as depression, anxiety, insomnia, psychosis, and neurosis, with fatigue being observed in a group of 106 pSS patients, among whom 32 were considered as fatigued and 74 nonfatigued. However, there was no difference in IDO mRNA levels in pSS patients with and without fatigue in peripheral blood leukocytes.[51] In our cohort, no correlation was found between fibromyalgia and serum levels of Kyn pathway metabolites.

The limitations of our study are mainly due to the limited number of patients. Secondly, almost all of our patients were homogeneous for sicca symptoms and joint involvement, and the number of patients with other extraglandular involvement was very limited. This makes it difficult to establish a relationship between pSS and its involvement and disease activity. Multicenter studies with large patient numbers and different organ involvement are needed to evaluate future usefulness of this pathway in clinical routine.

In conclusion, our data suggest that the Trp metabolic pathway is activated in pSS patients and confirm previous studies that the Kyn pathway is altered. Increased activity of metabolites in the Kyn pathway may have a role in the pathogenesis of pSS. Larger prospective studies are needed to better understand the role of this metabolic route in persons with pSS.

REFERENCES

1. Nguyen CQ, Peck AB. Unraveling the pathophysiology of Sjogren syndrome-associated dry eye disease. *Ocul Surf.* 2009;7(1):11–27. doi:10.1016/s1542-0124(12)70289-6.
2. Stefanski A-L, Tomiak C, Pleyer U, et al. The diagnosis and treatment of Sjögren's syndrome. *Dtsch Ärztebl Int.* 2017;114(20):354.
3. Tomiak C, Dörner T. Sjögren-Syndrom: Aktuelle Aspekte aus Rheumatologischer Sicht. *Hautarzt* 2008;59(12):1011–23; quiz 1024. doi:10.1007/s00105-008-1671-3.
4. Kvarnström M, Ottosson V, Nordmark B, et al. Incident cases of primary Sjögren's syndrome during a 5-year period in Stockholm County: a descriptive study of the patients and their characteristics. *Scand J Rheumatol.* 2015;44(2):135–142.

5. Weng M-Y, Huang Y-T, Liu M-F, et al. Incidence and mortality of treated primary Sjögren's syndrome in Taiwan: a population-based study. *J Rheumatol.* 2011;38(4):706–708. doi:10.3899/jrheum.100883.
6. Maldini C, Seror R, Fain O, et al. Epidemiology of primary Sjögren's syndrome in a French multiracial/multiethnic area. *Arthritis Care Res.* 2014;66(3):454–463.
7. Brito-Zeron P, Baldini C, Bootsma H, et al. Sjögren syndrome. *Nat Rev Dis Primers.* 2016;2(1):1–20.
8. Parisis D, Chivasso C, Perret J, et al. Current state of knowledge on primary Sjögren's syndrome, an autoimmune exocrinopathy. *J Clin Med.* 2020;9(7):2299.
9. Chivasso C, Sarrand J, Perret J, et al. The Involvement of innate and adaptive immunity in the initiation and perpetuation of Sjögren's syndrome. *Int J Mol Sci .* 2021;22(2):658.
10. Kramer JM. Early events in Sjögren's syndrome pathogenesis: the importance of innate immunity in disease initiation. *Cytokine.* 2014;67(2):92–101. doi:10.1016/j.cyto.2014.02.009.
11. Schwarcz R, Bruno JP, Muchowski PJ, et al. Kynurenines in the mammalian brain: when physiology meets pathology. *Nat Rev Neurosci.* 2012;13(7):465–477. doi:10.1038/nrn3257.
12. Frumento G, Rotondo R, Tonetti M, et al. Tryptophan-derived catabolites are responsible for inhibition of T and natural killer cell proliferation induced by indoleamine 2, 3-dioxygenase. *J Exp Med.* 2002;196(4):459–468. doi:10.1084/jem.20020121.
13. Moffett JR, Namboodiri MA. Tryptophan and the immune response. *Immunol Cell Biol.* 2003;81(4):247–265. doi:10.1046/j.1440-1711.2003.t01-1-01177.x.
14. Schroecksnadel K, Winkler C, Duftner C, et al. Tryptophan degradation increases with stage in patients with rheumatoid arthritis. *Clin Rheumatol.* 2006;25(3):334–337.
15. de Jong RA, Nijman HW, Boezen HM, et al. Serum tryptophan and kynurenine concentrations as parameters for indoleamine 2, 3-dioxygenase activity in patients with endometrial, ovarian, and vulvar cancer. *Int J Gynecol Cancer.* 2011;21(7):837-845.
16. Chavele KM, Shukla D, Keteepe-Arachi T, et al. Regulation of myeloperoxidase-specific T cell responses during disease remission in antineutrophil cytoplasmic antibody–associated vasculitis: the role of Treg cells and tryptophan degradation. *Arthritis Rheumatol.* 2010;62(5):1539–1548.
17. Fallarino F, Grohmann U, Vacca C, et al. T cell apoptosis by tryptophan catabolism. *Cell Death Differ.* 2002;9(10):1069–1077. doi:10.1038/sj.cdd.4401073.
18. Szántó S, Koreny T, Mikecz K, et al. Inhibition of indoleamine 2, 3-dioxygenase-mediated tryptophan catabolism accelerates collagen-induced arthritis in mice. *Arthritis Res Ther.* 2007; 9(3):1–7.
19. Munn D, Sharma MD, Baban B, et al. GCN2 kinase in T cells mediates proliferative arrest and anergy induction in response to indoleamine 2, 3-dioxygenase. *Immunity.* 2005;22(5):633–642.
20. Pallotta MT, Orabona C, Volpi C, et al. Indoleamine 2, 3-dioxygenase is a signaling protein in long-term tolerance by dendritic cells. *Nat Immun.* 2011;12(9):870–878.
21. Schroecksnadel K, Kaser S, Ledochowski M, et al. Increased degradation of tryptophan in blood of patients with rheumatoid arthritis. *J Rheumatol.* 2003;30(9):1935–1939.
22. Widner B, Sepp N, Kowald E, et al. Enhanced tryptophan degradation in systemic lupus erythematosus. *Immunobiology.* 2000;201(5):621–630. doi:10.1016/s0171-2985(00)80079-0.
23. Leblhuber F, Walli J, Jellinger K, et al. Activated immune system in patients with Huntington's disease. *Clin Chem Lab Med.* 1998;36(10):747-750.
24. Shiboski CH, Shiboski SC, Seror R, et al. 2016 American College of Rheumatology/European League Against Rheumatism classification criteria for primary Sjögren's syndrome: a consensus and data-driven methodology involving three international patient cohorts. *Ann Rheum Dis.* 2017;76(1):9–16. doi:10.1136/annrheumdis-2016-210571.
25. Seror R, Ravaud P, Bowman SJ, et al. EULAR Sjögren's syndrome disease activity index: development of a consensus systemic disease activity index for primary Sjögren's syndrome. *Ann Rheum Dis.* 2010;69(6):1103–1109. doi:10.1136/ard.2009.110619.
26. Seror R, Ravaud P, Mariette X, et al. EULAR Sjögren's Syndrome Patient Reported Index (ESSPRI): development of a consensus patient index for primary Sjögren's syndrome. *Ann Rheum Dis.* 2011;70(6):968–972. doi:10.1136/ard.2010.143743.
27. Huang Y, Louie A, Yang Q, et al. A simple LC-MS/MS method for determination of kynurenine and tryptophan concentrations in human plasma from HIV-infected patients. *Bioanalysis.* 2013;5(11):1397–1407. doi:10.4155/bio.13.74.
28. İriz A, Şemsi R, Eser B, et al. The evaluation of serum tryptophan and kynurenine levels in patients with obstructive sleep apnea syndrome. *Sleep Breath.* 2021;25(3):1389–1398. doi:10.1007/s11325-020-02250-7.
29. Grohmann U, Bronte V. Control of immune response by amino acid metabolism. *Immunol Rev.* 2010;236(1):243–264. doi:10.1111/j.1600-065X.2010.00915.x.
30. Murray PJ. Amino acid auxotrophy as a system of immunological control nodes. *Natur Immun.* 2016;17(2):132–139.
31. King NJ, Thomas SR. Molecules in focus: indoleamine 2, 3-dioxygenase. *Int J Biochem Cell Biol.* 2007;39(12):2167–2172. doi:10.1016/j.biocel.2007.01.004.
32. Thackray SJ, Mowat CG, Chapman SK. Exploring the mechanism of tryptophan 2, 3-dioxygenase. *Biochem Soc Trans.* 2008;36(6):1120–1123.
33. Richard DM, Dawes MA, Mathias CW, et al. L-tryptophan: basic metabolic functions, behavioral research and therapeutic indications. *Int J Tryptophan Res*. 2009;2:IJTR. S2129.
34. Taylor MW, Feng G. Relationship between interferon-γ, indoleamine 2, 3-dioxygenase, and tryptophan catabolism. *FASEB J.* 1991;5(11):2516–2522. doi:10.1096/fasebj.5.11.1907934.
35. Pertovaara M, Raitala A, Uusitalo H, et al. Mechanisms dependent on tryptophan catabolism regulate immune responses in primary Sjögren's syndrome. *Clin Exp Immunol.* 2005;142(1):155–161. doi:10.1111/j.1365-2249.2005.02889.x.
36. Valim V, Zandonade E, Brun JG, et al. Kynurenines pathway biomarkers for primary Sjogren's syndrome. *Clin Exp Rheumatol.* 2018;36(3):290.
37. Bengtsson AA, Trygg J, Wuttge DM, et al. Metabolic profiling of systemic lupus erythematosus and comparison with primary Sjögren's syndrome and systemic sclerosis. *PLoS One.* 2016;11(7):e0159384. doi:10.1371/journal.pone.0159384.
38. Spiera H, Vallarino R. Serum kynurenine in rheumatoid arthritis. *J Clin Investig.* 1969;48(5):856–859.
39. Nguyen CH, Nakahama T, Dang TT, et al. Expression of aryl hydrocarbon receptor, inflammatory cytokines, and incidence of rheumatoid arthritis in Vietnamese dioxin-exposed people. *J Immunotoxicol.* 2017;14(1):196–203. doi:10.1080/1547691X.2017.1377323.
40. Nguyen NT, Nakahama T, Nguyen CH, et al. Aryl hydrocarbon receptor antagonism and its role in rheumatoid arthritis. *J Exp Pharmacol.* 2015;7:29–35. doi:10.2147/JEP.S63549.
41. Ro W. Exploitation of the IDO pathway in the therapy of rheumatoid arthritis. *Int J Tryptophan Res.* 2013;21(6):67–63.
42. Forrest CM, Kennedy A, Stone TW, et al. Kynurenine and neopterin levels in patients with rheumatoid arthritis and osteoporosis during drug treatment. In: *Developments in Tryptophan and Serotonin Metabolism.* Springer; 2003:287–295.
43. Åkesson K, Pettersson S, Ståhl S, et al. Kynurenine pathway is altered in patients with SLE and associated with severe fatigue. *Lupus Sci Med.* 2018;5(1):e000254. doi:10.1136/lupus-2017-000254.
44. Onmaz DE, Sivrikaya A, Isik K, et al. Altered kynurenine pathway metabolism in patients with ankylosing spondylitis. *Int Immunopharmacol.* 2021;99:108018.

45. Ter Borg E, Kelder J. Development of new extra-glandular manifestations or associated auto-immune diseases after establishing the diagnosis of primary Sjögren's syndrome. *Rheumatol Int.* 2017;37(7):1153–1158.
46. Campochiaro C, Lytton S, Nihtyanova S, et al. Elevated kynurenine levels in diffuse cutaneous and anti-RNA polymerase III positive systemic sclerosis. *Clin Immunol.* 2019;199:18–24. doi:10.1016/j.clim.2018.12.009.
47. Badawy AA. Tryptophan availability for kynurenine pathway metabolism across the life span: control mechanisms and focus on aging, exercise, diet and nutritional supplements. *Neuropharmacology.* 2017;112:248–263. doi:10.1016/j.neuropharm.2015.11.015.
48. Yamashita M, Yamamoto T. Excessive brain tryptophan and kynurenic acid lead to abnormal social behavior in central fatigue induced by chronic sleep disorder. *Int J Psychophysiol.* 2014;2(94):229–230.
49. Kolodziej LR, Paleolog EM, Williams RO. Kynurenine metabolism in health and disease. *Amino Acids.* 2011;41(5):1173–1183. doi:10.1007/s00726-010-0787-9.
50. Ogbechi J, Clanchy FI, Huang Y-S, et al. IDO activation, inflammation and musculoskeletal disease. *Exp Gerontol.* 2020;131:110820. doi:10.1016/j.exger.2019.110820.
51. Karageorgas T, Fragioudaki S, Nezos A, et al. Fatigue in primary Sjögren's syndrome: clinical, laboratory, psychometric, and biologic associations. *Arthritis Care Res.* 2016;68(1):123–131.

Central Line Access Is Predictive of Diagnostic Blood Loss and Transfusion in the Surgical Intensive Care Unit

Brian D. Adkins, MD,[1] Abe DeAnda Jr, MD,[2] Judy A. Trieu, MD, MPH,[3] Srinivas Polineni, MHA,[4] Anthony Okorodudu, PhD, MBA,[1] Sean G. Yates, MD[1,]*

[1]The University of Texas Southwestern Medical Center—Pathology, Dallas, TX, USA, [2]University of Texas Medical Branch, Galveston, TX, USA, [3]Parkland Health and Hospital System, Dallas, TX, USA, [4]University of Texas Medical Branch—Pathology, Galveston, TX, USA. *To whom correspondence should be addressed: sean.yates@utsouthwestern.edu.

Keywords: anemia, patient blood management, lab stewardship, central venous catheter, iatrogenic anemia, phlebotomy

Abbreviations: DLT, diagnostic laboratory testing; CVC, central venous catheter; LOS, length of stay; STROBE, Strengthening the Reporting of Observational Studies in Epidemiology; EHRs, electronic health records; HIPAA, Health Insurance Portability and Accountability Act; CCI, Charlson Comorbidity Index; PICCs, peripherally inserted central catheters; LIS, laboratory information system; Hb, hemoglobin; IR, interventional radiology; BCDs, blood-conserving devices; CLABSI, central line–associated bloodstream infection; NA, nonapplicable; EPO, erythropoietin-stimulating

Laboratory Medicine 2023;54:173–181; https://doi.org/10.1093/labmed/lmac071

ABSTRACT

Background: Most patients in the surgical intensive care unit (SICU) have anemia and undergo extensive diagnostic laboratory testing (DLT). Consequently, patients undergo RBC transfusion, and many are discharged with anemia, both of which are associated with poorer outcomes.

Objective: To characterize DLT blood loss in the SICU.

Materials and Methods: We performed a 1-year retrospective study of 291 patients admitted to a SICU. The number of draws, average volume, and estimated discard volume were recorded, along with clinical and laboratory findings.

Results: Patients who underwent greater amounts of DLT had lower hemoglobin levels at discharge ($P \leq .001$). Admissions requiring central venous catheter (CVC) access (49.8%) demonstrated significantly higher DLT draws and rates of transfusion.

Conclusion: Findings from this study suggest that DLT blood loss contributes to anemia in the SICU, and that the presence and duration of CVC leads to increased testing, anemia, and RBC transfusion.

Diagnostic laboratory testing (DLT) plays an integral role in the clinical management of patients with critical illness. Although DLT provides invaluable information, helping guide diagnostic, prognostic, and therapeutic decisions, volume lost due to high testing burden has been shown to contribute to the development of anemia and may lead to an increased rate of transfusion.[1–4] An estimated 16.2 laboratory tests are collected daily from patients in the ICU and account for a daily DLT-associated blood loss of 15 to 100 mL.[2,4–9] In the ICU, blood needed for DLT is frequently collected from a central venous catheter (CVC). Approximately half of patients in the ICU will undergo placement of a CVC.[10] The ease at which CVCs permit collection of DLT and the clinical acuity of information from the patients who often require CVC appear to promote increased access, with an approximately 30% increase in testing and a 40% increase blood volumes collected in patients with CVCs relative to those without CVCs.[11,12] Ultimately, an increase in DLT and increased DLT-associated blood loss has been shown to correspond with a higher incidence of anemia.[1–4]

Anemia is a common development in the critical care setting, with a reported incidence of anemia in 98% of patients admitted to the ICU.[9] Moreover, patients undergoing certain procedures, such as cardiothoracic surgery, may require higher numbers of draws, contributing to an overall greater loss of blood, with 1 group showing a median blood loss of 454 mL.[13] Likewise, suppressed erythropoiesis in patients with critical illness can occur due to inflammatory iron sequestration and decreased erythropoietin activity.[14–19] Other etiologies include nutritional deficiencies; major surgical interventions; bleeding; length of stay (LOS); and receipt of care at a teaching institution, likely due to increased testing for educational purposes.[18,20,21,22–24] Together, these factors lead to the development of multifactorial anemia at discharge in patients treated in the ICU, with severe discharge anemia being associated with a number of adverse outcomes, including increased 30-day mortality rates and readmissions, which further contribute to increasing health care spending.[14,22]

The prevalence of anemia in patients with critical illness often prompts RBC transfusions, occurring in 26.3% to 50.0% of patients

in the ICU.[25–27] The high rate of RBC transfusions is concerning, given the observed association between liberal RBC transfusions and poor outcomes, such as a higher incidence of serious health care–associated infections and increased LOS.[20,26,28] Similarly, mortality rates are appreciably higher in patients who received transfusions in the ICU, relative to such patients who did not receive any transfusion—30.0% vs 19.6%, respectively.[27]

Measures aimed at mitigating factors that contribute to the incidence of anemia and the extent of RBC transfusions have the potential to significantly improve outcomes for patients with critical illness. Our study aimed to characterize DLT-associated blood loss and the impact of CVC placement, as well as the association of these factors with anemia and rate of RBC transfusion.

Materials and Methods

Design and Setting

This retrospective study was conducted at a large academic center between January 1, 2017, and December 31, 2017, and was approved by our local IRB (protocol No. 190161). Data from hospitalization were recorded, and no follow-up data were obtained. Cost analysis was performed at a large public hospital affiliated with an academic center in April of 2022 and did not involve the use of patient data. We used the Strengthening the Reporting of Observational Studies in Epidemiology (STROBE) guidelines in preparation of this manuscript.[29]

Study Population

Our study population comprised consecutive adult patients admitted to the SICU. Patients younger than 18 years, as well as those who were members of vulnerable populations, such as prisoners, were excluded from the study. The study size was a convenience sample derived from the period reviewed.

Data Collection

Electronic medical records (EHRs) were manually reviewed to obtain patient demographics and clinical information (**TABLE 1**), laboratory results, progress notes, and discharge summaries. Data collection was performed by physicians, recorded in standardized deidentified abstraction sheets, and met the requirements of the Health Insurance Portability and Accountability Act (HIPAA). To account for the acuity of illness, we calculated the Charlson Comorbidity Index (CCI) for each patient, as previously described.[30] The CCI helps predict mortality, or relative risk of death, based on patient comorbidities, with a lower score characterizing healthier patients (score of 0–1) vs sicker patients (score of 3–8).

To estimate the total blood volume collected for a given laboratory test, tube volumes were confirmed by injecting the contents with water and then decanting the final volume into tubes. The number and source (ie, peripheral access, or CVC) of DLT was identified in the electronic medical records for each patient. The product of the average 7-day blood volume and the number of each test type was then calculated to estimate the daily and total blood volumes collected for a given patient. Volume of blood discarded from CVCs, arterial lines, and peripherally inserted central catheters (PICCs) was estimated based on internal nursing protocol requirements for minimum volume for discarding. The laboratory information system (LIS) was queried to determine tests that were reflexed for tubes containing already-obtained specimens, to not overestimate blood loss associated with DLT.

The following information was also recorded: incidence of anemia (female patients, hemoglobin [Hb] <12 mg/dL; males, Hb <13 mg/dL) based on WHO definitions), frequency of phlebotomy per patient per day, volume of blood loss via phlebotomy per patient per day, number and volume of RBC transfusions, number of RBC units transfused intraoperatively/immediately postoperatively, and number of RBC units transfused in the SICU (not immediately postoperatively). Additionally, we recorded the Hb level at SICU admission; pretransfusion Hb (Hb ≤3 hours before transfusion); and the primary indication for RBC transfusion, as reported by the ordering health care provider.[31]

Statistical Analysis

Statistical analyses were performed using Wizard statistical software, version 1.9.48 (Evan Miller). The normality of distribution of continuous variables was tested with the 1-sample Kolmogorov-Smirnov test. Frequencies were determined for categorical variables. Continuous variables are expressed as mean (SD). A Fisher exact test was used for categorical variables. We used a Student *t* test for variables with normal distribution and a Mann-Whitney *U* test for continuous variables without normal distribution. We assumed statistical significance at an alpha value of 0.05. Bonferroni correction was used to account for the multiple testing hypothesis. Hospital charges were obtained from the publicly available data for fiscal year 2022 from the Parkland Hospital chargemaster.[32] Data were utilized to calculate the estimated cost for a single RBC transfusion, CVC placement at bedside, and CVC placement using interventional radiology (IR).

TABLE 1. Study Demographic Data (n = 299)

Variable	All Admissions
Anemia on admission, No. (%)[a]	153 (51.2)
Anemia on discharge, No. (%)[a]	285 (95.3)
CCI, mean (SD)	4.4 (2.6)
LOS, mean (SD), days	15.8 (11.2)
Admission Hb, mean (SD), g/dL	12.1 (2.5)
Nadir Hb, mean (SD), g/dL	7.9 (1.7)
CVC access, No. (%)	149 (49.8)
Discharge Hb, mean (SD), g/dL	9.4 (1.6)
Delta Hb from admission to discharge, mean (SD), g/dL	2.8 (2.6)
Patients requiring RBC transfusion, No. (%)	95 (31.8)
RBC units transfused overall, No. (mean [SD]; range)	1 (0.73 [1.6]; 0–16)
Total No. of blood draws, mean (SD)	
Per day	5.8 (4.5)
Per hospitalization	93.25 (115.5)
DLT blood loss per patient (mL), mean (SD)	
Per day	14.3 (9.8)
Per hospitalization	229.5 (253.7)
Total iatrogenic blood loss per patient (mL), (including discard), mean (SD)	
Per day	20.0 (16.7)
Per hospitalization	346.9 (490.9)

CCI, Charslon Comorbidity Index; CVC, central venous catheter; DLT, diagnostic laboratory testing; Hb, hemoglobin; LOS, length of stay
[a]Anemia classification is based on based on WHO definitions: females, Hb <12 mg/dL; males, Hb <13 mg/dL.

Results

Patient Characteristics

Patient demographics and study outcomes are summarized in **TABLE 1**. A total of 291 patients (mean, 62.2 years; male to female ratio, 1:5) underwent 299 hospitalizations, with an LOS of 15.8 days. Comorbidity status, as assessed by CCI, was 4.4. Mean (SD) DLT-associated blood loss was 14.3 mL/day (229.5 mL/hospitalization). The overall rate of vascular access was 75.3% (225/299). The rates of vascular access by type were as follows: CVC access, 49.8% (149/299); PICC access, 17.1% (51/299); and arterial access, 69.6% (208/299). We believed arterial discarded blood volume to be negligible and counted it as 0 mL. The mean (SD) daily discard amount in patients with CVC only was 16.32 (11.0) mL, and this amount for patients with PICC only was 13.2 (7.4) mL ($P \geq .99$). Cumulative blood loss during hospital admission with CVC and PICC access was greater than for CVC only: 132.2 mL vs 524.1 mL ($P \leq .001$). The cumulative blood loss at admission was predictive of the magnitude of anemia at discharge, with the largest diagnostic-associated blood loss group corresponding to a discharge Hb level of 8.6 g/dL vs the lowest blood loss group being associated with an Hb level of 9.7 g/dL ($P \leq .001$; **FIGURE 1**). The overall rate of transfusion was 31.7% (95/299), and the overall change in hemoglobin from admission to discharge was not significantly different in patients undergoing transfusion vs those not receiving transfusion ($P \geq .99$).

CVC Access vs No CVC Access

Patients with and without CVC had similar length of hospital stay and CCI (**TABLE 2**). However, patients with CVC access had a significantly higher number of total blood draws, total blood drawn or discarded for access and DLT, and rate of transfusion. Patients with CVC require flushing of the access site with a small volume of fluid, typically normal saline, which is subsequently discarded prior to drawing a specimen, with a total discard volume of blood of 204 mL/hospitalization. Rates of anemia at the time of hospital discharge were significantly higher in the CVC group. Also, nadir Hb and discharge Hb levels were significantly lower in patients with CVC placement. The number of total blood draws per day was significantly higher in patients with a longer duration of CVC (**FIGURE 2**), and the total number of draws was significantly higher in patients with CVC vs those without CVC. The volume of combined DLT-associated blood loss was predictive of receipt of RBC transfusion, independent of any surgical procedure or the acuity of illness as complicated by comorbidities by CCI (**FIGURE 3**), although the range of CCI was greater in patients with prolonged CVC access (**FIGURE 4**). Most patients had concurrent placement of an arterial line (142/149 [95.3%]), and fewer had PICC access (26/149 [17.4%]).

Patients with Anemia at Hospital Admission vs Patients without Anemia at Admission

Patients with and without anemia at hospital admission had a similar length of stay and CCI (**TABLE 3**). Anemia at admission was significantly associated with lower Hb nadir, lower Hb at discharge, and higher rate of anemia at discharge. Preexisting anemia was not predictive of the need for transfusion.

Surgical Admissions vs Nonsurgical Admissions

Patients treated in the surgical department and those treated outside the surgical department had a similar length of hospital stay and CCI (**TABLE 4**). Patients who underwent at least 1 operation had higher rates of CVC placement, lower Hb nadir, and lower Hb at discharge. Undergoing a surgical procedure was not predictive of anemia at discharge or nonoperative transfusion.

Charge Analysis

We performed a charge analysis comparing CVC placement and the cost of blood transfusion. The charge for a transfusion procedure was $1507.00 and an RBC unit was $799.00, with the overall cost of transfusion with associated testing being $2778.00 (**TABLE 5**). The cost for bedside CVC and the cost of single RBC transfusion were similar ($3511.04 vs $2778.00). IR placement of CVC is approximately 3 times more expensive than bedside CVC placement ($10,993.04 vs $3511.04).

Discussion

The findings of our study suggest that the total volume of DLT-associated blood loss contributes to the incidence and magnitude of anemia which, in turn, was associated with more frequent RBC transfusions in patients with critical illness. Likewise, the severity of anemia correlated with the volume of blood drawn (**FIGURE 1**). Further, CVC access was predictive of increased total blood loss, transfusion, and anemia. The observations derived from our investigation correspond with those reported in previous studies.[1,4–9]

Although CVC placement will largely occur in patients with higher-acuity disease, as demonstrated in our cohort by higher CCI values, it is associated with an increase in blood draws for laboratory testing and a resultant increase in iatrogenic blood loss, for DLT and line-clearance blood discarding. Patients with critical illness require extensive DLT to guide their therapy; however, the number of accesses, as well as the utilization of blood-conserving devices (BCD) to reduce specimen discarding, represent modifiable factors. BCDs were not used at our institution but could be especially impactful because there was a significant amount of cumulative blood loss associated with line clearance—204 mL/admission—which nears the volume of 1 unit of RBCs.

Although the overall rate of transfusion was 31.7% (95/299), CVC access was predictive of a higher transfusion rate, compared with patients without CVC access. Transfusion has been associated with morbidity and mortality among patients in the ICU, an association which likely acts as a marker of sicker patients. We found that CVC line placement of >7 days was predictive of a higher rate of RBC transfusions. ICUs often have goals to remove CVCs as quickly as possible, to reduce the risk of central line–associated bloodstream infection (CLABSI), which is associated with high mortality. Our findings suggest that reduction in DLT blood loss provides a further rationale for early CVC removal.[33]

A recent meta-analysis by Whitehead et al[5] demonstrated that utilization of BCDs were associated with a reduction in iatrogenic blood loss, although another group[13] had reported technical issues with implementation. BCDs attach to an access site and work by filling a reservoir to flush the line, which allows uncontaminated patient blood to fill a distal specimen site; the blood specimen is then removed, and afterwards the residual volume is returned to the body of the patient.[34] Implementation requires nurse training, and kits may fail requiring swapping of BCDs, but BCDs can be easily attached to a CVC.[34]

Small interventions, such as use of pediatric tubes in addition to BCD, have been shown to be effective in reduction of DLT-associated blood loss.[34,35] Another future consideration may be implementation of decision support for laboratory test ordering, which has been shown to be effective in RBC transfusion stewardship. These interventions, including hard stops for

FIGURE 1. Discharge hemoglobin level vs volume of diagnostic laboratory blood loss ($P \leq .001$). Each group represents 1/6 of the admissions, or approximately 50 admissions.

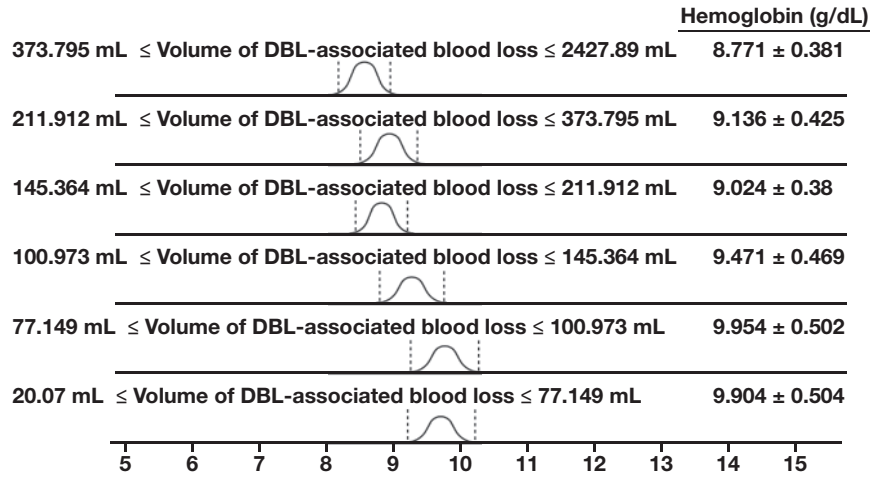

TABLE 2. Admissions with CVC Access vs Patients without CVC Access

Variable	CVC (n = 149)	No CVC (n = 150)	*P* Value
Age, y, mean (SD)	63.2 (12.6)	60.9 (16.5)	<.001
CCI, mean (SD)	4.6 (2.3)	4.2 (2.9)	<.001
LOS, mean (SD)	17.1 (11.4)	14.5 (10.9)	.11
Admission Hb (g/dL), mean (SD)	12.3 (2.7)	11.9 (2.3)	>.99
Nadir Hb (g/dL), mean (SD)	7.4 (1.4)	8.4 (1.9)	<.001
Discharge Hb (g/dL), mean (SD)	8.9 (1.2)	9.8 (1.8)	<.001
Delta Hb from admission to discharge, g/dL, mean (SD)	3.4 (2.9)	2.1 (2.1)	<.001
Anemia on admission, No. (%)[a]	68 (45.6)	85 (56.7)	>.99
Anemia on discharge, No. (%)[a]	149 (100)	135 (90.0)	.004
Rate of RBC transfusion, No. (%)	63 (42.3)	33 (22.0)	.01
No. of RBC units transfused, mean (SD)	1 (2.1)	0.4 (0.9)	.06
Total No. of blood draws, mean (SD)	121.1 (149.3)	60.6 (48)	<.001
Per day, mean (SD)	7 (5.1)	4.6 (3.5)	<.001
Total DLT-associated blood loss, mL, mean (SD)	297.8 (324.3)	161.6 (122.6)	<.001
Total DLT-associated blood loss, mL per day, mean (SD)	16.5 (10.7)	12.2 (8.3)	.007
Total discard volume per admission, mL, mean (SD)	204 (322)	NA	NA
Duration of CVC access, mL, mean (SD)	7.4 (5.5)	NA	NA
Total iatrogenic blood loss per patient (including discard), mL, mean (SD)	501.7 (632.8)	193.2 (191.3)	<.001

CCI, Charslon Comorbidity Index; CVC, central venous catheter; DLT, diagnostic laboratory testing; Hb, hemoglobin; LOS, length of stay; NA, nonapplicable.
[a]*Anemia classification based on WHO definitions: females, Hb <12 mg/dL; males, Hb <13 mg/dL.*

certain tests, may further contribute to a decrease in laboratory draws.[36] To that end, numerous studies have shown efficacy in reducing unnecessary laboratory testing through the Choosing Wisely campaign; recommendations by many medical societies support a more conservative approach to testing.[37–39] Examples of actionable measures are reviewed in **TABLE 6**.

Transfusion is commonly cited as one of the most common procedures for hospitalized patients and is associated with numerous costs that may not be considered by clinical staff, such as donor outreach, collection, transport, storage, laboratory testing, and laboratory staff salaries. A charge analysis examining RBC transfusion and associated charges demonstrated that RBC transfusion were similarly priced vs bedside CVC placement ($2778.00 vs $3511.04).

Although many medical services place lines at the bedside, there has been a shift in some centers to having most lined placed by IR, which our findings show is significantly more expensive than other methods ($10,993.04). Although determining clear pricing information is challenging, utilization of interventions may prevent excess spending on transfusion.

CVC placement was associated with lower Hb nadirs, lower discharge Hb levels, and a greater delta in Hb from admission to discharge.

FIGURE 2. Number of laboratory blood draws compared with length of central venous catheter (CVC) placement (days). The mean (SD) blood draws per day was 5.8 (4.5).

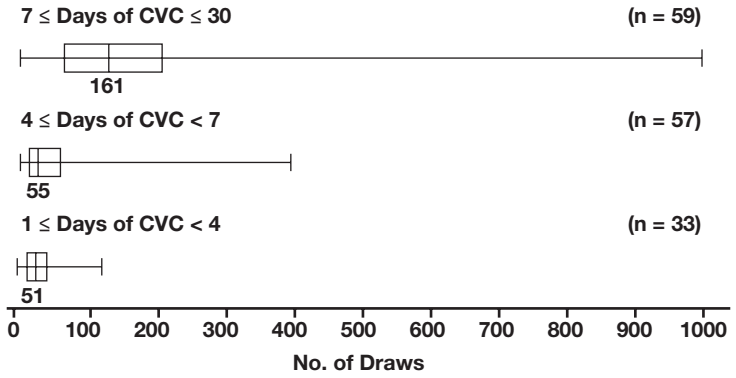

FIGURE 3. Number of nonperioperative RBC transfusions (volume in units) compared with length of central venous catheter (CVC) placement (days).

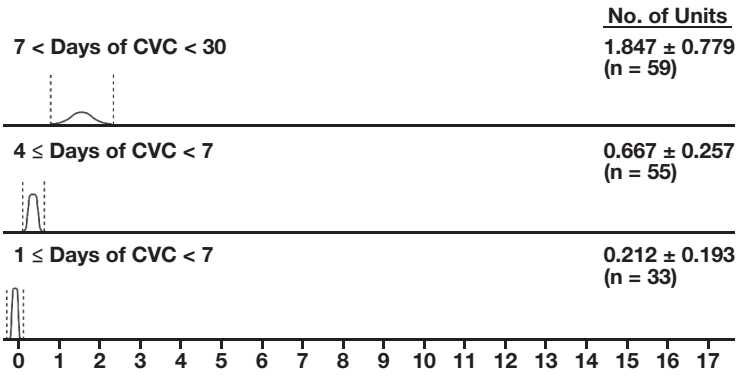

FIGURE 4. Charlson Comorbidity Index comparison among patients with central venous catheter (CVC) placement (distributed by number of days).

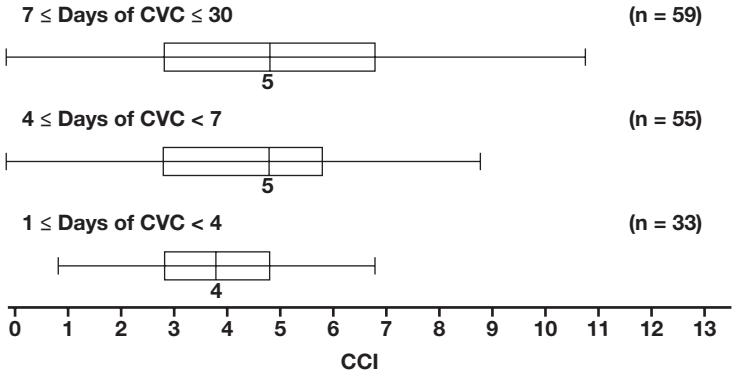

Although a restrictive transfusion strategy has been shown to be more effective in numerous studies, severe anemia at discharge has been shown to be predictive of anemia on long-term follow-up for patients of the ICU, further contributing to readmission, need for transfusion, and poor general health as an outpatient. These findings have supported efforts to reduce iatrogenic anemia.[14,17]

Under physiologic conditions the body can readily produce sufficient RBC mass for maintenance of Hb levels at ~10–20 mL per day. Although this number may increase exponentially in conditions of anemia with adequate iron stores, patients with critical illness have been shown to have reduced RBC production, making any blood loss likely more impactful.[19,40–43] Many patients treated in the ICU have anemia on presentation, with nutritional deficiency being a contributing factor in 13% of these patients as follows: 2% have B_{12} deficiency, 2% have folate deficiency, and 9% have iron deficiency.[18] Ongoing blood draws represent an identifiable loss of RBC mass and iron, which the patient with critical illness cannot effectively replace, further contributing to iatrogenic anemia.

Although we observed a total mean daily loss of blood of 20.0 mL (a volume below the observed ~50–100 mL in other studies), this

TABLE 3. Patients with Anemia on Admission vs Patients without Anemia on Hospital Admission[a]

Variable	Anemia on Admission (n = 153)	No Anemia on Admission (n = 146)	*P* Value
Age, y, mean (SD)	61.7 (15.1)	62.4 (14.6)	>.99
CCI, mean (SD)	4.9 (2.8)	3.9 (2.3)	.07
LOS, mean (SD)	16.5 (12.1)	15.1 (10.4)	>.99
Admission Hb (g/dL), mean (SD)	10.1 (1.7)	14.3 (1.3)	<.001
Nadir Hb (g/dL), mean (SD)	7.3 (1.2)	8.6 (1.9)	<.001
Discharge Hb (g/dL), mean (SD)	8.9 (1.3)	9.9 (1.8)	<.001
Delta Hb from admission to discharge (g/dL), mean (SD)	4.4 (2.1)	1.3 (2.0)	<.001
Anemia at discharge, No. (%)	153 (100)	132 (90.4)	.002
Patients requiring RBC transfusion, No. (%)	58 (61.0)	38 (26.0)	>.99
RBC transfusions, No., mean (SD)	1 (0.8 [1.7])	1 (0.7 [1.6])	>.99
CVC access, No. (%)	68 (44.4)	81 (55.5)	>.99
Duration of CVC access, mean (SD)	3.6 (5.7)	3.8 (5.4)	>.99
Blood draws per stay, mean (SD)	85.8 (102.0)	91.1 (124.2)	>.99
Blood draws per day, mean (SD)	6.1 (5.1)	5.5 (3.8)	>.99
DLT-associated blood loss per patient, mL, mean (SD)	214.8 (214.0)	220.3 (284.5)	>.99
Per day, mL, mean (SD)	15.2 (10.9)	13.4 (8.4)	>.99
Total iatrogenic blood loss per patient (including discard, mL, mean (SD)	361.7 (420.6)	331.4 (556.3)	.77
Per day, mL, mean (SD)	21.6 (18.12)	18.4 (14.9)	>.99

CCI, Charslon Comorbidity Index; CVC, central venous catheter; DLT, diagnostic laboratory testing; Hb, hemoglobin; LOS, length of stay.
[a]Anemia classification based on World Health Organization definitions: females, Hb <12 mg/dL; males, Hb <13 mg/dL.

TABLE 4. Values for Patients with Surgical Admissions vs Those Not Admitted to the Surgical Department

Variable	Surgical Admissions (n = 210)	Nonsurgical Admissions (n = 89)	*P* Value
Age, y, mean (SD)	62.2 (13.9)	61.7 (16.3)	>.99
CCI, mean (SD)	4.3 (2.3)	4.7 (3.2)	>.99
LOS, mean (SD)	16.7 (12.5)	13.6 (6.7)	>.99
Admission Hb (g/dL), mean (SD)	12.3 (2.6)	11.8 (2.3)	>.99
Nadir Hb (g/dL), mean (SD)	7.6 (1.5)	8.6 (2)	<.001
Discharge Hb (g/dL), mean (SD)	9.1 (1.4)	9.9 (1.9)	.009
Delta Hb from admission to discharge, g/dL, mean (SD)	3.1 (2.7)	1.9 (2.0)	<.001
Anemia on admission, No. (%)[a]	104 (49.5)	49 (55.1)	>.99
Anemia on discharge, No. (%)[a]	206 (98.1)	79 (88.8)	.06
Patients requiring RBC transfusion, No. (%)	74 (35.2)	22 (24.7)	>.99
RBC units transfused number, No. (mean [SD])	1 (0.8 [1.7]	1 (0.6 [1.5])	>.99
CVC access, No. (%)	127 (60.5)	22 (24.7)	.005
Duration of CVC access, mean (SD)	7.2 (5.6)	8.7 (6.6)	>.99
Blood draws, total No., mean (SD)	99.6 (124.3)	78.3 (89.7)	>.99
Per day, mean (SD)	5.9 (4.6)	5.5 (4.3)	>.99
DLT-associated blood loss per hospitalization, mL, mean (SD)	241.8 (279.8)	200.4 (175.7)	>.99
Per day, mL, mean (SD)	142.2 (10.2)	14.6 (8.6)	>.99
Total iatrogenic blood loss per patient (including discard), mL, mean (SD)	375.7 (541.3)	279 (337.3)	>.99
Per day, mL, mean (SD)	20.3 (16.7)	19.5 (16.6)	>.99

CCI, Charslon Comorbidity Index; CVC, central venous catheter; DLT, diagnostic laboratory testing; Hb, hemoglobin; LOS, length of stay.
[a]Anemia classification based on World Health Organization definitions: females, Hb <12 mg/dL; males, Hb <13 mg/dL.

TABLE 5. Charge Analysis of CVC Placement and Blood-Transfusion Cost[a]

Procedure	Overall Charge	Charge Components (*Current Procedural Terminology* Code)	Charge
RBC transfusion	$2778.00	Blood typing (86905)	$180.00
		RBC antibody screen (86850)	$292.00
		RBC LR (P9016)	$799.00
		Transfuse blood/comp (36430)	$1507.00
Bedside CVC placement	$3511.04	Guide wire (C1769)	$209.04
		Catheter, infusion, inserted peripherally, centrally, or midline (C1751)	$2687.00
		Chest X-ray, single view (71010)	$615.00
Interventional radiology CVC placement	$10,993.04	Moderate sedation (9153)	$597.00
		Guide wire (C1769)	$209.04
		Catheter, infusion, inserted peripherally, centrally, or midline with image guidance (36560 and 76937)	$9572.00
		Chest X-ray, single view (71010)	$615.00

CVC, central venous catheter.
[a]All values are in United States dollars. Overall charges for each procedure were calculated from associated products and processes required for performance.

TABLE 6. Interventions for Reducing Diagnostic Laboratory Testing Blood Loss or Improving Hospital-Acquired Anemia

Intervention	Mechanism	Caveats	Outcome	Level of Evidence[a]
Small-volume collection tubes	These tubes require smaller volumes reducing blood lost to laboratory draws.	Limited volume for add-on testing	Decreased anemia	Suggestive evidence[5]
Provider education	Staff can educate providers to use best practice by limiting duplicate orders and discouraging unnecessary testing.	Time-consuming Challenging to encourage participation	Fewer tests ordered	Insufficient evidence[5]
EHR decision support	Automated messages, or pop-ups, can be placed into the EHR to encourage best practice or to prevent ordering via hard stop.	Providers may disagree with evidence Providers may ignore evidence due to pop-up fatigue	5.8% improvement in patients receiving desired intervention (example: more appropriate lab testing)[b]	Heterogeneous quality of studies[46]
Blood-conservation devices	These devices recirculate the port flush volume, leading to less discarded blood with lab draws.	More expensive than typical ports Implementation requires training Devices can fail	Reduced blood loss	Moderate evidence[5]/unclear quality (biased)[34]
Point-of-care testing	Point-of-care machines require less volume and are more convenient.	Perhaps increased testing due to convenience Expensive to purchase new equipment Implementation requires training	Decreased transfusion	Insufficient evidence[5]
Intravenous iron supplementation	Parenteral iron can replenish storage iron.	Iron bound by hepcidin Infusion reactions Expensive Theoretical risk for infection	Improved hemoglobin level at 10- to 30-day follow-up	Very low level of certainty[47]
EPO agents	These drugs can change EPO levels in patients with decreased production and perhaps overcome the blunted EPO response in patients with critical illness.	Expensive Large number needed to treat Risk of thromboembolic events or acute myocardial infarction	Reduction in number of units transfused (1–2) and somewhat decreased mortality	Low or unclear quality[16,48]

EHR, electronic health record; EPO, erythropoietin-stimulating.
[a]As defined by meta-analysis.
[b]This meta-analysis reviewed the impact of decision support in general, as opposed to in the setting of impact on iatrogenic anemia.

volume is actually equivalent to steady-state RBC production in healthy individuals.[4–7,42,44] A mathematical model by Lyon et al[45] suggested that patients with critical illness who have compromised RBC production would demonstrate anemia in approximately 9–14 days. The observed SICU LOS in our study was 15 days, and although 20 mL was significantly less than 50–100 mL, 95.3% of patients had anemia at the time of SICU discharge.

One limitation of our study is that many patients had CVC and PICC placement. As such, those with only CVC were compared with those receiving PICC, and with those receiving PICC and CVC, to compare discard volumes. As a single predictor, DLT-associated plus total blood loss was significantly lower in patients without CVC, and CVC placement by itself was predictive of increased blood draws.

Because this is a retrospective analysis, we could not actively monitor these patients or obtain additional studies that may have been informative, such as of nutritional or inflammatory markers. Moreover, these patients have complex critical illness, and numerous factors, as discussed earlier herein, contribute to the incidence of anemia. Still we attempt to characterize anemia in patients based on their underlying

illness or health status as determined by CCI and by comparing data from patients who had surgical procedures with data from those who did not. Our cohort shows a contemporary baseline of iatrogenic blood loss in an SICU setting, which may be generalizable to other SICU services. Likewise, our results also showed lower rates of transfusion, compared with the findings of previous studies, indicating some movement toward more conservative transfusion practice.

The goal of a "bloodless" ICU admission without transfusion should still be pursued because RBC transfusion in this population is associated with higher rates of mortality, increased LOS, and ongoing anemia as an outpatient.[14,20] Moreover, the decision to transfuse RBCs was left to the discretion of the treating physician, and therefore the rationale for RBC transfusions was not always clear, highlighting the importance of institutional policies for transfusion. Negotiated rates were unavailable at this time, so chargemaster data represent an approximation of the final cost.

Conclusion

Although onset or persistence of anemia in this context is multifactorial, an association is clear between DLT, CVCs, and hospital-acquired anemia. Patients in the ICU especially require numerous laboratory tests, given the high acuity of care; however, physicians should be aware that this increased testing is associated with higher rates of anemia and the need for RBC transfusion. Our results highlight a need for increased health care provider education and a multidisciplinary approach to laboratory testing for these patients, involving hematology and transfusion medicine specialists.

Our results also support the implementation of waste-reducing measures such as BCDs, pediatric tubes, decision support, and institutional policies for frequency of laboratory testing. Given the associated increase in morbidity and mortality associated with hospital-acquired anemia and transfusion, efforts should be made to reduce unnecessary DLT and associated adverse events, to improve quality of care.

REFERENCES

1. Salisbury AC, Reid KJ, Alexander KP, et al. Diagnostic blood loss from phlebotomy and hospital-acquired anemia during acute myocardial infarction. *Arch Intern Med.* 2011;171(18):1646–1653.
2. Chant C, Wilson G, Friedrich JO. Anemia, transfusion, and phlebotomy practices in critically ill patients with prolonged ICU length of stay: a cohort study. *Crit Care.* 2006;10(5):R140. doi:10.1186/cc5054
3. Eyster E, Bernene J. Nosocomial anemia. *JAMA.* 1973;223(1):73–74.
4. Henry ML, Garner WL, Fabri PJ. Iatrogenic anemia. *Am J Surg.* 1986;151(3):362–363.
5. Whitehead NS, Williams LO, Meleth S, et al. Interventions to prevent iatrogenic anemia: a Laboratory Medicine Best Practices systematic review. *Crit Care.* 2019;23:278. doi:10.1186/s13054-019-2511-9
6. Silver MJ, Li Y-H, Gragg LA, Jubran F, Stoller JK. Reduction of blood loss from diagnostic sampling in critically ill patients using a blood-conserving arterial line system. *Chest.* 1993;104(6):1711–1715.
7. Ba VN, Bota DP, Mélot C, Vincent J-L. Time course of hemoglobin concentrations in nonbleeding intensive care unit patients. *Crit Care Med.* 2003;31(2):406–410.
8. Zimmerman JE, Seneff MG, Sun X, Wagner DP, Knaus WA. Evaluating laboratory usage in the intensive care unit: Patient and institutional characteristics that influence frequency of blood sampling. *Crit Care Med.* 1997;25(5):737–748.
9. Thomas J, Jensen L, Nahirniak S, Gibney RTN. Anemia and blood transfusion practices in the critically ill: a prospective cohort review. *Heart Lung.* 2010;39(3):217–225.
10. Martín C, Silva J, Romo J, et al. Analysis of the use of central venous catheters, mortality and catheter-related bloodstream infections in patients admitted to the ICU and after discharge to ward. *Intensive Care Med Exp.* 2015;3(suppl 1):A8911–A8912.
11. Low LL, Harrington GR, Stoltzfus DP. The effect of arterial lines on blood-drawing practices and costs in intensive care units. *Chest.* 1995;108(1):216–219.
12. Page C, Retter A, Wyncoll D. Blood conservation devices in critical care: a narrative review. *Ann Intensive Care.* 2013;3:141–146.
13. Koch CG, Reineks EZ, Tang AS, et al. Contemporary bloodletting in cardiac surgical care. *Ann Thorac Surg.* 2015;99(3):779–784.
14. Warner MA, Hanson AC, Frank RD, et al. Prevalence of and recovery from anemia following hospitalization for critical illness among adults. *JAMA Netw Open.* 2020;3(9):e2017843–e2017843.
15. Griffith DM, Vale ME, Campbell C, Lewis S, Walsh TS. Persistent inflammation and recovery after intensive care: a systematic review. *J Crit Care.* 2016;33:192–199.
16. Litton E, Latham P, Inman J, Luo J, Allan P. Safety and efficacy of erythropoiesis-stimulating agents in critically ill patients admitted to the intensive care unit: a systematic review and meta-analysis. *Intensive Care Med.* 2019;45(9):1190–1199.
17. Bateman AP, McArdle F, Walsh TS. Time course of anemia during six months follow up following intensive care discharge and factors associated with impaired recovery of erythropoiesis. *Crit Care Med.* 2009;37(6):1906–1912.
18. Rodriguez RM, Corwin HL, Gettinger A, et al. Nutritional deficiencies and blunted erythropoietin response as causes of the anemia of critical illness. *J Crit Care.* 2001;16(1):36–41.
19. Shander A. Anemia in the critically ill. *Crit Care Clin.* 2004;20(2):159–178.
20. Corwin HL, Gettinger A, Pearl RG, et al. The CRIT study: anemia and blood transfusion in the critically ill—current clinical practice in the United States. *Crit Care Med.* 2004;32(1):39–52.
21. Napolitano LM. Understanding anemia in the ICU to develop future treatment strategies. *Am J Respir Crit Care Med*. 2018;198(5):554–555.
22. Makam AN, Nguyen OK, Clark C, Halm EA. Incidence, predictors, and outcomes of hospital-acquired anemia. *J Hosp Med.* 2017;12(5):317–322.
23. Smoller BR, Kruskall MS. Phlebotomy for diagnostic laboratory tests in adults. *N Engl J Med.* 1986;314:1233–1235.
24. Ezzie ME, Aberegg SK, O'Brien JM. Laboratory testing in the intensive care unit. *Crit Care Clin.* 2007;23(3):435–465.
25. Cable CA, Razavi SA, Roback JD, Murphy DJ. RBC transfusion strategies in the ICU: a concise review. *Crit Care Med.* 2019;47(11):1637–1644.
26. Vlaar AP, Oczkowski S, de Bruin S, et al. Transfusion strategies in non-bleeding critically ill adults: a clinical practice guideline from the European Society of Intensive Care Medicine. *Intensive Care Med.* 2020;46:673–696.
27. Vincent J-L, Jaschinski U, Wittebole X, et al. Worldwide audit of blood transfusion practice in critically ill patients. *Crit Care.* 2018;22:102.
28. Rohde JM, Dimcheff DE, Blumberg N, et al. Health care–associated infection after red blood cell transfusion: a systematic review and meta-analysis. *JAMA.* 2014;311(13):1317–1326.
29. von Elm E, Altman DG, Egger M, et al. Strengthening the Reporting of Observational Studies in Epidemiology (STROBE) statement: guidelines for reporting observational studies. *J Clin Epidemiol.* 2008;61:344–349.
30. Charlson M, Szatrowski TP, Peterson J, Gold G. Validation of a combined comorbidity index. *J Clin Epidemiol.* 1994;47(11):1245–1251.
31. World Health Organization. Anaemia. https://www.who.int/health-topics/anaemia#tab=tab_1. Accessed July 8, 2022.

32. Hospital Price Index. https://search.hospitalpriceindex.com/hpi2/hospital/ParklandHospital/8213. Accessed July 8, 2022.
33. Ziegler MJ, Pellegrini DC, Safdar N. Attributable mortality of central line associated bloodstream infection: systematic review and meta-analysis. *Infection.* 2015;43(1):29–36.
34. Siegal DM, Manning N, Jackson Chornenki NL, Hills CM, Heddle NM. Devices to reduce the volume of blood taken for laboratory testing in ICU patients: a systematic review. *J Intensive Care Med.* 2020;35(10):1074–1079.
35. Riessen R, Behmenburg M, Blumenstock G, et al. A simple "blood-saving bundle" reduces diagnostic blood loss and the transfusion rate in mechanically ventilated patients. *PLoS One.* 2015;10(9):e0138879.
36. Goodnough LT, Baker SA, Shah N. How I use clinical decision support to improve red blood cell utilization. *Transfusion.* 2016;56(10):2406–2411.
37. Eaton KP, Levy K, Soong C, et al. Evidence-based guidelines to eliminate repetitive laboratory testing. *JAMA Intern Med.* 2017;177(12):1833–1839.
38. Iams W, Heck J, Kapp M, et al. A multidisciplinary housestaff-led initiative to safely reduce daily laboratory testing. *Acad Med.* 2016;91(6):813–820.
39. Choosing Wisely. Search Recommendations. https://www.choosingwisely.org/clinician-lists/. Accessed July 8, 2022.
40. Hoffman R. *Hematology: Basic Principles and Practice*. 7th ed. Philadephia, PA: Elsevier; 2017.
41. Hillman RS, Henderson PA. Control of marrow production by the level of iron supply. *J Clin Invest.* 1969;48(3):454–460.
42. Hayden SJ, Albert TJ, Watkins TR, Swenson ER. Anemia in critical illness: insights into etiology, consequences, and management. *Am J Respir Crit Care Med.* 2012;185(10):1049–1057.
43. Giblett ER, Coleman DH, Pirzio-Biroli G, et al. Erythrokinetics: quantitative measurements of red cell production and destruction in normal subjects and patients with anemia. *Blood.* 1956;11(4):291–309.
44. Liu S, McConnell SC, Ryan TM. Erythropoiesis in the absence of adult hemoglobin. *Mol Cell Biol.* 2013;33(11):2241–2251.
45. Lyon AW, Chin AC, Slotsve GA, Lyon ME. Simulation of repetitive diagnostic blood loss and onset of iatrogenic anemia in critical care patients with a mathematical model. *Comput Biol Med.* 2013;43(2):84–90.
46. Kwan JL, Lo L, Ferguson J, et al. Computerised clinical decision support systems and absolute improvements in care: meta-analysis of controlled clinical trials. *BMJ.* 2020;370:m3216.
47. Geneen LJ, Kimber C, Doree C, Stanworth S, Shah A. Efficacy and safety of intravenous iron therapy for treating anaemia in critically ill adults: a rapid systematic review with meta-analysis. *Transfus Med Rev.* 2021;36(2):97–106.
48. Turaga KK, Sugimoto JT, Forse RA. A meta-analysis of randomized controlled trials in critically ill patients to evaluate the dose-response effect of erythropoietin. *J Intensive Care Med.* 2007;22(5):270–282.

A New Auto-RPA-Fluorescence Detection Platform for SARS-CoV-2

Jing Tian, MD,[1,a] Biao Chen, PhD,[2,a] Bin Zhang, PhD,[3,a] Tantan Li,[4] Zhiqiang Liang,[5] Yujin Guo,[6] Huping Jiao,[7] Fenghong Liang,[2] Longquan Xiang,[8] Fanzhong Lin,[8] Ruiwen Ren, MD,[1,] Qingbin Liu, PhD[2,*]*

[1]Centers for Disease Control and Prevention, People's Liberation Army Southern Theater Command, Guangzhou, China, [2]Laboratory of Medical Mycology, Jining No. 1 People's Hospital, Jining, China, [3]Computational Bioscience Research Center (CBRC), Computer, Electrical and Mathematical Sciences and Engineering Division, King Abdullah University of Science and Technology, Thuwal, Saudi Arabia, [4]Jining Precision Medical Test Center, Jining No. 1 People's Hospital, Jining, China, [5]Medical Laboratory Department, Jining No. 1 People's Hospital, Jining, China, [6]Institute of Clinical Pharmacy & Pharmacology, Jining No. 1 People's Hospital, Jining, China, [7]Jilin University, Changchun, China, [8]Department of Pathology, Jining No. 1 People's Hospital, Jining, China. *To whom correspondence should be addressed: renruiwen@hotmail.com; jnmclqb@mail.jnmc.edu.cn. [a]First authors.

Keywords: SARS-CoV-2, auto-RPA-fluorescence, limit of detection, specificity, diagnosis

Abbreviations: qRT-PCR, quantitative reverse transcription–polymerase chain reaction; RPA, recombinase polymerase amplification; CDC, Centers for Disease Control and Prevention; LAMP, loop-mediated isothermal amplification; CRISPR, clustered regularly interspaced short palindromic repeats; Cas, CRISPR-associated; STC, Southern Theater Command; S, spike, N, nucleocapsid; BLAST, basic local alignment search tool; FAM, carboxyfluorescein; HEX, hexachlorofluorescein; Ct, cycle threshold.

Laboratory Medicine 2023;54:182–189; https://doi.org/10.1093/labmed/lmac093

ABSTRACT

Objective: The outbreak of COVID-19 caused by SARS-CoV-2 has led to a serious worldwide pandemic. Quantitative reverse transcription–polymerase chain reaction (qRT-PCR)–based methods were recommended for routine detection of SARS-CoV-2 RNA. Because the reaction time and analytical sensitivity of qRT-PCR limits the diagnosis of SARS-CoV-2, development of a quick process of SARS-CoV-2 detection technology with high analytical sensitivity remains urgent.

Methods: We combined isothermal amplification and fluorescence detection technology to develop a new auto-recombinase polymerase amplification (RPA)-fluorescence platform that could be used in the diagnosis of SARS-CoV-2.

Results: By optimization of primers and probes, the RPA platform could detect SARS-CoV-2 nucleotides within 15 min. The limits of detection and specificity of the auto-RPA-fluorescence platform were 5 copies/μL and 100%, respectively. The accuracy of detection of the auto-RPA-fluorescence platform in the 16 positive samples was 100%.

Conclusion: The RPA platform is a potential technology for the diagnosis of SARS-CoV-2 infection.

Since the outbreak of COVID-19, caused by SARS-CoV-2, this infectious disease has become a global pandemic that affects many countries in the world. According to the World Health Organization homepage (https://www.who.int), more than 500 million people have been infected with COVID-19, and more than 6 million people have died as of April 2022. Quantitative reverse transcription–polymerase chain reaction (qRT-PCR) is a common approach for the detection of SARS-CoV-2 infection. It is routinely performed worldwide, including in the Centers for Disease Control and Prevention (CDC) and other clinical laboratories.[1,2] Globally, qRT-PCR has been defined as a standard method for the detection of COVID-19. However, this method is time-consuming (the process takes more than 2 h), and requires high purity samples, sophisticated equipment, and well-trained personnel, which can delay the diagnosis of COVID-19. In addition, this method has relatively low analytical sensitivity and poor-quality nucleotide extraction, which causes false-negative results.[3,4] Therefore, more rapid, sensitive, and accurate diagnostic methods are greatly needed to deal with the COVID-19 pandemic.

To detect COVID-19 infection rapidly, scientists have made various efforts to develop a series of novel detection methods with great potential.[5] For example, loop-mediated isothermal amplification (LAMP) starts amplification by using *Bst* DNA polymerase at a constant temperature of approximately 65°C. The LAMP can cycle, elongate, and continue subsequent rounds of amplification with 6 specially designed primers and has high reaction efficiency. The reaction generates magnesium pyrophosphate and results in color change, which can be judged by the naked eye under blue light.[6,7] However, such a method is mediated by detecting the by-products of loop amplification, which may cause false-positive results due to nonspecific reactions. [8–11] Clustered regularly interspaced short palindromic repeats (CRISPR)-associated (Cas) nuclease-based methods have properties that can be used for ultrasensitive diagnostic tests. The Cas nucleases, such as RNA-guided RNase Cas13a and DNase Cas12a, cause collateral cleavage when activated by the recognition of target nucleotide sequences.[5] Recently,

researchers have developed exciting (CRISPR)-based methods by integrating PCR, LAMP, or recombinase polymerase amplification (RPA) with Cas-mediated collateral cleavage,[6,9,12–15] which were amplified by diverse reaction systems.[5] However, current CRISPR strategies have some disadvantages, including multiple-step operations and long incubation times. A new approach that is more rapid, accurate, and simple for detecting SARS-CoV-2 is urgently needed.

To achieve more rapid and accurate detection of SARS-CoV-2 infection, we applied RPA and a fluorescence detection system to develop an auto-RPA–fluorescence assay for detecting SARS-CoV-2 RNA. The results show that the new assay described here is more rapid and simple than the standard qRT-PCR used currently to detect SARS-CoV-2 and has potential to detect other major pathogenic microorganisms as well.

Materials and Methods

RNA Extraction

Oropharyngeal swabs were used to collect samples from participants and qRT-PCR was used to determine whether the samples were positive or negative for SARS-CoV-2. Briefly, RNA was extracted using the SSNP-9600A Thermo Fisher Scientific nucleic acid extraction workstation in the P3 laboratory of the Center for Disease Control and Prevention of Southern Theater Command (CDC-STC). Prior to the experiment, the purity and concentration of each virus RNA sample was determined using Qubit 3.0 fluorometer (Thermo Fisher Scientific). Subsequent experiments were performed at Jining No. 1 People's Hospital. All samples were frozen at −80°C or transferred on dry ice and kept for less than 6 mo.

Design and Analysis of Primers and Probes

The complete genomic sequence of SARS-CoV-2 was obtained from GenBank (MN985325.1) and used as reference sequence for the design of primers and probes. To establish the auto-RPA-fluorescence assay, we first designed RPA-specific primers and probes for targeting the spike (S) gene and nucleocapsid (N) gene sequences of SARS-CoV-2 using the PrimedRPA online bioinformatic tool.[16,17] The panel of primers and probes used in the RPA reaction are listed in **TABLE 1**. We used Primer-basic local alignment search tool (BLAST) to determine whether the primer and probe sequences were specific for the SARS-CoV-2 genome. The primer region sequence was then compared with the genomes of other viruses using BLAST to calculate homology. Fluorescence and modifications were then labeled following principles that were suggested previously.[17] The S gene and N gene fragments of SARS-CoV-2 were synthesized and cloned in pcDNA3 vectors (Sangon Biotech). According to the criteria suggested in the TwistAmp amplification guidelines (TwistDx), the primers/probes with better amplification efficiency and fluorescent quantity were used for subsequent detection.

Construction of a New Auto-RPA–Fluorescence Platform

We designed a new auto-RPA-fluorescence platform based on the RPA principle and a fluorescence detection system. Briefly, tetrahydrofuran is added to the probe between two adjacent thymine residues that are separated by 1, 3, or 5 intervening nucleotides when synthesized. In this study, a fluorescent dye—carboxyfluorescein (FAM) or hexachlorofluorescein (HEX)—was added to the upstream thymine, and Black Hole Quencher dye was added to the downstream thymine in the probe (Genomics).

TABLE 1. Primers and Probes Used in the Auto-RPA–Fluorescence Platform[a]

Primer/Probe	Sequence 5'→ 3'
N256For	ACTACCGAAGAGCTACCAGACGAAT
N540Rev	CGTGATGAGGAACGAGAAGAGGCTTG
N540For	CAAGCCTCTTCTCGTTCCTCATCAC
N689Rev	GCCTTTACCAGACATTTTGCTCTCA
N860For	GGACCAGGAACTAATCAGACAAGGAA
N1167Rev	GCAGCAGGAAGAAGAGTCACAGTTTG
S3053For	CAGAGCTTCTGCTAATCTTGCTGCTA
S3202Rev	TTGTGAAGTTCTTTTCTTGTGCAGGG
S2531For	TGCTGCTAGAGACCTCATTTGTGCAC
S2850Rev	AAAGCTTGTGCATTTTGGTTGACCAC
Probe N645 exo	GGTGATGCTGCTCTTGCTTTGCTGCTGCTTGACAGATT GAACCA
Probe N408 exo	GAGGGAGCCTTGAATACACCAAAAGATCACATTGGCAC CCGCAAT
Probe S2560 exo	AACGGCCTTACTGTTTTGCCACCTTTGTCACAGATGAA ATGA
Probe S2760 exo	CTATTGGCAAAATTCAAGACTCATTTCTTCCACAGCAA
Probe S3135 exo	GCTATCATCTTATGTCCTTCCCTCGTCAGCACCTCATGG

[a]Primers and probes were designed and selected by the online tool PrimedRPA (see Materials and Methods). All primers and probes were tested by BLAST to detect specificity for SARS-CoV-2 virus genome and subsequently tested in the auto-RPA-fluorescence platform.

During detection with the auto-RPA-fluorescence platform, we first used the RPA exo kit (Weifang Amp-Future Biotech) to perform reverse-transcribed isothermal amplification in a 50 μL reaction volume. The 50 μL reaction mixture contained 2 μL primer mix (10 μmol/L each), 1 μL probe (10 μmol/L), and 5 μL RNA sample. For the positive control group, we used synthesized gene fragments that covered the amplification regions. For the negative control group, the template DNA was replaced with scrambled synthesized DNA. The reactions were performed in a SLAN-96P fluorescence qPCR detection system (Shanghai Hongshi Medical Technology), and the reaction mixtures were incubated at 42°C for 2 min followed by 40 cycles. Since the temperature was consistent in RPA reaction and there were no real cycles, the program automatically defined 42°C/40 sec/step as a cycle. The fluorescence signal was monitored for each cycle using a fluorescence qPCR detection system. For reactions with cycle threshold (Ct) values of less than 38, the results were determined as positive and otherwise determined as negative.

Limit of Detection and Specificity of the Auto-RPA–Fluorescence Platform in Detecting SARS-CoV-2

To assess the limit of detection of the auto-RPA–fluorescence platform for detecting SARS-CoV-2, the virus gene template was diluted from 50,000,000 to 5 copies/μL with double-distilled water and applied to the platform. The specificity of the new platform was evaluated using RNA extractions from influenza, HCoV-229E, measles, mumps, HIV, and coxsackie viruses.

Application and Assessment of the Auto-RPA–Fluorescence Platform for Detecting SARS-CoV-2-Infected Samples

A total of 16 positive samples and 2 negative samples were collected from the CDC-STC (NBJJ-2020-007), Guangzhou, China. Specimen

FIGURE 1. The optimization of primer pairs and probes for auto RPA–fluorescence-based SARS-CoV-2 detection. A, Agarose gel electrophoresis analysis of amplification products by different primer pairs as indicated. B, Schematic representation of probe modification for SARS-CoV-2 detection in the auto-RPA–fluorescence detection platform. C, Fluorescent signal generated from S2531For/S2850Rev/ProbeS2560 in the platform. D, Fluorescent signal generated from S2531For/S2850Rev/ProbeS2760 in the platform.

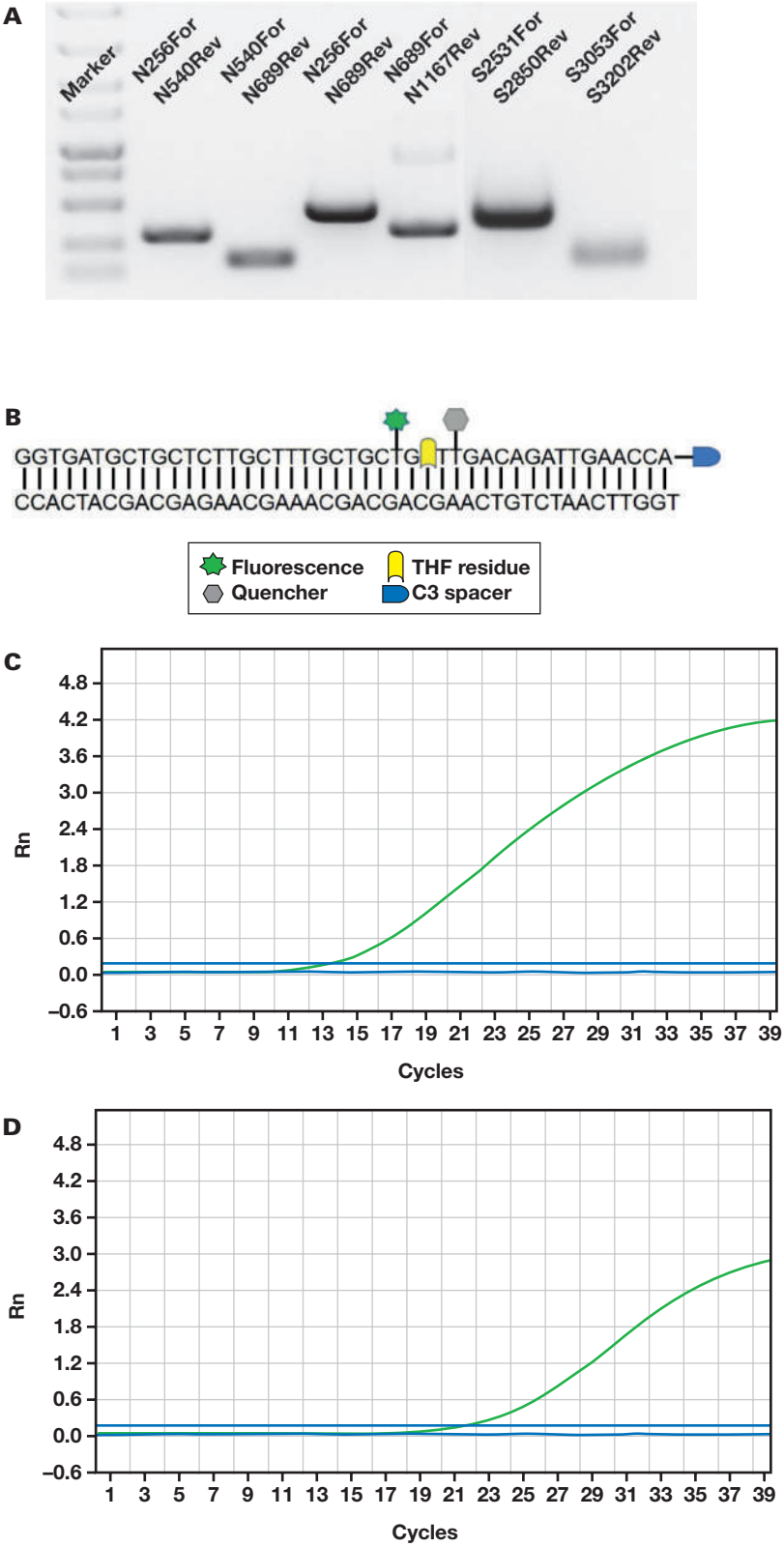

FIGURE 1. (cont) E, Fluorescent generated from N256For/N689Rev/ProbeN645 in the platform. F, Fluorescent signal generated from N256For/N689Rev/ProbeN408 in the platform. Signals are presented as normalized reporter (Rn).

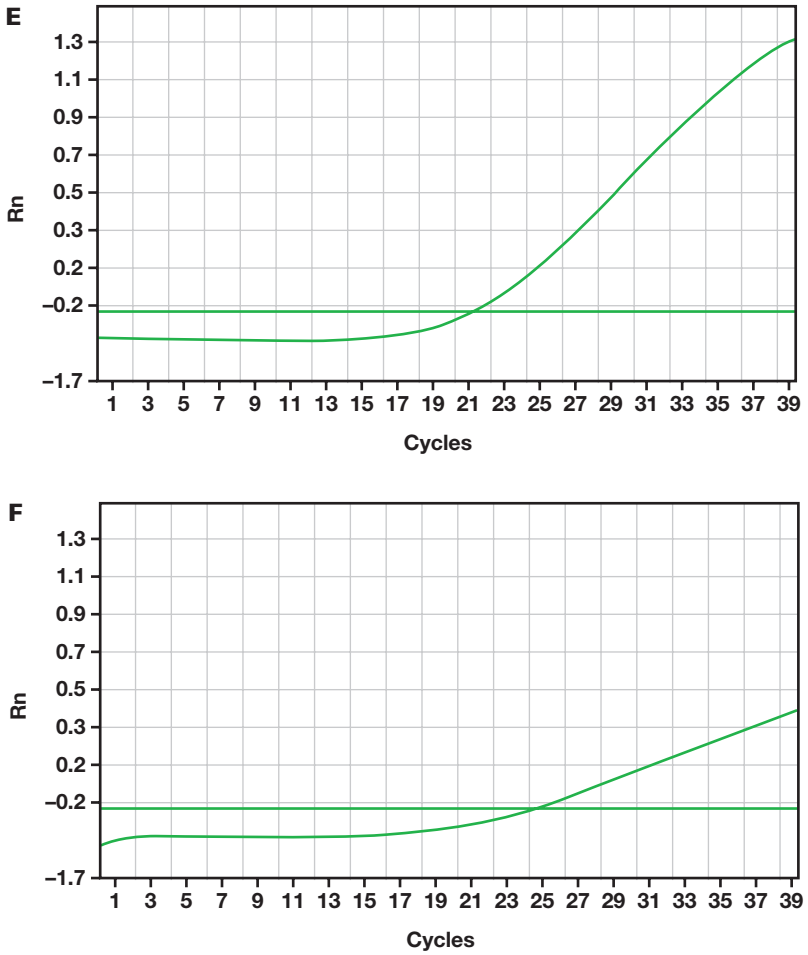

RNA was subsequently extracted and evaluated using the new auto-RPA–fluorescence platform.

Ethical Statement

Sample collection and analysis were approved by the CDC-STC. The internal use of samples accorded with the medical and ethical rules pertaining to participating individuals.

Results

Efficiency of the Auto-RPA–Fluorescence Assay for SARS-CoV-2 Detection

As described in Materials and Methods, we designed RPA-specific primers and probes for targeting the N and S gene sequences of SARS-CoV-2 using PrimedRPA. After the analysis of specificity, we selected 10 primers and 5 probes with their genomic locations, as shown in **TABLE 1**.

To select the primer with optimal efficiency, we compared the sequences of the primers with those of other virus genomes (including 7 similar coronaviruses, 2 influenza viruses, and 2 other coronaviruses) using BLAST. We found that the sequences were not similar to most of the viral sequences we chose. The amplification efficiency of different pairs of primers was then tested by normal PCR with synthesized gene fragments, as suggested by TwistDx. Agarose gel electrophoresis revealed that N256For/N689Rev and S2531For/S2850Rev were the best primer pairs for amplification with the highest efficiency (**FIGURE 1A**). We modified the probes for fluorescence detection, as indicated in the Materials and Methods section (**FIGURE 1B**). To compare the efficiency of probes N408, N645, S2560, and S2760—which are located in the region confined by the selected primer pairs—we performed RPA reactions and obtained quantified real-time fluorescence signals using the SLAN-96S fluorescence detection system. The results showed that although all the primer sets generated fluorescence, the N256For/N689Rev/ProbeN645 and S2531For/S2850Rev/ProbeS2560 sets produced the strongest signals with lower Ct values (**FIGURE 1C–1F**).

The Auto-RPA–Fluorescence Platform Was Sensitive in the Detection of SARS-CoV-2

Next, to explore the limits of the single auto-RPA-fluorescence assay in the detection of SARS-CoV-2, we prepared reaction mixtures containing serially 10-fold-diluted S and N gene fragments (from 50,000,000 to 5 copies). In the established reaction system, we applied FAM-labeled N256For/N689Rev/ProbeN645 for detecting the N gene and HEX-labeled S2531For/S2850Rev/ProbeS2560 sets for detecting the S gene and monitored the resulting real-time fluorescence signals. As indicated in **FIGURE 2**, the auto-RPA-fluorescence platform was able to detect

FIGURE 2. The limit of detection of the auto-RPA–fluorescence detection platform in detecting SARS-CoV-2 gene fragments. A, The limit of detection with FAM-labeled N256For/N689Rev/ProbeN645 in detecting SARS-CoV-2 N gene. Fluorescent curves of reactions with 10-fold gradually diluted the N gene template from 50 million copies/μL to 5 copies/μL. B, The limit of detection with HEX-labeled S2531For/S2850Rev/ProbeS2560 in detecting SARS-CoV-2 S gene. Fluorescent curves of reactions with 10-fold gradually diluted the S gene fragments from 50 million copies/μL to 5 copies/μL.

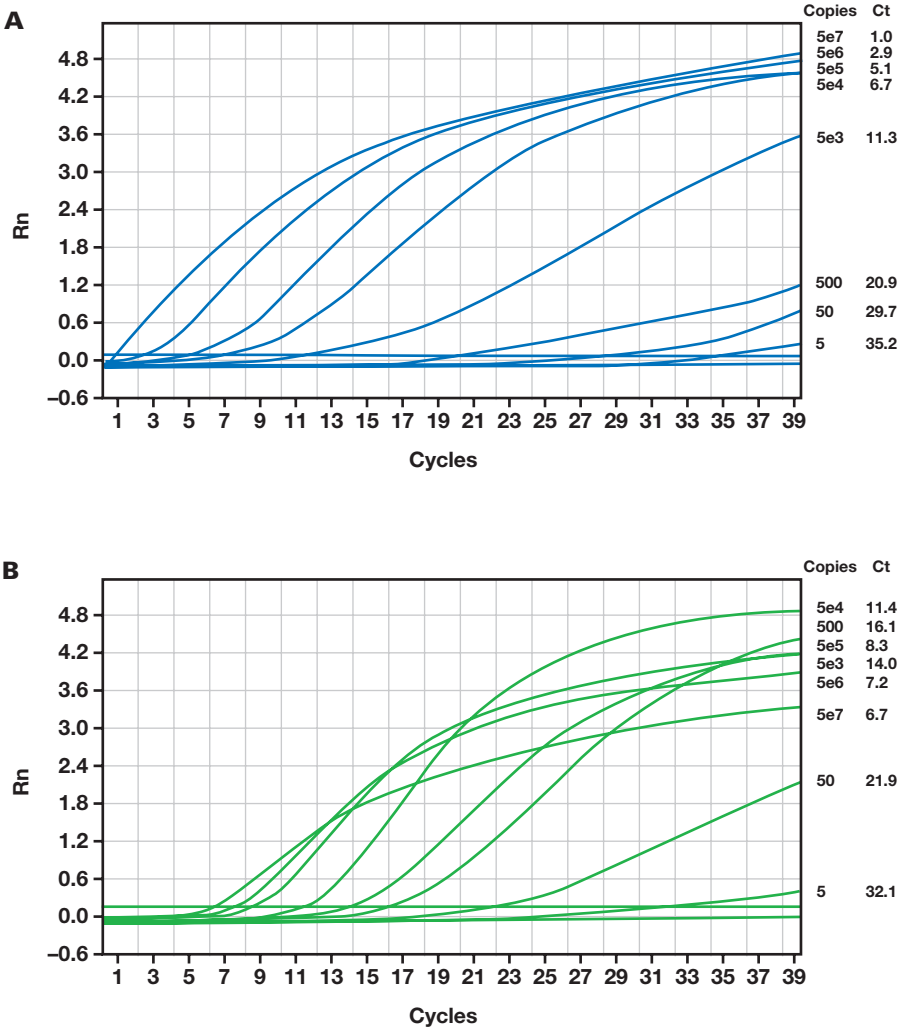

5 copies/μL prior to the 38 Ct cutoff, which suggested positive results in detecting SARS-CoV-2 gene fragments. Additionally, both primer/probe sets were able to detect as few as 5 copies/μL S gene or N gene templates. (**FIGURE 2**).

The Auto-RPA–Fluorescence Detection Platform Is Specific in Detecting SARS-CoV-2

To assess its detection specificity, we tested the auto-RPA-fluorescence platform on the nucleotide sequences of influenza, HCoV-229E, measles virus, mumps, HIV, and coxsackie viruses. The FAM-labeled N256For/N689Rev/ProbeN645 and HEX-labeled S2531For/S2850Rev/ProbeS2560 were applied in the reaction. Only the RNA from SARS-CoV-2 generated positive signals (**FIGURE 3**), demonstrating that the primers and probes were highly specific for SARS-CoV-2 detection.

The Auto-RPA–Fluorescence Platform Was Accurate and Reliable for the Detection of SARS-CoV-2 in Clinical Samples

To investigate the diagnostic accuracy and reliability of the auto-RPA–fluorescence detection method, we applied it to oropharyngeal swab samples obtained during the 2020 epidemic. A total of 16 samples from SARS-CoV-2–infected patients and 2 SARS-CoV-2–negative samples—which were initially detected using qPCR—were tested using the auto-RPA–fluorescence assay. The N256For/N689Rev/ProbeN645 and HEX-labeled S2531For/S2850Rev/ProbeS2560 were applied in the PRA reaction. The results showed that all the samples validated by our assay were consistent with those detected using the qRT-PCR method. Moreover, the results were reported in less than 15 min with Ct values less than 10 (**FIGURE 3**). The SARS-CoV-2–negative samples did not show fluorescence signals (**FIGURE 3**). The Ct values of 16 positive samples detected by auto-RPA–fluorescence are shown in **TABLE 2**. The qRT-PCR results of samples that were used in the auto-RPA–fluorescence detection platform are shown in **Supplementary Figure S1**.

Discussion

Although the most popular approach for SARS-CoV-2 detection is based on qRT-PCR, it is unsuitable for large-scale diagnostics since it is time-consuming and requires special equipment and well-trained

FIGURE 3. **The specificity of the auto-RPA–fluorescence detection platform in detecting SARS-CoV-2. Figures represent the fluorescent curves generated by the platform in detecting SARS-CoV-2–positive samples (A), SARS-CoV-2–negative samples (B), and an influenza sample (C) as representative of the control virus. FAM-labeled N256For/N689Rev/ProbeN645 and HEX-labeled S2531For/S2850Rev/ProbeS2560 were applied in the reaction.**

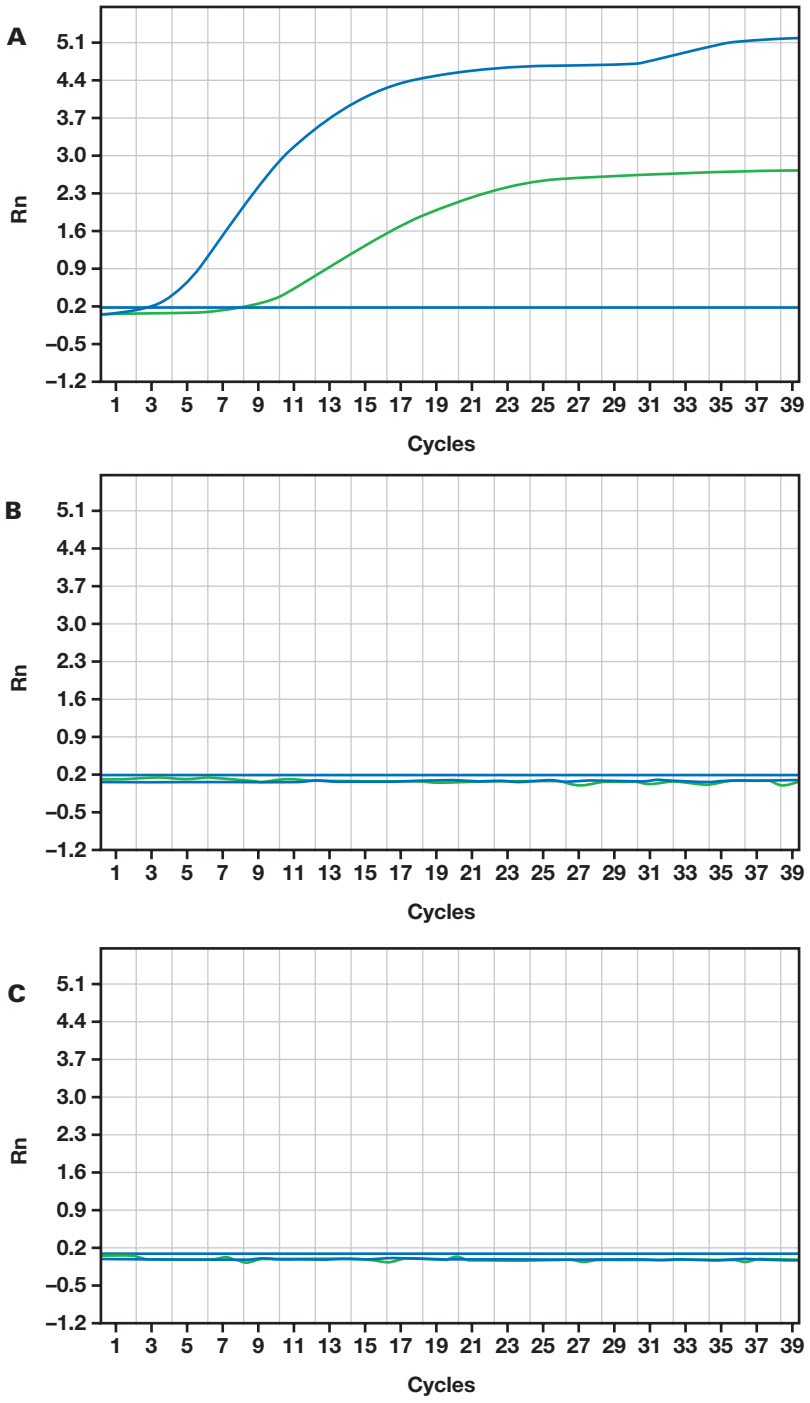

personnel. The emerging isothermal amplification-based technologies have mostly been reported for SARS-CoV-2 detection. For rapid and convenient testing, colorimetric methods coupled with RT-LAMP amplification have been proposed.[18,19] However, the colorimetric methods developed for LAMP lack specificity because their detection objects are based on factors such as H^+-induced pH change and the level of magnesium pyrophosphate.[7,19] To improve specificity and limits of detection, researchers have developed LAMP- or RPA-based methods using CRISPR-Cas9/Cas12. Such methods can achieve nearly single-copy detection of CRISPR-RNA and can recognize specific target sequences.[6,13,20,21] However, such isothermal reactions are followed by the mixing of amplicons with Cas9/Cas12 reagents for probe cleavage, which complicates SARS-CoV-2 detection. Recently, 1-step CRISPR-based methods coupled with RPA have been developed.[22,23] However, these assays present a high

TABLE 2. The Ct Values of 16 Positive Samples Detected by the Auto-RPA–Fluorescence Platform

Sample	Ct Value (N Gene)	Ct Value (S Gene)
1	3.1	7.8
2	5.0	13.2
3	2.8	7.9
4	4.2	14.5
5	5.3	14.3
6	5.1	14.7
7	4.3	12.4
8	4.0	11.9
9	2.1	9.0
10	4.0	8.8
11	2.3	7.3
12	5.1	15.3
13	2.3	1
14	7.0	18.1
15	5.1	15.7
16	3.1	9.9

Ct, cycle threshold; N, nucleocapsid; S, spiked.

background in visual detection, which decreases the analytical sensitivity and specificity of CRISPR detection. Therefore, there is still an urgent need for a more rapid, accurate, and simple methods for SARS-CoV-2 detection.

Herein, we combined the multienzyme RPA principle with a fluorescence detection system to create a new auto-RPA–fluorescence platform that simplifies laboratory operation and can be implemented for point-of-care testing. The probe modification strategy deployed in the new auto-RPA–fluorescence assay generates reaction yields that are suitable for real-time fluorescent monitoring with high analytical sensitivity. We propose an operation protocol that requires minimal equipment—that is, pipettes, heat blocks, and reagent tubes—and takes place at the relatively low temperature of approximately 42°C.[16] Thus, it has potential for next-generation point-of-care molecular diagnosis. We expect this assay could be widely applied to detect various pathogenic microbes, including infectious bacteria, fungi, and viruses.

In this study, the single auto-RPA–fluorescence assay for SARS-CoV-2 demonstrated several comparative advantages over its counterparts. First, it was much faster than qRT-PCR. The entire amplification process of single auto-RPA–fluorescence can be completed within 15 min, whereas qRT-PCR usually takes approximately 2 h. To our knowledge, single auto-RPA-fluorescence requires the least amount of time to diagnose SARS-CoV-2 infection of any system. Second, the single auto-RPA–fluorescence assay can be performed at a constant temperature of approximately 39 to 42°C, which can be achieved in a water bath. It is very convenient for use where an energy supply is unavailable. The auto-RPA–fluorescence platform provided 100% accuracy in testing SARS-CoV-2–positive and –negative samples. Third, the detection limit of the auto-RPA–fluorescence platform was as low as 5 copies/μL, which is comparable with other CRISPR/isothermal-based methods. Isothermal methods such as LAMP are relatively inaccurate because they involve a robust reaction.[10–12] Further, the limit of detection makes this platform adaptable for analyzing the mixed nucleic acids of samples from suspected COVID-19 patients and thus improves the throughput of detection.

In conclusion, we establish a promising single auto-colorimetric assay that can detect SARS-CoV-2 infection with high analytical sensitivity using a more rapid and simple detection process. The assay also has potential for the detection of other major pathogenic microorganisms. However, the present assay still requires an RNA preparation module. Thus, further efforts are required to combine RNA extraction with the single auto-RPA method to achieve simplified SARS-CoV-2 detection.

Acknowledgments

This work was sponsored by the Doctoral Fund of Jining No.1 People's Hospital (2019004, 2020005), Technology Development Program of Shandong Province (2018WS469), China Postdoctoral Science Foundation (2020T130073ZX), and Natural Science Foundation of Shandong Province (NM ZR2020QH272), China.

We gratefully acknowledge the assistance of Professor Huabao Xiong and Professor Dongmei Shi with the writing of the manuscript.

REFERENCES

1. Jiang S, Du L, Shi Z. An emerging coronavirus causing pneumonia outbreak in Wuhan, China: calling for developing therapeutic and prophylactic strategies. *Emerg Microbes Infect* 2020;9(1):275–277. doi:10.1080/22221751.2020.1723441.
2. Chu DKW, Pan Y, Cheng SMS, et al. Molecular diagnosis of a novel coronavirus (2019-nCoV) causing an outbreak of pneumonia. *Clin Chem.* 2020;66(4):549–555. doi:10.1093/clinchem/hvaa029.
3. Trisnawati I, El Khair R, Puspitarani DA, Fauzi AR, Gunadi. Prolonged nucleic acid conversion and false-negative RT-PCR results in patients with COVID-19: a case series. *Ann Med Surg (Lond).* 2020;59:224–228.
4. Xiao AT, Tong YX, Zhang S. False negative of RT-PCR and prolonged nucleic acid conversion in COVID-19: Rather than recurrence. *J Med Virol.* 2020;92(10):1755–1756. doi:10.1002/jmv.25855.
5. Gootenberg JS, Abudayyeh OO, Lee JW, et al. Nucleic acid detection with CRISPR-Cas13a/C2c2. *Science.* 2017;356(6336):438–442. doi:10.1126/science.aam9321.
6. Wang R, Qian C, Pang Y, et al. opvCRISPR: one-pot visual RT-LAMP-CRISPR platform for SARS-cov-2 detection. *Biosens Bioelectron.* 2021;172:112766. doi:10.1016/j.bios.2020.112766.
7. Yu L, Wu S, Hao X, et al. Rapid detection of COVID-19 coronavirus using a reverse transcriptional loop-mediated isothermal amplification (RT-LAMP) diagnostic platform. *Clin Chem.* 2020;66(7):975–977. doi:10.1093/clinchem/hvaa102.
8. Wang X, Zhong M, Liu Y, et al. Rapid and sensitive detection of COVID-19 using CRISPR/Cas12a-based detection with naked eye readout, CRISPR/Cas12a-NER. *Sci Bull (Beijing).* 2020;65(17):1436–1439. doi:10.1016/j.scib.2020.04.041.
9. Wang B, Wang R, Wang D, et al. Cas12aVDet: a CRISPR/Cas12a-based platform for rapid and visual nucleic acid detection. *Anal Chem.* 2019;91(19):12156–12161. doi:10.1021/acs.analchem.9b01526.
10. Huang WE, Lim B, Hsu CC, et al. RT-LAMP for rapid diagnosis of coronavirus SARS-CoV-2. *Microb Biotechnol.* 2020;13(4):950–961. doi:10.1111/1751-7915.13586.
11. Lu R, Wu X, Wan Z, Li Y, Jin X, Zhang C. A novel reverse transcription loop-mediated isothermal amplification method for rapid detection of SARS-CoV-2. *Int J Mol Sci* . 2020;21(8):2826.

12. Zhang M, Liu C, Shi Y, Wu J, Wu J, Chen H. Selective endpoint visualized detection of Vibrio parahaemolyticus with CRISPR/Cas12a assisted PCR using thermal cycler for on-site application. *Talanta.* 2020;214:120818. doi:10.1016/j.talanta.2020.120818.

13. Kellner MJ, Koob JG, Gootenberg JS, Abudayyeh OO, Zhang F. SHERLOCK: nucleic acid detection with CRISPR nucleases. *Nat Protoc.* 2019;14(10):2986–3012. doi:10.1038/s41596-019-0210-2.

14. Ali Z, Aman R, Mahas A, et al. iSCAN: An RT-LAMP-coupled CRISPR-Cas12 module for rapid, sensitive detection of SARS-CoV-2. *Virus Res.* 2020;288:198129. doi:10.1016/j.virusres.2020.198129.

15. Sun Y, Yu L, Liu C, et al. One-tube SARS-CoV-2 detection platform based on RT-RPA and CRISPR/Cas12a. *J Transl Med.* 2021;19(1):74. doi:10.1186/s12967-021-02741-5.

16. Daher RK, Stewart G, Boissinot M, Bergeron MG. Recombinase polymerase amplification for diagnostic applications. *Clin Chem.* 2016;62(7):947–958. doi:10.1373/clinchem.2015.245829.

17. Higgins M, Ravenhall M, Ward D, et al. PrimedRPA: primer design for recombinase polymerase amplification assays. *Bioinformatics.* 2019;35(4):682–684. doi:10.1093/bioinformatics/bty701.

18. Notomi T, Mori Y, Tomita N, Kanda H. Loop-mediated isothermal amplification (LAMP): principle, features, and future prospects. *J Microbiol.* 2015;53(1):1–5. doi:10.1007/s12275-015-4656-9.

19. Notomi T, Okayama H, Masubuchi H, et al. Loop-mediated isothermal amplification of DNA. *Nucleic Acids Res.* 2000;28(12):E63.

20. Tsang J, LaManna CM. Open sharing during COVID-19: CRISPR-based detection tools. *CRISPR J.* 2020;3(3):142–145. doi:10.1089/crispr.2020.0030.

21. Broughton JP, Deng X, Yu G, et al. CRISPR-Cas12-based detection of SARS-CoV-2. *Nat Biotechnol.* 2020;38(7):870–874. doi:10.1038/s41587-020-0513-4.

22. Ding X, Yin K, Li Z, et al. Ultrasensitive and visual detection of SARS-CoV-2 using all-in-one dual CRISPR-Cas12a assay. *Nat Commun.* 2020;11(1):4711. doi:10.1038/s41467-020-18575-6.

23. Ding X, Yin K, Li Z, Liu C. All-in-one dual CRISPR-Cas12a (AIOD-CRISPR) assay: a case for rapid, ultrasensitive and visual detection of novel coronavirus SARS-CoV-2 and HIV virus. *bioRxiv.* 2020. doi: 10.1101/2020.03.19.998724.

Comparison of RhD Typing Results by Serology and Molecular Methods

Richard R. Gammon, MD,[1] Michelle Conceicao, BS, SBB(ASCP)CM,[2] Nancy Benitez, MPH, SBB(ASCP)CM,[3] Frieda Bright, MPH, MT(ASCP)SBBCM,[4] Kelley Counts, MS, MBA,[5] Claribel Resto, MPH, MT(ASCP)SBBCM,[3] and Karl Rexer, PhD[5,6]

[1]Scientific, Medical, Technical Direction, OneBlood, Orlando, FL, USA, [2]Immunohematology Reference Laboratory, OneBlood, St Petersburg, FL, USA, [3]Immunohematology Reference Laboratory, OneBlood, Fort Lauderdale, FL, USA, [4]Centralized Transfusion Service, OneBlood, St Petersburg, FL, USA, [5]Information Technology Administration, OneBlood, St Petersburg, FL, USA, [6]Rexer Analytics, Winchester, MA, USA. *To whom correspondence should be addressed: richard.gammon@oneblood.org.

Keywords: serology, molecular, D-alloimmunization, immunohematology reference laboratory, turnaround time, concordance

Abbreviations: IRL, immunohematology reference laboratory; RBCs red blood cells; TAT, turnaround time; RhIG, Rh immune globulin.

Laboratory Medicine 2023;54:190–192; https://doi.org/10.1093/labmed/lmac097

ABSTRACT

Objective: Molecular testing determines D antigen status when abnormal serologic results are observed. Molecular testing is routinely batched, resulting in longer turnaround time for abnormal D status resolution. During the interim, obstetric patients with questionable/uninterpretable and weak D typing results by serology, per the immunohematology reference laboratory (IRL) policy, will receive RhD negative blood. This study aimed to determine whether serology results achieved a concordance.

Methods: Six hospitals provided samples to the IRL (first IRL) for RhD status by DNA. De-identified samples were sent for serology RhD (second IRL). A concordance of ≥80% was acceptable.

Results: Forty-nine samples were evaluated. Results were concordant (65.3% [32/49]) and discordant (34.7% [17/49]). This is significantly lower than clinically acceptable 80% ($z = 2.57$, $P < .05$). The turnaround-time was 3.0 hours for serology and 4.4 days for molecular evaluation.

Conclusion: Due to a low concordance, serology could not be used in place of molecular testing.

When the D type of antigen is determined in a patient, a weak D test is not recommended except to assess the red blood cells (RBCs) of a newborn to determine maternal risk for D alloimmunization.[1] Today, monoclonal IgM reagents type many samples as D-positive by immediate spin that would have previously been detected only by indirect antiglobulin testing.[1]

Although molecular testing is the preferred method to determine D status when questionable, uninterpretable, or weak D typing results are observed by conventional serologic methods, indicating the patient has a possible D variant, it has a longer turnaround time (TAT). During the period when molecular D status confirmation is pending, per our institution's immunohematology reference laboratory (IRL) policy, those with discrepant results (obstetric patients being the highest priority) need to receive RhD negative blood components or Rh immune globulin (RhIG) as a precaution to avoid risk of anti-D formation.[1] This study compared the results of a serological-based test to those of a molecular-based test and their TATs to determine whether there was sufficient concordance between methodologies to allow serology results to be used to make transfusion decisions regarding administration of RhD positive or RhD negative RBCs or platelets and RhIG administration that would avoid alloimmunization and formation of anti-D while limiting use of O negative blood products. Since a serology evaluation can be available within a few hours, this study aim was to evaluate whether it could produce the same results as the molecular test at least 80% of the time.

Materials and Methods

This study is an institutional review board–approved (WCG IRB 20200027) comparison of molecular and serologic methodologies to determine RhD status. The study included 6 affiliated hospitals. The participating hospitals submitted samples to the IRL for *RHD* genotyping to resolve discrepant or questionable serologic D typing results. Samples were tested for RhD status by DNA using the BioArrary BeadChip Assay RUO (Research Use Only) (Immucor). The RHD BeadChip Test Kit uses 35 genetic markers associated with RhD phenotypes to make variant calls. In total, 66 phenotypical variants are detected as well as 5 D negative hybrid alleles. Results were reported per policy to the submitting hospital.

Molecular testing was prioritized based on the clinical need of the patient; cases involving pregnant women with weak D serologic typing or difficult serologic cases needing accurate RhD status to help with the antibody identification were considered a priority. Subsequently, samples were de-identified and sent for RhD testing by serology to a second IRL using the ALBAclone RhD Variant Kit RUO (Quotient). Results and turnaround time were recorded and placed into 2 categories: weak

D/D+ (not at risk for anti-D production) and partial D/D– (at risk for anti-D production). Those categorized as weak D/D+ included weak D types 1, 2, and 3, along with "possible D," which corresponds to a D+ phenotype per RhD BeadChip package insert. All other results were categorized as partial D/D–. The data were analyzed for concordance. A one proportion *z*-test was used to compare the observed concordance rate to the clinically acceptable concordance rate.

The TATs for D status by molecular and serologic methods were evaluated. The TAT for the molecular BeadChip methodology was determined using the time between when a sample was received in the IRL to the day the results were reported to the hospital. The RhD Variant Kit takes 3.0 hours to obtain results from start to finish, so TAT for the serology testing was based on this time for each sample.

Results

A total of 49 samples were evaluated from March 10, 2020, through September 14, 2021. Serological compared to molecular results was concordant (65.3% [32/49]) and discordant (34.7% [17/49]). This observed concordance rate is significantly lower than the clinically acceptable 80% concordance rate ($z = 2.57$, $P < .05$).

Samples tested with RhD by DNA were classified as weak D/D+ (61.2% [30/49]) and partial D/D– (38.8% [19/49]). Samples tested for RhD by serology were classified as weak D/D+ (71.4% [35/49]) and partial D/D– (28.6% [14/49]). The 17 discordant results were due to the following: 64.7% (11/17) were classified as weak D type 4.0 or 4.3 (at risk of forming anti-D) by DNA but simply as weak D/D+ (not at risk of forming anti-D) by serology. The remainder (35.3% [6/17]) were classified as weak D/D+ (not at risk of forming anti-D) by DNA but had an unidentified pattern by serology with a final result of partial D/D– (at risk of forming anti-D) (**TABLE 1**).

The TAT was 3.0 hours for each serology evaluation and a mean of 4.4 days (range, 1–14 days; median, 5 days) for molecular evaluation. No statistical testing was needed to compare the TAT of the serology and molecular testing; for every sample, the serology evaluation was available substantially faster than the molecular evaluation. Molecular test results were available the next day for 26.5% of samples (13/49) and required multiple days for 73.5% of samples (36/49).

Discussion

The long history of providing recipients who have weak D phenotype cells with D positive RBCs has suggested that some weak D phenotypes are unlikely to make anti-D.[1] In 2015, a work group evaluated the scientific literature on anti-D alloimmunization among individuals whose RBCs have a weak D phenotype and concluded that weak D types 1, 2, and 3 can be safely treated as D positive in pregnancy.[2] The recommendations have been adopted by the Association for the Advancement of Blood and Biotherapies, the College of American Pathologists, the American College of Obstetrics and Gynecologists, and the Armed Services Blood Program.[1] Thus, implementing the committee recommendations can help to avoid exposing pregnant women to RhIG unnecessarily and unnecessary costs to the treating facility.[1] Recent data suggest that anti-D immunization in weak D type 4.0 and 4.1 is very rare, too, but opinions on the transfusion strategy in these genotypes remain controversial, and at this institution's IRLs, these are considered partial-D and capable of forming anti-D.[3–5]

Performing *RHD* genotyping is useful to distinguish partial D from weak D or to resolve serologic D typing discrepancies.[1] Although patients with uncertain D status can be treated as D-negative for transfusion and RhIG administration, this approach may be unsatisfactory for those of childbearing potential who face unnecessary RhIG injections, and it places a strain on the limited D-negative blood supply. Performing *RHD* genotyping in pregnancy allows an informed decision to be made on the administration of antenatal RhIG.[1]

RHD genotyping can be performed with reasonable cost recovery that is in line with the those associated with unnecessary administration of RhIG.[6] One study constructed a Markov-based model to evaluate the costs of *RHD* genotyping for pregnant participants with serologic weak D phenotypes to determine the need for RhIG prophylaxis.[6] Using a comparison strategy of managing these participants conservatively as D–, direct medical costs were assessed over 10- and 20-year periods for a simulated population of US women.[6] Using base-case variables, *RHD* genotyping for pregnant women with serologic weak D phenotypes was expected to marginally reduce overall costs.[6] The authors concluded that *RHD* genotyping these subjects, rather than conservatively managing them as D–, would be cost-saving when the fee of genotyping is below $256 US.[6]

A limitation of *RHD* molecular testing is its longer TAT when compared to serological testing. Serology testing may be performed with a shorter TAT, and if the results could be considered for making transfusion and RhIG administration decisions, this may help to prevent unnecessary use of resources and decrease health care costs. For example, O negative is the universal donor blood type and may be used for any patient; however, it is sometimes used inappropriately. In the US population, 7% to 10% of individuals have the O negative type; however, usage is about 5% greater.[7,8] Therefore, it is important to conserve RhD negative blood products when this does not affect patient care. Also, as the average cost of RhIG in 2017 was $97 US (this does not include nursing time or direct and indirect costs), reduction of unnecessary administration and avoidance of the small risk of adverse effects would be beneficial to both patients and hospitals.[9]

A limitation of the serology test was observed during this study. In serology, weak D type 4.0 or 4.3 was not detected as a D variant. This is a known limitation of the serology test. Additionally, unidentified

TABLE 1. Final Interpretation of Test Results

Serology	Molecular	Number	Result
D+; not at risk for anti-D production	D+; not at risk for anti-D production	24	Concordant
Partial D; at risk for anti-D	Partial D; at risk for anti-D	8	Concordant
D+; not at risk for anti-D production	Partial D; at risk for anti-D	11	Discordant
Partial D; at risk for anti-D	D+; not at risk for anti-D production	6	Discordant

patterns were observed that could not be interpreted. These results may have contributed to a high discordant rate and a statistically significant difference in concordance with molecular testing.

Study limitations include that it was performed at 1 blood center and involved just 2 of its IRLs. Only a limited number of affiliated hospitals, located within 2 states in the southeastern US, agreed to participate in the study. Only 1 testing vendor was used for molecular testing and 1 for serology testing. Patient demographics and sample size may not be representative of results that could be seen with other IRLs that perform testing for their affiliated hospitals. Additional variables could lead to results discrepant from this study. These include the use of different methods (eg, slides, tube, microplate, gel, and automated analyzers using enzyme-treated RBCs), the phase of testing, different IgM clones in manufacturer's reagents, and the large number of *RHD* gene variations that affect the level of expression and epitopes of the D antigen.[1]

Although many serology and molecular testing results were concordant, a significant minority (34.7%) were discordant. Given the study results of a concordance rate of less than 80% and the concerns with development of anti-D, especially in women of childbearing age, it is evident that except in limited cases, serological-based testing should not be used to quickly determine whether RhD negative blood is required or RhIG administration is necessary.

Acknowledgments

The authors thank Anthony Trinkle for assistance with molecular testing. This work was supported by a Coastal Blood Foundation grant.

REFERENCES

1. Peyrard, T, Wagner FF. The Rh system. In: Cohn CS, Delaney M, Johnson ST, Katz LM. Eds. *Technical Manual*. 20th ed. Bethesda, MD: AABB Press, 2020.
2. Sandler, SG, Flegel, WA, Westhoff, CM, et al. It's time to phase in *RHD* genotyping for patients with a serologic weak D phenotype. *Transfusion.* 2015;55:680–689. doi:10.1111/trf.12941.
3. Ouchari, M, Srivastava, K, Romdhane, H, Yacoub SJ, Flegel, WA. Transfusion strategy for weak D Type 4.0 based on *RHD* alleles and *RH* haplotypes in Tunisia. *Transfusion.* 2018;58(2):306–312. doi:10.1111/trf.14411.
4. Flegel, WA, Peyrard, T, Chiaroni, J, Tournamille, C, Jamet D, Pirenne, F. A proposal for a rational transfusion strategy in patients of European and North African descent with weak D type 4.0 and 4.1 phenotypes. *Blood Transfus.* 2019;17(2):89–90.
5. Westhoff, CM, Nance, S, Lomas-Francis, C, Keller, M, Chou, ST. Experience with *RHD*weak D type 4.0* in the USA. *Blood Transfus.* 2019;17(2):91–93.
6. Kacker S, Vassallo R, Keller MA, et al. Financial implications of *RHD* genotyping of pregnant women with a serologic weak D phenotype. *Transfusion.* 2015;55(9):2095–2103. doi:10.1111/trf.13074.
7. Gammon RR, Rosenbaum L, Cooke R, et al. Maintaining adequate donations and a sustainable blood supply: lessons learned. *Transfusion.* 2021;61(1):294–302. doi:10.1111/trf.16145.
8. Sapiano MRP, Savinkina AA, Ellingson KD, et al. Supplemental findings from the National Blood Collection and Utilization surveys, 2013 and 2015. *Transfusion.* 2017;57(suppl 2):1599–1624. doi:10.1111/trf.15715.
9. Mikulic M. Average prices for a immune globulin injection in selected countries in 2017 (in U.S. dollars. *Statista*. Available at https://www.statista.com/statistics/1089187/price-of-immune-globulin-injection-by-country/. Accessed December 9, 2021.

Association of the *rs3856806* Polymorphism in the *PPARG* Gene with Type 2 Diabetes Mellitus: A Meta-Analysis of 11,811 Individuals

Raphael Enrique Tiongco, RMT, MSMT,[1,] Henry Basilio, RMT,[1] Dharleen Ryanne Camacho, RMT,[1] Willie Mae Ellorin, RMT,[1] Clarisse Arianne Sico, RMT,[1] and Engracia Arceo, RMT, MPH, DrPH[1]*

[1]Department of Medical Technology, College of Allied Medical Professions, Angeles University Foundation, Angeles City, Philippines. *To whom correspondence should be addressed: tiongco.raphael@auf.edu.ph.

Keywords: type 2 diabetes mellitus, PPARG, single nucleotide variant, gene polymorphism, rs3856806, meta-analysis

Abbreviations: SNV, single nucleotide variant; T2DM, type 2 diabetes mellitus; OR, odds ratio; CI, confidence interval; PPARG, peroxisome proliferator-activated receptor γ

Laboratory Medicine 2023;54:193–198; https://doi.org/10.1093/labmed/lmac095

ABSTRACT

This study investigated the role of the *rs3856806* single nucleotide variant (SNV) on the peroxisome proliferator-activated receptor γ with the development of type 2 diabetes mellitus (T2DM) by conducting a meta-analysis. Relevant studies were searched in PubMed and were selected according to the inclusion criteria. Data were extracted and subjected to analysis using Review Manager 5.4.1. Pooled odds ratios (OR) and 95% confidence intervals (CI) were computed to measure the association of the SNV with T2DM development. Nine studies published in English were retrieved up to October 1, 2021. Homogeneity (I^2 = 3%, P = .41) was achieved for the allelic model with significant outcomes (OR: 0.82; 95% CI: 0.76-0.89; P < .00001). Genotypic models also yielded significant associations for the co-dominant, dominant, and recessive models. All genotypic analysis showed homogeneity (I^2 = 0-31%, P = .17-0.76) of the pooled outcomes. Our findings suggest that carrying the T allele of the *rs3856806* SNV significantly decreases the risk of acquiring T2DM. However, further studies are necessary to support our claims.

The continuous rise in cases of diabetes mellitus (DM) makes it one of the most prevalent chronic metabolic disorders in the world.[1] A total of 537 million adult cases of DM were reported by the International Diabetes Federation in 2021.[2] It is considered a major threat to public health, as it is considered a principal cause of mortality worldwide.[3] From a local perspective, the Philippines have indicated DM as the fourth highest cause of mortality, reporting approximately 20,000 cases of DM-related deaths on the first 2 quarters of 2021 alone.[4] The pathophysiology of the disease involves various biochemical pathways that contribute to the overall inability of an individual to properly regulate blood glucose levels, resulting in its abnormal increase.[5] Type 2 DM (T2DM) is considered the predominant type, as it comprises about 90% to 95% of all DM cases in the world. The presence of insulin resistance brings about the mechanism of impaired glucose regulation present in T2DM.[6] One of the investigated mechanisms in the development of T2DM is the occurrence of point mutations such as single nucleotide variants (SNVs). Studies suggest that the specific SNV are critical in regulating insulin resistance, contributing to developing T2DM.[7]

SNVs are genetic mutations resulting from defects in the process of DNA replication.[8] Studies have shown that SNVs can be markers for increased susceptibility to various diseases.[9] In recent years, various SNVs have been consistently associated with the onset of T2DM, where a probable contribution of genetic variations was described, including the peroxisome proliferator-activated receptors (PPARs). These PPARs are nuclear transcription factors activated by lipid-soluble ligands, which are involved in the differentiation of adipocytes and the metabolism of glucose and lipids.[10] The PPARs have subtypes, namely PPARα, PPARβ, and PPARγ. Among these subtypes, PPARγ (PPARG) has been mostly associated with obesity and diabetes.[11] Studies suggest that PPARG holds a vital role in insulin regulation and may be a factor in the development of T2DM in genetic variations in the *PPARG* gene.[10] Polymorphisms in the *PPARG* gene have described several variants that could be linked with increased susceptibility to T2DM, such as the *rs3856806*.[12] The *rs3856806* SNV (also referred to as His447His, C1431T, CAC478CAT, His449His, and C161T)[13] is 1 of the 2 most common variants of the *PPARG* gene associated with insulin resistance and T2DM, with Pro12Ala being the other variant. Some studies suggest that the *rs3856806* variant is better at predicting insulin resistance than the Pro12Ala.[14]

Some studies[15,16] show that the presence of the polymorphism in the *PPARG* gene may decrease the likelihood of T2DM development. However, only a minor effect in genetic association studies was noted. The lack of reproducibility and consistency may be attributed to small

sample sizes and ethnic differences; thus, evidence may be limited. On the other hand, other studies[14,17] do not find any significant relationship. Hence, we performed a meta-analysis to determine the association of the SNV with T2DM development by pooling together the results of individual studies that contain genotypic data on the *rs3856806* polymorphism and T2DM.

Materials and Methods

Search Strategy

The related publications used in this meta-analysis were searched using both PubMed and Google Scholar (title search only). The following combination of key search terms was used: "diabetes" AND "His447His" OR "C161T" OR "C1431T" OR "CAC478CAT" OR "His449His" OR "rs3856806." The rs3856806 has many alternative names. Hence, all these were incorporated into the search strategy.

Selection of Included Studies and Data Extraction

Titles and abstracts of the resulting text were initially screened for relevance and any duplicates. Studies were included if (1) they were written in English, (2) they contained case-control (patients with T2DM and healthy patients) groups, and (3) they contained the genotypic frequencies for the *rs3856806* SNV (CC, CT, and TT). After irrelevant studies were removed, the full text of the selected articles was obtained for further screening. Studies that did not have full text were removed. For the full-text screening, the previous criteria were used together with the following: genotypic data were expressed in raw numbers and not in percentages, and SNV results were within the Hardy-Weinberg equilibrium; this was computed from the data of each study together with the minor allele frequency. Once the list of studies was finalized, the cited references from these studies were also assessed for additional articles.

From the final list of studies, the following data were then extracted: first author's last name, year of publication, country where the participants were recruited, criteria used for T2DM identification, method of SNV detection used, number of DM and non-DM participants, and the genotypic frequencies for the *rs3856806* SNV (CC, CT, and TT).

Power Analysis and Quality Assessment of the Included Studies

Methods for power analysis and quality assessment of the included studies were based on a previous report.[18] For the power analysis, G*Power 3.1. was used, and the adequacy was set at ≥80%, assuming an odds ratio (OR) of 1.5 and a genotypic risk level of $\alpha = 0.05$. The quality of the included studies was assessed using the tool developed by Clark and Baudouin.[19] The scores range from 0 (worst) to 10 (best), where <5, 5–7, and >7 indicate low, moderate, and high quality, respectively.

Data Analysis

The protocol for the data analysis used was based on the procedures done by the same author.[20,21] The OR and 95% confidence interval (CI) were computed using Review Manager version 5.4 (Nordic Cochrane Centre, Cochrane Collaboration). To better determine the association of the SNV with T2DM development, 3 genotypic (co-dominant, dominant, and recessive) and an allelic model were used. This was used to highlight the effect of the heterozygous genotype in the association. For the *rs3856806* polymorphism, the T allele is considered the alternative allele and the C allele as the reference allele. Consequently, the CC genotype is considered the wild type or the reference genotype, the CT genotype as the heterozygous genotype, and the TT genotype as the mutant genotype.

The fixed- and random-effects model was used to compute the ORs and 95% CIs depending on the presence of heterogeneity, as determined using the χ^2-based Q test, and I^2 statistics were used to determine the presence of heterogeneity.[22,23] The fixed-effects model was used if heterogeneity was nonsignificant; the random-effects model was used if heterogeneity results were significant.[24,25] The computed pooled ORs and 95% CIs were considered significant if the *P* value obtained was less than .05. Heterogeneity was considered significant if the *P* value obtained was less than .10, especially if few studies were present.[26]

Sensitivity and Publication Bias Analysis

The robustness of the pooled ORs was determined through sensitivity analysis. This was done by repeating the overall statistical analysis while omitting 1 study at a time. This was done to check the influence of the individual study in the pooled OR. Finally, publication bias analysis was omitted due to the low number (n < 10) of studies in this meta-analysis.[27]

Results

Search Results and Characteristics of the Included Studies

A total of 62 studies were screened for their eligibility. From the 62 studies, only 9 were included in this meta-analysis.[14–17,28–32] One study was obtained from checking the cited references from each included text. The full summary of the literature search is presented in **FIGURE 1**. A complete summary of the characteristics of the included studies is shown in **TABLE 1**. Overall, a total sample size of 11,811 (4519 DM and 7292 non-DM) was included in this meta-analysis. All studies were conducted in various geographic locations from 2001 to 2014. The Clark-Baudouin scores (mean 5.8, median 5.0, interquartile range 5.0–7.0) indicated that the methodological quality of the studies was moderate.

Meta-Analysis Results

FIGURE 2 shows the fixed-effects model analysis of the association between the *rs3856806* polymorphism and T2DM development in the allelic model. Homogeneity (I^2 = 3%, P = .41) was achieved for the allelic model with significant outcomes (OR: 0.82; 95% CI: 0.76–0.89; P < .00001). Forest plot analysis of the genotypic models (**FIGURES 3–5**) also yielded significant associations for the co-dominant (OR: 0.64; 95% CI: 0.51–0.81; P = .0002), dominant (OR: 0.81; 95% CI: 0.74–0.89; P < .0001), and recessive (OR: 0.70; 95% CI: 0.56–0.89; P = .003) models. All analysis showed homogeneity (I^2 = 0-31%, P = .17–.76) of the pooled outcomes. On the other hand, sensitivity analysis showed the robustness of the meta-analysis outcomes (data not shown).

Discussion

Summary and Interpretation of Findings

The study outcomes suggest that the *rs3856806* polymorphism in the *PPARG* gene is associated with T2DM development. Based on the pooled

ORs and 95% CIs generated from the genotypic and allelic models, individuals that carry the T allele are less likely to develop T2DM. These findings are supported by the homogeneity of the post-outlier outcomes, the consistency and high degree of significant associations, and the robustness of the outcomes, which enhance the level of evidence presented in this meta-analysis.

Protective Role of the SNV in T2DM Development

T2DM is a complex metabolic disorder where susceptibility to the disease has been related to various genes localized at different chromosomes. The association of SNVs with diseases like cancer, ischemic stroke, and sepsis has already been studied. In diabetes, several reports show that PPRAG is a key agent in the development and pathophysiology of T2DM.[33]

The *PPARG* gene codes for a member of the PPAR subfamily of nuclear receptors to form heterodimers with retinoid X receptors and influence the transcription of many target genes. The PPARG is a nuclear hormone receptor involved in regulating adipocyte differentiation. It also plays a role in enhancing gene expression responsible for encoding proteins involved in glucose and lipid metabolism.[34] The PPARG has many functional roles across all kinds of tissues, such as in macrophages, which is said to improve insulin sensitivity.[35] The PPARG works in peripheral tissues by modifying the secretion of adipocytokines.[36] Activation of PPARG may lead to the expansion of adipocyte tissue mass by differentiating new adipocytes to release hormones responsible for insulin sensitivity. With this beneficial phenomenon, the concentration of circulating lipid substrates is reduced, and glucose utilization is stimulated in insulin-sensitive tissues.[37]

The SNV *rs3856806* is a mutation found at exon 6, and it has been shown to produce better predictions of insulin resistance than other SNVs. This SNV is also known by another name, C1431T, depicting the substitution from a C to T at nucleotide 1431. This silent mutation may regulate the expression of PPARG by altering mRNA processing, which may lead to increased differentiation of adipocytes. This study showed that the presence of the T allele in the SNV *rs3856806* demonstrated a remarkable association with diabetes and was found to significantly reduce the risk of acquiring diabetes.[38] It is the polymorphism that may affect the balance of energy metabolism and cell differentiation and presumably alter the susceptibility of T2DM. These results are in accordance with the study conducted by Jaziri et al[30] where the T allele in exon 6 of C1431T was associated with a lower risk of acquiring diabetes. This is further proven in previous studies where it was stated that the presence of the T allele might increase adipocyte differentiation and is associated with insulin sensitivity.[38–40] In the study of Du et al,[15] it was further indicated that adiponectin might have a significant association where their findings suggested that patients with the TT genotype of rs3856806 had higher adiponectin levels. Adiponectin increases insulin sensitivity and is associated with diabetes, especially at low levels.

Although there are studies that have similar results to ours, there are also studies that show otherwise. In a study conducted among the Chinese Han population,[41] results show that the *rs3856806* T allele of PPARG is significantly associated with higher T2DM risk. The

FIGURE 1. Summary of the literature search.

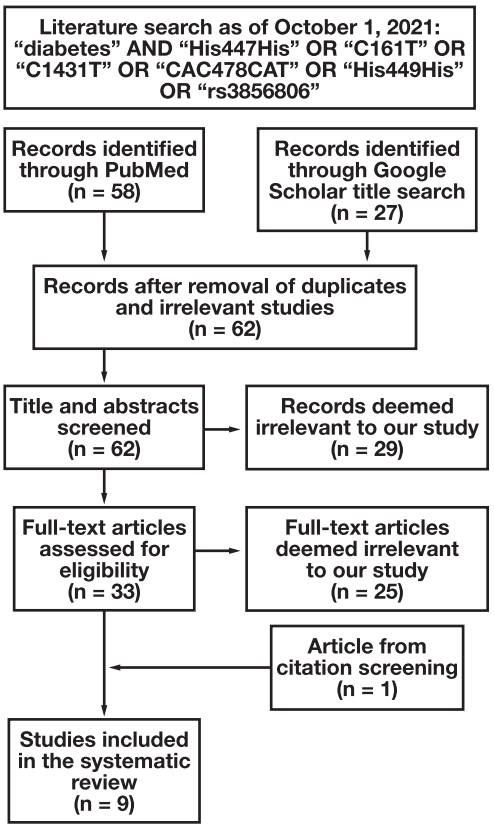

TABLE 1. Characteristics of the Included Studies

First Author	Year	Country	T2DM Identification	Method of SNV Detection	DM	Non-DM	Total	Power (%)	HWE	maf	CB Score
Doney	2004	Scotland	Not mentioned	Taqman	1997	983	2980	99	0.4	0.13	4
Du	2011	China	WHO criteria	Taqman	1105	1107	2212	99	0.09	0.24	8
Evans	2001	Germany	WHO criteria	SSCP	219	426	645	68	0.58	0.14	4
Jaziri	2006	France	1997 ADA Criteria	PCR	43	3213	3256	25	0.85	0.12	5
Lu	2011	China	WHO criteria	PCR-RFLP	538	601	1139	92	0.31	0.26	8
Tavares	2005	Brazil	Santa Casa Hospital criteria	PCR	207	170	377	49	0.6	0.09	7
Vergotine	2014	South Africa	WHO criteria	RT-PCR	222	598	820	72	0.77	0.14	5
Wan	2010	China	ADA criteria	PCR	86	89	175	26	0.86	0.21	6
Yilmaz-Aydogan	2011	Turkey	Not mentioned	PCR-RFLP	102	105	207	30	0.75	0.24	5

ADA, American Diabetes Association; CB, Clark-Baudouin score; DM, diabetes mellitus; FBG, fasting blood glucose; HWE, Hardy-Weinberg equilibrium; maf, minor allele frequency; PCR, polymerase chain reaction; PCR-RFLP, polymerase chain reaction-restriction fragment length polymorphism; RT-PCR, real-time polymerase chain reaction; SNV, single nucleotide variant; SSCP, single-strand conformation polymorphism; T2DM, type 2 diabetes mellitus; WHO, World Health Organization .

FIGURE 2. **Forest plot analysis for the association of the *rs3856806* polymorphism in the *PPARG* gene with type 2 diabetes mellitus (allelic model). CI, confidence interval.**

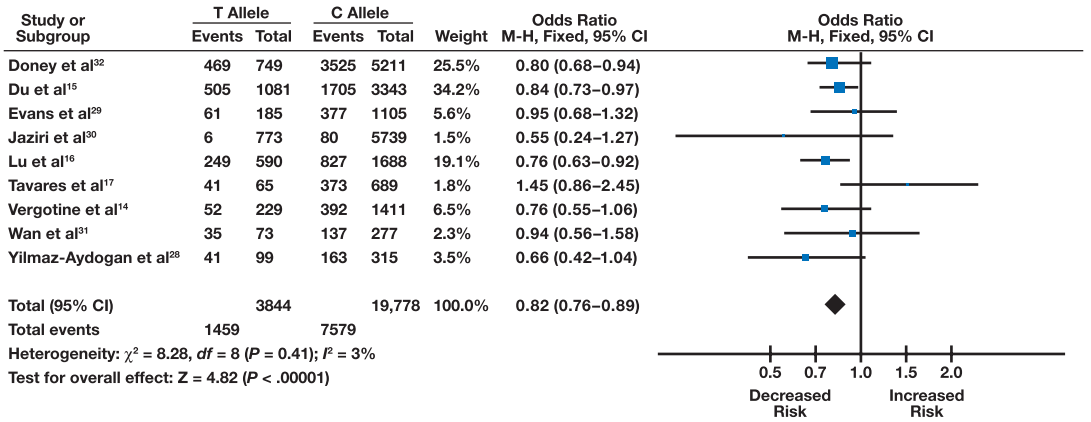

FIGURE 3. **Forest plot analysis for the association of the *rs3856806* polymorphism in the *PPARG* gene with type 2 diabetes mellitus (co-dominant model). CI, confidence interval.**

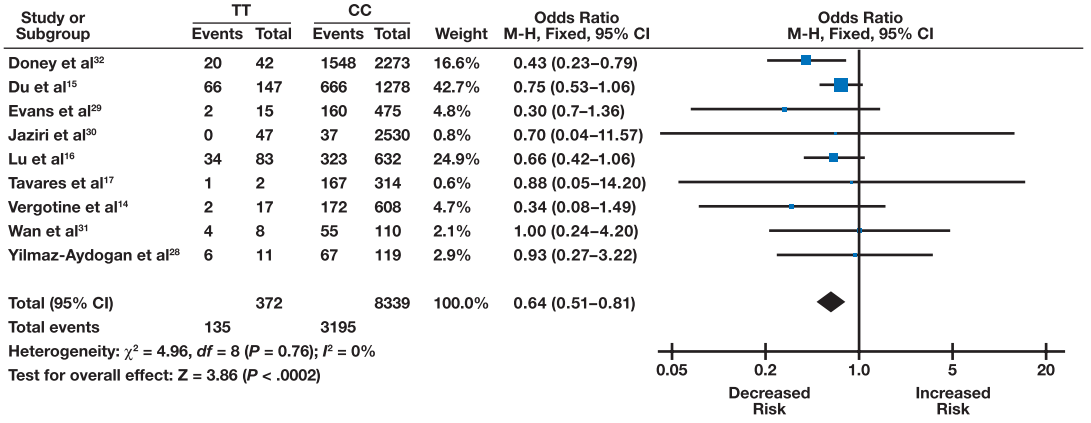

FIGURE 4. **Forest plot analysis for the association of the *rs3856806* polymorphism in the *PPARG* gene with type 2 diabetes mellitus (dominant model). CI, confidence interval.**

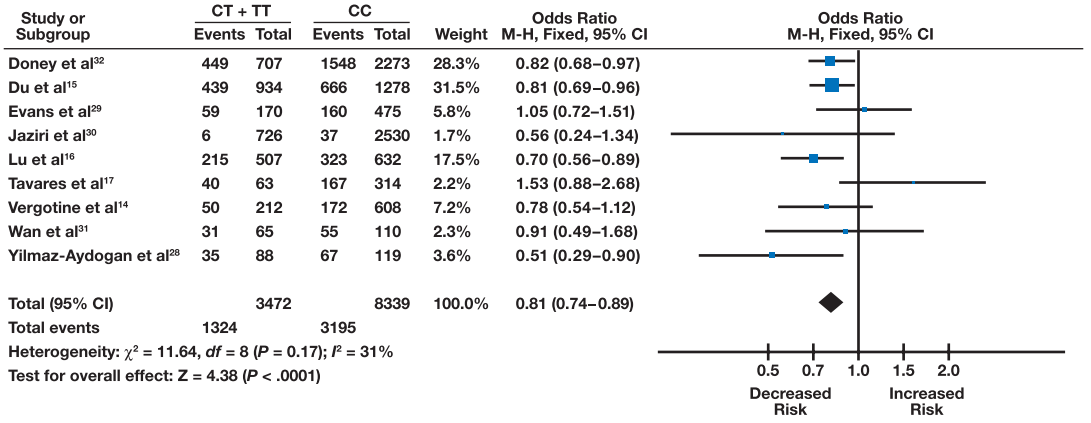

researchers cited explanations such as the genotypes with minor allele variants at the *rs180592*, *rs709158*, and *rs3856806* loci are associated with increased low-density lipoprotein cholesterol levels, which was a risk factor of T2DM. Furthermore, they also explained that in the co-dominant and log-additive models, *rs1805192* and *rs3856806* were all associated with increased dyslipidemia risk. The differences in the ethnicity and environment of the participants may have accounted for the difference in the results. In the meta-analysis of *rs3856806* with atherosclerosis, researchers noted an increased risk among Caucasians and decreased risk among Asians.[42] This shows the need for further studies in a wider and more population-specific setting to better elucidate the results.

FIGURE 5. Forest plot analysis for the association of the *rs3856806* polymorphism in the *PPARG* gene with type 2 diabetes mellitus (recessive model). CI, confidence interval.

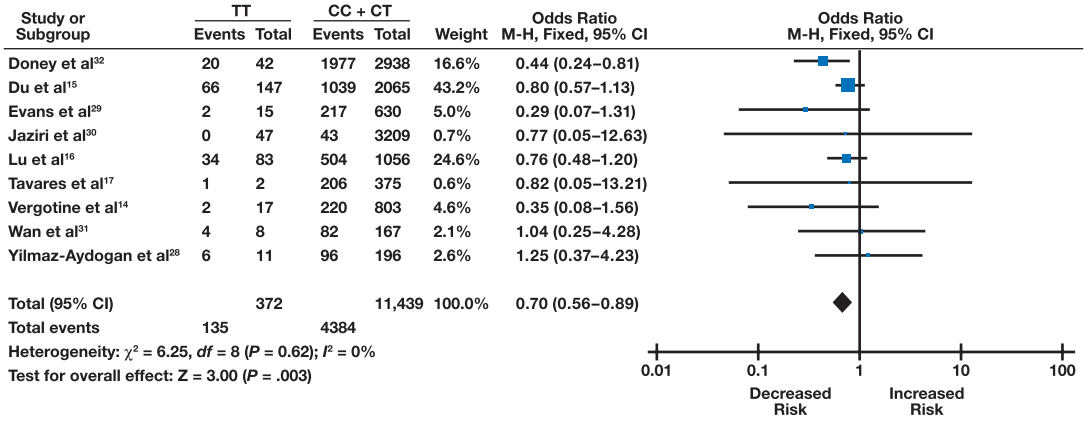

Limitations of the Study

Even with the promisingly high degree of significant association in this study, caution should be taken when interpreting these results, especially when applied clinically. Some of the study's limitations include no representation of other ethnic groups in the study, studies included have a large gap in the year of publication (from 2001 to 2014), no recent study was included in the meta-analysis (the latest was published in 2014), identification of T2DM across the studies is not standardized, an inconsistent method of SNV identification was used, and some studies failed to describe the controls they used. Since T2DM is a complex disorder, interaction with other genetic variants, ethnicity, and the environment must be considered when applying the results of the study.

Conclusion

In summary, our meta-analysis of 11,811 individuals shows that *rs3856806* polymorphism in the *PPARG* gene is associated with T2DM development. To our knowledge, this is the first meta-analysis that identified the association of the *rs3856806* polymorphism with T2DM development. However, care should be taken when interpreting these findings since the exact mechanism of how the SNV influences T2DM development is still in question. Further studies regarding the association of the SNV with processes related to T2DM pathophysiologies such as insulin resistance and inflammation should be conducted. Also, studies among the Filipino population may be pursued to determine the applicability of these findings among various ethnic groups.

REFERENCES

1. Kaul K, Tarr JM, Ahmad SI, Kohner EM, Chibber R. Introduction to diabetes mellitus. *Adv Exp Med Biol.* 2012;771:1-11. doi: 10.1007/978-1-4614-5441-0_1.
2. International Diabetes Federation. *IDF Diabetes Atlas.* 10th ed. Brussels, Belgium; 2021. Available at https://www.diabetesatlas.org.
3. Lin X, Xu Y, Pan X, et al. Global, regional, and national burden and trend of diabetes in 195 countries and territories: an analysis from 1990 to 2025. *Sci Rep.* 2020;10(1):1–11.
4. Philippine Statistics Authority. Causes of deaths in the Philippines (preliminary): January to June 2021. Available at: https://psa.gov.ph/content/causes-deaths-philippines-preliminary-january-june-2021.
5. Lovic D, Piperidou A, Zografou I, Grassos H, Pittaras A, Manolis A. The growing epidemic of diabetes mellitus. *Curr Vasc Pharmacol.* 2019;18(2):104–109.
6. American Diabetes Association. Diagnosis and classification of diabetes mellitus. *Diabetes Care.* 2011;34(suppl 1):S62–S69. doi: 10.2337/dc11-S062.
7. Zhang Y, Bai R, Liu C, et al. MicroRNA single-nucleotide polymorphisms and diabetes mellitus: a comprehensive review. *Clin Genet.* 2019;95(4):451–46 20221.
8. Hanchard NA. Genetic susceptibility and single-nucleotide polymorphisms. *Semin Fetal Neonatal Med.* 2005;10(3):283–289.
9. Bell JI. Single nucleotide polymorphisms and disease gene mapping. *Arthritis Res.* 2002;4(Suppl 3):S273.
10. Mohamed MBH, Mtiraoui N, Ezzidi I, Chaieb M, Mahjoub T, Almawi WY. Association of the peroxisome proliferator-activated receptor-Γ2 Pro12Ala but not the C1431T gene variants with lower body mass index in type 2 diabetes. *J Endocrinol Invest.* 2007;30(11):937–943.
11. Butt HS, Hasnain S. The C1431T polymorphism of peroxisome proliferator activated receptor γ (PPARγ) is associated with low risk of diabetes in a Pakistani cohort. *Diabetol Metab Syndr.* 2016;8(1):67.
12. Costa V, Casamassimi A, Esposito K, et al. Characterization of a novel polymorphism in PPARG regulatory region associated with type 2 diabetes and diabetic retinopathy in Italy. *J Biomed Biotechnol.* 2009;2009:1–7. doi:10.1155/2009/126917.
13. Moffett SP, Feingold E, Barmada MM, et al. The C161→T polymorphism in peroxisome proliferator–activated receptor gamma, but not P12A, is associated with insulin resistance in Hispanic and Non-Hispanic White women: evidence for another functional variant in peroxisome proliferator–activated receptor gamma. *Metabolism.* 2005;54(11):1552–1556.
14. Vergotine Z, Kengne AP, Erasmus RT, Yako YY, Matsha TE. Rare mutations of peroxisome proliferator-activated receptor gamma: frequencies and relationship with insulin resistance and diabetes risk in the mixed ancestry population from South Africa. *Int J Endocrinol.* 2014;2014. doi: 10.1155/2014/187985.
15. Du J, Shi H, Lu Y, et al. Tagging single nucleotide polymorphisms in the PPAR-γ and RXR-α gene and type 2 diabetes risk: a case-control study of a Chinese Han population. *J Biomed Sci.* 2011;25(1):33–41.
16. Lu Y, Ye X, Cao Y, et al. Genetic variants in peroxisome proliferator-activated receptor-γ and retinoid x receptor-α gene and type 2 diabetes risk: a case-control study of a Chinese Han population. *Diabetes Technol Ther.* 2011;13(2):157–164.
17. Tavares V, Hirata RDC, Rodrigues AC, et al. Effect of the peroxisome proliferator-activated receptor-γ C161T polymorphism on lipid profile in Brazilian patients with type 2 diabetes mellitus. *J Endocrinol Invest.* 2005;28(4):129–136.
18. Kunjantarachot A, Pabalan N, Jarjanazi H, et al. Paraoxonase single nucleotide variants show associations with polycystic ovary syndrome: a meta-analysis. *Reprod Biol Endocrinol.* 2020;18(1):114.

19. Clark MF, Baudouin SV. A systematic review of the quality of genetic association studies in human sepsis. *Intensive Care Med.* 2006;32(11):1706–1712.
20. Tiongco RE, Cabrera FJ, Clemente B, Flake CC, Salunga MA, Pineda-Cortel MR. G276T polymorphism in the ADIPOQ gene is associated with a reduced risk of polycystic ovarian syndrome: a meta-analysis of Asian population. *Taiwan J Obstet Gynecol.* 2019;58(3):409–416.
21. Tiongco RE, Aguas IS, Cabrera FJ, et al. The role of the TNF-α gene –308 G/A polymorphism in the development of diabetic nephropathy: an updated meta-analysis. *Diabetes Metab Syndr.* 2020;14(6):2123–2129.
22. Higgins JPT, Thompson SG, Deeks JJ, Altman DG. Measuring inconsistency in meta-analyses. *BMJ.* 2003;327(7414):557–560.
23. Lau J, Ioannidis JPA, Schmid CH. Quantitative synthesis in systematic reviews. *Ann Intern Med.* 1997;127(9):820–826. doi: 10.7326/0003-4819-127-9-199711010-00008.
24. Mantel N, Haenszel W. Statistical aspects of the analysis of data from retrospective studies of disease. *J Natl Cancer Inst.* 1959;22(4):719–748.
25. DerSimonian R, Laird N. Meta-analysis in clinical trials. *Control Clin Trials.* 1986;7(3):177–188.
26. Higgins JPT, Thompson SG. Quantifying heterogeneity in a meta-analysis. *Stat Med.* 2002;21(11):1539–1558.
27. Ioannidis JA, Trikalos TA. The appropriateness of asymmetry tests for publication bias in meta-analyses: a large survey. *CMAJ.* 2007;176(8):1091–1096.
28. Yilmaz-Aydogan H, Kurnaz O, Kurt O, et al. Effects of the PPARG P12A and C161T gene variants on serum lipids in coronary heart disease patients with and without type 2 diabetes. *Mol Cell Biochem.* 2011;358(1–2):355–363.
29. Evans D, de Heer J, Hagemann C, Wendt D, Wolf A, Beisiegel U, Mann WA. Association between the P12A and c1431t polymorphisms in the peroxisome proliferator activated receptor gamma (PPAR gamma) gene and type 2 diabetes. *Exp Clin Endocrinol Diabetes.* 2001;109(3):151–154. doi: 10.1055/s-2001-14838.
30. Jaziri R, Lobbens S, Aubert R, et al; DESIR Study Group. The PPARG Pro12Ala polymorphism is associated with a decreased risk of developing hyperglycemia over 6 years and combines with the effect of the APM1 G-11391A single nucleotide polymorphism: the Data From an Epidemiological Study on the Insulin Resistance Syndrome (DESIR) study. *Diabetes.* 2006;55(4):1157–1162. doi: 10.2337/diabetes.55.04.06.db05-0676.
31. Wan J, Xiong S, Chao S, Xiao J, Ma Y, Wang J, Roy S. PPARgamma gene C161T substitution alters lipid profile in Chinese patients with coronary artery disease and type 2 diabetes mellitus. *Cardiovasc Diabetol.* 2010;24;9:13. doi: 10.1186/1475-2840-9-13.
32. Doney ASF, Fischer B, Cecil JE, et al. Association of the Pro12Ala and C1431T variants of PPARG and their haplotypes with susceptibility to type 2 diabetes. *Diabetologia.* 2004;47(3):555–558.
33. Zhu L, Huang Q, Xie Z, et al. PPARGC1A Rs3736265 G>A polymorphism is associated with decreased risk of type 2 diabetes mellitus and fasting plasma glucose level. *Oncotarget.* 2017;8(23):37308–37320.
34. Tyagi S, Sharma S, Gupta P, Saini A, Kaushal C. The peroxisome proliferator-activated receptor: a family of nuclear receptors role in various diseases. *J Adv Pharm Technol Res.* 2011;2(4):236.
35. He W. Polymorphism and human health. *PPAR Res.* 2009;2009:1–15. doi: 10.1155/2009/849538.
36. Kilpeläinen TO, Lakka TA, Laaksonen DE, et al. SNPs in PPARG associate with type 2 diabetes and interact with physical activity. *Med Sci Sports Exerc.* 2008;40(1):25–33.
37. Ferré P. The biology of peroxisome proliferator-activated receptors. *Diabetes.* 2004;53(suppl 1):S43–S50.
38. Minge CE, Robker RL, Norman RJ. PPAR gamma: coordinating metabolic and immune contributions to female fertility. *PPAR Res.* 2008;2008:1–19. doi: 10.1155/2008/243791.
39. Orio F, Matarese G, di Biase S, et al. Exon 6 and 2 peroxisome proliferator-activated receptor-γ polymorphisms in polycystic ovary syndrome. *J Clin Endocrinol Metab.* 2003;88(12):5887–5892.
40. Antoine HJ, Pall M, Trader BC, Chen YI, Azziz R, Goodarzi MO. Genetic variants in peroxisome proliferator-activated receptor gamma influence insulin resistance and testosterone levels in normal women, but not those with polycystic ovary syndrome. *Fertil Steril.* 2007;87(4):862–869.
41. Lv X, Zhang L, Sun J, et al. Interaction between peroxisome proliferator-activated receptor gamma polymorphism and obesity on type 2 diabetes in a Chinese Han population. *Diabetol Metab Syndr.* 2017;9(1):7.
42. Wang P, Wang Q, Yin Y, et al. Association between peroxisome proliferator-activated receptor gamma gene polymorphisms and atherosclerotic diseases: a meta-analysis of case-control studies. *J Atheroscler Thromb.* 2015;22(9):912–925.

Usefulness of Genetic Aberration and Shorter Telomere Length in Myelodysplastic Syndrome: A Pilot Study

Hee Sue Park, MD, PhD,[1,2] *Bo Ra Son, MD, PhD,*[1,2] *Jihyun Kwon, MD, PhD*[3,4]

[1]Laboratory Medicine, Chungbuk National University Hospital, Cheongju, South Korea, [2]Laboratory Medicine, Chungbuk National University College of Medicine, Cheongju, South Korea, [3]Internal Medicine, Chungbuk National University Hospital, Cheongju, South Korea, and [4]Internal Medicine, Chungbuk National University College of Medicine, Cheongju, South Korea. *To whom correspondence should be addressed: marioncrepe@chungbuk.ac.kr.

Keywords: IPSS-R, myelodysplastic syndrome, next-generation sequencing, telomere length, prognosis, transfusion dependency

Abbreviations: TL, telomere length; MDS, myelodysplastic syndrome; IPSS-R, International Prognostic Scoring System-revised; PCR, polymerase chain reaction.

Laboratory Medicine 2023;54:199–205; https://doi.org/10.1093/labmed/lmac100

ABSTRACT

Objective: We aimed to evaluate the clinical usefulness of genetic aberration and shorter telomere length (TL) in individuals with myelodysplastic syndrome (MDS).

Methods: A targeted sequencing panel with 49 genes and TL measurement by quantitative real-time polymerase chain reaction were performed for 46 subjects.

Results: According to the revised International Prognostic Scoring System (IPSS-R) subtypes, the mutation frequency was 33.3%, 57.9%, and 100% in the very low/low, intermediate, and very high/high risk groups, respectively. A shorter telomere was detected in 43.5%. We defined group 1 as IPSS-R-high or -very high risk, group 2 as having 1 or more genetic aberrations, group 3 as having a shorter TL, and group 4 as having a longer TL than the age-matched reference. Group 1 and group 2 showed an adverse prognosis. The TL was not strongly correlated with MDS prognosis. However, it may be related to a poor long-term prognosis.

Conclusion: Genetic variation and shorter TL may be helpful in reclassifying non–high-risk groups.

The revised International Prognostic Scoring System (IPSS-R) is a gold standard prognostic model for myelodysplastic syndrome (MDS). It classifies patients using cytogenetics, complete blood count, and blast percentage into the following 5 risk groups: very low, low, intermediate, high, and very high.[1] This model was validated in patients receiving first-line therapy with hypomethylating agents, lenalidomide, or allogenic stem cell transplantation.[2,3] However, it has clinical utility limitations in the non–high-risk group, unlike in the high- and very high–risk groups. The classification of the intermediate-risk group is ambiguous owing to risk uncertainty, as clinical outcomes are diverse. Moreover, this new model was devised recently based on age, peripheral blood percentage, and red blood cell (RBC) transfusion history.[4] Additionally, the low-risk group is mostly classified as a dysplasia subtype, without excess blasts, which can be confusing during differential diagnosis, as MDS symptoms overlap with those of syndromes from age-related or nonclonal cytopenia.[5,6] As the IPSS-R prognostic model concentrates on the high-risk groups, a differentiated prognostic model is needed.

Telomeres, which are nucleotide repeats (TTAGGG)n at chromosome ends, indicate chromosomal stability.[7] Shortening of telomeres reflects telomeropathy-related genetic mutations, a physiological result of regenerative stress or secondary DNA damage.[8] Telomere shortening triggers cellular transformation by causing genome instability, which plays a key role in tumorigenesis.[9] Therefore, telomere length (TL) might be a cancer prognostic biomarker and a potential therapeutic target.[9,10] Previous studies have reported that a short telomere predicts a poor prognosis in patients with chronic lymphocytic leukemia and colorectal cancer.[9] There are several technical methods to measure TL, such as terminal restriction fragment analysis, single TL analysis, quantitative polymerase chain reaction (PCR), and quantitative fluorescence in situ hybridization; however, it is not yet clear which method is the most appropriate.[11]

Furthermore, as molecular genetic tests are common, a new approach that uses these results is required. There have been only a few studies on whether the prognostic significance of TL in cancers can be applied to MDS. In addition, as the molecular characteristics of MDS have been gaining importance in terms of diagnosis and prognosis, the relationship between genetic mutations and TL should also be investigated. Therefore, in this study, we aimed to evaluate whether the measurement of TL can compensate for the blind spots of the current MDS risk-grouping system.

Materials and Methods

Subjects

Forty-six individuals diagnosed with MDS at Chunbuk National University Hospital between June 2016 and January 2021 were enrolled in this study. The study group comprised 34 men and 12 women (median age, 73 years). The participants were classified using the 2016 World Health Organization (WHO) classification for MDS as excess blasts-1 (n = 5), excess blasts-2 (n = 15), single lineage dysplasia (n = 3), ring sideroblasts with single lineage dysplasia (n = 1), multilineage dysplasia (n = 16), ring sideroblasts with multilineage dysplasia (n = 4), and unclassifiable (n = 2). The IPSS-R for MDS is composed of very high– (n = 10), high- (n = 8), intermediate- (n = 19), low- (n = 5), and very low–risk (n = 4) groups (**TABLE 1**). This study was approved by the institutional review board of Chunbuk National University Hospital (CBNUH 2021-04-017-001), and the requirement of informed consent was exempted by the institutional review board.

TABLE 1. Characteristics of Subjects

Clinical Variable	Result
Sex (male:female)	34:12
Age, median (range), y	73 (31–87)
<60	8 (17.4%)
≥60	38 (82.6%)
CBC, median (range)	
Hemoglobin (g/dL)	8.3 (4.0–14.0)
White blood cell count ($\times 10^9$/L)	2.9 (0.2–8.0)
Platelet count ($\times 10^9$/L)	65 (5–446)
WHO 2016 subtype criteria, No. (%)	
EB-1	5 (10.9%)
EB-2	15 (32.6%)
SLD	3 (6.5%)
MLD	16 (34.8%)
RS-SLD	1 (2.2%)
RS-MLD	4 (8.7%)
U	2 (4.3%)
Cytogenetics, No.	
Normal karyotype	24
Complex	8
-Y	3
del(20)	3
del(5)	2
del(1)	1
Others (derivate chromosome, translocation)	3
IPSS-R, No. (%)	
Very low	4 (8.7%)
Low	5 (10.9%)
Intermediate	19 (41.3%)
High	8 (17.4%)
Very high	10 (21.7%)
Followed up days (median, range)	298 (12–1382)
Survival	26 (56.5%)

CBC, complete blood count; EB, excess blasts; IPSS-R, International Prognostic Scoring System-revised; MLD, multilineage dysplasia; RS, ring sideroblasts; SLD, single lineage dysplasia; U, unclassifiable; WHO, World Health Organization.

Next-Generation Sequencing

We performed next-generation sequencing (NGS) with a target panel for the 46 participants using Illumina Nextseq 550 Dx (Green Cross Laboratories). Genomic DNA was extracted from the bone marrow sample collected at the time of diagnosis. The NGS panel comprised 49 genes related to hematologic neoplasms: *ANKRD26*, *ASXL1*, *ATRX*, *BCOR*, *BCORL1*, *BRAF*, *CALR*, *CBL*, *CBLB*, *CEBPA*, *CSF3R*, *DDX41*, *DNMT3A*, *ETV6*, *EZH2*, *FLT3*, *GATA1*, *GATA2*, *HRAS*, *IDH1*, *IDH2*, *JAK2*, *JAK3*, *KIT*, *KDM6A*, *KRAS*, *MPL*, *NOTCH1*, *NPM1*, *NRAS*, *PDGFRA*, *PHF6*, *PPM1D*, *PTPN11*, *RAD21*, *RUNX1*, *SETBP1*, *SF3B1*, *SMC1A*, *SMC3*, *SRSF2*, *STAG1*, *STAG2*, *STAT3*, *TET2*, *TP53*, *U2AF1*, *WT1*, and *ZRSR2*. The mean coverage of sequencing depth for the targeted regions was 674-fold. The percentage of target bases that read more than 50-fold was 99.7% in all samples. We selected genes with tier 1 (variants with strong clinical significance) and tier 2 (variants with potential clinical significance) mutations according to the American Society of Clinical Oncology guidelines.[12]

Measurement of TL

TL was measured using samples of the 46 subjects at the Seoul Clinical Laboratory (Seoul, South Korea) with TB green premix Ex Taq II (Takara Biomedical Technology) for the 7500 FAST quantitative real-time polymerase chain system (Applied Biosystems). The samples used for TL measurement were bone marrow aspirates at initial diagnosis. The TLs determined from the peripheral blood of age-matched normal healthy donors, provided by Seoul Clinical Laboratory, were used as a reference. The accuracy range was 97.26% to 103.45% and precision range was 0.23% to 4.44%. Statistical analysis was performed using SPSS version 21.0 (SPSS).

Statistical Analysis

Mann–Whitney *U* test was used for continuous variables to compare 2 groups. Statistical analyses were performed using SS version 21.0 (IBM). Results with $P < .05$ were considered statistically significant.

Results

The median TL of the 46 subjects was 6.26 kilobase (kb) and the difference compared to age-matched reference was 2.19% (–30.2% to 40.0%). Twenty participants had a TL shorter than the aged-matched reference, and the difference between these groups was –6.3% (–0.6% to –30.2%). On the other hand, 26 subjects had a TL longer than aged-matched reference value; the difference was +12.9% (0.0% to 40.0%).

As a result of NGS testing, tier 1 or 2 clinical significance variants were detected in 32 of the 46 participant samples. According to IPSS-R subtypes, no significant mutations were detected in 66.7% (6/9) of subjects in the very low– and low-risk groups and in 42.1% (8/19) of subjects in the intermediate-risk group. On the contrary, all subjects in the high- and very high–risk groups had more than 1 pathogenic variant (**FIGURE 1**). The frequencies of detection of gene mutations were as follows: *TP53* (n = 14); *ASXL1* (n = 6); *DDX41* and *STAG2* (n = 5); *RUNX1*

FIGURE 1. Frequency of tier 1 or 2 variant according to the International Prognostic Scoring System-revised (IPSS-R) risk subtypes in 46 subjects.

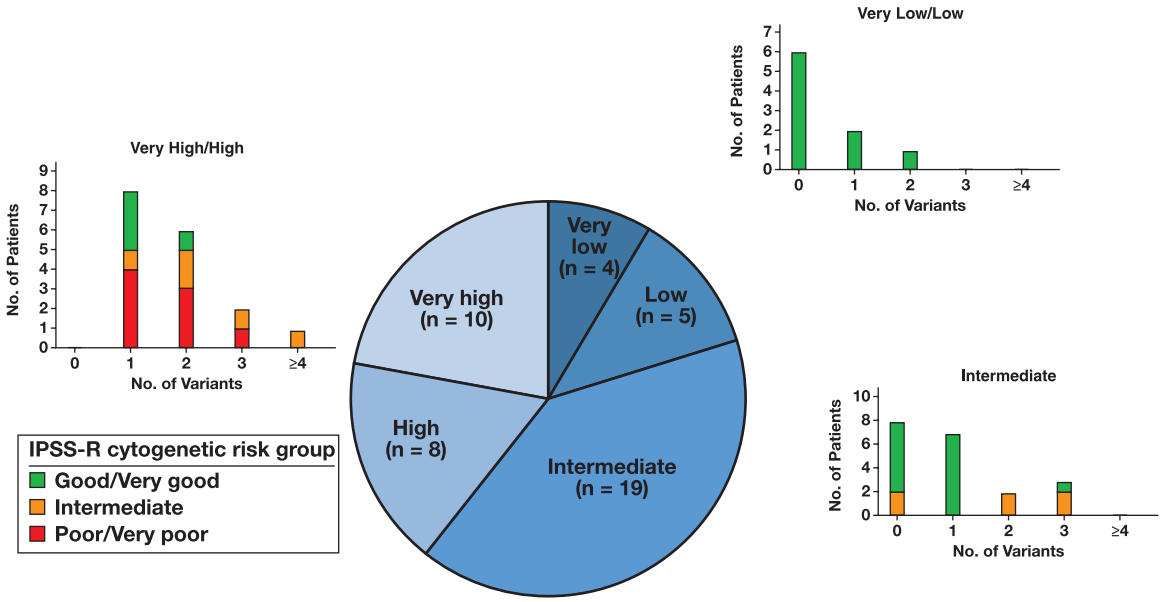

and *TET2* (n = 4); *U2AF1, SETBP1*, and *SRSF2* (n = 3); *ZRSR2, PHF6, DNMT3A, EZH2, PTPN11*, and *CEBPA* (n = 2); and *STAT3, SF3B1,* and *PPM1D* (n = 1). In addition, of the 46 subject samples, 24 (52.1%) had no numerical and structural abnormalities in chromosomes, and 14 had more than 1 genetic mutation (**TABLE 2**). Of these 14, 8 subjects were in the non–high risk group, and 3 showed adverse prognosis defined as death or transformation.

TL tended to be shorter than the reference value in participants under 60 years of age, with a tendency to be higher in older individuals (**FIGURE 2A**). There was no relationship between TL and IPSS-R risk groups or WHO subtypes (**FIGURE 2B, C**). The median TL in each group was 6.27 kb for the very low– or low-risk group, 6.29 kb for the intermediate-risk group, and 6.22 kb for the very high– or high-risk group. The association between individual genetic variation and the total number of mutations and TL was also not statistically significant.

We defined group 1 as IPSS-R high or very high (**FIGURE 3A**). As expected, these participants were diagnosed in the excess blasts subtype and showed adverse prognosis for acute myeloid leukemia (AML). Seven participants (38.9%) died or showed transformation to AML. Thereafter, we included in group 2 those individuals having 1 or more genetic aberrations. Among them, 2 participants died and 1 showed transformation to AML (**FIGURE 3B**). The remaining subjects were divided into group 3 or group 4 according to TL, compared with the age-matched reference. Neutropenia was more significant in groups 1 and 2 than in group 4 (median absolute neutrophil count, 0.94 vs 0.90 vs 2.37 × 10^3/μL, P = .048, .025). Group 3 had shorter telomeres than groups 1, 2, and 4. Furthermore, there was a no significant difference between groups 3 and 4 (P = .073) (**FIGURE 3C**). Four subjects among the 7 in group 3 had partial hypocellular marrow compared with their age-matched reference. However, the 7 participants who had telomeres longer than the age-matched reference showed normal to hypercellular marrow. Although there was no significant difference in the initial median hemoglobin level between group 3 and group 4 (8.0 vs 7.9 g/dL), transfusion dependency, which was defined as the need for recurrent RBC transfusion within 60 days, was distinct in group 4. The absolute neutrophil count of group 3 was also lower than that of group 4 with no statistical significance (1.25 vs 2.37 × 10^3/μL, P = .383). None of the participants in group 3 or 4 died or progressed to AML, and there was a no statistically significant difference between groups 3 and 4 (P = .073) (**FIGURE 3C**).

Discussion

Despite being a conventionally used prognostic tool, the IPSS-R weighted scoring system has a limitation; that is, it is difficult to distinguish the non–high-risk groups.[13] In our study, we aimed to evaluate the clinical usefulness of genetic aberration and shorter telomeres in the non–high-risk groups. Thirty-two of the 46 study participants (69.6%) had tier 1 or tier 2 mutations. The frequency appears to be low compared with that in previous studies, but it is probably because we excluded tier 3 variants. As expected, the number of significant genetic mutations increased as the risk increased.

Interestingly, 18 of the 22 participants with abnormal karyotypes showed more than 1 mutation. The remaining 4 patients without mutation had nonpoor cytogenetic prognostic subgroups such as loss Y, del(20q), and trisomy 8. In the case of normal karyotypes, the subjects with more than 1 mutation showed an adverse prognosis. Therefore, genetic mutations may have a greater effect on prognosis than good prognostic chromosomal abnormalities. Mutations in some specific genes, such as *TP53*, *RUNX1*, and *EZH2*, are well correlated with an adverse prognosis, but the prognostic effects of the majority of genetic aberrations are controversial.[3] Additionally, a few genes, such as *ASXL1*, *DNMT3A*, and *TET2*, should also be distinguished from somatic mutations found in normal elderly individuals.[6,14] However, in this study,

TABLE 2. Fourteen Patients with Genetic Mutations but Normal Karyotype

IPSS-R	Patient	Sex	Age, y	WHO Subtype	Gene	DNA Change	Protein Change	VAF	Tier
Very high	1	M	80	EB-2	*DDX41*	c.455T > G	p.Val152Gly	46	1
						c.1574G > A	p.Arg525His	10	1
High	2	F	77	EB-2	*DDX41*	c.776A > G	p.Tyr259Cys	53	1
						c.1574G > A	p.Arg525His	10	1
	3	M	52	EB-2	*RUNX1*	c.1200dupG	p.Pro401Alafs*199	40	1
					PTPN11	c.218C > T	p.Thr73Ile	28	2
	4	M	65	EB-2	*ASXL1*	c.419dupT	p.Leu1339Phefs*25	38	1
					PHF6	c.385C > T	p.Arg129Ter	19	2
					PTPN11	c.1508G > A	p.Gly503Glu	8	2
					STAG2	c.215delG	p.Gly72Valfs*11	48	2
					ZRSR2	c.247C > T	p.Gln83Ter	85	2
					SETBP1	c.2602G > A	p.dAsp868Asn	44	2
	5	M	66	EB-2	*TET2*	c.2414delG	p.Gly805Aspfs*8	85	1
					SRSF2	c.284C > T	p.Pro95Leu	50	1
					STAG2	c.1400delT	p.Phe467Serfs*3	29	1
					STAG2	c.1840C > T	p.Arg614Ter	41	1
					CEBPA	c.859dupG	p.Val287Glyfs*34	16	1
					CEBPA	c.884C > T	p.Ala295Val	12	1
	6	M	79	EB-1	*SRSF2*	c.284C > A	p.Pro95His	45	1
					SETBP1	c.2608G > A	p.Gly870Ser	34	1
					STAG2	c.2556_2558delins	p.Ser853Glufs*20	62	1
Intermediate	7	M	74	MLD	*DDX41*	c.455T > G	p.Val152Gly	47	1
	8	M	76	MLD	*DNMT3A*	c.1123-2A > G	.	5	1
	9	M	81	MLD	*RUNX1*	c.284_285dup	p.Asn96Profs*27	7	1
	10	M	52	MLD	*ASXL1*	c.3202C > T	p.Arg1068Ter	3	1
					ZRSR2	c.984delT	p.Leu329Phefs*?	4	1
					U2AF1	c.101C > T	p.Ser34Phe	23	1
	11	M	65	EB-2	*TP53*	c.517G > A	p.Val173Met	35	
Low	12	M	57	U	*BCOR*	c.3982C > T	p.Gln1328Ter	4	1
Very low	13	M	80	SLD	*SRSF2*	c.284C > A	p.Pro95His	45	1
					IDH2	c.419G > A	p.Arg140Gln	44	1
	14	F	70	MLD	*TET2*	c.3594 + 1G > A	.	40	1
						c.4640_4644delins	p.Gln1547Leufs*24	34	1

EB, excess blasts; MLD, multilineage dysplasia; SLD, single lineage dysplasia; U, unclassifiable; VAF, variant allele frequency; WHO, World Health Organization.

there was no evidence to show that the genetic variations, including variations in these genes, which are known to be related to aging, are associated with TL. It can be speculated that TL and gene mutations function in independent domains in the aging process and MDS pathogenesis. In addition, in terms of the relationship between TL and the clinical characteristics of MDS revealed in this study, the possibility that the role of aging may be limited cannot be excluded. However, as the number of subjects in this study was small, additional research is needed to confirm this hypothesis. Nevertheless, it appears that the presence of mutations is important in determining disease progression and predicting the prognosis. In the case of predisposition genes, monoallelic *DDX41* mutation was observed in the intermediate risk group (**TABLE 2**); it is expected that an additional *DDX41* mutation leads to disease progression. As biallelic *DDX41* mutations in AML are known to lead to a poor prognosis,[15] close clinical follow-up may be necessary for persons with these mutations. Additionally, 14 subjects in the non–high-risk groups with no genetic aberration (groups 3 and 4) did not show disease progression during follow-up (median 273 days, range 12 to 973 days).

The TL reflects not only aging but also disease characteristics, leading to confusion in interpretation. Müezzinler et al[16] estimated a mean leukocyte TL loss of 24.7 bp per year using weighted linear regression. Therefore, shortening TL is a concern, as it indicates that aging influences disease pathophysiology such as cancers and neurodegenerative diseases. The prevalence of MDS also increases with age, but due to heterogeneity in the disease, previous reports on the TL of individuals with MDS are not consistent.[17,18] Previous studies have reported that progressive shortening of TL reflects continuous DNA damage, which leads to progression to AML.[19–21] Nevertheless, Warny et al[22] reported that they did not detect any prognostic significance through TL at disease diagnosis and during

FIGURE 2. Measurement of telomere length (TL) using a quantitative real-time polymerase chain system. A, A comparison of TL between myelodysplastic syndrome (MDS) and age-matched reference value. B, TL according to the 2016 World Health Organization classification. EB, excess blasts; MLD, multilineage dysplasia; SLD, single lineage dysplasia; U, unclassifiable. C, TL according to the revised International Prognostic Scoring System subtypes.

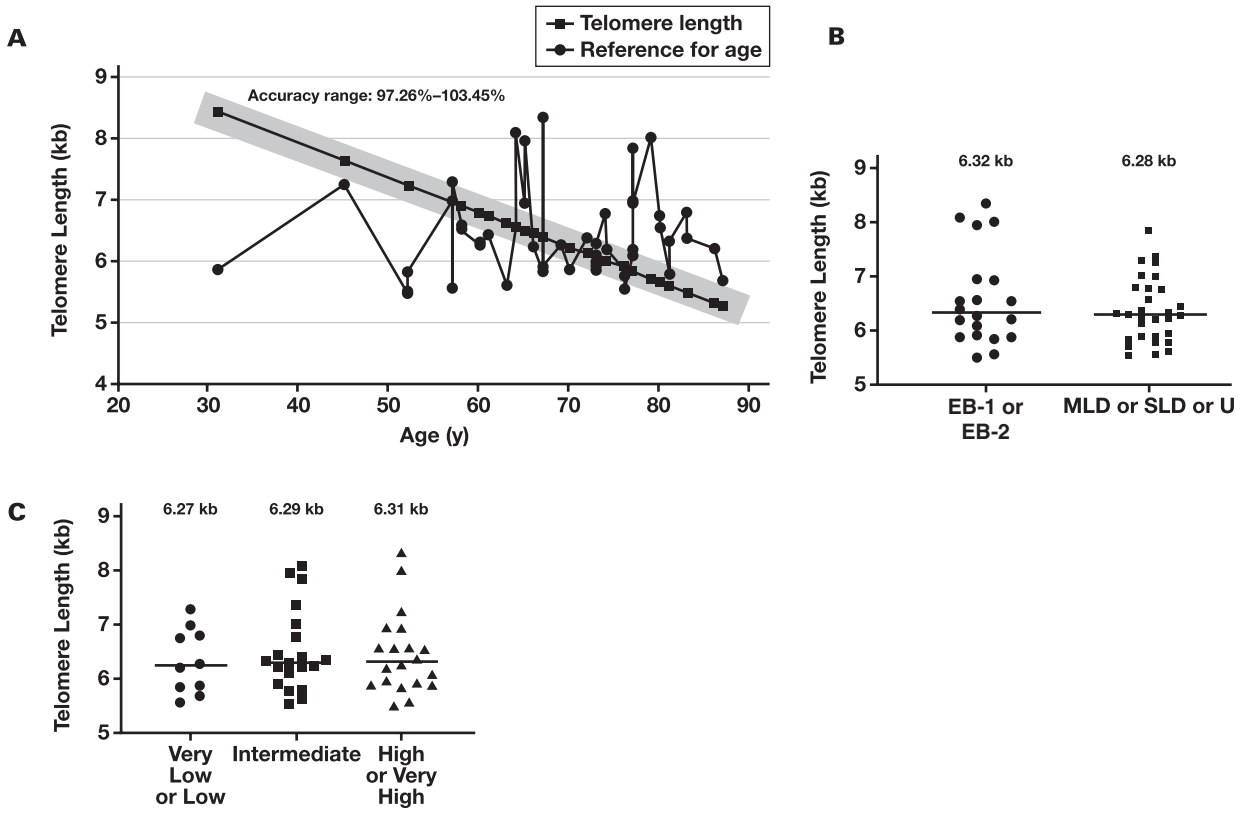

treatment even when the disease relapsed. Similarly, in our study, TL was not found to be directly related to survival prognosis. However, some of the clinical features related to TL influence the course of a disease or indirectly suggest prognosis. For example, recurrent RBC transfusion is known as a risk factor for shorter survival and disease progression in MDS.[23] In addition, the TL of subjects in groups 1 and 2, which were classified as relatively high-risk groups, tended to be shorter than that of subjects in group 4. Except in the case of persons with hypoplastic MDS, who were mainly classified into group 3, this result can be considered to be consistent with the results of previous studies that reported telomere shortening during disease progression.[18,24] Similar to the findings of a previous study,[25] specific gene mutations did not correlate with a shorter telomere, but cells with gene mutations seem to be related to a short telomere. Therefore, a shorter telomere reflects disease progression in the high-risk groups, but differential diagnosis from bone marrow failure syndrome should be considered in the non–high-risk groups. In addition, even if a short telomere has little effect on short-term prognosis, it may indicate a poor long-term prognosis and predict disease progression.

The subjects classified into groups 1 and 2 showed a high risk of progression to AML based on previously well-known prognostic factors such as age, sex, and the pattern of genetic mutation. In contrast, groups 3 and 4 lacked the aforementioned strong prognostic factors but showed differences in clinical features, such as bone marrow cellularity and transfusion dependence according to TL. Although the possibility that some of the individuals in group 3 may have early-stage aplastic anemia cannot be excluded, it can be hypothesized that short telomere has some association with hypoplastic MDS. In this case, the differential diagnosis of hypoplastic MDS or early-phase aplastic anemia in individuals with a shorter telomere should be considered; this should be followed up with bone marrow examination even if they do not meet the diagnostic criteria initially.

This study has some limitations. First, the number of participants was too small to draw any conclusions. Although our study does not draw firm conclusions, the association of TL with the onset and course of bone marrow diseases, including MDS, is likely to be elucidated through further studies. Second, we did not do enough validation of the TL in normal population and a shorter telomere. There is no standard method to measure TL and there is no standardized definition for a shorter telomere in previous reports. The quantitative PCR method is preferred for its high throughput, but its variability within and between samples remains relatively high.[11] Therefore, when interpreting TL, clinical course and additional test results such as complete blood count and bone marrow examination must be considered, and it appears that additional studies are needed to sufficiently verify this.

In conclusion, we showed that genetic variation and a shorter telomere may be helpful in the diagnosis and prognosis of patients in the non–high-risk groups. Although our results did not reach statistical significance because the number of subjects was very small, they indicate

FIGURE 3. **A, New grouping for myelodysplastic syndrome incorporating genetic mutations and telomere length. EB, excess blasts; IPSS-R, International Prognostic Scoring System-revised; MLD, multilineage dysplasia; SLD, single lineage dysplasia; TD, transfusion dependent, TI, transfusion independent; U, unclassfiable; WHO, World Health Organization. B, Kaplan-Meier cumulative survival graph according to the new model (*P* = .094). C, Comparison of telomere length between the new model groups.**

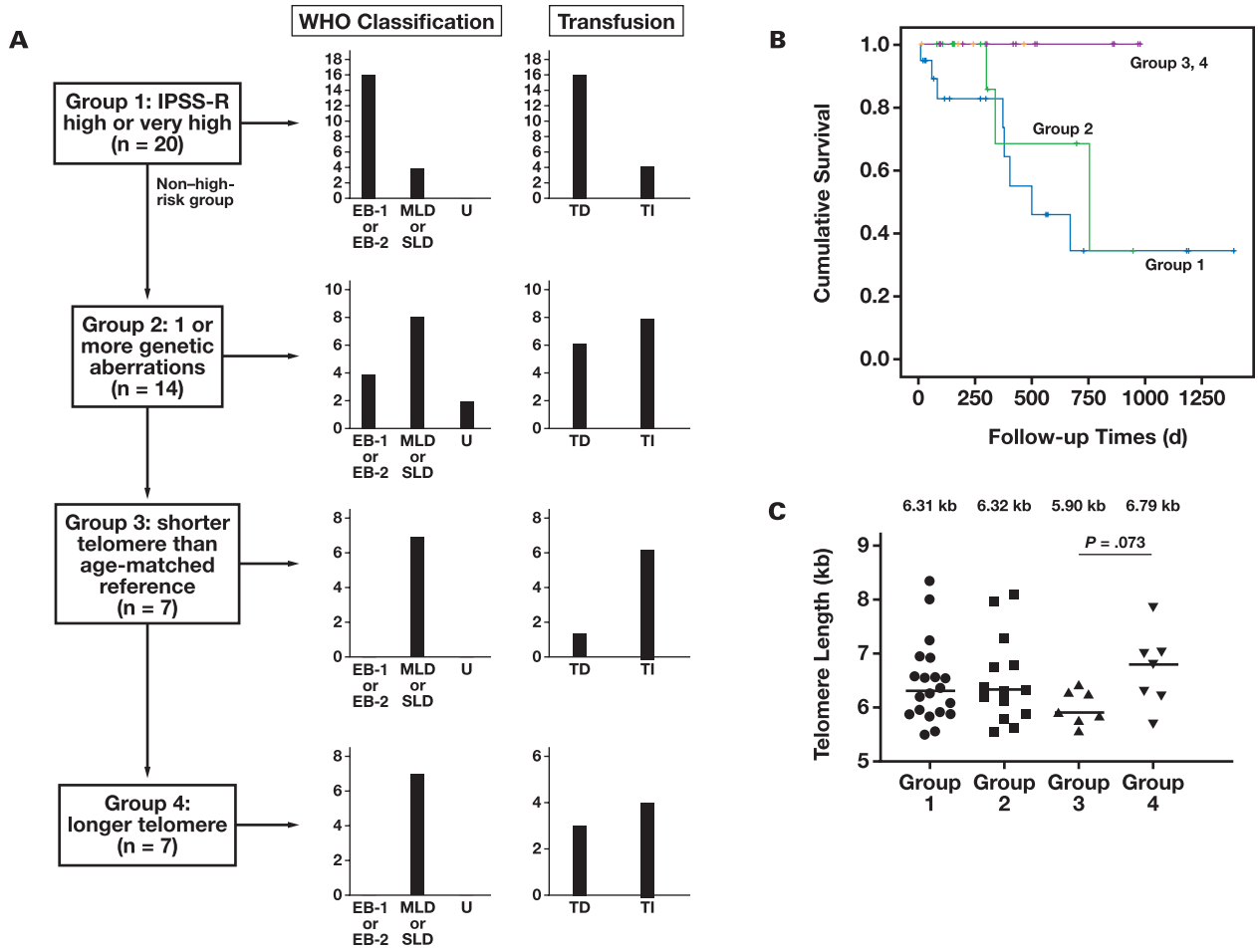

that these new variables can be meaningful for the prognosis of patients with MDS. It is necessary to draw more significant conclusions through subsequent validation studies.

Acknowledgments

This work was supported by the research grant of the Chungbuk National University Hospital in 2021.

REFERENCES

1. Greenberg PL, Tuechler H, Schanz J, et al. Revised international prognostic scoring system for myelodysplastic syndromes. *Blood.* 2012;120(12):2454–2465. doi:10.1182/blood-2012-03-420489.
2. Della Porta MG, Alessandrino EP, Bacigalupo A, et al. Predictive factors for the outcome of allogeneic transplantation in patients with MDS stratified according to the revised IPSS-R. *Blood.* 2014;123(15):2333–2342. doi:10.1182/blood-2013-12-542720.
3. Nazha A, Bejar R. Molecular data and the IPSS-R: how mutational burden can affect prognostication in MDS. *Curr Hematol Malig Rep.* 2017;12(5):461–467. doi:10.1007/s11899-017-0407-9.
4. Benton CB, Khan M, Sallman D, et al. Prognosis of patients with intermediate risk IPSS-R myelodysplastic syndrome indicates variable outcomes and need for models beyond IPSS-R. *Am J Hematol.* 2018;93(10):1245–1253. doi:10.1002/ajh.25234.
5. Mufti GJ, McLornan DP, van de Loosdrecht AA, Germing U, Hasserjian RP. Diagnostic algorithm for lower-risk myelodysplastic syndromes. *Leukemia.* 2018;32(8):1679–1696. doi:10.1038/s41375-018-0173-2.
6. Valent P. ICUS, IDUS, CHIP and CCUS: diagnostic criteria, separation from MDS and clinical implications. *Pathobiology.* 2019;86(1):30–38. doi:10.1159/000489042.
7. Gadalla SM, Cawthon R, Giri N, Alter BP, Savage SA. Telomere length in blood, buccal cells, and fibroblasts from patients with inherited bone marrow failure syndromes. *Aging (Albany NY).* 2010;2(11):867.
8. Townsley DM, Dumitriu B, Young NS. Bone marrow failure and the telomeropathies. *Blood.* 2014;124(18):2775–2783. doi:10.1182/blood-2014-05-526285.
9. Zhang C, Chen X, Li L, Zhou Y, Wang C, Hou S. The association between telomere length and cancer prognosis: evidence from a meta-analysis. *PLoS One.* 2015;10(7):e0133174. doi:10.1371/journal.pone.0133174.
10. Martínez P, Blasco MA. Telomere-driven diseases and telomere-targeting therapies. *J Cell Biol.* 2017;216(4):875–887. doi:10.1083/jcb.201610111.

11. Aubert G, Hills M, Lansdorp PM. Telomere length measurement—caveats and a critical assessment of the available technologies and tools. *Mutat Res.* 2012;730(1-2):59–67. doi:10.1016/j.mrfmmm.2011.04.003.
12. Li MM, Datto M, Duncavage EJ, et al. Standards and guidelines for the interpretation and reporting of sequence variants in cancer: a joint consensus recommendation of the Association for Molecular Pathology, American Society of Clinical Oncology, and College of American Pathologists. *J Mol Diagn.* 2017;19(1):4–23. doi:10.1016/j.jmoldx.2016.10.002.
13. Mittelman M, Oster HS, Hoffman M, Neumann D. The lower risk MDS patient at risk of rapid progression. *Leuk Res.* 2010;34(12):1551–1555. doi:10.1016/j.leukres.2010.05.023.
14. Jaiswal S, Fontanillas P, Flannick J, et al. Age-related clonal hematopoiesis associated with adverse outcomes. *N Engl J Med.* 2014;371(26):2488–2498. doi:10.1056/NEJMoa1408617.
15. Maciejewski JP, Padgett RA, Brown AL, Müller-Tidow C. DDX41-related myeloid neoplasia. *Semin Hematol.* 2017;94:97.
16. Müezzinler A, Zaineddin AK, Brenner H. A systematic review of leukocyte telomere length and age in adults. *Ageing Res Rev.* 2013;12(2):509–519. doi:10.1016/j.arr.2013.01.003.
17. Wang L, Xiao H, Zhang X, Wang C, Huang H. The role of telomeres and telomerase in hematologic malignancies and hematopoietic stem cell transplantation. *J Hematol Oncol.* 2014;7(1):1–10.
18. Göhring G, Lange K, Hofmann W, et al. Telomere shortening, clonal evolution and disease progression in myelodysplastic syndrome patients with 5q deletion treated with lenalidomide. *Leukemia.* 2012;26(2):356–358. doi:10.1038/leu.2011.193.
19. Nogueira BMD, Machado CB, Montenegro RC, De Moraes MEA, Moreira-Nunes CA. Telomere length and hematological disorders: a review. *In Vivo.* 2020;34(6):3093–3101. doi:10.21873/invivo.12142.
20. Vasko T, Kaifie A, Stope MB, Kraus T, Ziegler P. Telomeres and telomerase in hematopoietic dysfunction: prognostic implications and pharmacological interventions. *Int J Mol Sci* . 2017;18(11):2267.
21. Jones CH, Pepper C, Baird DM. Telomere dysfunction and its role in haematological cancer. *Br J Haematol.* 2012;156(5):573–587. doi:10.1111/j.1365-2141.2011.09022.x.
22. Warny M, Helby J, Sengeløv H, Nordestgaard BG, Birgens H, Bojesen SE. Bone marrow mononuclear cell telomere length in acute myeloid leukaemia and high-risk myelodysplastic syndrome. *Eur J Haematol.* 2019;102(3):218–226. doi:10.1111/ejh.13196.
23. Pereira A, Nomdedeu M, Aguilar JL, et al. Transfusion intensity, not the cumulative red blood cell transfusion burden, determines the prognosis of patients with myelodysplastic syndrome on chronic transfusion support. *Am J Hematol.* 2011;86(3):245–250. doi:10.1002/ajh.21959.
24. Lange K, Holm L, Vang Nielsen K, et al. Telomere shortening and chromosomal instability in myelodysplastic syndromes. *Genes Chromosomes Cancer.* 2010;49(3):260–269. doi:10.1002/gcc.20737.
25. Hwang SM, Kim SY, Kim JA, et al. Short telomere length and its correlation with gene mutations in myelodysplastic syndrome. *J Hematol Oncol.* 2016;9(1):1–13.

Evaluation of Oxidative Stress by Dynamic Thiol/Disulfide Homeostasis and Ischemia-Modified Albumin Levels in Children with β-Thalassemia Major

Elif Güler Kazancı, MD,[1] Muhammet Furkan Korkmaz, MD,[2,] Funda Eren, MD,[3] Özcan Erel, MD[4]*

[1]Department of Pediatric Hematology, University of Health Sciences, Bursa City Training and Research Hospital, Bursa, Turkey, [2]Department of Pediatrics, University of Health Sciences, Bursa City Training and Research Hospital, Bursa, Turkey, [3]Department of Biochemistry, University of Health Sciences, Ankara City Training and Research Hospital, Ankara, Turkey, [4]Department of Biochemistry, Faculty of Medicine, Yıldırım Beyazıt University, Ankara, Turkey. *To whom correspondence should be addressed: korkmazmfurkan@gmail.com.

Keywords: β-thalassemia major, children, ischemia-modified albumin, oxidative stress, thiol/disulfide homeostasis, chelation therapy

Abbreviations: β-TM, β-thalassemia major; TDH, thiol/disulfide homeostasis; IMA, ischemia-modified albumin; NT, native thiol; TT, total thiol; D/NT, disulfide/native thiol; D/TT, disulfide/total thiol; NT/TT, native thiol/total thiol; Hb, hemoglobin; DFO, desferrioxamine; DFP, deferiprone; DFR, deferasirox; OS, oxidative stress; ROS, reactive oxygen species; AUC, area under the curve; AST, aspartate aminotransferase

Laboratory Medicine 2023;54:206–211; https://doi.org/10.1093/labmed/lmac098

ABSTRACT

Objective: β-thalassemia major (β-TM) is a hemoglobinopathy characterized by reduced or absent β-globin production. A balance remains between the production of free radicals and suppression of increased levels of reactive oxygen species by the antioxidant system. This study aimed to examine thiol/disulfide homeostasis (TDH) and serum ischemia-modified albumin (IMA) levels to evaluate the oxidant/antioxidant balance in healthy children and persons with β-TM receiving and not receiving chelation therapy.

Methods: This prospective study was carried out from January to June 2021 among 46 individuals with β-TM and 35 healthy controls. A spectrophotometric method was used to analyze TDH and IMA concentrations.

Results: We found that, compared to controls, native thiol (NT) (P = .048) and total thiol (TT) (P = .027) values were lower in the patient group, whereas disulfide (P < .001), disulfide/native thiol (D/NT) (P = .004), disulfide/total thiol (D/TT) (P = .005), native thiol/total thiol (NT/TT) (P = .004) and IMA (P = .045) values were higher. NT and TT levels were significantly lower in the chelation– group compared to the chelation+ and control groups (P = .002, P = .001). D/NT, D/TT, and NT/TT levels were higher in the chelation+ group than the control group (P = .007), and IMA levels were significantly higher in the chelation+ and chelation– groups compared to the control group (P = .002). The receiver operating characteristic analysis demonstrated that IMA levels were significantly higher in the children with β-TM not taking regular chelation therapy.

Conclusion: Thiol/disulfide homeostasis was observed to be weakened in children with β-TM in our study. Our findings show that when children with β-TM do not receive regular chelation therapy, their oxidant imbalance worsens.

Thalassemia is an autosomal recessive inherited disease that presents with the hypochromic microcytic anemia. Thalassemia group diseases develop as a result of faulty synthesis of 1 or more of the hemoglobin (Hb) chains.[1] Deficient or no synthesis of the Hb chain or chains defined as α, β, γ, δ causes thalassemia. α-thalassemia results from deficient α chain synthesis, whereas deficient synthesis of β chain leads to β thalassemia. β-thalassemia major (β-TM), on the other hand, presents a clinical picture where Hb levels are below 7 g/dL, typically observed together with excessive iron deficiency, and therefore routine blood transfusions at intervals of 2 to 5 weeks are performed to keep Hb levels above 10 g/dL.[2,3] About 3% of the global population are β-thalassemia carriers, whereas 5% to 10% of the population in Southwest Asia are α-thalassemia carriers. In Turkey, there is a high number of thalassemia carriers in the Çukurova, Mediterranean coastline, Aegean, and Marmara regions. There are approximately 1,300,000 β-thalassemia carriers and around 4000 β-thalassemia patients in Turkey.[4]

Regular blood transfusions applied to β-TM patients, hemolysis, and increased intestinal iron absorption cause iron overload in the body.[5,6] In an attempt to prevent iron accumulation in the body, reduce existing iron accumulation, and thereby prevent complications linked to elevated iron accumulation in the body, these patients are treated with chelation therapy. Treatments for this purpose employ desferrioxamine (DFO), deferiprone (DFP), deferasirox (DFR), and their combinations.[7]

Generation of reactive oxygen products increases in β-TM patients. It has been shown that oxidative stress (OS), caused by the shift of the balance between reactive oxygen products and the antioxidant defense system towards reactive oxygen products, has a fundamental role in the pathogenesis of many diseases, including β-TM.[8,9] Some indicators express OS levels in the body. Oxidant molecules oxidize the thiols

consisting of sulfhydryl groups to form reversible disulfide bridges, and this process forms 1 of the main defense systems against the negative effects of reactive oxygen species (ROS).[10–12]

Although only thiol levels could be evaluated since 1979, a method developed by Erel et al[13] in 2014 now makes it possible to measure both thiol and disulfide levels (thiol-disulfide homeostasis [TDH]), enabling better evaluation of OS levels. Recent studies of this method have noticed that impaired TDH is related to diverse disorders such as diabetes mellitus, chronic kidney failure, asthma, acute malnutrition, obesity, sickle cell anemia, familial Mediterranean fever, and cancer. However, it should be noted that studies with β-thalassemia patients are very limited.[14–20]

In this study, we aim to demonstrate potential OS changes between healthy individuals and children with β-TM by way of comparison. Additionally, this study, where we will compare the TDH of β-TM patients receiving and not receiving chelation therapy, will be the first of its kind in the literature.

Material and Methods

Study Population and Design

This single-center prospective study was carried out among 46 individuals with β-TM and 35 healthy controls. Patients were admitted from January to June 2021 to the pediatric hematology department of the University of Health Sciences City Training and Research Hospital, Bursa, Turkey. Ethical approval was obtained from the University Ethics Committee (2011-KAEK-25 2020/12-15). Written informed consent was obtained from all parents or legal educators of patients prior to inclusion in the study.

The subjects were diagnosed with β-TM on examination of complete blood count, peripheral blood smear, and high-performance liquid chromatography. The individuals received regular erythrocyte transfusions. Chelation was performed as DFR and/or DFP. The DFR was given in a dose of 25 to 35 mg/kg/d and DFP in a dose of 75-100/mg/d to those over the age of 2 years, at least 1 hour before food orally daily. To investigate the effect of iron-chelating agents, we categorized the patients into 2 groups, those receiving regular chelation therapy and those that do not. Individuals with chronic childhood diseases such as thalassemia minor or intermedia, endocrinological, cardiac, neurological, or infectious diseases were excluded from the study. The healthy control group comprised healthy children who were age- and gender-compatible with the patient group, presented to our Pediatric Health and Diseases polyclinic for routine examinations, did not have any chronic diseases, did not use any medication, and did not have any symptoms or complaints in the previous 14 days that would suggest infection.

Blood samples were collected in the early morning from healthy controls and β-TM subjects. Blood transfusion of β-TM patients was performed after blood samples were collected. We used EDTA-containing tubes and an automated analyzer for complete blood count (Siemens ADVIA 2120i). Serum samples were centrifuged at 1500*g* for 10 minutes and stored at −80°C until analysis.

Baseline laboratory tests such as liver-kidney-thyroid function tests, vitamins, and albumin were conducted with standard methods. An automatic chemical analyzer (Roche, Cobas 501) with a novel spectrophotometric method was used to test the serum concentrations of native and total thiol and ratios of disulfide.[13] A colorimetric method described by Bar-Or et al[21] was used to measure serum IMA concentrations, and the obtained results were included in the text as absorbance units.

Statistical Analyses

Categorical variables are expressed as No. (%), and continuous variables are presented as mean ± SD or median (minimum-maximum values), where appropriate. To compare the qualitative variables, χ^2 or Fisher's exact tests were performed. The difference among three groups was measured with 1-way analysis of variance, and the Bonferroni test among post hoc tests was used to make binary comparisons. Correlations were analyzed using Spearman's Rho correlation analysis. The independent sample test was used to evaluate the differences between the 2 groups in the presence of parametric test conditions. When the conditions were not met, the Mann-Whitney *U* test was used.

The performance of TDH parameters in terms of predicting β-TM not using chelation therapy was assessed using the receiver operating characteristic (ROC). The 95% confidence intervals of the area under the curve (AUC) were calculated.

All tests were 2-tailed and $P < .05$ was considered statistically significant. Statistical analyzes were performed by using SPSS version 21.0 (SPSS).

Results

We included 81 children between the ages of 2 and 252 months (46 children diagnosed with β-TM and 35 healthy controls). There was no statistically significant difference between age and gender in both groups. Compared to the healthy controls, the patient group had low levels of Hb ($P < .001$) and hematocrit ($P < .001$) and high serum iron ($P < .001$), ferritin ($P < .001$), and vitamin D ($P = .002$). The data related to demographic and laboratory characteristics of the study population are shown in **TABLE 1**.

In comparison to the healthy controls, the patient group had lower native thiol (NT) ($P = .048$) and total thiol (TT) ($P = .027$) values and showed higher levels of disulfide ($P<.001$), disulfide/native thiol (D/NT) ($P = .004$), disulfide/total thiol (D/TT) ($P = .005$), native thiol/total thiol (NT/TT) ($P = .004$), and IMA ($P = .045$). TDH parameters in the patient and control groups are shown in **TABLE 2**.

We report that 11 (23.9%) of β-TM patients included in the study did not receive chelation therapy. When we examined the patient group by categorizing them into 2 groups, those taking chelation therapy (chelation+) and those that do not (chelation−), it was determined that NT and total TT were significantly lower in the chelation− group than the chelation+ and control groups ($P = .002$, $P = .001$). Disulfide levels were higher in both patient groups compared to the control group ($P < .001$). The D/NT and D/TT levels were found to be higher in both patient groups compared to the control group ($P = .007$). Although IMA levels were determined to be significantly higher in the chelation+ and chelation− groups than in the control group ($P = .002$), we observed no differences among the patient groups. A detailed comparison of TDH parameters in the patient groups and control group is provided in **TABLE 3**.

The results of correlation analyses performed for OS and other parameters are given in **TABLE 4**. Age (month) has a weak positive correlation with NT and TT, whereas Hb values have a weak positive correlation with NT and TT and a moderate positive correlation with disulfide levels. Ferritin values have a weak negative correlation with disulfide. Vitamin D, on the other hand, has a weak negative correlation with disulfide and D/NT. Aspartate aminotransferase (AST) values

TABLE 1. Demographics and Laboratory Characteristics Among Study Participants[a]

Parameters	Study Group (n = 46)	Control Group (n = 35)	*P* Value
Age, months	34 (2–252)	100 (13–205)	.554[b]
Female/Male	27/19	19/16	.432[c]
Hemoglobin (g/dL)	9.27 ± 1.61	12.78 ± 0.64	<.001[d]
Hematocrit (%)	27.36 ± 2.45	38.78 ± 5.54	<.001[d]
MCV (µg/dL)	79.04 ± 9.46	82.11 ± 4.51	.058[d]
RDW (%)	17.65 ± 5.07	16.26 ± 4.58	.677[d]
Serum iron (µg/dL)	226.12 ± 63.38	114.89 ± 36.03	<.001[d]
TIBC	271 (17–1022)	245 (152–333)	.154[b]
Ferritin (nmol/L)	1333 (115–4012)	54 (8–2029)	<.001[b]
Vitamin B_{12} (ng/L)	358 ± 132	336 ± 123	.461[d]
Folic acid (ng/mL)	9.82 (2.30–39.68)	10.70 (3.20–96.40)	.117[b]
Vitamin D (µg/L)	22.50 (4.52–50.00)	14.55 (4.70–27.40)	.002[b]
AST (U/L)	29 (8–52)	24 (11–51)	.240[b]
ALT (U/L)	19 (4–78)	13 (8–232)	.139[b]
TSH (µIU/L)	3.12 ± 1.65	2.60 ± 0.94	.118[d]
fT4 (ng/dL)	1.19 ± 0.20	1.26 ± 0.39	.360[d]
Albumin (g/dL)	4.58 (1.30–5.24)	4.70 (4.00–5.30)	.156[b]

ALT, alanine aminotransferase; AST, aspartate aminotransferase; fT4, free T4; MCV, mean corpuscular volume; RDW, red cell distribution width; TIBC, total iron-binding capacity; TSH, thyroid-stimulating hormone.
[a]*Data are presented as mean ± standard deviation or median (minimum-maximum values).*
[b]*Mann-Whitney U test.*
[c]*χ^2 test.*
[d]*Independent-samples t test.*

demonstrated a weak negative correlation with NT, TT, and disulfide levels.

An ROC analysis was performed to see the utility of the TDH parameters for β-TM chelation– group. The cut-off values affording the optimum balance between sensitivity and specificity and AUC values are given in **TABLE 5**.

Discussion

Oxidative stress occurs upon disruption of the balance between oxidant and antioxidant mechanisms in the body.[18] Thiol groups act as antioxidants and regulate the redox system. The thiols containing a sulfhydryl group are oxidized by oxidants to form reversible disulfide bridges. Oxidation-reduction reactions have a key role in maintaining the dynamic TDH.[22,23] The TDH balance is crucial in terms of apoptosis, antioxidant protection, signal transduction, detoxification, enzyme activity, and regulation of cellular signaling mechanisms by the transcription factor. Disruption of these vital cellular functions is observed in case of an abnormality in the TDH.[11,13]

Many studies have evaluated OS in adults with β-TM. Higher malondialdehyde levels and lower vitamin E and total antioxidant capacity in individuals with β-TM compared with controls were shown in 1 of these studies.[9] On the contrary, Kassab-Chekir[24] and Kalpravidh et al[25] found that antioxidant mechanisms were more dominant. Some studies evaluate OS in those with β-TM by measuring only NT levels. However, these do not provide information about the TDH.[26,27] Developed by Erel and Neselioğlu,[13] the method that we used in our study not only measures separate variables but also enables both individual and integral evaluations and provides an overall picture of the TDH. This method is an easy, cheap, practical, and fully automated (optionally manual) spectrophotometric test. Being the first researchers to use this method, Güzelçiçek et al[8] showed that OS increased in children with β-TM compared to healthy children. In our study, we found NT and TT values to be lower in the patient group than in the healthy control group, whereas disulfide, D/NT, D/TT, NT/TT, and IMA values were higher in the patient group. These results indicate that the TDH shifted to the oxidized side in our patient group.

As a result of repeating blood transfusions and hemolysis, individuals with β-TM suffer from iron overload in their body tissues. Iron overload causes increased ROS production and OS in these persons.[28] Due to these undesirable effects, the need to use iron chelators and antioxidants individually or in combination has arisen during treatment.[29] The chelator DFO, which is the most widely used, has significant contributions to morbidity and mortality rates in persons needing transfusions. The need for daily administration with a parenteral or portable infusion pump is the biggest disadvantage of this chelator. Two new oral chelators, DFP and DFR, developed due to these disadvantages, improved the practices, conformity, and quality of life for persons needing transfusions. The DFP is able to direct and push iron from tissues to the circulation, and the iron in circulation binds with DFO, which is then excreted via the kidneys. Widely referred to as the "shuttle hypothesis," this chelator combination also manages to eliminate the labile iron pool and decrease the level of labile plasma iron.[30,31] The quality of chelation therapy is directly related to life expectancy. Inadequate adherence to treatment increases the risk of complications and shortens survival. Measurement of serial serum ferritin is useful for close and frequent monitoring to show changes in iron burden and determine current treatment needs. In the case of increased ferritin levels, dosage may be lowered and the choice of chelator may be better adapted to patient preference.[32]

When we examined the patient group by categorizing them into 2 groups, those taking chelation therapy and those that do not, it was determined that disulfide, D/NT, and D/TT levels were higher in both patient groups than the control group. The NT and TT levels, on the other hand, were significantly lower in the chelation– group than the chelation+ and control groups. We believe that these results support the hypothesis that regular chelation therapy reduces OS in those with β-TM. Our study is the first in the literature to test this hypothesis by measuring the TDH in children with β-TM.

Ischemia-modified albumin is produced by ROS that occurs as a result of ischemic attacks. A recent and sensitive marker, IMA is used for ischemia and OS to determine several conditions.[33–35] Some studies with adults showed an increase in IMA levels in patients with chronic kidney failure and β-TM.[5,36] Although Topal et al[12] found a similar level of IMA in the control group in their study in which they examined children with iron deficiency anemia, Mengen et al[17] reported that IMA levels increased in children with obesity. In our study, IMA levels were significantly higher in the chelation+ and chelation– groups than in the control group. Performed to further ex-

amine this situation, the ROC analysis showed that IMA levels were significantly higher in those with β-TM not taking regular chelation therapy. With 0.736 AUC, IMA had the highest rate among all parameters. Similarly, NT and TT levels were found to be low in this group. In light of these results, we believe that IMA levels are one of the important indicators of OS in β-TM.

Ateş et al[37] reported negative correlations between patient age and TDH in their study. Another study reported that OS increases with age, leading to TDH imbalance.[13] In our study, age (month) has a weak positive correlation with NT and TT levels. On the other hand, Hb demonstrated weak and moderate positive relationship with TDH indicators, and ferritin, vitamin D, and AST values showed a weak negative relationship.

This study was conducted at a single center with a small group of patients. Therefore, the limited sample size for some analyses may not have allowed us to draw definitive conclusions. Furthermore, we could not examine the relationship between TDH and other OS parameters and β-TM. To the best of our knowledge, despite these limitations, our study is the first in the literature to evaluate TDH and OS in children with a diagnosis of β-TM, especially with its focus on the use of chelation therapy.

Conclusion

Our study shows that the TDH deteriorates and OS increases in children diagnosed with β-TM. The IMA levels, and hence OS, increased even more in children diagnosed with β-TM who did not receive regular

TABLE 2. Thiol/Disulfide Hemostasis Parameters Among Study Participants[a]

Parameters	Study Group (n = 46)	Control Group (n = 35)	*P* Value
Native thiol (μmol/L)	490.57 ± 97.92	532.22 ± 49.48	.048
Total thiol (μmol/L)	532.57 ± 103.60	584.31 ± 50.70	.027
Disulfide (μmol/L)	31.00 ± 4.46	26.04 ± 4.31	<.001
Disulfide/native thiol (%)	5.34 ± 0.77	4.94 ± 0.94	.004
Disulfide/total thiol (%)	4.99 ± 0.64	4.48 ± 0.77	.005
Native thiol/total thiol (%)	92.02 ± 1.29	91.04 ± 1.54	.004
IMA (ABSU)	0.81 ± 0.21	0.73 ± 0.06	.045

ABSU, absorbance units; IMA, ischemia-modified albumin.
[a]The values are presented as mean ± standard deviation. Mann-Whitney U test was performed. P < .05 was considered significant.

TABLE 3. Thiol/Disulfide Hemostasis Parameters in the Study Groups and Control Group[a]

Parameters	Chelation+ (n = 35)	Chelation– (n = 11)	Control Group (n = 35)	*P* Value
Native thiol (μmol/L)	508.13 ± 98.18[b]	434.72 ± 76.60[c]	532.22 ± 49.48	.002
Total thiol (μmol/L)	551.07 ± 104.20[b]	473.73 ± 79.84[c]	584.31 ± 50.70	.001
Disulfide (μmol/L)	30.47 ± 4.75[c]	31.50 ± 3.05[c]	26.04 ± 4.31	<.001
Disulfide/native thiol (%)	5.32 ± 0.79[c]	5.38 ± 0.67[c]	4.94 ± 0.94	.007
Disulfide/total thiol (%)	4.93 ± 0.66[c]	5.06 ± 0.56[c]	4.48 ± 0.77	.007
Native thiol/total thiol (%)	92.13 ± 1.33[c]	91.67 ± 1.13	91.04 ± 1.54	.007
IMA (ABSU)	0.77 ± 0.20[b]	0.94 ± 0.21[c]	0.73 ± 0.06	.002

ABSU, absorbance units; IMA, ischemia-modified albumin.
[a]The values are presented as mean ± standard deviation. ANOVA test was performed. P < .05 was considered significant.
[b]Different from the chelation– group
[c]Different from the control group

TABLE 4. Correlation Between Variables in Patients with β-Thalassemia Major

	Native Thiol		Total Thiol		Disulfide		Disulfide/Native Thiol	
Variables	*r*	*P*[a]	*r*	*P*[a]	*r*	*P*[a]	*r*	*P*[a]
Age	0.334	.002	0.323	.003	0.153	.172	–0.174	.119
Hemoglobin	0.308	.005	0.336	.002	0.410	.001	0.109	.332
Hematocrit	0.297	.007	0.323	.003	0.431	.001	0.127	.259
Serum iron	0.097	.429	0.073	.552	–0.197	.107	-0.235	.053
Ferritin	–0.129	.267	–0.078	.504	–0.328	.004	–0.210	.068
Vitamin B_{12}	0.173	.131	0.117	.307	–0.013	.912	–0.010	.934
Folic acid	0.074	.523	0.133	.253	0.025	.828	0.002	.988
Vitamin D	–0.006	.959	–0.106	.395	–0.391	.001	–0.352	.004
AST	–0.343	.002	–0.315	.005	–0.277	.015	0.003	.980
ALT	0.071	.539	0.135	.242	0.088	.445	0.044	.701
TSH	–0.002	.986	–0.027	.827	–0.234	.055	–0.116	.177
fT4	0.040	.743	0.033	.740	–0.089	.468	–0.104	.400
Albumin	0.216	.059	0.042	.717	0.059	.202	0.135	.242

ALT, alanine aminotransferase; AST, aspartate aminotransferase; fT4, free T4; TSH, thyroid-stimulating hormone.
[a]P < .05 was considered significant.

TABLE 5. Receiver Operator Curve Evaluating Parameters and Cut-Off Values for β-Thalassemia Major Chelation– Patients

Parameters	Cut-Off Value	Sensitivity (%)	Specificity (%)	AUC (95 % CI)	*P* Value
Native thiol (μmol/L)	425.5	63.6	77.1	0.270 (0.119–0.422)	.023
Total thiol (μmol/L)	463.1	63.6	77.1	0.271 (0.125–0.418)	.023
Disulfide (μmol/L)	17.88	81.8	71.4	0.374 (0.208–0.540)	.212
Disulfide/native thiol (%)	3.76	90.9	68.6	0.635 (0.452–0.818)	.181
Disulfide/total thiol (%)	3.50	90.9	68.6	0.636 (0.454–0.819)	.176
Native thiol/total thiol (%)	91.36	63.6	80.0	0.364 (0.181–0.546)	.176
IMA (ABSU)	0.68	90.9	68.6	0.736 (0.589–0.884)	.019

ABSU, absorbance units; AUC, area under the curve; CI, confidence interval; IMA, ischemia-modified albumin.

chelation therapy. We believe that IMA levels are one of the important indicators of OS in β-TM.

REFERENCES

1. Cappellini MD, Cohen A, Eleftheriou A, et al. *Guidelines for the Clinical Management of Thalassaemia*. Rev 2nd ed. 2008. https://pubmed.ncbi.nlm.nih.gov/24308075/. Accessed April 22, 2022.
2. Taher AT, Weatherall DJ, Cappellini MD. Thalassaemia. *Lancet.* 2018;391(10116):155–167.
3. Abd IK, Zainal IG. Assessment of biochemical parameters and study its correlation in ß-thalassemia major patients and healthy controls in Kirkuk City, Iraq. *Med J Babylon.* 2020;17:172–176.
4. Beta thalassemia. *Diagnosis and Treatment Guide. National Treatment Guide 2011*. http://www.thd.org.tr/thdData/Books/94/bolum-viii-beta-talasemi-tani-ve-tedavi-kilavuzu.pdf. Accessed April 22, 2022.
5. Awadallah SM, Atoum MF, Nimer NA, et al. Ischemia modified albumin: an oxidative stress marker in β-thalassemia major. *Clin Chim Acta.* 2012;413(9-10):907–910.
6. Leecharoenkiat K, Lithanatudom P, Sornjai W, et al. Iron dysregulation in beta-thalassemia. *Asian Pac J Trop Med.* 2016;9(11):1035–1043.
7. Borgna-Pignatti C, Marsella M. Iron chelation in thalassemia major. *Clin Ther.* 2015;37(12):2866–2877.
8. Guzelcicek A, Cakirca G, Erel O, et al. Assessment of thiol/disulfide balance as an oxidative stress marker in children with β-thalassemia major. *Pak J Med Sci.* 2019;35(1):161–165.
9. Ghone RA, Kumbar KM, Suryakar AN, et al. Oxidative stress and disturbance in antioxidant balance in beta thalassemia major. *Indian J Clin Biochem.* 2008;23(4):337–340.
10. Topal I, Mertoğlu C, Sürücü Kara I, et al. Thiol-disulfide homeostasis, serum ferroxidase activity, and serum ischemia modified albumin levels in childhood iron deficiency anemia. *Fetal Pediatr Pathol.* 2019;38(6):484–489.
11. Erenler AK, Yardan T. Clinical utility of thiol/disulfide homeostasis. *Clin Lab.* 2017;63:867–870. doi:10.7754/Clin.Lab.2017.161117
12. Topal I, Mertoglu C, Surucu Kara I, et al. Thiol-disulfide homeostasis, serum ferroxidase activity, and serum ischemia modified albumin levels in neonatal jaundice. *Fetal Pediatr Pathol.* 2019;11:1–18.
13. Erel O, Neselioglu S. A novel and automated assay for thiol/disulphide homeostasis. *Clin Biochem.* 2014;47:326–332. doi:10.1016/j.clinbiochem.2014.09.026
14. Gulpamuk B, Tekin K, Sonmez K, et al. The significance of thiol/disulfide homeostasis and ischemia-modified albumin levels to assess the oxidative stress in patients with different stages of diabetes mellitus. *Scand J Clin Lab Inv.* 2018;78(1):136–142.
15. Dirican N, Dirican A, Sen O, et al. Thiol/disulfide homeostasis: a prognostic biomarker for patients with advanced nonsmall cell lung cancer? *Redox Rep.* 2016;21:197–203. doi:10.1179/1351000215Y.0000000027
16. Cakirca G, Celik MM, Erdal H. Investigation of thiol/disulfide homeostasis in familial Mediterranean fever patients. *J Clin Anal Med.* 2018;9(3):231–234.
17. Mengen E, Ucakturk SA, Kocaay P, et al. The significance of thiol/disulfide homeostasis and ischemia-modified albumin levels in assessing oxidative stress in obese children and adolescents. *J Clin Res Pediatr Endocrinol.* 2020;12(1):45–54.
18. Demir M, Erel O. Dynamic thiol/ disulfide balance in children with acute malnutrition. *Eur J Ther.* 2020;26(2):92–96.
19. Nar R, Calıs AG. Assessment of dynamic thiol/disulfide homeostasis in patients with asthma. *J Lab Med.* 2018;42(3):99–104.
20. Ozcan O, Erdal H, Ilhan G, et al. Plasma ischemia-modified albumin levels and dynamic thiol/disulfide balance in sickle cell disease: a case-control study. *Turk J Hematol.* 2018;35(4):265–270.
21. Bar-Or D, Lau E, Winkler JV. A novel assay for cobalt-albumin binding and its potential as a marker for myocardial ischemia-a preliminary report. *J Emerg Med.* 2000;19:311–315. doi:10.1016/s0736-4679(00)00255-9
22. Nagy P. Kinetics and mechanisms of thiol–disulfide exchange covering direct substitution and thiol oxidation-mediated pathways. *Antioxid Redox Signal.* 2013;18(13):1623–1641.
23. Circu ML, Aw TY. Reactive oxygen species, cellular redox systems, and apoptosis. *Free Radic Biol Med.* 2010;48(6):749–762.
24. Kassab-Chekir A, Laradi S, Ferchichi S, et al. Oxidant, antioxidant status and metabolic data in patients with beta-thalassemia. *Clin Chim Acta.* 2003;338(1-2):79–86.
25. Kalpravidh RW, Tangjaidee T, Hatairaktham S, et al. Glutathione redox system in beta-thalassemia/Hb E patients. *Sci World J.* 2013;2013:543973.
26. Laksmitawati DR, Handayani S, Udyaningsih-Freisleben SK, et al. Iron status and oxidative stress in beta thalassaemia patients in Jakarta. *Biofactors.* 2003;19(1-2):53–62.
27. Livrea MA, Tesoriere L, Pintaudi AM, et al. Oxidative stress and antioxidant status in beta-thalassemia major: iron overload and depletion of lipid soluble antioxidants. *Blood.* 1996;88(9):3608–3614.
28. Vichinsky E, Butensky E, Fung E, et al. Comparison of organ dysfunction in transfused patients with SCD or beta thalassemia. *Am J Hematol.* 2005;80(1):70–74. doi:10.1002/ajh.20402.
29. Fibach E, Rachmilewitz EA. The role of antioxidants and iron chelators in the treatment of oxidative stress in thalassemia. *Ann N Y Acad Sci.* 2010;1202(1):10–16.
30. Odame I, Rund D. Evidence-based treatment of thalassemia major. In: Mark A, Crowther JG, Ginsberg J, et al, eds. *Evidence-Based Hematology.* Hoboken, NJ: Blackwell Publishing; 2008.
31. Prus E, Fibach E. Effect of iron chelators on labile iron and oxidative status of thalassaemic erythroid cells. *Acta Haematol.* 2009;123:14–20. doi:10.1159/000258958

32. Cappellini MD, Cohen A, Porter J, Taher A, Viprakasit V, eds. *Guidelines for the Management of Transfusion Dependent Thalassaemia (TDT)*. 3rd ed. Nicosia, Cyprus: Thalassaemia International Federation; 2014.
33. Roy D, Quiles J, Sharma R, et al. Ischemia modified albumin concentrations in patients with peripheral vascular disease and exercise-induced skeletal muscle ischemia. *Clin Chem.* 2004;50:1656–1660. doi:10.1373/clinchem.2004.031690
34. Piwowar A, Knapik-Kordecka M, Warwas M. Ischemia-modified albumin level in type 2 diabetes mellitus—preliminary report. *Dis Markers.* 2008;24:311–317. doi:10.1155/2008/784313
35. Chang D, Sha Q, Zhang X, et al. The evaluation of the oxidative stress parameters in patients with primary angle-closure glaucoma. *PLoS One.* 2011;6:e27218. doi:10.1371/journal.pone.0027218
36. Cichota L, Moresco R, Duarte M, et al. Evaluation of ischemia-modified albumin in anemia associated to chronic kidney disease. *J Clin Lab Anal.* 2008;22:1–5.
37. Ates I, Altay M, Yilmaz FM, et al. Dynamic thiol/disulfide balance in patients with autoimmune subclinical hypothyroidism. *Endocr Res.* 2016;41(2):343–349. doi:10.3109/07435800.2016.1156124

Clinical Application of Prostatic Exosomal Protein and Prostate-Specific Antigen Levels in the Detection of Prostate-Related Diseases

Qiuxia Ge, MS,[1] *Jianfang Lou, MS*[1,*]

[1]Department of Laboratory Medicine, First Affiliated Hospital of Nanjing Medical University, Nanjing, China. *To whom correspondence should be addressed: loujianfang@126.com.

Keywords: prostatitis, prostate cancer, prostatic small extracorporeal protein, prostate-specific antigen, types, combination

Abbreviations: PSEP, prostatic exosomal protein; PSA, prostate-specific antigen; AP, acute prostatitis; CP, chronic prostatitis; PCa, prostate cancer

Laboratory Medicine 2023;54:212–214; https://doi.org/10.1093/labmed/lmac103

ABSTRACT

Objective: Our aim was to study the use of prostatic exosomal protein (PSEP) and prostate-specific antigen (PSA) in diagnosis of prostate-related diseases.

Methods: A total of 54 cases of acute prostatitis (AP), 72 cases of chronic prostatitis (CP), and 36 cases of prostate cancer (PCa) were enrolled. Levels of PSEP and PSA were analyzed.

Results: The positive rate and level of PSEP in CP was highest (both $P < .05$). The total PSA (tPSA) level in PCa was the highest ($P < .05$), followed by AP and CP. The free PSA (fPSA) level was lowest in CP ($P < .05$); fPSA/tPSA in AP was the highest ($P < .05$). The PSEP level in type II CP was higher than in type IIIa and type IIIb (both $P < .05$), and it was higher in type IIIa than in type IIIb ($P < .05$). The tPSA level in type IIIb was the lowest in the 3 types (both $P < .05$). The fPSA/tPSA in type IIIb was the highest in the 3 types ($P < .05$).

Conclusion: The PSEP combined with PSA better distinguishes prostate-related diseases.

Prostate-related diseases are diseases with a high incidence in men, and clinical diagnosis is generally based on clinical symptoms combined with the results of routine examinations such as urine routine, prostatic fluid microscopy, urine bacteriological culture, etc. Due to certain limitations and difficulty of diagnosis caused by the inconvenience of some inspections or individuals' intolerance, timely and effective targeted treatment in some cases has been missed.[1,2] With the increase in new diagnostic factors, prostatic exosomal protein (PSEP) has been gradually applied clinically as a new indicator of prostate-related diseases in recent years, but its diagnostic value requires evaluation. In this study, we discuss the levels of PSEP of prostate-specific antigen (PSA) in different prostate diseases and the value in distinguishing prostate diseases.

Materials and Methods

Study Subjects

A total of 54 cases of acute prostatitis (AP), 72 cases of chronic prostatitis (CP), and 36 cases of prostate cancer (PCa) in patients admitted to the First Affiliated Hospital of Nanjing Medical University from August 2018 to October 2019 were included in the study. All study subjects had relevant clinical symptoms and underwent auxiliary examinations. The diagnosis of prostatitis complied with the diagnostic criteria in the *Guidelines for the Diagnosis and Treatment of Prostatitis*. All participants were diagnosed by needle biopsy and pathology. Participants diagnosed with AP were aged 28 to 65 years, with an average age of 34.4 ± 3.2 years; those diagnosed with CP were aged 31 to 65 years with an average age of 37.8 ± 5.5 years; subjects diagnosed with PCa were aged 35 to 67 years, with an average age of 39.8 ± 5.6 years. There was no significant difference in age among the 3 groups. The study had been approved by the First Affiliated Hospital of Nanjing Medical University of Medicine Institutional Review Board and the consent was informed.

Methods

Morning urine was centrifuged to take the supernatant for use. Fasting blood was centrifuged at 3500 rpm for 5 min to take serum for use. The PSEP detection was done using enzyme-linked immunosorbent assay with a commercial kit (Angke). All evaluations were performed in strict accordance with the manufacturer's instructions. The PSEP concentration of the sample was calculated with a standard curve, which was generated according to different concentrations of standard products. The normal reference range is ≤1.2 ng/mL. The PSA detection were performed using Roche e602 electrochemiluminescence and its supporting reagents, and the value of free to total PSA (fPSA/tPSA) ratio was calculated automatically. The reference ranges of the 2 are ≤4 ng/mL and 0.05 to 0.3 ng/mL, respectively.

Statistical Analysis

Quantitative data were expressed as medians ± standard deviation (± SD) range. Statistical analysis was operated by using Graphpad

Prism8 software package. One-way analysis of variance and the least significant difference method were used to compare data among different groups.

Results

Levels of PSEP, tPSA, fPSA, and the fPSA/tPSA Ratio

The positive rates of PSEP in the AP group, CP group, and PCa group were 51.9% (48/54), 88.9% (64/72) and 25% (9/36), respectively. The PSEP levels in CP and AP were significantly higher than those in PCa (both $P < .05$), and the PSEP level in CP was higher than that in AP as well ($P < .05$). The tPSA level in PCa was significantly higher than that in the CP and AP groups (both $P < .05$), and tPSA level in the AP group was significantly higher than that in CP ($P < .05$); fPSA in the CP group was significantly lower than that in the PCa and AP groups ($P < .05$),but there was no significant difference between PCa and AP groups; fPSA/tPSA in the PCa and CP groups was significantly lower than in the AP group ($P < .05$), but there was no difference between the PCa and CP groups. Results are shown in **TABLE 1**.

Levels of PSEP, tPSA, fPSA, and fPSA/tPSA in Different Types of CP

According to the classification criteria of the National Institutes of Health, CP was divided into type II (25 cases), type IIIa (31 cases), and type IIIb (16 cases), and the positive rates of the 3 were 88.0% (21/25), 90.3% (28/31), and 93.8% (14/16), respectively. The PSEP level in type II was significantly higher than that in type IIIa and type IIIb (both $P < .05$), and the PSEP level in type IIIa was significantly higher than that in type IIIb ($P < .05$). The tPSA level in type IIIb was significantly lower than that in type II and type IIIa ($P < .05$). The fPSA level showed no significant difference among 3 types. The fPSA/tPSA was significantly higher in type IIIb than in type II and type IIIa ($P < .05$), but there was no significant difference between the latter 2. Results are shown in **TABLE 2**.

Discussion

Prostate disease is a common disease in men around the world. The diagnosis generally is made based on clinical symptoms and results of tests such as prostate fluid examination, culture, and urine routine, etc. However, a considerable part of the examinations typically cause discomfort to individuals, making it difficult to undergo them. Moreover, some tests lack specificity and are easily affected by a variety of factors, so it is necessary to explore suitable noninvasive markers in the clinic.

PSA belongs to a kind of prostate tissue-specific marker that is synthesized by prostate epithelial cells, including free and bound forms. In addition to tumor lesions, studies have also shown that PSA in peripheral blood abnormally increases when prostate tissue is inflamed, so there may be limitations in distinguishing prostate inflammation from tumors using PSA only. The prostate corpuscle is a kind of vesicle secreted by prostate epithelial cells that secrete PSEP. The PSEP level as an indicator of prostatitis is a method that has been applied in the clinic in recent years. Stimulation of prostate tissue in an inflammation state can induce increased production of prostatic corpuscles followed by increased secretion of PSEP, which enter the male genitourinary tract and ultimately appear in the urine.[3] Therefore, the degree of inflammation in prostatitis can be reflected by the levels of PSEP in urine.[4] This study explored the value of PSEP and PSA in the diagnosis of prostate-related diseases. It was found that the positive rate of PSEP in CP was as high as 88.9%, which was significantly higher than that in AP and PCa, and the level was also significantly higher than the latter two as well. The PSEP level in PCa was the lowest. The tPSA level in PCa was significantly higher than that in AP and CP, whereas CP had the lowest tPSA level. The fPSA level in CP was lower than that in AP and PCa, but there was no difference between AP and PCa. In the different types of CP, the PSEP level in type II was the highest, which can be 5 times higher than the upper limit of the reference, which may be related to type II inflammation caused by bacterial infection. The tPSA level in type IIIb was the lowest, but the fPSA among the 3 groups showed no difference. The value of the fPSA/tPSA ratio was significantly higher in type IIIb than in type II and type IIIa. Therefore, the types of CP can be distinguished when PSA was combined with PSEP.

The concentration of PSEP in the normal urine of men is extremely low,[5] and reports have shown that the content of PSEP in the urine of men with CP will increase with the increased release of prostatic corpuscles in the reproductive channel due to the release of various chemokines and the permeability changes of prostate duct epithelial cells caused by inflammation progression.[6] In addition, PSEP will also significantly increase when PCa is accompanied by inflammation, although the level will not significantly change compared with the male population without inflammation.[7] Therefore, changes in the level of PSEP can also be observed in the diagnosis of PCa, allowing clinicians to distinguish the disease and provide appropriate treatment.

Conclusion

The combination of PSEP and PSA can be used to discriminate prostatic inflammation from PCa. Further, examination of urine PSEP

TABLE 1. Levels of PSEP, tPSA, fPSA, and fPSA/tPSA in Different Prostate-Related Diseases

	Acute Prostatitis Group (n = 54)	Chronic Prostatitis Group (n = 72)	Prostate Cancer Group (n = 36)
PSEP	2.69 ± 0.34	5.44 ± 0.72[a,b]	0.74 ± 0.31[b]
tPSA	6.47 ± 2.80	3.23 ± 0.56[a,b]	11.42 ± 2.47[b]
fPSA	3.53 ± 1.24	1.04 ± 0.48[a,b]	3.56 ± 1.22
fPSA/t PSA	0.46 ± 0.17	0.33 ± 0.07[b]	0.30 ± 0.06[b]

fPSA, free PSA; PSA, prostate specific antigen; PSEP, prostatic exosomal protein; tPSA, total PSA.
[a]Compared with the prostate cancer group, P < .05.
[b]Compared with the acute prostatitis group, P < .05.

TABLE 2. Levels of PSEP, tPSA, fPSA, and fPSA/tPSA in Different Types of Chronic Prostatitis

	Type II (n = 25)	Type IIIa (n = 31)	Type IIIb (n = 16)
PSEP	6.57 ± 0.99	5.65 ± 0.48[a]	3.26 ± 0.76[a,b]
tPSA	3.26 ± 1.14	3.43 ± 0.84	2.12 ± 0.89[a]
fPSA	1.21 ± 0.05	1.56 ± 0.27	1.32 ± 0.14
fPSA/t PSA	0.39 ± 0.06	0.42 ± 0.09	0.66 ± 0.12[a]

fPSA, free PSA; PSA, prostate-specific antigen; PSEP, prostatic exosomal protein; tPSA, total PSA.
[a]Compared with type II chronic prostatitis, $P < .05$.
[b]Compared with type IIIa chronic prostatitis, $P < .05$.

using PSA as a simple, noninvasive operation provides a method in distinguishing prostate-related diseases,[8,9] which is worthy of clinical application.

Conflict of Interest Disclosure

The authors have nothing to disclose.

REFERENCES

1. Magistro G, Stief CG, Wagenlehner FME. Chronic prostatitis/chronic pelvic pain syndrome. *Der Urologe Ausg A.* 2020;59(6):739–748. doi:10.1007/s00120-020-01226-5.
2. Motamedinia P, Scott AN, Bate KL, et al. Urine exosomes for non-invasive assessment of gene expression and mutations of prostate cancer. *PLoS One.* 2016;11(5):e0154507. doi:10.1371/journal.pone.0154507.
3. Li X, Jiang T, Liu F, et al. Clinical evaluation of urine prostatic exosomal protein in the diagnosis of chronic prostatitis. *Urol Int.* 2018;100(1):112–118.
4. Liang W, Wu Z, Zhang G, et al. A urine-based biomarker for chronic prostatitis/chronic pelvic pain syndrome: a retrospective multi-center study. *Transl Androl Urol.* 2020;9(5):2218–2226. doi:10.21037/tau-20-1268.
5. Yin L, Tang Y, Pan A, et al. The application of IL-10 and TNF-α in expressed prostatic secretions and prostatic exosomal protein in urine in the diagnosis of patients with chronic prostatitis. *Medicine.* 2019;98(33):e16848e16848. doi:10.1097/md.0000000000016848.
6. Tang Y, Pan A, Liu Y, Yin L. The diagnostic value of urine heat shock protein 70 and prostatic exosomal protein in chronic prostatitis. *J Clin Lab Anal.* 2021;35(6):e23778. doi:10.1002/jcla.23778.
7. Kim JH, Hong SK. Clinical utility of current biomarkers for prostate cancer detection. *Investig Clin Urol.* 2021;62(1):1–13. doi:10.4111/icu.20200395.
8. Gu CY, Huang YQ, Han CT, et al. Clinical significance of urine prostatic exosomal protein in the diagnosis of prostate cancer. *Am J Cancer Res.* 2019;9(5):1074–1078.
9. Hatano K, Fujita K. Extracellular vesicles in prostate cancer: a narrative review. *Transl Androl Urol.* 2021;10(4):1890–1907. doi:10.21037/tau-20-1210.

CASE STUDY

Minor Cross-Matching in the Diagnosis of Pneumococcal Hemolytic Uremic Syndrome in an 18-Month-Old Boy

Suman Sudha Routray, MD,[1] Sukanta Tripathy, MD,[1] Palash Das, MD,[2] and Gopal Krushna Ray, MD[1,]*

[1]Department of Transfusion Medicine and Blood Centre and [2]Department of Paediatrics, Kalinga Institute of Medical Sciences, Bhubaneswar, India. *To whom correspondence should be addressed: ray.gopal88@gmail.com.

Keywords: polyagglutination, *Streptococcus pneumoniae*, T-antigen, therapeutic plasma exchange, direct antiglobulin test, rapid immunochromatographic test

Abbreviations: HUS, hemolytic uremic syndrome; TTP, thrombotic thrombocytopenic purpura; DAT, direct antiglobulin test; sp-HUS, HUS induced by *Streptococcus pneumoniae* infections; T-Ag, Thomsen-Friedenreich antigen; PCV-13, 13-valent conjugated pneumococcal vaccine; IH, immunohematological; CRP, C-reactive protein; AST, antimicrobial susceptibility testing; PICU, pediatric ICU; aHUS, atypical hemolytic uremic syndrome; TPE, therapeutic plasma exchange; FFP, fresh frozen plasma; WBDPs, whole blood–derived platelets; ICT, immunochromatographic testing; CAT, column agglutination testing; DIC, disseminated intravascular coagulation; IPD, invasive pneumococcal disease; UIP, universal immunization program; C3, complement 3; ASFA, American Society for Apheresis; IDSA, Infectious Diseases Society of America; ATS, American Thoracic Society; Hb, hemoglobin; TPC, total platelet count; Sr, serum; MAHA, microangiopathic hemolytic anemia; PRBCs, packed RBCs; RDP, random donor platelets; C3, complement 3; ET, endotracheal

Laboratory Medicine 2023;54:215–219; https://doi.org/10.1093/labmed/lmac092

ABSTRACT

In developing nations, limitations in diagnostic facilities act as a barrier for differentiation of hemolytic uremic syndrome (HUS) based on the etiology. A sick-looking 18-month-old boy presented to our hospital in Bhubaneswar, India, with clinical signs and symptoms of left lobar pneumonia, abnormal hematological and renal parameters, no growth in blood culture, a negative direct antiglobulin test (DAT) result, and low complement levels. A rapid deterioration in his clinical condition necessitated intensive care support, blood transfusion, and renal replacement therapy (peritoneal dialysis and hemodialysis). Because his health care team suspected atypical HUS, therapeutic plasma exchange (TPE) was initiated as soon as possible. In the absence of a lectin panel, minor cross-matching confirmed T-antigen exposure. With a diagnosis of HUS induced by *Streptococcus pneumoniae* (sp-HUS), TPE was stopped immediately, and washed blood components were administered. Despite the aforementioned measures, the boy died of HUS on day 20 after presentation. This case emphasized the role of minor cross-matching in the detecting of polyagglutination in resolving the diagnostic dilemma of sp-HUS.

Hemolytic uremic syndrome (HUS) and thrombotic thrombocytopenic purpura (TTP) often present a diagnostic dilemma to clinicians due to the overlapping clinical features of these conditions. The European Paediatric Research Group for HUS has classified HUS arbitrarily based on etiology (class 1) and clinical associations with unknown etiology (class 2).[1] Accurate diagnosis based on etiology is important in developing rational approaches to treatment and prognosis. The presence of thrombotic microangiopathic hemolytic anemia, thrombocytopenia, and acute renal failure is characteristic of HUS. Further evaluation in the form of blood culture, stool culture, chest X-ray, direct antiglobulin test (DAT), and estimation of serum complements factor H and I and C3 level are required for differentiation of HUS based on etiology.

Infection associated with HUS is the major cause of HUS in the pediatric age group, mostly due to verocytotoxin.[1] HUS induced by *Streptococcus pneumoniae* infections (sp-HUS) is a distinctive disorder characterized by Thomsen-Friedenreich antigen (T-Ag) expression and is associated with increased mortality. A report from the United Kingdom[2] has reported a significant decrease in its incidence with the introduction of 13-valent conjugated pneumococcal vaccine (PCV-13) in the infant immunization schedule.

The burden of HUS in India is unclear because of the limited access to diagnostic and therapeutic facilities in that country. A consensus guideline was developed in India for diagnosis and management of HUS in 2019.[3] Herein, we report the role of the immunohematological (IH) workup in evaluating a case of apparent sp-HUS with negative blood culture requiring transfusion support.

Patient History

An 18-month-old boy, born to nonconsanguineous parents, was presented to a local physician with the chief complaints of fever, tachypnea, and cough for the past 6 days. After experiencing no improvement in his symptoms despite the treatment he received, which included oral antibiotics and other supportive measures, the child was referred to our institute. At admission, he was conscious, sick-looking,

and in respiratory distress. Clinical examination revealed pallor and generalized edema with periorbital puffiness. Systemic examination revealed crepitations on the left side of the chest. Abdominal examination showed an enlarged liver, with a liver span of 12 cm.

There was no history of gastroenteritis or similar illness in the recent past, nor any known history of similar illness in the family. After sending the results of relevant investigations, empirically intravenous amoxycillin clavulanic acid, nebulization with levosalbutamol, and other forms of supportive management were started.

Clinical and Laboratory Information

The results of initial investigations on admission showed anemia, thrombocytopenia, the presence of schistocytes in the peripheral blood smear, abnormal renal parameters, and raised levels of C-reactive protein (CRP). There had been no culture report before hospital admission, and no growth was noted in blood culture as assayed in this hospital. Hence, the antimicrobial susceptibility testing (AST) results could not be ascertained. The results of tests for malaria antigen and IgM antibody of scrub typhus were negative. Chest X-ray showed bilateral opacities and white-out appearance of the left lower lobe of the lung. DAT results were negative. Changes in hematological and renal parameters throughout the period of hospitalization are depicted in **FIGURE 1**.

The patient was shifted to the pediatric ICU (PICU) because of deteriorating arterial blood-gas levels and multisystem involvement, with a provisional diagnosis of atypical hemolytic uremic syndrome (aHUS). Subsequent clinical features and the results of clinical management (injected doxycycline, injected piperacillin, and IV tazobactam) during hospitalization are shown in the timeline graph in **FIGURE 2**.

Management of the patient in the PICU included peritoneal dialysis, hemodialysis (dialysis equipment malfunction [tubing block]), therapeutic plasma exchange (TPE) using fresh frozen plasma (FFP) instead of 5% albumin as replacement fluid, injected methyl prednisolone, and transfusion support with 1 unit of RBCs and 2 units of whole-blood–derived platelets (WBDPs). The condition of the toddler deteriorated further as he developed parapneumonic effusion, for which intercostal drainage was required. On day 7 after admission, the patient tested positive for urinary C-polysaccharide antigen of *Streptococcus pneumoniae*, via rapid immunochromatographic testing (ICT). This finding, along with the aforementioned features of HUS, raised the suspicion of sp-HUS. As a result, an IH workup was performed.

FIGURE 1. Line graph showing hematological (A) and renal (B) parameters for the patient, an 18-month-old boy, during the hospitalization period. Hb, hemoglobin; Sr, serum; TPC, total platelet count.

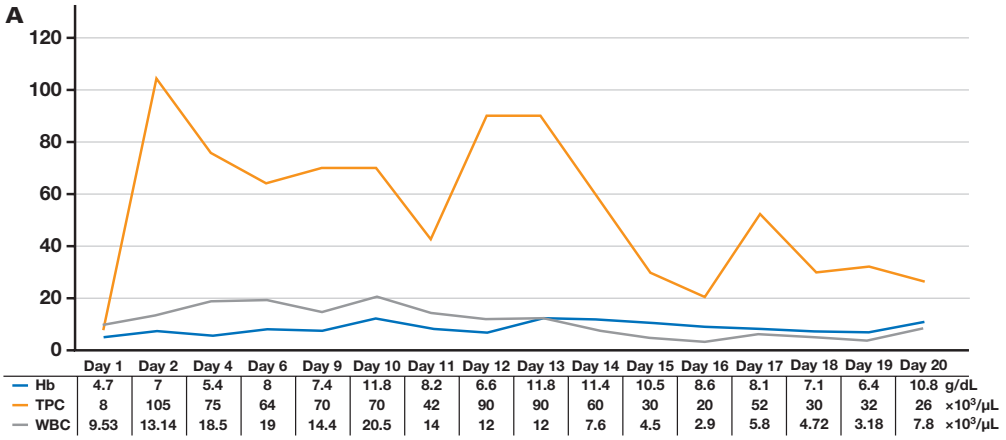

	Day 1	Day 2	Day 4	Day 6	Day 9	Day 10	Day 11	Day 12	Day 13	Day 14	Day 15	Day 16	Day 17	Day 18	Day 19	Day 20	
Hb	4.7	7	5.4	8	7.4	11.8	8.2	6.6	11.8	11.4	10.5	8.6	8.1	7.1	6.4	10.8	g/dL
TPC	8	105	75	64	70	70	42	90	90	60	30	20	52	30	32	26	$\times 10^3/\mu L$
WBC	9.53	13.14	18.5	19	14.4	20.5	14	12	12	7.6	4.5	2.9	5.8	4.72	3.18	7.8	$\times 10^3/\mu L$

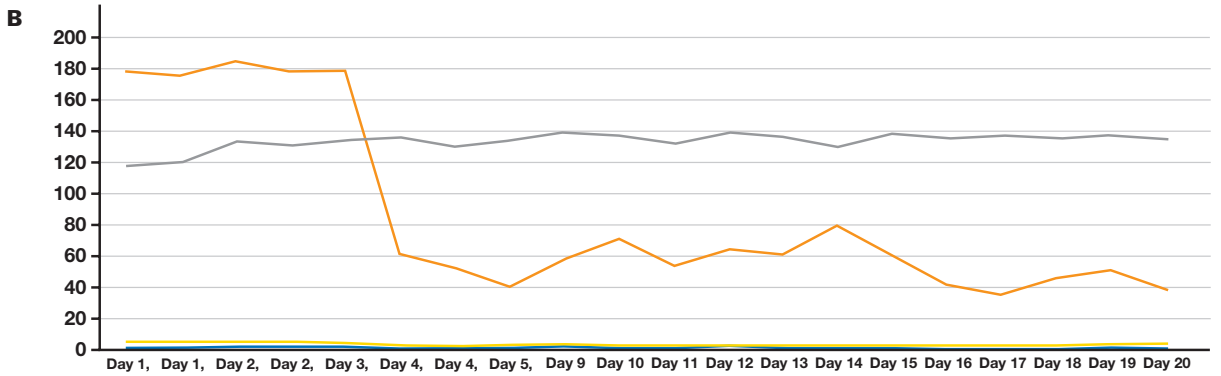

	Day 1, 6 AM	Day 1, 6 PM	Day 2, 6 AM	Day 2, 6 PM	Day 3, 6 AM	Day 4, 6 AM	Day 4, 6 PM	Day 5, 6 AM	Day 9	Day 10	Day 11	Day 12	Day 13	Day 14	Day 15	Day 16	Day 17	Day 18	Day 19	Day 20	
Sr creatinine	1.65	1.82	2.23	2	2	1.07	1.25	1.34	2	1.93	1.4	2.06	1.66	1.9	1.42	1.11	1.12	1.21	1.42	1.12	mg/dL
Sr urea	178.3	176	184.3	178	179	61	53	40.7	57.4	71	54	64.2	61	80	61	42	36	46	51	39	mg/dL
Na+	118	120	133	131	134	136	130	134	139	137	132	139	137	130	138	136	137	136	137	135	mmol/L
K+	5.5	5.7	5.5	5.3	4.5	3.4	2.6	3.1	3.6	3.4	3	3.4	3.2	2.9	3.2	3.2	3.5	3.5	3.9	4	mmol/L

FIGURE 2. Timeline of the condition of our patient, an 18-month-old boy, during the hospitalization period. aHUS, atypical hemolytic uremic syndrome; C3, complement 3; DAT, direct antiglobulin testing; DIC, disseminated intravascular coagulation; ET, endotracheal; Hb, hemoglobin; MAHA, microangiopathic hemolytic anemia; PICU, pediatric ICU; PRBCs, packed RBCs; RDP, random donor platelets; sp-HUS, HUS induced by *Streptococcus pneumoniae*; TPC, total platelet count; T-Ag, Thomsen-Friedenreich antigen; ?, suspected.

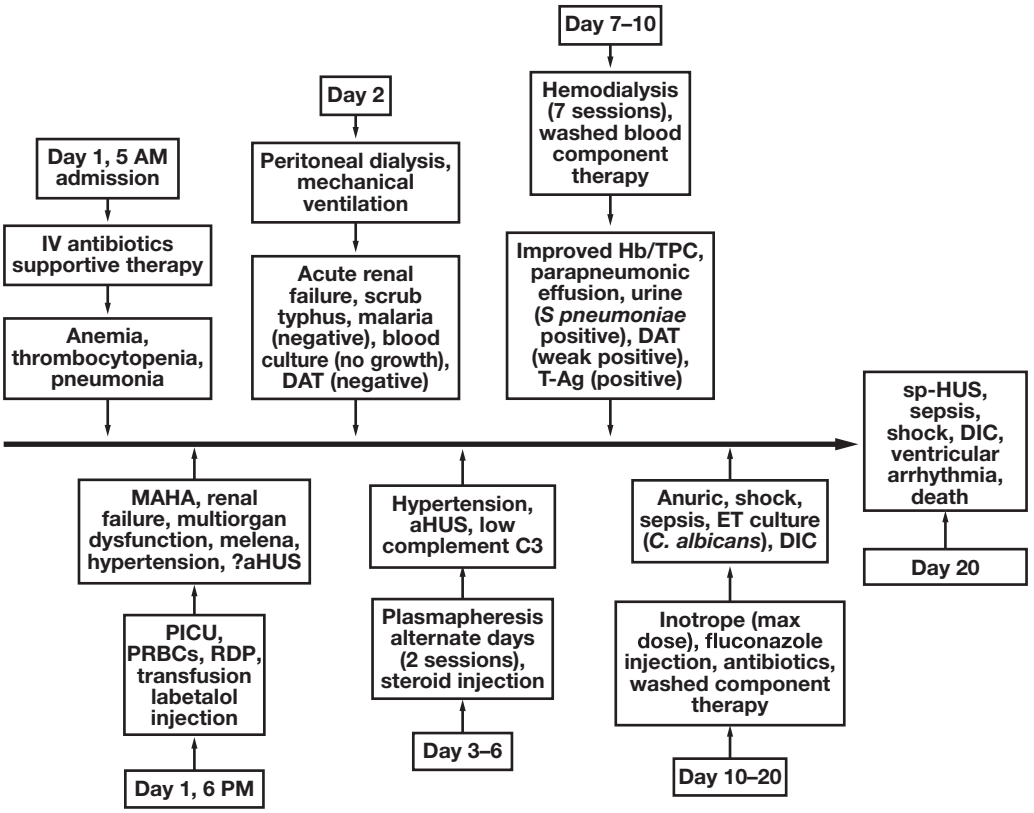

IH Workup and Transfusion Support

Blood grouping was performed by column agglutination testing (CAT) using a gel card; the blood type of the patient was determined to be A-positive, without any mismatch between forward and reverse grouping. A weak positive result was found via DAT. Monospecific DAT using IgG and C3d antisera was performed via conventional test tube technique; the results were negative. We perceived no evidence of auto-/allo-antibodies.

The RBCs of the patient were cross-matched with plasma from the A and AB groups from adult and umbilical cord blood specimens at room temperature. The presence of agglutination with adult serum and absence of agglutination with the cord blood specimen and with autoantibody serum suggested the presence of polyagglutination (T-Ag activation), as shown in **FIGURE 3**. The RBCs of the patient were tested against the available lectins (*Dolichos biflorus* and *Ulex europaeus*) and yielded a positive (4+) reaction. A positive DAT result, along with the presence of polyagglutination and other features, was suggestive of sp-HUS. Washed blood component therapy was advised to remove the plasma proteins because of polyagglutination.

The repeat sepsis screening result was positive. Despite all supportive measures, the toddler developed disseminated intravascular coagulation (DIC) and shock, and he died of sp-HUS on day 20 after admission.

FIGURE 3. Findings from immunohematological workup for polyagglutination. DAT, direct antiglobulin test; T-Ag, Thomsen-Friedenreich antigen.

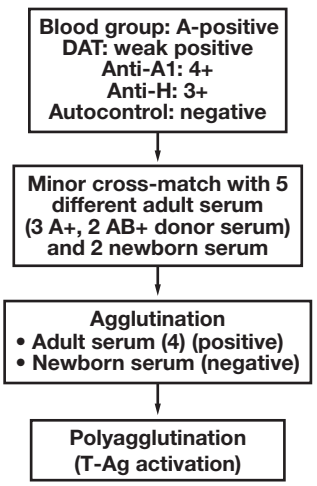

Discussion

sp-HUS is a rare disease and remains an underdiagnosed complication of invasive pneumococcal disease (IPD). Although more than 200 sp-HUS cases have been reported in the literature, diagnosis of this central complication remains challenging.[2,4] sp-HUS has been classified into the following categories: definite, probable, and possible.[4] In this case, the presence of HUS, DIC, invasive *S pneumoniae* infection, and T-Ag activation puts the diagnosis of sp-HUS into the probable category. The key pathogenesis occurs due to the exposure of cryptic

T-Ag present on the erythrocytes, platelets, and renal endothelium by the neuraminidase-producing *S pneumoniae* serotypes.[5] A heavy bacterial load leads to *S pneumoniae* infiltration of the lung, pleural space, or subarachnoid space, with the development of sp-HUS. T-Ag is also present on the hepatocytes, which leads to transient hepatic dysfunction.

Definite diagnosis of IPD is made by isolating the organism from blood culture. The rate of culture positivity is approximately 3% to 8% in adults and even lower in children. Many factors are responsible for the low positivity rate, including previous administration of antibiotics; intermittent bloodstream invasion by pneumococcus; and the release of autolysins leading to cell death, which make bacterial growth difficult.[6] Previous antimicrobial therapy could have been the cause of culture-negative results in our patient, thus delaying the diagnosis of IPD. Rapid ICT, developed to detect the C-polysaccharide cell wall antigen in the urine of patients with IPD, has revived interest among scientists in Ag-detection methods for an early diagnosis with good sensitivity and specificity.[7]

Per recent guidelines, confirmation of T-Ag activation has been included in the definite diagnosis of sp-HUS. However, approximately 50% of the children with IPD who do not have HUS were found to have T-Ag, but T-Ag is not detected in all children with HUS.[8] It is suggested that DAT, polyagglutination testing, and peanut lectin agglutination assay can identify T-Ag.[4,5]

DAT is simple, and the positive DAT result yielded in our investigation suggests complement-mediated sensitization of RBCs (T-Ag) by the IgM type of anti-T antibody. However, DAT positivity is not specific for sp-HUS, and the rate of positivity varies from 60% to 90% among the sp-HUS cases.[4] In our case, DAT was negative on the day of admission but came to be weakly positive on day 7, as discovered during the IH workup.

Although guidelines recommend a peanut lectin agglutination assay for definite diagnosis, its unavailability causes undue delay in diagnosis. Moreover, in-house preparation of lectin is time-consuming, labor-intensive, and has the disadvantage of a lack of standardization. In the absence of peanut lectin agglutination assay, the use of polyclonal antisera (human serum) or minor cross-matching could simply detect T-Ag activation.[9] Minor cross-matching with adult human serum and cord serum could have helped us to derive an earlier diagnosis and could have prevented us from transfusing unwashed blood components and undertaking plasma infusion during the plasmapheresis, both of which might have worsened the disease progression.

The CDC recommends PCV13 for all infants as a series of 4 doses given at ages 2 months, 4 months, 6 months, and 12 through 15 months, to reduce invasive pneumococcal infections and other pneumococcal infections worldwide.[2] Although pneumonia accounts for a major proportion of mortality in children younger than 5 years in India (17.1%), only the vaccine that protects against pneumonia due to *Haemophilus influenzae* type B is covered by the universal immunization program (UIP). Conjugated pneumococcal vaccine is available only in 5 states per the UIP and is optional in the other 23 states, including ours. The high cost of this vaccine also acts as a barrier to low-income families. In this case, our patient was unvaccinated, making him prone to IPD.

In this case, low complement (C3) level and no growth in blood culture pointed towards atypical HUS. TPE was initiated at the earliest possible time with FFP as replacement fluid instead of albumin because of cost constraints. sp-HUS can also present with low complement levels (C3 and/or C4) due to complement dysregulation.[10]

In our patient, it is unclear whether a genetic defect in the complement system of the host or an acquired complement defect secondary to pneumococcal infection contributed to the development of sp-HUS. As soon as the diagnosis of sp-HUS was made, plasmapheresis was deferred due to insufficient evidence for this form of treatment, which is labeled as category III per the American Society for Apheresis (ASFA) guidelines.[11] Washed blood components were advised, to avoid further anti-T–mediated hemolysis.[4] Some reports, such as one by Spinale et al,[5] suggest a beneficial effect with TPE to reduce the anti-T antibody and neuraminidase with albumin or low titer anti-T antibody–containing plasma as the replacement fluid. A transient improvement in the renal and hematological parameters of our patient was observed after initiation of TPE. The role of TPE in sp-HUS could not be ascertained due to the lack of randomized control trials and merits further evaluation.

Patients with sp-HUS are very sick at presentation and require treatment in the PICU for a median duration of 19 days; half of all patients with this condition require mechanical ventilation for a median duration of 6.6 days. Two-thirds of patients with sp-HUS undergo invasive procedures such as tube insertion into the chest, lobectomy/pneumonectomy, or thoracoscopic surgical procedures. More than half of the patients with sp-HUS undergo renal replacement therapy and washed component therapy, to treat their greater degree and longer duration (since presentation) of oligoanuria, anemia, and thrombocytopenia.[12] Our patient had early PICU admission, was supported with renal replacement therapy and mechanical ventilation, and required a chest tube placement for the duration of his hospital stay.

A high mortality rate is observed in sp-HUS complicated with pneumococcal meningitis, rather than with isolated pneumonia.[4] Advancements in critical care and early diagnosis have resulted in a decline in the mortality rate. Nonlytic antimicrobial therapy (quinolones and macrolides) in patients with IPD is recommended by the Infectious Diseases Society of America (IDSA) and the American Thoracic Society (ATS), although occasionally, it is used in combination with lytic regimens (such as β-lactamase). Multidrug resistance in half of the isolates of patients with IPD, and the presence of DIC along with HUS, makes the disease progression and treatment more complicated and increases the mortality risk. In our patient, delayed diagnosis of sp-HUS and development of DIC could have been the reasons for his death.

IH workup employing minor cross-matching in case of a diagnostic dilemma helps to detect polyagglutination and can aid in the differentiation of HUS based on etiology. Universal vaccination when feasible and early diagnosis can result in better disease management, with avoidance of FFP and administration of washed blood components to prevent anti-T antibody-mediated complications of HUS.

REFERENCES

1. Besbas N, Karpman D, Landau N, et al. A classification of hemolytic uremic syndrome and thrombotic thrombocytopenic purpura and related disorders. *Kidney Int.* 2006;70(3):423–431.
2. Makwana A, Sheppard C, Fry NK, Ladhani SN. Pneumococcal-related hemolytic uremic syndrome in the United Kingdom National Surveillance, 2006–2016. *Pediatr Infect Dis J.* 2019;38(10):e254–e259.
3. Bagga A, Khandelwal P, Mishra K, et al. Hemolytic uremic syndrome in a developing country: consensus guidelines. *Pediatr Nephrol.* 2019;34(8):1465–1482.

4. Agarwal HS, Latifi SQ. *Streptococcus pneumoniae*-associated hemolytic uremic syndrome in the era of pneumococcal vaccine. *Pathogens.* 2021;10(6):727.
5. Spinale JM, Ruebner RL, Kaplan BS, Copelovitch L. Update on *Streptococcus pneumoniae* associated hemolytic uremic syndrome. *Curr Opin Pediatr.* 2013;25(2):203–208.
6. Petti CA, Woods CW, Reller LB. *Streptococcus pneumoniae* antigen test using positive blood culture bottles as an alternative method to diagnose pneumococcal bacteremia. *J Clin Microbiol.* 2005;43(5):2510–2512.
7. Briones ML, Blanquer J, Ferrando D, Blasco ML, Gimeno C, Marín J. Assessment of analysis of urinary pneumococcal antigen by immunochromatography for etiologic diagnosis of community-acquired pneumonia in adults. *Clin Vaccine Immunol*. 2006;13(10):1092–1097.
8. Huang DT-N, Chi H, Lee H-C, Chiu N-C, Huang F-Y. T-antigen activation for prediction of pneumococcus-induced hemolytic uremic syndrome and hemolytic anemia. *Pediatr Infect Dis J.* 2006;25(7):608–610.
9. Ray GK, Mukherjee S, Routray SS, Prakash S. Tn red cell polyagglutination in a healthy blood donor: a case report. *Transfus Apher Sci.* 2021;60(1):103013.
10. Gómez Delgado I, Corvillo F, Nozal P, et al. Complement genetic variants and FH desialylation in *S. pneumoniae*-haemolytic uraemic syndrome. *Front Immunol.* 2021;12:641656.
11. Padmanabhan A, Connelly-Smith L, Aqui N, et al. Guidelines on the Use of Therapeutic Apheresis in Clinical Practice – Evidence-Based Approach from the Writing Committee of the American Society for Apheresis: The Eighth Special Issue. *J Clin Apher*. 2019;34(3):171–354.
12. Banerjee R, Hersh AL, Newland J, et al. *Streptococcus pneumoniae*-associated hemolytic uremic syndrome among children in North America. *Pediatr Infect Dis J.* 2011;30(9):736–739.

Reviewer List

The *Laboratory Medicine* staff would like to extend a warm thank you to our 2022 ad hoc reviewers. We appreciate your time and dedication to the journal.

N. S. Abbai
Omneya AbdelKarem
Ahmed Abdel-Razik
Laila Abdel-Wareth
Gyorgy Abel
Stephan W. Aberle
Emad S. Abood
Roshini Abraham
Brooj Abro
Ramzia Abu Hamad
Bodhraj Acharya
Sergio A. Acuna
Paul C. Adams
Tobi Adelaja
Cigdem Usul Afsar
Bernice Agana
Ritu Aggarwal
James Aguanno
Niyaz Ahmed
Mohammad Akbari
Ayse Akbas
Aysegul Aksan
Kalichamy Alagarasu
Mohammad Alam
Nazire Albayrak
Mohammed Al-Beltagi
Kevin Alby
Laith N. Al-Eitan
Evan Alexander
Mahesheema Ali
Mahmoud Ali
Youssif Ali
Murat Alisik
Gunay Aliyeva
David Alland
Karel Allegaert
John Allen
Kathleen Allen
Jenifer E. Allsworth
Yaser Alnaam
Caroline Alquist
Bahaudin Al-Shawwa
Fatemeh Amiri
Konstantinos Anagnostopoulos
Benjamin Andress
Brooke Andrews
John Anetor
Laura Anfossi
Donna P. Ankerst
Marianna Antonelou
Sophie Arbefeville
Luca Arcaini
Robert Arena
Emiliano Aroasio
Juwairiya Arshi
Saja Asakrah
Alice Assinger
Eray Atalay
John J. Atherton
Frederic Auvray
Hassan Azzazy
Ghufran Babar
Mukhtiar Baig
Matthew Baker
Steven Baker
Adriana Balduzzi
Kayode Balogun
Richard Baltaro
Monisha Banerjee
Ritu Banerjee
Daniel Bankson
Liming Bao
Mustafa Barbhuiya
Yousif Barzani
Luisa Barzon
Davood Bashash
Ingrid V. Bassett
Haim H. Bau
Linnea Baudhuin
Nikola Baumann
Isabel Bazan
Anette Beck-Sickenger
Tamer Bego
Rasheedunnisa Begum
Kristina Behan
Erdal Benli
Andrea Bennett
Isabela Judith Martins Bensenor
Mary Berg
Andreas Bergthaler
Jess Francisco Bermejo-Martn
Gaetano Bernardi
Alexa M. E. Bersenas
Stefano Bertolini
Monica Bhatia
Jeremy Biggs
Paul Billoir
Julie E. Bines
Zuleyha Bingol
Rob S. van Binnendijk
Marcelo De Carvalho Bittencourt
Stefan Bittner
Martin Bitzan
Giulia Bivona
Marc Blondon
Yair Blumenfeld
Daniel M. Blumenthal
Emily Blyth
C-Thomas Bock
Francesco Bonfante
Maria R. Bonsignore
Anwar Borai
Eduardo F. Borba
P Borsky
David Bosler
Brendan Boyce
Ibrahim Bozgeyik
Cosimo Bruni
Janetta Bryksin
Dustin Bunch
Eileen Burd
Carey-Ann D. Burnham
Joshua Buse
Sheraz Butt
Alexander J. Butwick
Ritchard G. Cable
Boris Calderon
George Calin
Neil Came
Sean Campbell
Adrian Canizalez-Roman
Simone Canovi

Jing Cao
Liyun Cao
Zheng Cao
Zhimin Cao
David Carpentieri
Anne Carroll
Marcia Carvalho
Stefano Castellana
Brian Castillo
Jorge J. Castillo
Gian Caviglia
Ferruccio Ceriotti
Lynette Chakkaphak
Elham Chamani
Allison Chambliss
Jae Hyuck Chang
Chung-Hwan Chen
Hsiang-Cheng Chen
Mingyi Chen
Chia Cheng
Zhikai Chi
Asako Chiba
Charles Y. Chiu
Anil Kiran Chokkalla
Jacky Chow
O. D. Christophe
Soie Chung
Marcello Ciaccio
Michal Ciborowski
Frederik Banch Clausen
Felix Claverie-Martin
Steven Coca
Claudia Cohn
Cristoforo Comi
Hui Cong
Mark Cooper
Sandra Cooper
Luca Coppeta
Victor M. Corman
Marianna Cortese
Aloyce Costantine
Jesse Cox
Daisy Crispim
Elliott Crouser
Elisa Cupolillo
Brian R Curtis
Martina Curto
M. Cushman
Albert Czaja
Bakul Dalal
Fram Dalal
Tine Dalby
Siddhartha Dalvi
Ann K. Daly
Alfredo Damasceno
Maryam Daneshpazhooh
Bereczki Dániel
Hisham Darwish
Madhusudan Das
Riku Das
Sanchita Das
Shatavisha Dasgupta
Stella Daskalopoulou
Masja De Haas
Walter Demczuk
Barbara A. Demeneix
Zhaoqun Deng
Susan Dent
Sridevi Devaraj
Jane Dickerson
Dennis Dietzen
Anand Dighe
Huiguo Ding
Monica Dinu
Kurosh Djafarian
Kamal Djenouhat
Michelle Dolan
Fei Dong
Nebiye Yentur Doni
Susan E. Dorman
Todd Bradley
Luciano F. Drager
Paul Drain
Guochen Duan
Thomas Durant
Walter Dzik
Wisdom Ebong
Cumali Efe
Wael Elayat
Mahmoud El-Bendary
Paula C. L. Elias
Vincent Escuyer
Lise Estcourt
James Faix
Soudabeh Fallah
Deanna Fang
Silvia Fare
Evan Farkash
Christopher Farnsworth
Maryam Fathi
Francesco Fazio
Yuri Fedoriw
Yong Feng
Angela Ferguson
Giovanna Ferraioli
Dolores Figueroa
Eric Fitts
Maribeth Flaws
Richard Francis
Jun Fu
Yulong Fu
Craig Fuller
Jenny Alfaro García
Bahram Pourghassem Gargari
Emily Garnett
Wendy Garrett
José Antonio Garrote-Adrados
Charlotte A. Gaydos
Eric Gehrie
Nina T. Gentile
Jonathan Genzen
Glenn George
Zofia Gerlicz-Kowalczuk
Kanjaksha Ghosh
Brain Gilfix
Alessandra Giuliani
Todd Glenski
Carolina Cavalieri Gomes
Manuela E. Gomes
Anne Goodeve
Andrew Goodwin
Cheryl Goss
Marcin Grabowicz
Melanie L. Graham
Stewart E. Graham
Jonathan Grant
Michele Grant
S Gray
Siri Atma W. Greeley
Dina Greene
Graeme Greenfield
John E. Greenlee
David Grenache
David Grier
Damien Gruson
Luke E. Grzeskowiak
Bing Gu
Paola Guglielmelli
Xianyong Gui
Canan Gunduz
Junming Guo
Shicheng Guo
Jones Gyamfi
Hoda Hagrass
Won-Ho Hahn
Young Hahn
Diane Halstead
Mouhamed Halwani
Kimberly Hanson
Timm Harder
Justin Hardick
Mehmet Harman
Amanda Harrington
Neil Harris
Thomas S. Harrison

Cornelis Harteveld
Mandana Hasanzad
Marwa Hassan
Jane Hata
Pierre Hausfater
Chuanglong He
Rong He
Alicia K. Heath
Robert A. Hegele
Markus H. Heim
Debora Heller
Javad Heshmati
John Hess
Allan Hildesheim
Pravin Hissaria
Eveline Hitti
Clement KM Ho
Vanessa Hoang
Bastian Hoechst
Noah Hoffman
Johannes Hoffmann
Daniel Holmes
Sang-Bum Hong
Sen-Kuang Hou
Lydia Howell
Rongrong Huang
Maite Huarte
Anke Huckriede
Virginia Hughes
Laura K. Hummers
Mina Hur
Mihaela Iancu
Giacchin Iannolo
Toshiaki Iba
Kiyoshi Ichihara
Fumiaki Imamura
Akihiro Inazu
Cesare Indiveri
Tina Ipe
Osamu Ishibashi
Joannes FM Jacobs
Musharraf Jelani
Mark T. Jennings
Selma Maria Bezerra Jeronimo
Ishwarlal Jialal
Yan-Fang Jiang
Zifeng Jiang
Zhicheng Jin
Jian Jing
Nathan Johnson
Graham Jones
Patricia Jones
Ajith Joseph
Parag Joshi
Carmen Julius
Sevgi Kalayoglu-Besisik
Rashmi Kanagal-Shamanna
Stefan C. Kane
Jia-Horng Kao
Mehmet Karakus
Amy Karger
Subhradip Karmakar
Irena Kasacka
Dara Kass
Adetola Kassim
Sukhbir Kaur
Peter Kavsak
Roop Kaw
Miwa Kawanaka
Alexander Kay
Deborah Keil
Rhett Ketterling
Ali Khademhossieni
Nisreen Khambati
Akram Kharroubi
Hasan Khudhair
Chang-Seok Ki
Laura Kidd
Frederick Kiechle
Jan T. Kielstein
Annette Kim
Won Kim
Hiroshi Kimura
Thomas King
Dianne Kirk
Joseph E. Kiss
Gregory Kline
Ivana Klun
Joel Kniep
Yukio Kobayashi
Fatma Emel Kocak
Ravindra Kolhe
Adam Komorowski
Benjamin Korman
Steven J. Korzeniewski
Paulo G. Kotze
Peter Kouides
Ioannis E. Koutroubakis
Aleksander Krag
Mauricio Krause
Manisha Kumar
Sachin Kumar
Samantha Kumarage
Kristine Kuus
Paul A. Kyrle
Sarrah Lahorewala
Pietro Lampertico
Stephen E. Langabeer
Nicholas Larkey
Avani Latchireddi
Frank Leebeek
Christopher Lehman
Julia Lehman
Natalia Emerim Lemos
Antonio M Lerario
Emilio Letang
Edward Leung
Wai Keung Leung
Van Leung-Pineda
Jerrold Levy
Deborah A. Lewinsohn
Paul Lewis
Jian Li
Ke Li
Xia Li
Carmen Lima
Jin Lin
Yuh-Feng Lin
Mark Little
Christine Litwin
Bao Liu
Bin Liu
Chen-Hua Liu
Jingping Liu
Sanxiong Liu
Shan Liu
John Loannidis
Rosa Lombardi
Amedeo Lonardo
S. Wesley Long
James D. Lord
Andrea Hsiu Ling Low
Diego Lucero
Ralf J. Ludwig
Gifford Lum
Ruben Luo
Fabrizio Luppi
Patricia Maguire
Lisa Mamone
Arduino Mangoni
Karen Mann
Shemoon Marleen
Marisa Marques
Theodore K. Marras
Francis Martin
Constantino Martinez
Annalaura Mastrangelo
Celestina Mazzotta
Karissa McCall-Culbreath
Christopher McCudden
Christopher A. Mecoli
Jeffrey Meeusen
Pierluigi Meroni
Ryan Metcalf
Ozgur Mete

Malgorzata Michalska-Jakubus
Wolfgang Miesbach
Arianna Miglio
Paola Migliorini
Douglas Miller
Ranjana Minz
Kamran Mirza
Jenny Mjosberg
Kristin Moberg
Nathan Montgomery
M.-C. Morel-Kopp
Christian Moro
Francesca Moro
Karen Moser
Seyedreza Mousavi
M. R. Mozafari
Barbara Mroczko
Anupam Mukherjee
Banibrata Mukhopadhyay
Omar Munoz
Kazunori Murata
Caitlin N. Murphy
Reem Mustafa
Alagarraju Muthukumar
Anita Nadkarni
Michael Nagler
Mahdi Najafi
Elizabeth Nalintya
Anna Namuganga
Muhammad Nawaz
Heather Nelson
James New
Olivier Neyrolles
Ferdinando Nicoletti
Slav Ninkovic
Lenka Novakova
David Novis
Kandai Nozu
Hitoshi Okada
Anthony Okorodudu
Claudia P. Oliveira
Catherine Omosule
Mohamed Omran
Sarah Ondrejka
Michal Ordak
S. R. Ostrowski
Eric Oswald
Julie J. Paik
Kyoungjune Pak
Octavia Palmer
Doreen Palsgrove
Preeti Pancholi
Aditya K. Panda
Suchitra Pandey
Vrajesh Pandya
Vivek Pant
Hyung-Doo Park
Kyong Park
Sung-Gyoo Park
Giustino Parruti
Geraldo A. Passos
Arvind H. Patel
Sumit Patel
Janton Paulman
Vera Paulson
Can Peng
Yaguang Peng
Jeffrey Petersen
Jess Peterson
Jonathan Pham
Tho Pham
Michael Phelan
Christina Pierre
B. Pilmis
Fred Plapp
Marija Pljesa-Ercegovac
Krizia Pocino
Christopher R. Polage
Polina Popova
Sakorn Pornprasert
Mohammad Reza Pourmand
Andrea Prinzi
Bobbi Pritt
Ger J. M. Pruijn
Rivak Punchoo
Maritza Puray-Chavez
Amy Pyle-Eilola
Hongbo Qi
Chao Qiu
Geetha Raghuveer
Claude A. Ragle
Christian Ramakers
Veerabathiran Ramakrishnan
Rema Rao
Farideh Razi
Andreas Recke
Rekha Reddy
Melissa Reeves
Alan Remaley
Jyothi Rengarajan
Koert Ritmeijer
John Roback
J. Robert
Karina Rodriguez-Capote
Gabriele Roehrig
Jorge Rojas-Serrano
Gustavo Romero
Silvio Roncella
Mikael Roussel
Dipnarayan Saha
Takayuki Saitoh
Hany Sakr
Eric Salazar
Max Salfinger
Carlos Salomon
Aga Syed Sameer
Sandra Sánchez Barbosa
Billy Sánchez-Jacinto
Ramin Saravani
Jinous Saremian
Gulbanu Sarsenbayeva
Emilia Inoue Sato
Shuzo Sato
Natasha Savage
Emin Savik
Jonathan Savitz
Enrico Scala
Kristian Schafernak
Janna Schill
Dustin Schlawin
Robert Schmidt
Tina Schmidt
Markus Schmugge
Frank Schneider
Kathryn Schnippel
Henk Schonewille
Jacques Schrenzel
Casey Schroeder
Audrey Schuetz
Wilhelm Schwaeble
Isolde SeidenLong
Figen Abatay Sel
Lisa Senzel
Damilola Seyi-Amole
Reham M. Shaat
Zahra Shajani-Yi
Jitender Sharma
Aditi Shastri
Lo Sheng-Ying
Yusuf Othman Sheriff
Qiuying Shi
Muhammad J. A. Shiddiky
David Shiembob
Joel Shilling
Kazuyuki Shimada
Joshua Shirley
James Sikora
Tatjana Simic
Gurmukh Singh
Rance Siniard
Damian Skrypnik
Patricia Slev
Carolijn Smids
James Snyder
Craig Soderquist

Una Orvim Solvik
Snehal Sonawane
Jukun Song
Cynthia So-Osman
Pinar Soysal
Jerry Squires
Pooja Srivastava
Sucheta Srivastava
Francesco Staffieri
Kyle Staller
Daniel Starczynowski
Anne Stavelin
Ewa Stepien
Douglas Stickle
Goran Stimac
Mirjana Stojkovic
Jan Styczynski
Brenda Suh-Lailam
Harold C Sullivan
Jon Sussex
Raoul Sutter
Rei Suzuki
Erica Swenson
Tom Syer
Anna Szpakowicz
Yoshitaka Takuma
Marilina Tampoia
Giovanni Targher
Yohei Tateishi
Safaa Tayel
Seyithan Taysı
Anne Tebo
Mark W. Tenforde
Matthew J. Thoendel
Richard Thomson
Philipp J. Thurner
Funda Tihminlioglu
Sojit Tomo
Patrizia Tosi
Valerie Trapp-Stamborski
Giorgio Treglia
Hung-Wen Tsai
Jia-Huei Tsai
Alexandra Tsirogianni
Kenneth L. Tyler
Eric Ubil
F. Uhel
Turgay Ulas
Takeji Umemura
Melissa Upton
Hiroshi Ureshino
Eloisa Urrechaga
Muhammad Usman
Amena Usmani
Jamuna Vadivelu
Bijay Vaidya
Farzam Vaziri
Fabien B. Vincent
Stefanie Vincken
Mrigender Virk
Miguel Viveiros
Moiz Vora
Mislav Vrsalovic
Emmanuel B. Walter
Guiqiang Wang
Jun Wang
Pingyu Wang
Zhiqianq Wang
Arjumand Warsy
Miguel Waterhouse
Rafal Watrowski
Jun Wei
Christian Wejse
Mike Wells
Mark Wener
Zhihong Weng
Lars Westblade
Astrid M. Westendorf
Gillian A. Whalley
L. Whitby
Carilyn Wieland
Joesph Wiencek
Diana Wilkins
Lance Williams, III
Lawrence Williams
Margaret Williams
Maria Alice Willrich
Terra Wineman
William Winter
Aneta Wojnicz
Chun-Ming Wong
Ka-Leung Wong
Martin Wong
Jennifer Woo
Malgorzata Wrzosek
Dongling Wu
Jindao Wu
Bing Xia
Jun Xia
Lei Xu
Xinjie Xu
hideyuki Yamawaki
Yun Yan
Noriyuki Yanagida
Oscar Yanes
Marianne Yee
Xin Yi
Zhou Yong
Kumiko Yoshimatsu
Hai-Sheng You
Brittany Young
Beiwei Yu
Di Yu
P Yuen
Liu Yuhan
Monika Zajkowska
Nicole Zantek
Hong-Tao Zhang
Linsheng Zhang
Litu Zhang
Qingjiong Zhang
Victoria Zhang
Wenhao Zhang
Yanzhong Zhang
Ying E. Zhang
Yue Zhang
Zhen Zhao
Jie Zheng
Sean L. Zheng
Hebing Zhou
Arthur Zieske
Polona Zigon
A. Zoff
H. Zou

2023;54;220–224 | https://doi.org/10.1093/labmed/lmad008

SCIENCE

Combined Diagnosis of SARS-CoV-2: Rapid Antigen Detection as an Adjunct to Nucleic Acid Detection

Xuewen Li, MD,[1] Yiting Wang, MD,[1] Junqi Pan, BS,[2] Jiancheng Xu, PhD,[1] Qi Zhou, PhD[3,]*

[1]Department of Laboratory Medicine, First Hospital of Jilin University, Changchun, China, [2]Bachelor of Biomedicine, University of Melbourne, Melbourne, Victoria, Australia, [3]Department of Pediatrics, First Hospital of Jilin University, Changchun, China.*To whom correspondence should be addressed. zhou_qi@jlu.edu.cn

Key words: RT-PCR, COVID-19, Lateral flow immunoassay, Early screening, Sensitivity

Abbreviations: RT-PCR, reverse transcriptase–polymerase chain reaction; RAD, rapid antigen detection; WHO, World Health Organization; NAAT, nucleic acid amplification test; ORFs, open reading frames, S, spike, E, envelope, N, nucleocapsid; Ct, cycle threshold; POCT, point-of-care testing; LFIA, lateral flow immunoassay, ECLIA, electrochemiluminescence immunoassay, CLIA, chemiluminescence immunoassay, CLEIA, chemiluminescence enzyme immunoassay, ELISA, enzyme-linked immunosorbent assay.

Laboratory Medicine 2023;54:e37–e43; https://doi.org/10.1093/labmed/lmac089

ABSTRACT

Coronavirus disease 2019 is a serious threat to human life, and early diagnosis and screening can help control the COVID-19 pandemic. The high sensitivity of reverse transcriptase–polymerase chain reaction (RT-PCR) assay is the gold standard for the diagnosis of COVID-19, but there are still some false-negative results. Rapid antigen detection (RAD) is recommended by the World Health Organization (WHO) as a screening method for COVID-19. This review analyzed the characteristics of RDT and found that although the overall sensitivity of RAD was not as high as that of RT-PCR, but RAD was more sensitive in COVID-19 patients within 5 days of the onset of symptoms and in COVID-19 patients with Ct ≤ 25. Therefore, RAD can be used as an adjunct to RT-PCR for screening patients with early COVID-19. Finally, this review provides a combined diagnostic protocol for RAD and nucleic acid testing with the aim of providing a feasible approach for COVID-19 screening.

As of March 6, 2022, more than 433 million confirmed cases and more than 5.9 million deaths have been reported worldwide for COVID-19 caused by SARS-CoV-2.[1] The spread of COVID-19 can be effectively controlled by extensive screening, close contact tracing, and isolation of infected individuals. Currently, the nucleic acid amplification test (NAAT) is still the gold standard for COVID-19 diagnosis, and RT-PCR is mostly used[2]; however, NAAT has some disadvantages, such as strict testing environment, high personnel and technical requirements, expensive instruments and reagents, and long testing time, etc. Moreover, NAAT has false negatives and false positives, which may lead to a certain probability of wrong and missed tests. The World Health Organization (WHO) and some countries have issued guidelines for the use of rapid antigen detection (RAD).[3–5] The RAD is relatively simple and inexpensive to perform, can be performed without trained specialists or specialized instruments, and can report and interpret results in less than 30 minutes. However, RAD also has shortcomings, such as lower sensitivity. Therefore, either method alone cannot simultaneously maximize the accuracy or efficiency or minimize the cost of SARS-CoV-2 detection. The RAD, if used as an adjunct to COVID-19 diagnosis, will contribute to the accurate diagnosis of COVID-19 in combination with NAAT methods and play a crucial role in the control of the COVID-19 pandemic. This review analyzes the characteristics of RAD and RT-PCR testing and provides a combined testing protocol intending to provide a feasible method for COVID-19 screening in different populations.

Nucleic Acid Testing

About two-thirds of the 5'-terminal of the SARS-CoV-2 genome is composed of overlapping open reading frames (ORFs) ORF1a and ORF1b, which are mainly responsible for encoding nonstructural proteins such as enzymes related to viral replication and transcription. The other one-third of the genome encodes major structural proteins such as spike (S) protein, envelope (E) membrane protein, membrane protein, and nucleocapsid (N) protein. The structural proteins determine the replication, stability, and invasiveness of the virus.[6] The S protein on the surface of SARS-CoV-2 specifically recognizes the angiotensin-converting enzyme 2 receptor on the host cell membrane and mediates the binding of the virus to the host cell membrane. The SARS-CoV-2 stimulates the body's defense system during viral replication, amplification, and release. Persons with COVID-19 fight the virus through autoimmune function and adjuvant therapy against inflammation.[7] However, an over-activated inflammatory response and cytokine storm may trigger viral pneumonia. There is no specific treatment for COVID-19; therefore, early diagnosis and timely prevention are the keys to controlling the outbreak. The gold standard for SARS-CoV-2 diagnosis is RT-PCR, the principle of which is to monitor the growth of the number of products in real time by specific

fluorescent-labeled probes and calculate the initial template amount based on the amplification curve. The kits are designed with specific primers for the detection of SARS-CoV-2 against the ORF1ab fragment and the N gene, and the diagnosis of positive cases requires 2 positive targets in the same specimen. A study optimizing the detection of SARS-CoV-2 suggested the use of PCR targeting the E gene followed by confirmation using RNA-dependent RNA polymerase primers in combination with SARS-CoV-2-specific probes.[8]

The number of copy amplification cycles recorded by RT-PCR is the cycle threshold (Ct) value, and the critical level for Ct value for RT-PCR is generally set at 37 to 40 globally and results greater than the critical value are considered negative.[9] The Ct value threshold for RT-PCR varies from laboratory to laboratory due to differences in population, geography, instrumentation, and reagents. The Ct value is widely used as a semi-quantitative indicator of SARS-CoV-2 viral load; a lower Ct value corresponds to higher severity of the disease.[10] In contrast, asymptomatic infected patients may have higher Ct values leading to false-negative results.[11] Therefore, the sensitivity of RT-PCR in asymptomatic infected patients needs to be improved. The RNA count of COVID-19 pharyngeal virus peaks on the fourth day of symptom onset,[12] One study found that the false-negative rate of RT-PCR decreased gradually to a minimum from the day of infection to the third day of symptom onset and then increased gradually on the fourth day of symptom onset.[13] In addition, RT-PCR assay results are also susceptible to sampling site effects, with the following viral loads for different specimen types: alveolar lavage >deep cough sputum >nasopharyngeal swab >oropharyngeal swab >blood.[14] Currently, nasopharyngeal swabs and oropharyngeal swab sampling methods are most common. Therefore, early in the patient's infection, low nasopharyngeal and oropharyngeal viral loads lead to an increased likelihood of false-negative RT-PCR results.

The RT-PCR method also has some obvious disadvantages: (i) the test requires sophisticated instruments, which are usually expensive and limited in number, and the population in need cannot perform point-of-care testing (POCT) on their own; (ii) testing personnel and the population in need must go to a designated location for professional specimen collection, which may lead to clustering of infections; (iii) the assay takes longer, the experiment itself requires a certain amount of cycle time, and in the case of relatively large numbers of samples, the test needs to be performed in batches. In addition, patients with the virus may still spread the virus while the results are not reported. During the SARS-CoV-2 pandemic, new variants of the virus have emerged, such as the Delta and Omicron variants. The Delta variant is more transmissible, has an increased viral load, is more pathogenic, and has a longer duration of the transmission.[15] The Omicron variant was first identified in southern Africa in November 2021. The Omicron variant has a greatly enhanced immune escape and infectious ability, resulting in the rapid global spread of the Omicron variant.[16] Due to the emergence of variant strains such as these, existing probes may be insensitive, resulting in false-negative results. Numerous reports have evaluated nucleotide sequence variants in RT-PCR primers and probes that produce mismatches and may lead to false-negative results.[17]

RAD

The WHO recommends RAD that meets the minimum performance requirements of ≥ 80% sensitivity and ≥ 97% specificity. Antigen detection mainly targets the N-protein antigen locus of SARS-COV-2, and the overall sensitivity of RAD is lower than RT-PCR, so RAD cannot replace RT-PCR as a diagnostic method for COVID-19. However, RAD also has certain advantages, such as short detection time and the possibility of POCT. Therefore, RAD can be used as an auxiliary method to improve the diagnostic efficiency of COVID-19 in combination with RT-PCR. Most of the RAD tests are performed using nasopharyngeal swabs, oropharyngeal swabs, or bilateral anterior nasal swabs, and the detection methods include both qualitative and quantitative assays. Qualitative assays are mainly performed by lateral flow immunoassay (LFIA): 2 horizontal lines appear on the membrane, 1 in the quality control (QC) area and the other in the test area. The color intensity of the horizontal lines in the test area may vary depending on the concentration of SARS-CoV-2 antigen in the sample. The presence of a horizontal line in both the test and QC areas is considered a positive result, and the presence of a horizontal line in the QC area only is considered a negative result. If no horizontal line appears in the QC area, it is an invalid result. Generally, the test result can be determined as negative or positive by visual inspection within 15 to 20 minutes, and the test method is easy to learn. Quantitative assays mainly use automated antigen detection, which requires specific detection instruments and platforms that can detect specific antigen content.

LFIA

LFIA Sensitivity and Number of Days to Symptom Onset in Persons with COVID-19

Patients with COVID-19 often present with symptoms such as fever, cough, and weakness at the beginning of the infection. Many studies have performed LFIA tests on patients with COVID-19 at different days after the onset of symptoms and tracked the sensitivity of the tests on different periods. Various LFIA kits were used to test persons infected with SARS-CoV-2 and found that the sensitivity was generally lower than that of RT-PCR assays, with the highest sensitivity occurring at 1 to 3 days,[18,19]1 to 4 days,[20]1 to 5 days,[21,22] and 1 to 7 days.[23] As shown in **FIGURE 1A**, the first time-inflection point of the decrease in LFIA sensitivity occurred mostly within 5 days of symptom onset, the second time inflection point was on day 7 of symptom onset, and the third time inflection point was around 11 days after symptom onset. The results of the included studies were fitted to a curve showing that the sensitivity of LFIA was higher in the first 5 days and decreased significantly after 5 days. Therefore, the use of LFIA during this period has a high SARS-CoV-2 detection rate and can be used for self-testing and mass screening of COVID-19 when the person initially feels unwell; however, this method is not suitable for disease surveillance of persons with COVID-19 1 week after the onset of symptoms. In addition, a large proportion of persons with COVID-19 do not show any symptoms but are infectious. Frequent screening for SARS-CoV-2 in asymptomatic populations using antigen-based POCT has a very low detection rate and a high false-alarm rate.[24] Therefore, before using LFIA for COVID-19 screening, the characteristic distribution of the infected population, the accuracy of the LFIA kit, and the variation in sensitivity over time need to be carefully evaluated. When using LFIA for COVID-19 screening, it is necessary to increase the number of LFIA tests or combine LFIA with NAAT tests, especially in asymptomatic people and persons with symptomatic episodes >5 days.

LFIA Sensitivity and Ct Values in Different Ranges of RT-PCR in COVID-19 Diagnosis

Ct value is inversely proportional to viral RNA copy number[25]; a lower Ct value means a higher viral load. Subjects with COVID-19 were classified

FIGURE 1 A, Sensitivity of different LFIA kits in COVID-19 patients at different days after the onset of symptoms. B, Sensitivity of different LFIA kits for Ct values in different ranges of RT-PCR. The legend indicates the types of kits used in the different references.

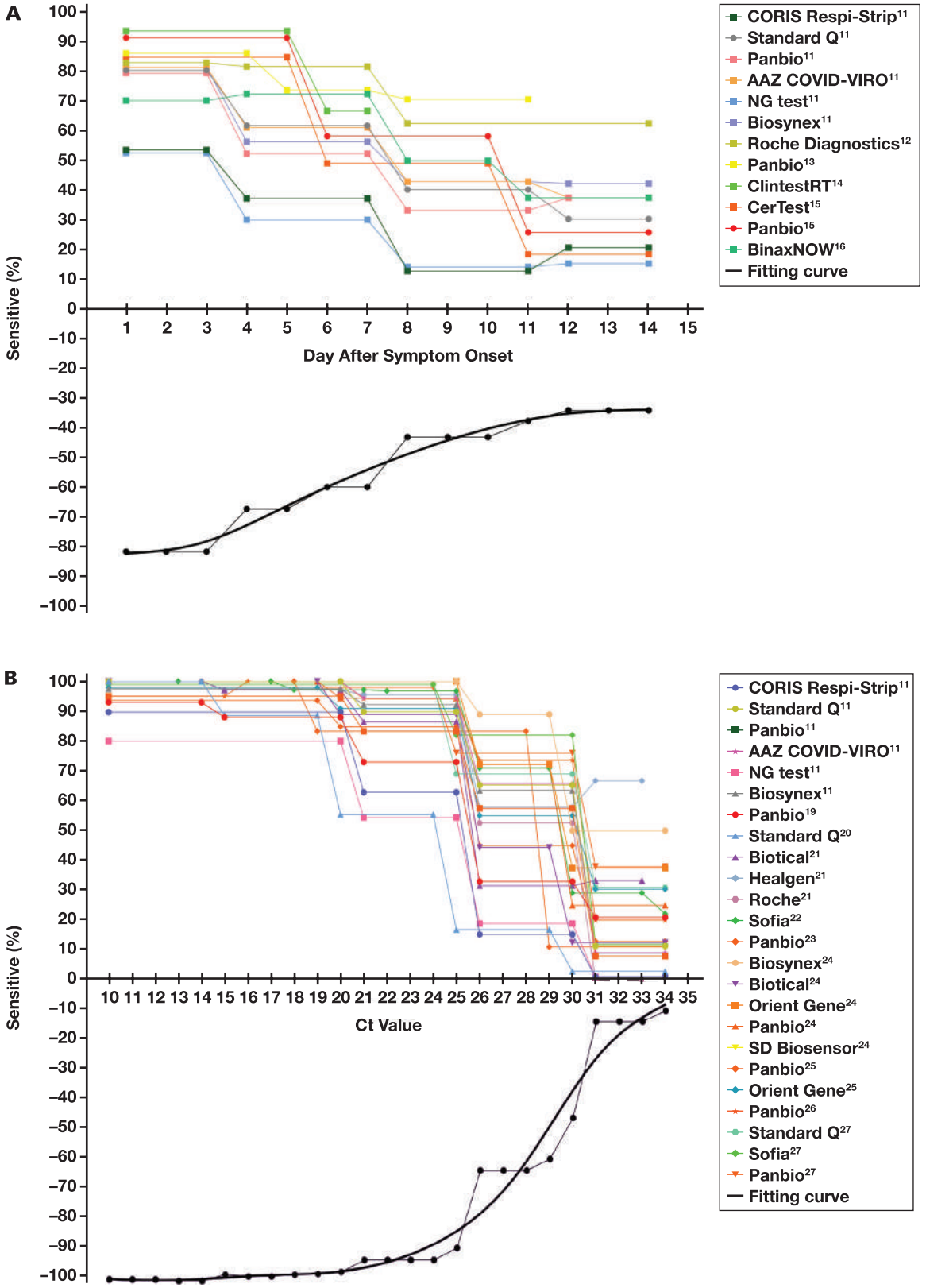

and categorized according to Ct values derived from RT-PCR, and subjects with different Ct values were tested by LFIA. The study showed that the sensitivity of RAD detection varied at different viral loads. The phases with higher sensitivity occurred in Ct < 15,[26–28] Ct ≤ 18,[29,30] Ct < 20,[18,31–33] and Ct < 25.[31,34] As shown in **FIGURE 1B**, the sensitivity of LFIA is highest when the Ct value is ≤ 20. The first inflection point of sensitivity decrease

occurs at the Ct value of 19 to 20, the second inflection point occurs at the Ct value of 24 to 26, and the third inflection point occurs at the Ct value of 29 to 31. Fitting the results of the included studies to a curve showed that LFIA has good sensitivity in detecting COVID-19 in those with Ct ≤ 25, whereas persons with Ct values between 30 and 35 receive a high false negative. In a study testing 31 RAD kits, 26 of the 31 RAD kits had sensitivities above 80% for viral loads above 10^6 genomic copies/mL (Ct < 25); 10 of the 31 RAD kits had sensitivities of 80% or higher for Ct values between 25 and 30, and the other 5 RAD kits had sensitivities only slightly below 80%; for viral loads ≤ 10^6 genomic copies/mL (Ct ≥ 25), all tests evaluated had sensitivities below 80%[35]; this demonstrates the dependence of RAD on viral load. The LFIA is more suitable for detecting COVID-19 in persons with high viral load at the beginning of SARS-CoV-2 infection when there is a large amount of upper respiratory virus shedding. The sensitivity of the LFIA was reduced in asymptomatic infected individuals relative to the symptomatic population, but the sensitivity was significantly higher at Ct < 20,[36] with sensitivity of 86% at Ct value < 25.[37] In general, the use of LFIA in late presentation individuals and the asymptomatic infected population should take into account its lower sensitivity by using RT-PCR as a co-diagnostic method.

The LFIA has good recognition of high SARS-COV-2 load, and the severity of COVID-19 determines the viral load.[38] Therefore, LFIA helps to identify and predict the severity of the disease.

Automated Antigen Assays

Currently, automated antigen assays are mainly used for the quantitative detection of the N antigen of SARS-CoV-2, and the detection principles can be broadly classified into four types: electrochemiluminescence immunoassay (ECLIA), chemiluminescence immunoassay (CLIA), chemiluminescence enzyme immunoassay (CLEIA), and enzyme-linked immunosorbent assay (ELISA).

The Roche Elecsys SARS-CoV-2 antigen assay uses ECLIA to quantify the N antigen in the sample. Roche Elecsys SARS-CoV-2 antigen detects nasopharyngeal swab specimens for SARS-CoV-2 infection status with an overall sensitivity of 65.85% and a specificity of 100%. When the cutoff value for antigen determination was set to >0.673, the sensitivity could be increased to 74.8%.[39] Using RT-PCR as a reference, the sensitivity was over 90% at Ct ≤ 30, and the sensitivity of the assay was higher within the first week of onset than after 1 week.[40]

The LIAISON SARS-CoV-2 antigen assay uses CLIA to quantify the N antigen in the sample. The overall sensitivity and specificity of the LIAISON SARS-CoV-2 antigen assay, using RT-PCR as a reference, were 75.33% and 100%, respectively. The overall sensitivity increased to 96.55% with high viral load (Ct < 18.57),[41] and sensitivity was 91.1% for Ct ≤ 23, 89.8% for Ct ≤ 25, and 67.9% for Ct ≤ 33.[42] The LIAISON SARS-CoV-2 antigen assay has shown good performance in identifying SARS-CoV-2 infection in individuals with medium to high viral loads.

The VITROS SARS-CoV-2 antigen test uses CLEIA to quantify the N antigen in the sample. The sensitivity of VITROS SARS-CoV-2 antigen for detecting SARS-CoV-2 samples ranged from 72.0% to 100% within 1 week of symptom onset and decreased from 25% to 75% after 1 week, from 93.8% to 100% for Ct ≤ 30 and from 15.4% to 72.7% for Ct > 30.[43] The Lumipulse G SARS-CoV-2 antigen assay provides another platform for quantification of N antigens in samples using ECLIA. The overall sensitivity and specificity of the Lumipulse G SARS-CoV-2 antigen assay were 84.0% and 89.1%, respectively, compared to the molecular assay, and showed 86.4% agreement with RT-PCR results.[44] In a study comparing the Roche and Lumipulse automated assays,[45] both antigen tests were shown to accurately detect SARS-CoV-2 antigen in RT-PCR–positive samples with high viral loads. In addition, antigen levels were correlated with viral load and Ct values determined by RT-PCR. The performance of the Roche and Lumipulse antigen tests was nearly identical, indicating that both tests have high diagnostic accuracy up to 9 days after symptom onset, with a gradual decline after 9 days.

The N-antigen SARS-CoV-2 antigen test uses ELISA to quantify the N antigen in the sample. The overall sensitivity was 90.1% compared to RT-PCR and showed high agreement with RT-PCR results, with a negative correlation between antigen concentration and Ct values.[46]

Automated antigen detection is more sensitive than LFIA but the detection speed is not as fast as LFIA, and automated antigen detection requires specific instruments that cannot perform POCT; automated antigen testing is faster than NAAT and gives a specific viral load, but is still not as sensitive as NAAT and can be used as a prescreening tool but not as a replacement for NAAT.

Sensitivity of RAD Detection in SARS-COV-2 Variants

The COVID-19 mutation occurs mainly in the S protein of the virus, so other structural proteins, especially the N protein, can be better targets for detection due to the lower mutation rate. The newly detected Omicron variant contains only 2 mutations in the region encoding the N protein, whereas it contains more than 30 mutations in the S protein.[47] One study found reduced sensitivity of 9 antigen detection kits for both Delta and Omicron variants.[48] However, despite the slight difference in sensitivity, RAD is, in principle, effective in detecting Delta variants.[49] BinaxNOW detects high SARS-CoV-2 carriage during Omicron surge but should be repeated in high-risk populations with negative BinaxNOW results.[50] The RAD detected significantly fewer cases of COVID-19 with the Alpha variant than the Alpha nonvariant. This implies that the efficiency of antigen detection needs to be reevaluated in other areas where SARS-CoV-2 variants are predominant.[51] In the detection of nonvariant SARS-CoV-2, RAD showed a sensitivity of 90% (20 ≤ Ct < 25) and 10% (25 ≤ Ct < 30); In Beta or Gamma-associated SARS-CoV-2 variants, RAD has a detection sensitivity of 42.8% in samples with 20 ≤ Ct < 25.[52] The marked decrease in sensitivity in SARS-CoV-2 variants suggests that special care must be taken when using RAD at the large-scale diagnostic level, especially in the current context of the emergence of several new SARS-CoV-2 variants that may produce false-negatives. The use of either RAD or RT-PCR alone increases false-negatives in the detection of SARS-CoV-2 variants, and the use of both RAD and nucleic acid diagnostics for SARS-CoV-2 can rapidly correct false-negative results and control and prevent COVID-19 outbreaks.

Combined RAD and RT-PCR Protocol

The RAD detection site contains the bilateral anterior nostrils, and studies have shown that bilateral anterior nasal swabs have slightly lower or similar sensitivity than nasopharyngeal swabs.[53,54] The bilateral anterior nostril collection method caused significantly less severe coughing, sneezing, and pain and was more acceptable to the subjects than if the NAAT test site was the nasopharynx or oropharynx.[55] In addition, the combination of the 2 assays will increase the number of sites tested and reduce the number of missed diagnoses due to differences in viral load at the sampling site.

Different assays for RAD have different sensitivities, so the choice of a RAD as a prescreen for COVID-19 requires a thorough clinical

FIGURE 2 Flow chart of the combined detection of SARS-COV-2 using NAAT and RAD in different populations. NAAT, nucleic acid amplification test; RAD, rapid antigen detection.

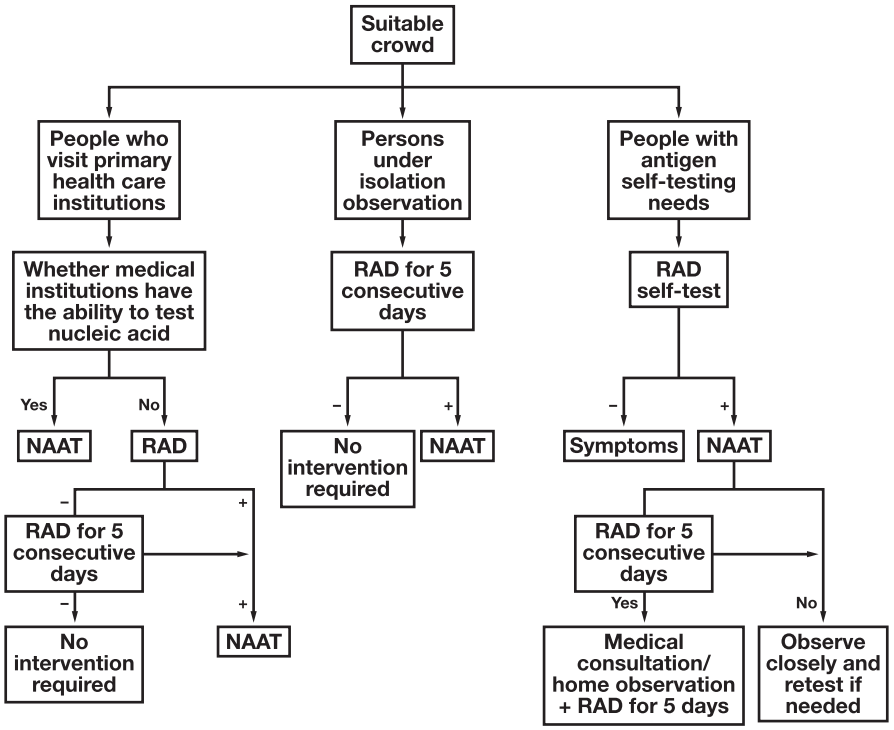

evaluation in advance. The COVID-19 Outbreak Screening Centre in Hong Kong used a combination of RAD and RT-PCR methods to screen asymptomatic individuals through 2 processes.[56] In the first process, individual with initial positive RADs accelerated the testing of RT-PCR samples for these individuals by their laboratories, reducing the average time to confirm results from 10.85 hours to 7.0 hours. In the second process, individuals with an initial positive RAD undergo on-site rapid RT-PCR testing, reducing the average time to confirm results to less than 1 hour.

The population currently undergoing mass screening falls into 3 broad categories: (i) persons who visit primary health care institutions with respiratory and fever symptoms and have symptoms for 5 days or less; (ii) isolation observation personnel, including home isolation observation, close contact and subclose contact, inbound isolation observation, sealing control area, and control area personnel; (iii) community residents who have a need for antigen self-testing. Nucleic acid testing, when available, is preferred in the first category because of the presence of symptoms of COVID-19. The second and third categories are suitable for 5 consecutive days of self-testing with RAD. The testing process is shown in **FIGURE 2**. The RAD can play an important role in prescreening, and a positive RAD result must be confirmed with the gold standard (RT-PCR). Although using the 2 methods will improve the diagnostic efficiency and accuracy of COVID-19, the detection method should be continuously improved with probes and N-protein antibodies in response to the due to the continuous mutation of the strain.

Conclusion

Due to some limitations of RT-PCR for SARS-CoV-2 detection, RAD can be used as an adjunct to RT-PCR. The overall sensitivity of RAD is lower than that of RT-PCR, but it has high sensitivity and specificity in the early stage of SARS-CoV-2 infection. Therefore, RAD can be used as a screening tool for early SARS-CoV-2 infection, and RT-PCR used to confirm the diagnosis when the result is positive. There are many types of RADs on the market with varying test quality, and a thorough clinical evaluation should be performed before use. This review provides a flow chart for the combined application of RAD and NAAT to screen COVID-19 in the population, and it is believed that this protocol can effectively shorten the screening time for COVID-19 in a large base population and provide assistance in the control of the COVID-19 pandemic.

Author Contributions

Xue-wen Li wrote the main parts of this manuscript and designed the figures; Yi-ting Wang wrote other parts and improved the language of the manuscript; Jian-cheng Xu conceived the structure and revised the manuscript; All authors read and approved the final manuscript.

REFERENCES

1. World Health Organization (WHO): Coronavirus disease (COVID-19) outbreak situation. https://www.who.int/emergencies/diseases/novel-coronavirus-2019. Accessed March 13, 2022.
2. Mathuria JP, Yadav R. Rajkumar. Laboratory diagnosis of SARS-CoV-2 - a review of current methods. *J Infect Public Health.* 2020;13(7):901–905. doi:10.1016/j.jiph.2020.06.005.
3. World Health Organization (WHO): Coronavirus Disease (COVID-19) Pandemic — Emergency Use Listing Procedure (EUL) Open for IVDs. https://extranet.who.int/pqweb/vitro-diagnostics/coronavirus-disease-covid-19-pandemic-%E2%80%94-emergency-use-listing-procedure-eul-open. Accessed March 13, 2022.

4. US Centers for Disease Control and Prevention. Interim Guidance for Rapid Antigen Testing for SARS-CoV-2. https://www.cdc.gov/coronavirus/2019-ncov/lab/resources/antigen-tests-guidelines.html. Accessed March 13, 2022.
5. European Centre for Disease Prevention and Control. Options for the Use of Rapid Antigen Tests for COVID-19 in the EU/EEA and the UK. (https://www.ecdc.europa.eu/en/publications-data/options-use-rapid-antigen-tests-covid-19-eueea-and-uk). Accessed 13 March 2022.
6. Perlman S. Another decade, another coronavirus. *N Engl J Med.* 2020;382(8):760–762. doi:10.1056/NEJMe2001126.
7. Wang Y, Wu M, Li Y, Yuen HH, He ML. The effects of SARS-CoV-2 infection on modulating innate immunity and strategies of combating inflammatory response for COVID-19 therapy. *J Biomed Sci.* 2022;29(1):27. doi:10.1186/s12929-022-00811-4.
8. Corman VM, Landt O, Kaiser M, et al Detection of 2019 novel coronavirus (2019-nCoV) by real-time RT-PCR. *Euro Surveill.* 2020;25(3):2000045.
9. Jamal SA, Farooq MU, Bidari V. Challenges associated with using cycle threshold (Ct) value of reverse-transcription polymerase chain reaction (RT-PCR) as a criteria for infectiousness of coronavirus disease 2019 (COVID-19) patients in India. *Infect Control Hosp Epidemiol.* 2021:1–2.
10. Rao SN, Manissero D, Steele VR, Pareja J. A systematic review of the clinical utility of cycle threshold values in the context of COVID-19. *Infect Dis Ther.* 2020;9(3):573–586.
11. Brummer LE, Katzenschlager S, McGrath S, et al. Accuracy of rapid point-of-care antigen-based diagnostics for SARS-CoV-2: an updated systematic review and meta-analysis with meta-regression analyzing influencing factors. *PLoS Med.* 2022;19(5):e1004011.
12. Wolfel R, Corman VM, Guggemos W, et al. Virological assessment of hospitalized patients with COVID-2019. *Nature.* 2020;581(7809):465–469.
13. Kucirka LM, Lauer SA, Laeyendecker O, Boon D, Lessler J. Variation in false-negative rate of reverse transcriptase polymerase chain reaction-based SARS-CoV-2 tests by time since exposure. *Ann Intern Med.* 2020;173(4):262–267.
14. Li L, Chen QY, Li YY, Wang YF, Yang ZF, Zhong NS. Comparison among nasopharyngeal swab, nasal wash, and oropharyngeal swab for respiratory virus detection in adults with acute pharyngitis. *BMC Infect Dis.* 2013;13:281.
15. Li B, Deng A, Li K, et al. Viral infection and transmission in a large, well-traced outbreak caused by the SARS-CoV-2 Delta variant. *Nat Commun.* 2022;13(1):460.
16. Yu X, Qi X, Cao Y, et al. Three doses of an inactivation-based COVID-19 vaccine induces cross-neutralizing immunity against the SARS CoV-2 Omicron variant. *Emerg Microbes Infect.* 2022;11(1):749–752.
17. Osorio NS, Correia-Neves M. Implication of SARS-CoV-2 evolution in the sensitivity of RT-qPCR diagnostic assays. *Lancet Infect Dis.* 2021;21(2):166–167.
18. Fourati S, Langendorf C, Audureau E, et al. Performance of six rapid diagnostic tests for SARS-CoV-2 antigen detection and implications for practical use. *J Clin Virol.* 2021;142:104930.
19. Thell R, Kallab V, Weinhappel W, et al. Evaluation of a novel, rapid antigen detection test for the diagnosis of SARS-CoV-2. *PLoS One.* 2021;16(11):e0259527.
20. Ngo Nsoga MT, Kronig I, Perez Rodriguez FJ, et al. Diagnostic accuracy of Panbio rapid antigen tests on oropharyngeal swabs for detection of SARS-CoV-2. *PLoS One.* 2021;16(6):e0253321.
21. Merino-Amador P, Gonzalez-Donapetry P, Dominguez-Fernandez M, et al. Clinitest rapid COVID-19 antigen test for the diagnosis of SARS-CoV-2 infection: a multicenter evaluation study. *J Clin Virol.* 2021;143:104961.
22. Perez-Garcia F, Romanyk J, Gomez-Herruz P, et al. Diagnostic performance of CerTest and Panbio antigen rapid diagnostic tests to diagnose SARS-CoV-2 infection. *J Clin Virol.* 2021;137:104781.
23. Almendares O, Prince-Guerra JL, Nolen LD, et al. Performance characteristics of the Abbott BinaxNOW SARS-CoV-2 antigen test in comparison to real-time reverse transcriptase PCR and viral culture in community testing sites during November 2020. *J Clin Microbiol.* 2022;60(1):e0174221.
24. Mitchell SL, Orris S, Freeman T, et al. Performance of SARS-CoV-2 antigen testing in symptomatic and asymptomatic adults: a single-center evaluation. *BMC Infect Dis.* 2021;21(1):1071.
25. Aykac K, Cura Yayla BC, Ozsurekci Y, et al. The association of viral load and disease severity in children with COVID-19. *J Med Virol.* 2021;93(5):3077–3083.
26. Thirion-Romero I, Guerrero-Zuniga DS, Arias-Mendoza DA, et al. Evaluation of Panbio rapid antigen test for SARS-CoV-2 in symptomatic patients and their contacts: a multicenter study. *Int J Infect Dis.* 2021;113:218–224.
27. Lee J, Kim SY, Huh HJ, et al. Clinical performance of the standard Q COVID-19 rapid antigen test and simulation of its real-world application in Korea. *Ann Lab Med.* 2021;41(6):588–592.
28. Favresse J, Gillot C, Oliveira M, et al Head-to-head comparison of rapid and automated antigen detection tests for the diagnosis of SARS-CoV-2 infection. *J Clin Med.* 2021;10(2):265.
29. Smith RD, Johnson JK, Clay C, et al Clinical evaluation of Sofia Rapid Antigen Assay for detection of severe acute respiratory syndrome coronavirus 2 (SARS-CoV-2) among emergency department to hospital admissions. *Infect Control Hosp Epidemiol.* 2021:1–6.
30. Mak GCK, Lau SSY, Wong KKY, et al. Evaluation of rapid antigen detection kit from the WHO Emergency Use List for detecting SARS-CoV-2. *J Clin Virol.* 2021;134:104712.
31. Van Honacker E, Van Vaerenbergh K, Boel A, De Beenhouwer H, Leroux-Roels I, Cattoir L. Comparison of five SARS-CoV-2 rapid antigen detection tests in a hospital setting and performance of one antigen assay in routine practice: a useful tool to guide isolation precautions? *J Hosp Infect.* 2021;114:144–152.
32. Nordgren J, Sharma S, Olsson H, et al. SARS-CoV-2 rapid antigen test: high sensitivity to detect infectious virus. *J Clin Virol.* 2021;140:104846.
33. Fenollar F, Bouam A, Ballouche M, et al Evaluation of the Panbio COVID-19 Rapid Antigen Detection Test device for the screening of patients with COVID-19. *J Clin Microbiol.* 2021;59(2):e02589–20.
34. Jaaskelainen AE, Ahava MJ, Jokela P, et al. Evaluation of three rapid lateral flow antigen detection tests for the diagnosis of SARS-CoV-2 infection. *J Clin Virol.* 2021;137:104785.
35. Puyskens A, Krause E, Michel J, et al Establishment of a specimen panel for the decentralised technical evaluation of the sensitivity of 31 rapid diagnostic tests for SARS-CoV-2 antigen, Germany, September 2020 to April 2021. *Euro Surveill.* 2021;26(44):2100442.
36. Escribano P, Sanchez-Pulido AE, Gonzalez-Leiva J, et al Different performance of three point-of-care SARS-CoV-2 antigen detection devices in symptomatic patients and close asymptomatic contacts: a real-life study. *Clin Microbiol Infect.* 2022;28(6):865–870.
37. Masia M, Fernandez-Gonzalez M, Sanchez M, et al. Nasopharyngeal Panbio COVID-19 antigen performed at point-of-care has a high sensitivity in symptomatic and asymptomatic patients with higher risk for transmission and older age. *Open Forum Infect Dis.* 2021;8(3):ofab059.
38. Imai M, Iwatsuki-Horimoto K, Hatta M, et al. Syrian hamsters as a small animal model for SARS-CoV-2 infection and countermeasure development. *Proc Natl Acad Sci USA.* 2020;117(28):16587–16595.
39. Ben Abdelhanin M, Mvumbi DM, Agathine A, Nanos N, Gidenne S. Evaluation of the Elecsys SARS-CoV-2 antigen assay for the detection of SARS-CoV-2 in nasopharyngeal swabs. *J Clin Virol.* 2021;144:104991.
40. Lau CS, Phua SK, Hoo SP, Jiang B, Aw TC. Evaluation and validation of the Roche Elecsys SARS-CoV-2 antigen electro-chemiluminescent immunoassay in a Southeast Asian region. *Vaccines (Basel).* 2022;10(2):198.

41. Altawalah H, Alfouzan W, Al-Fadalah T, Ezzikouri S. Diagnostic performance of automated SARS-CoV-2 antigen assay in nasal swab during COVID-19 vaccination campaign. *Diagnostics (Basel).* 2021;11(11):2110.

42. Petonnet D, Marot S, Leroy I, et al Comparison of rapid and automated antigen detection tests for the diagnosis of SARS-CoV-2 infection. *Diagnostics (Basel).* 2022;12(1):104.

43. Fourati S, Soulier A, Gourgeon A, et al. Performance of a high-throughput, automated enzyme immunoassay for the detection of SARS-CoV-2 antigen, including in viral "variants of concern": implications for clinical use. *J Clin Virol.* 2022;146:105048.

44. Sberna G, Basile F, Guarino ML, Capobianchi MR, Bordi L, Parisi G. Comparison of Allplex SARS-CoV-2 assay, easy SARS-CoV-2 WE and Lumipulse quantitative SARS-CoV-2 antigen test performance using automated systems for the diagnosis of COVID-19. *Int J Infect Dis.* 2021;113:113–115.

45. Hirotsu Y, Sugiura H, Maejima M, et al. Comparison of Roche and Lumipulse quantitative SARS-CoV-2 antigen test performance using automated systems for the diagnosis of COVID-19. *Int J Infect Dis.* 2021;108:263–269.

46. Mayanskiy N, Brzhozovskaya E, Fedorova N, Lebedin Y. Parallel detection of SARS-CoV-2 RNA and nucleocapsid antigen in nasopharyngeal specimens from a COVID-19 patient screening cohort. *Int J Infect Dis.* 2021;108:330–332.

47. Karim SSA, Karim QA. Omicron SARS-CoV-2 variant: a new chapter in the COVID-19 pandemic. *Lancet.* 2021;398(10317):2126–2128.

48. Osterman A, Badell I, Basara E, et al Impaired detection of omicron by SARS-CoV-2 rapid antigen tests. *Med Microbiol Immunol.* 2022;211(2-3):105–117.

49. Bekliz M, Adea K, Essaidi-Laziosi M, et al. SARS-CoV-2 antigen-detecting rapid tests for the delta variant. *Lancet Microbe.* 2022;3(2):e90.

50. Schrom J, Marquez C, Pilarowski G, et al Comparison of SARS-CoV-2 reverse transcriptase polymerase chain reaction and BinaxNOW rapid antigen tests at a community site during an Omicron surge: a cross-sectional study. *Ann Intern Med.* 2022;175(5):682–690.

51. van Ogtrop ML, van de Laar TJW, Eggink D, Vanhommerig JW, van der Reijden WA. Comparison of the performance of the PanBio COVID-19 antigen test in SARS-CoV-2 B.1.1.7 (Alpha) variants versus non-B.1.1.7 variants. *Microbiol Spectr.* 2021;9(3):e0088421.

52. Barrera-Avalos C, Luraschi R, Vallejos-Vidal E, et al. The rapid antigen detection test for SARS-CoV-2 underestimates the identification of COVID-19 positive cases and compromises the diagnosis of the SARS-CoV-2 (K417N/T, E484K, and N501Y) variants. *Front Public Health.* 2021;9:780801.

53. Patriquin G, LeBlanc JJ, Williams C, et al. Comparison between nasal and nasopharyngeal swabs for SARS-CoV-2 rapid antigen detection in an asymptomatic population, and direct confirmation by RT-PCR from the residual buffer. *Microbiol Spectr.* 2022;10(1):e0245521.

54. Wolfl-Duchek M, Bergmann F, Jorda A, et al. Sensitivity and specificity of SARS-CoV-2 rapid antigen detection tests using oral, anterior nasal, and nasopharyngeal swabs: a diagnostic accuracy study. *Microbiol Spectr.* 2022;10(1):e0202921.

55. Takeuchi Y, Akashi Y, Kato D, et al. Diagnostic performance and characteristics of anterior nasal collection for the SARS-CoV-2 antigen test: a prospective study. *Sci Rep.* 2021;11(1):10519.

56. Chiu RYT, Kojima N, Mosley GL, et al. Evaluation of the INDICAID COVID-19 rapid antigen test in symptomatic populations and asymptomatic community testing. *Microbiol Spectr.* 2021;9(1):e0034221.

SCIENCE

Comparison between the Sofia SARS Antigen FIA Test and the PCR Test in Detection of SARS-CoV-2 Infection

Manca Černila[1,4], Mateja Logar, MD, PhD[2], Hugon Možina, MD[3], Joško Osredkar, M Pharm, PhD[1,4]

[1]Institute of Clinical Chemistry and Biochemistry, University Medical Centre Ljubljana, Ljubljana Slovenia, [2]Department of Infectious Diseases, Department for Hospital Hygiene, University Medical Centre Ljubljana, Ljubljana, Slovenia, [3]Internist First Aid, University Medical Centre Ljubljana, Ljubljana, Slovenia, [4]Faculty of Pharmacy, University of Ljubljana, Ljubljana, Slovenia. *To whom correspondence should be addressed. mancacernila@gmail.com

Keywords: COVID-19, SARS-CoV-2, Sofia SARS antigen FIA, clinical validity, analytical validity, rapid antigen testing

Abbreviations: Sofia, Sofia SARS Antigen Fluorescent Immunoassay; rRT-PCR, real-time reverse transcription–polymerase chain reaction; FIA, fluorescent immunoassay; POCT, point-of-care testing; Ct, cycle threshold.

Laboratory Medicine 2023;54:e44–e48; https://doi.org/10.1093/labmed/lmac079

ABSTRACT

Objective: The purpose of this study was to compare Quidel's rapid antigen test Sofia SARS antigen Fluorescent Immunoassay (FIA) (Sofia) with the real-time reverse transcription–polymerase chain reaction (rRT-PCR) test.

Methods: Two samples were taken from each test subject—1 for testing with the Sofia test and 1 for testing with the rRT-PCR test. In total, swabs were taken from 146 subjects who presented symptoms of infection (group 1) and 672 subjects who were tested regardless of symptoms (group 2).

Results: In group 1, the sensitivity of the antigen test was 90.0% and its specificity 97.5%. In group 2, however, the sensitivity of the antigen test was 81.4% and the specificity 98.9%. In addition to asymptomatic patients, false-negative results of rapid antigen tests also occurred in subjects with high threshold values (cycle threshold > 30).

Conclusion: Our results show that the Sofia test meets the standards for diagnostic tests according to the criteria of the World Health Organization, as they show high sensitivity and specificity, and perhaps most importantly, a high negative predictive value (> 95%).

Frequent and rapid diagnostic testing is crucial to limit the spread of SARS-CoV-2 in the community, as it allows timely identification and isolation of infected individuals and thus breaks the transmission chain.[1] The quantitative detection of viral RNA in nasal swab or saliva samples based on the rRT-PCR test is the gold standard for sensitivity in detecting the presence of SARS-CoV-2. However, the lack of reagent supply, significant costs, and infrastructure constraints make it difficult to test sufficiently and report results quickly.[1,2] These conditions encouraged the development of rapid diagnostic tests, which are based on the detection of viral antigens. Their main advantages lie in the rapid availability of results and the possibility to perform point-of-care testing, which also relieves the burden on staff in diagnostic laboratories. According to the literature, however, the performance of these tests remains uncertain.[3] Rapid antigen detection kits have so far been described as suboptimally sensitive and specific. Nevertheless, the unique protein domains of the virus can be used to develop kits with higher sensitivity.[4]

Sofia SARS Antigen Fluorescent Immunoassay (FIA) (hereafter Sofia) is a type of antigen test. These tests are designed to detect viral proteins in respiratory samples of persons with COVID-19.[5] Sofia is an FIA that uses advanced immunofluorescence-based lateral flow technology. It uses the so-called "sandwich method" for qualitative detection of the virus's nucleocapsid proteins. Sofia, in combination with the Sofia 2 and Sofia analyzers, provides automated and objective results in 15 min, which also allows for the testing of persons with suspected COVID-19 in the person's immediate environment.[6] The FIAs are modern fluorescence-based tests that use a fluorescent component (a fluorescent dye-labelled antibody) as a detection reagent.[7] The Sofia test uses europium in the form of a chelate complex as the fluorescent component for detection.[8] The wavelength of the excitation light of these complexes is usually about 335 nm, and the wavelength of the emitted light is about 616 nm.[9] From this data, we can infer the interference caused by molecules that may appear in the sample. Hemoglobin, which absorbs light very efficiently at wavelengths below 600 nm, is the most common potential interferant in samples.[10] The molecule absorbs light and thus weakens the intensity of the excitation or the emission light of the test. The quenching efficiency also depends on the extinction coefficient of the molecule and its concentration in the sample. This can lead to false-negative results.[11] Some medicines can cause interference as well, but they are not specifically listed by the manufacturers. The accuracy of the result can be affected not only by interfering molecules that can cause autofluorescence or signal quenching but also by the volume of the sample—insufficient sample volume can give false-negative results.[5]

Materials and Methods

Participants and Samples

The experimental use of the Sofia test and its evaluation began in August 2020 at the Department of Infectious Diseases of the University Medical Centre Ljubljana. It was used on all symptomatic patients who were admitted and hospitalized in the grey zone (hereafter referred to as group 1). As the results were satisfactory, the use of the rapid test was extended to other locations of the University Clinical Centre Ljubljana in November. The results were also monitored and collected at the Internist First Aid of the University Medical Centre Ljubljana, where both symptomatic and asymptomatic patients (hereafter group 2) were tested. Prior to collecting the samples, we obtained the permission of the Commission for Medical Ethics (numbers 0120-211/ 2020/7 and 0120-60/ 2021/2), which allowed us to use the data for research purposes if the patient gave their verbal consent.

Laboratory Analysis

Two samples were taken from each patient using a nasopharyngeal swab. The first sample was used to detect viral antigen using the Sofia test, which was performed at the site of sampling. We used the Sofia SARS antigen FIA (Quidel, San Diego, CA, US) test kit and the fluorimeter SOFIA 2 (Quidel). The "walk away" method was selected in the device, so that the device incubated the plate itself and read the result after 15 min. The result was displayed as + (positive) or – (negative). If the control was valid, that was shown by a green tick mark. Otherwise, the device indicated an error and did not display the test result. In this case, the test must be repeated. The second sample was immersed in 2 to 3 mL virus transport medium and transported to the Institute of Microbiology and Immunology, where it was used for rRT-PCR testing. The transport was made in less than 2 hours and at room temperature.

Statistical Analysis

For the statistical analysis of the data, we used Excel (Microsoft Corp, Redmond, WA, US) to form contingency tables, the MedCalc Software Ltd statistical program to perform the analyses of sensitivity, specificity, positive and negative predictive values, and accuracy, and finally, the IBM SPSS statistical program was used to compare the tested methods with the McNemar and Kappa tests (α = .05).

Results

In total, we tested 818 people who were divided into 2 groups. Group 1 included 146 individuals who showed symptoms of the SARS-CoV-2 infection. Group 2, on the other hand, included 674 subjects who were tested regardless of whether they showed any symptoms of infection. In group 1, we only used the results of 132 symptomatic persons in our analysis—3 of the point-of-care testing (POCT) results showed an invalid result and the remaining 11 were excluded due to lack of data. The results of the screening test compared with the gold standard are presented in **TABLE 1**.

Among the 672 patients in group 2, 2 of the tests were not included in the analysis due to lack of data. Those tests with an invalid result were repeated, as further treatment of patients depended on the result of the tests. The results of the screening test compared with the gold standard are presented in **TABLE 2**.

The sensitivity and specificity of the tests were calculated using the data in **TABLES 1** and **2** (**TABLES 3** and **4**).

The results differ between the 2 tested groups. In addition, the values of diagnostic sensitivity and specificity, calculated from our results, also differ from the values stated by the manufacturer. The sensitivity stated by the manufacturer is slightly higher—87.5%, and the specificity is stated as more than 99.9%. It is important to note, that the manufacturer obtained these values when testing frozen samples, so the values of fresh samples may vary. Moreover, we do not have the data on the cycle threshold (Ct) values of the samples tested by the manufacturer.[5]

The values of sensitivity and specificity stated by the manufacturer are high and indicate a good diagnostic reliability of the tests. We observed, however, that the diagnostic reliability of the tests is significantly higher when testing symptomatic persons. The reasons for the differences in test performance may vary. Diagnostic efficiency can be affected, among other things, by the analytical sensitivity of the tests. For this purpose, we analyzed the data further to determine the analytical sensitivity of the tests with the help of the Ct value. In group 1, we only observed 1 false-negative result. The measured Ct value was 15.3, indicating a high concentration of viral RNA in the sample. It is important to note, however, that in this case, the subject had been tested and confirmed positive with the rRT-PCR test 6 weeks before the Sofia test was performed. The negative result was therefore most likely due to the low concentration of the virus in the upper respiratory tract as the disease had progressed.

TABLE 1. Presentation of the Screening Test Results for Group 1 Compared with the Gold Standard

Test Results	Positive Results rRT-PCR n (percentage)	Negative Results rRT-PCR n (percentage)	Total
Positive results Sofia n (percentage)	9 (6.8 %)	3 (2.3 %)	12
Negative results Sofia n (percentage)	1 (0.8 %)	119 (90.1 %)	120
Total	10	122	132

Sofia, Sofia SARS antigen Fluorescent Immunoassay; rRT-PCR, real-time reverse transcription–polymerase chain reaction.

TABLE 2. Presentation of the Screening Test Results for Group 2 Compared with the Gold Standard.

Test Results	Positive Results rRT-PCR n (percentage)	Negative Results rRT-PCR n (percentage)	Total
Positive results Sofia n (percentage)	524 (78.2 %)	6 (0.9 %)	530
Negative results Sofia n (percentage)	29 (3.8 %)	113 (17.0 %)	142
Total	553	119	672

TABLE 3. Sensitivity, Specificity, Positive and Negative Predictive Values, and Accuracy for Group 1.

Statistic	Value	95% Confidence Interval
Sensitivity	90.00%	55.50%–99.75%
Specificity	97.52%	92.93%–99.49%
Disease Prevalence	7.63%	3.72%–13.59%
Positive Predictive Value	75.00%	49.05%–90.34%
Negative Predictive Value	99.16%	94.84%–99.87%
Accuracy	96.95%	92.34%–99.16%

TABLE 4. Calculated Values of Sensitivity, Specificity, Positive and Negative Predictive Values, and Accuracy for Group 2.

Statistic	Value	95% Confidence Interval
Sensitivity	81.43%	73.98%–87.50%
Specificity	98.87%	97.55%–99.58%
Disease Prevalence	20.90%	17.88%–24.17%
Positive Predictive Value	95.00%	89.52%–97.69%
Negative Predictive Value	95.27%	93.44%–96.61%
Accuracy	95.22%	93.32%–96.71%

In group 2, we observed a higher number of false-negative results. These results are presented in **FIGURE 1**. In this figure, a significantly higher number of false negative values at higher Ct values can be observed. Nevertheless, these values are not extremely low, as the rRT-PCR test classifies Ct values below 29 as strongly positive or having high concentrations of the target nucleic acids, values from 30 to 37 as moderate amounts of the target nucleic acids, and values from 38 to 40 as extremely low amounts, which could also represent a state of infection or contamination of the sample.[12]

It is important to note that there were only 7 truly positive Sofia test results at Ct values greater than 30, as opposed to the 18 false-negative results. We can therefore conclude that the Sofia test only detects very high concentrations of the virus in the sample reliably (Ct values 10–25), whereas at low concentrations, it is significantly less reliable. However, the Ct values must be interpreted carefully as they are affected by sample type, sample collection timing, and assay design.[13]

Statistical Comparison of the Diagnostic Accuracy of the Tests

To compare the diagnostic accuracy of the Sofia test with the rRT-PCR test, we first performed the McNemar test. The result of the 2-way test in group 1 was 0.625. Since this value is higher than 0.05, we cannot reject the null hypothesis. Thus, there was no statistically significant difference between the Sofia and rRT-PCR tests in group 1. However, the result of the 2-way test in group 2 was less than 0.05, so we can reject the null hypothesis and accept the alternative hypothesis. Therefore, a statistically significant difference can be observed between the 2 tests in group 2.

Cohen's Kappa test was also performed for comparison purposes. The Kappa value in group 1 was 0.802, which shows a strong correspondence between the Sofia test and the rRT-PCR test. Additionally, our result confirms the correctness of the McNemar test result. The same

FIGURE 1 Presentation of the false-negative results in testing with the Sofia test with respect to the Ct values of the rRT-PCR test in group 2. Sofia, Sofia SARS Antigen Fluorescent Immunoassay; rRT-PCR, real-time reverse transcription–polymerase chain reaction; Ct, cycle threshold.

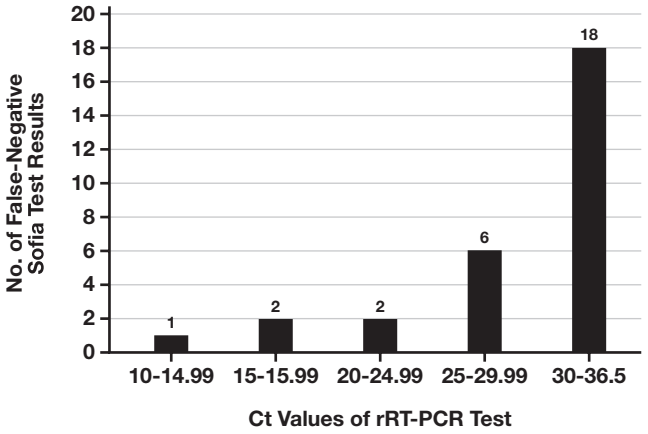

analysis was performed for group 2. The Kappa value in group 2 was also higher than 0.8, which indicates a strong agreement of the tests. Using the McNemar test, however, we proved a disagreement in the case of group 2, which, according to the data used by the test for analysis, indicates a low level of disagreement.

It can be concluded that the clinical sensitivity and specificity of the Sofia test in the case of symptomatic subject testing are comparable to the values of the rRT-PCR test. However, in the case of testing both asymptomatic and symptomatic patients, the Sofia test is clinically less reliable than the rRT-PCR test in terms of the number of false-positive results.

As already observed with analytical sensitivity, most false-negative results occurred in samples where Ct values were higher than 30. We were interested in the extent to which these results affect the statistical comparability of tests. For this purpose, we also performed a statistical comparison of the results of group 2, which did not include the results of samples with Ct values higher than 30.

The results of both the McNemar test ($p = .332$) and the Kappa test ($K = 0.914$) show a strong correspondence between the methods. We can therefore conclude that the Sofia test is comparable to the rRT-PCR method in the case of testing samples with high analyte concentration and significantly less reliable at lower concentrations (Ct > 30). This can pose an obstacle, especially when testing patients in the early stages of infection when the virus concentration in the sample may be low.

Sensitivity and specificity determine the operational characteristics of the test, but the predictive value (positive or negative) of the test is of great diagnostic importance to the physician and patient.[14] In **TABLES 3** and **4**, it can be observed that in group 1, the probability that a person with a positive test result has the disease is 75.0% (the probability of a person with a negative result not having the disease is 99.2%). Negative results can therefore be trusted in group 1, but regarding a positive result, there is a 25.0% probability that the positive result does not show the presence of an actual disease. This result would not be favorable in a disease where confirmatory tests are invasive or may even worsen the patient's health. In the case of COVID-19, all patients with a positive Sofia test can be tested with the rRT-PCR test to confirm their

infection. Significantly more important in SARS-CoV-2 infection is a good negative prognostic value, as any patient with a negative result that is actually positive remains unrecognized and consequently unknowingly spreads the infection. The negative predictive value in group 1 was 99.2% and 95.0% in group 2.

Positive and negative predictive values also depend, among other things, on the prevalence of the disease in the tested population.[15] This is the reason for the low positive predictive value in group 1, although the sensitivity and specificity values are high. However, it should also be emphasized that the prevalence of the disease differs between the 2 groups as the sampling period was completely different.

Discussion

The purpose of the study was to compare the Sofia test with the rRT-PCR test intended for the detection of SARS-CoV-2 virus. During the analysis of the data, we showed that there is no statistically significant difference in the diagnostic accuracy between the Sofia test and the rRT-PCR test when testing symptomatic subjects. However, the same is not true for asymptomatic persons. The concentration of the virus in the sample had a significant effect on the efficiency of the test, as we observed a significantly higher number of false-negative results in the samples with higher Ct values. The tests also differ in the way they are performed. The Sofia test is designed to be performed as POCT.[5] Its implementation is therefore less demanding and does not require specially trained staff. It can be performed by medical staff to whom the method and its proper implementation have been presented by an expert. The correct performance of the rRT-PCR test, however, is much more demanding and requires a high level of accuracy and precision of trained staff.[16] It should also be emphasized that the rRT-PCR test is significantly more expensive and time-consuming than the Sofia test due to its complexity.

Fundamentally, the analytical specificity of both methods is high. Antibodies to immune methods are capable of very specific recognition of a particular antigen.[17] The analytical specificity of PCR methods is based on the fact that specific nucleotide sequences can be determined in the viral RNA sequence, and specific oligonucleotide primers can be designed accordingly.[18] The analytical specificity of the Sofia test was not specifically defined by the manufacturers, nor could we define it in our research. However, we can compare data from the literature on the cross-reactivity of both tests. The cross-reactivity of the Sofia test was assessed by the manufacturer by testing various microbes, 16 viruses, and 3 negative matrices. All viruses and microbes were tested in the presence and absence of heat-inactivated SARS-CoV-2. The manufacturers demonstrated the absence of cross-reactivity with all tested microbes.

We can also infer the robustness of the methods. The robustness of the rRT-PCR assay stems from the fact that oligonucleotide primers are capable of close and specific binding to complementary nucleic acid sequences. The method itself is sensitive to contamination and the presence of inhibitors, but good optimization of the method significantly improves its robustness.[16] Automation can also help increase the robustness of the method. The Sofia test is intended for use with a patient, so it is important for the success of the test and the reliability of its results that the method is very robust. The device is portable and analysis can be performed by suitably qualified medical personnel. In the case of the Sofia test, the antibodies of the immune test are capable of close and specific binding to antigens, which significantly contributes to the robustness of the method itself.

The pitfall of both tests is that they are no longer reliable after the concentration of viral RNA and viral antigens falls below the detection limit.[19] The severity of the disease, the timing of sample collection, the types of sample, and sample handling techniques all influence antigen levels in samples.[13] The results discussed in this article were obtained as part of the testing of patients who were brought to 2 different departments of the University Medical Centre Ljubljana. Due to the nature of the testing, sampling and analysis were performed by several different individuals, so the possibility of errors in sample handling cannot be completely ruled out. We also do not possess the information on antigen levels in the samples; therefore, it is also hard to determine whether the difference in observed sensitivity is due to the test performance or the qualities of the samples used in the test.

Despite its shortcomings, rRT-PCR is still considered the gold standard for the diagnosis of SARS-CoV 2. Sources, however, point to shortcomings in diagnostics that rely solely on the detection of nucleic acids, mainly the large inconsistencies and a high rate of false-negative values. As a solution, they suggest combining testing with imaging of thoracic organs and other clinical signs.[19] We wondered whether combining the Sofia test with the rRT-PCR test would reduce these shortcomings. Due to the low detection limit of the Sofia test, combining these 2 methods would probably not significantly help to improve these deficiencies; however, the Sofia test can serve as a rapid screening test, as it can be performed at the point of care in significantly less time than rRT-PCR.

Our results therefore show that the Sofia test meets the standards of a reliable screening test according to the World Health Organization criteria. It shows high sensitivity and specificity, and perhaps most importantly, a high negative predictive value. This study confirms that the Sofia test can be used as a screening test, especially in circumstances that require rapid treatment and triage of patients, as the test can be quickly carried out at the point of care.

Acknowledgments

The authors would like to thank academic Prof. Dr. Tatjana Avšič Županc for collecting the results of the Ct values with her colleagues so that we could perform the necessary calculations.

The study was performed on samples routinely ordered in the context of patient care. Routine laboratory tests are covered by health insurance. There were no additional costs.

We have no conflicts of interest to disclose.

REFERENCES

1. Homza M, Zelena H, Janosek J, et al. Five antigen tests for SARS-CoV-2: virus viability matters. *Viruses.* 2021;13(4):684. doi:10.3390/v13040684.
2. Laboratory testing for 2019 novel coronavirus (2019-nCoV) in suspected human cases. https://www.who.int/publications-detail-redirect/10665-331501. Accessed January 14, 2022.
3. Options for the use of rapid antigen tests for COVID-19 in the EU/EEA - first update. European Centre for Disease Prevention and Control. https://www.ecdc.europa.eu/en/publications-data/options-use-rapid-antigen-tests-covid-19-eueea-first-update. Published October 26, 2021. Accessed January 14, 2022.
4. Cheng MP, Papenburg J, Desjardins M, et al. Diagnostic testing for severe acute respiratory syndrome–related coronavirus-2. *Ann Intern Med.* April 13, 2020:M20–1301. doi:10.7326/M20-1301.
5. Sofia SARS Antigen FIA. | Quidel. https://www.quidel.com/immunoassays/rapid-sars-tests/sofia-sars-antigen-fia. Accessed January 14, 2022.

6. Quidel Sofia 2 SARS Antigen Fluorescent Immunoassay (FIA) - diagnostic tests and controls. Flu and virus testing. https://www.fishersci.com/shop/products/sofia-2-sars-antigen-fluorescent-immunoassay-fia-2/23043151. Accessed January 14, 2022.
7. Kricka LJ, Park JY. Assay principles in clinical pathology. In: VLM McManus, RN. Mitchell (Ur.), eds. *Pathobiology of Human Disease,* pp. 3207–3221. Amsterdam: Academic Press;2014. doi:10.1016/B978-0-12-386456-7.06302-4.
8. Fluorescent Immunoassays. Direct & indirect fluorescent antibody tests. https://www.quidel.com/immunoassays/fluorescent-immunoassays-fia. Accessed January 21, 2022.
9. Nishioka T, Yuan J, Yamamoto Y, et al. New luminescent europium(III) chelates for DNA labeling. *Inorg Chem.* 2006;45(10):4088–4096. doi:10.1021/ic051276g.
10. Optical absorption of hemoglobin. https://omlc.org/spectra/hemoglobin/. Accessed January 21, 2022.
11. Simeonov A, Davis MI. Interference with fluorescence and absorbance. In: Markossian S, Grossman A, Brimacombe K, et al., eds. *Assay Guidance Manual*. Eli Lilly & Company and the National Center for Advancing Translational Sciences; 2004. http://www.ncbi.nlm.nih.gov/books/NBK343429/. Accessed January 14, 2022.
12. IslandPubDev518. Ct values simplified: a practical guide for researchers. https://bitesizebio.com/24581/what-is-a-ct-value/. Published November 17, 2020. Accessed January 14, 2022.
13. Chaimayo C, Kaewnaphan B, Tanlieng N, et al. Rapid SARS-CoV-2 antigen detection assay in comparison with real-time RT-PCR assay for laboratory diagnosis of COVID-19 in Thailand. *Virol J.* 2020;17(1):177. doi:10.1186/s12985-020-01452-5.
14. Saah AJ, Hoover DR. "Sensitivity" and "specificity" reconsidered: the meaning of these terms in analytical and diagnostic settings. *Ann Intern Med.* 1997;126(1):91–94. doi:10.7326/0003-4819-126-1-199701010-00026.
15. Parikh R, Mathai A, Parikh S, Chandra Sekhar G, Thomas R. Understanding and using sensitivity, specificity and predictive values. *Indian J Ophthalmol.* 2008;56(1):45–50. doi:10.4103/0301-4738.37595.
16. Bustin SA, Nolan T. Pitfalls of quantitative real-time reverse-transcription polymerase chain reaction. *J Biomol Tech.* 2004;15(3):155–166.
17. Dabbs DJ. *Diagnostic immunohistochemistry e-book: theranostic and genomic applications*. Philadelphia: Elsevier Health Sciences; 2021.
18. Barra GB, Santa Rita TH, Mesquita PG, Jácomo RH, Nery LFA. Analytical sensitivity and specificity of two RT-qPCR protocols for SARS-CoV-2 detection performed in an automated workflow. *Genes (Basel)* 2020;11(10):E1183. doi:10.3390/genes11101183.
19. Ravi N, Cortade DL, Ng E, Wang SX. Diagnostics for SARS-CoV-2 detection: a comprehensive review of the FDA-EUA COVID-19 testing landscape. *Biosens Bioelectron.* 2020;165:112454. doi:10.1016/j.bios.2020.112454.

SCIENCE

Lean Six Sigma Methodologies to Reduce the Cardiac Troponin Turnaround Time in the Core Laboratory

Niketa M. Vasani, MS, MLS(ASCP)[CM,1*] *Biren D. Patel, MD,*[2] *Brian J. Stanford, DO*[3]

[1]Core Laboratory, Robert Wood Johnson University Hospital, Somerset, New Jersey, USA, [2]St Joseph's University Medical Center, Paterson, New Jersey, USA, [3]Department of Pathology, Robert Wood Johnson University Hospital, Somerset, New Jersey, USA. *To whom correspondence should be addressed. niketaben.vasani@rwjbh.org

Keywords: turnaround time, compliance rate, troponin T, laboratory, lean six sigma, myocardial injury

Abbreviations: TAT, turnaround time; LIS, laboratory information system; DMAIC, define, measure, analyze , improve, control; hs-cTn, high-sensitive cardiac troponin.

Laboratory Medicine 2023;54:e49–e53; https://doi.org/10.1093/labmed/lmac088

ABSTRACT

Objective: Measurement of cardiac biomarker troponin T plays a vital role in the diagnosis of myocardial infarction. A quick turnaround time (TAT) for cardiac troponin T is crucial in managing patients in the emergency department and critical care unit. The goal of the study was to implement Lean Six Sigma methods to improve stat troponin T TAT compliance rate (the time specimen received in the laboratory to the reporting of results through the laboratory information system [LIS]) from 86% to 95% in an 8-month period.

Methods: We conducted a quality and process improvement project to reduce stat troponin T TAT in the core laboratory. We used a 5-stage Six Sigma methodology to simplify the laboratory work process and decrease the TAT by eliminating non-value-added steps. Data from April 2021 (baseline) and January 2022 (improved) are included in the analysis.

Results: In the core laboratory, we improved the TAT for the preanalytical and analytical process by eliminating the batch processing and prioritizing the stat samples. We improved the TAT for the postanalytical process by replacing manual result verification with auto result verification via an LIS. Improved stat troponin T TAT compliance rate has the potential to enhance the overall quality of patient care, especially in the emergency and critical care departments.

Conclusion: Using Lean Six Sigma methodologies in the core laboratory, we successfully improved the stat troponin T TAT compliance rate from 86% to 95% in an 8-month period.

Troponin T is used as a diagnostic marker for myocardial injury. Troponin T is frequently ordered as a stat priority test to manage patients in the emergency department or critical care unit. Delay in troponin test results may be harmful to critically ill patients. Every year, our core laboratory processes around 20,000 stat troponin T samples through all 3 shifts. One of the main quality indicators for our core laboratory is to monitor the TAT for stat troponin T. According to physician and national standard recommendations, the TAT target for Troponin is <60 min. At our facility, the troponin TAT target is set to 45 min from the time of specimen received in the laboratory to the reporting of results through the LIS. In the present study, using Lean Six Sigma methodology, we aim to improve the stat troponin T TAT compliance rate from 86% to 95% in an 8-month time period.

Materials and Methods

The 5-stage Six Sigma DMAIC methodology known as define (define the project), measure (collect the baseline data), analyze (analyze the measured data to reveal and confirm the possible root causes), improve (complete the test run of the solution implemented), and control (monitor the improvement) is used to simplify the project.

Define

We conducted a process walk to simplify and understand the entire process from specimen received in the laboratory to result verification. Based on our observation during the process walk, we divided the entire process into 3 phases: preanalytical, analytical, and postanalytical. The preanalytical phase includes sample collection, sample transportation, sample processing, and preparation. The analytical phase includes loading and running samples on the analyzer. The postanalytical phase includes result verification and releasing of results to the LIS. The process walk showed a potential for removing wasted time during the preanalytical, analytical, and postanalytical processes (**FIGURE 1**).

FIGURE 1 Process walk from specimen received in the laboratory to result verification.

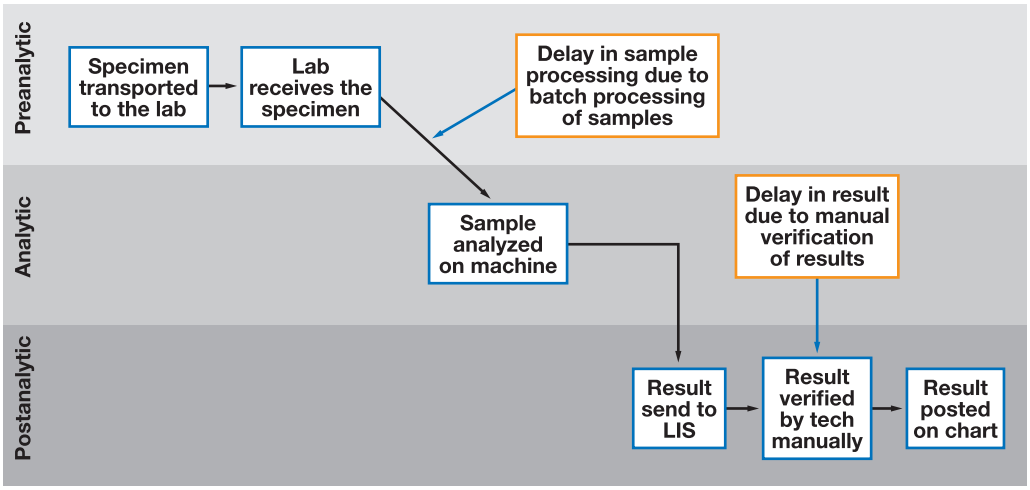

FIGURE 2 Baseline TAT for stat Troponin T (April 2021).

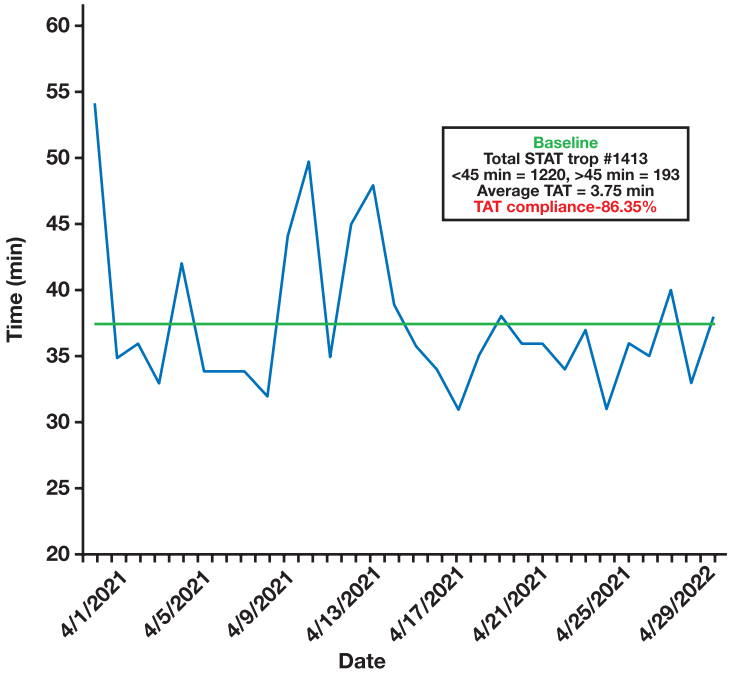

Measure

In the measure phase, we established baseline data for the current stat troponin T TAT compliance rate. Baseline TAT data was collected based on the time of stat troponin T specimen received in the laboratory to the reporting of results to the LIS. Using the LIS, we collected baseline troponin TAT data for April 2021 (**FIGURE 2**). The average TAT for stat troponin T was 37.5 min. The total number of stat troponin T we received in the laboratory was 1413. Out of 1413, 1220 troponin results were released within 45 min and 193 results were delayed over 45 min, which makes a baseline TAT compliance rate of 86%. The baseline stat troponin T TAT compliance rate was calculated using a formula where the number of the stat troponin T results (1220) released within 45 min is divided by the total number of stat troponin T received in the lab (1413), multiplied by 100.

Analyze

We used a fishbone diagram to further analyze the stat troponin T compliance rate. The 5-Why technique was used in combination with a fishbone diagram to discover and organize potential root causes for delayed TAT during preanalytical, analytical, and postanalytical phases of the process (**FIGURE 3**). Based on the fishbone diagram and 5 Why analysis, we derived root-cause hypotheses for each process phase (**TABLE 1**). For the preanalytical phase, we discovered a delay in the loading of stat troponin on the instrument (target 5 min). For the analytical

FIGURE 3 Fishbone diagram and derived hypothesis.

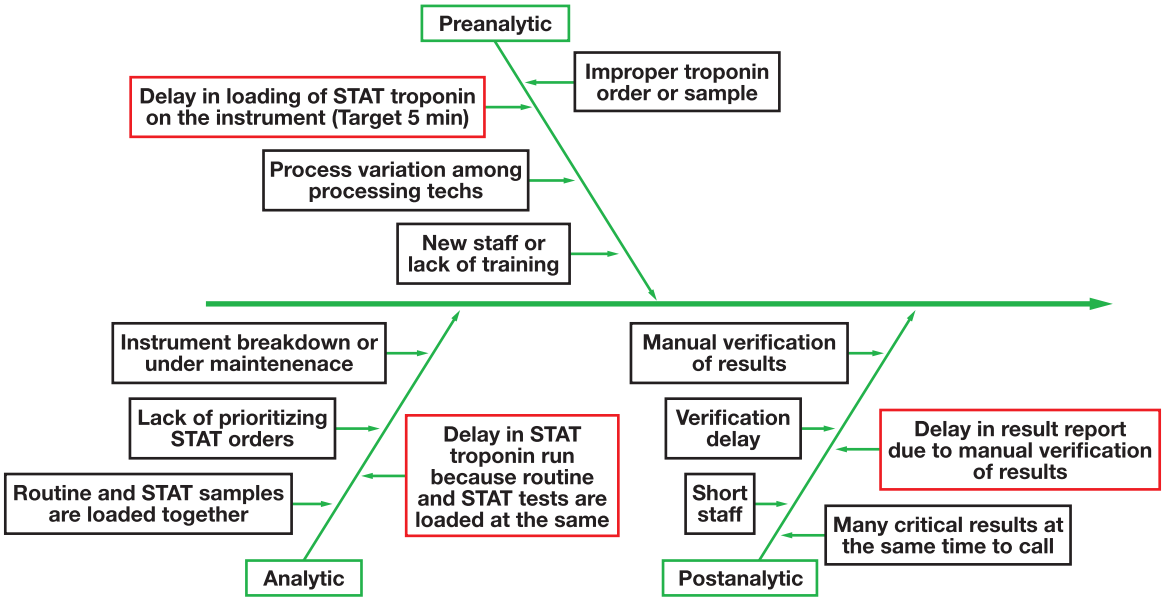

TABLE 1. Root Cause Hypotheses

Possible Root Cause	Root Cause Hypothesis
Preanalytical	1. Delay in loading of stat troponin on the instrument (Target 5 min)
Analytical	2. Delay in stat troponin TAT because routine and stat tests are loaded at the same time on the analyzer
Postanalytical	3. Delay in final result report due to manual verification of results

FIGURE 4 Hypothesis 1: delay in loading of stat troponin T on the instrument (Target 5 min) – true.

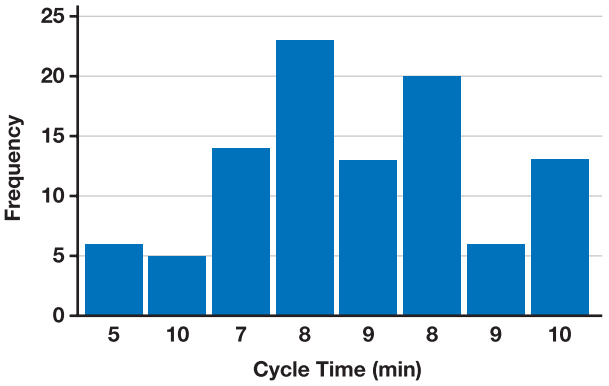

FIGURE 5 Hypothesis 2: delay in stat troponin T run because routine and stat tests are loaded at the same time on the analyzer – true.

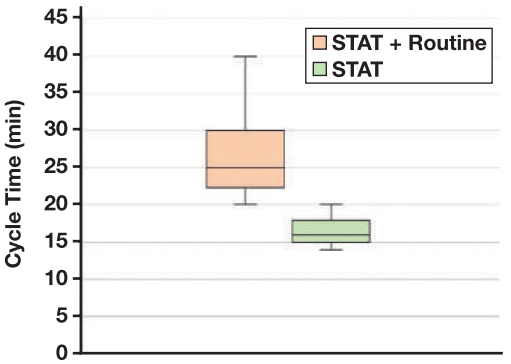

phase, we discovered a delay in stat troponin because routine and stat tests are loaded at the same time onto the analyzer. In the postanalytical phase, we revealed delays in result verification because technologists required manual verification of the results. Using the LIS, we collected baseline data for 100 random stat troponin T samples for preanalytical, analytical, and postanalytical processes. For the preanalytical baseline measure, TAT data from the specimen received to loading on the analyzer time was derived using the LIS system. For the analytical baseline measure, the troponin sample-loading process was monitored visually based on whether the sample was loaded on the stat lane or with routine tests. For the postanalytical baseline measure, TAT data from test completion on the analyzer to releasing results to the LIS was derived using the LIS system. Based on collected baseline data, all 3 hypotheses were created and validated using bar and box plots (**FIGURES 4–6**). The bar chart shows a delay in loading stat troponin T on the analyzer where the majority of samples have a loading time of 8 min (target 5 min) (**FIGURE 4**). The box plot shows the delay in sample run when stat and routine samples are loaded together in the same lane (**FIGURE 5**). The box plot shows a result delay due to manual verification of results by technologists (**FIGURE 6**).

Improve

The improvement includes the determination of solutions for problems identified in the analysis phase. Based on the analyzed hypothesis,

solutions were implemented for each phase of the process. For the preanalytical phase, samples were no longer processed in batches in the processing area. The processing technologist began to prioritize stat samples during sample processing. For the analytical phase, stat samples were no longer loaded with routine tests; stat samples were loaded on the analyzer in the stat lane only. For the postanalytical phase, technologists were no longer required to perform manual verification of test results. A complete result auto-verification system was implemented using the LIS.

Control

After implementing solutions to ensure improvement, TAT data was collected based on the time of stat troponin T specimen received in the laboratory to the reporting of results to the LIS.

FIGURE 6 Hypothesis 3: delay in final result report due to manual verification of results – true.

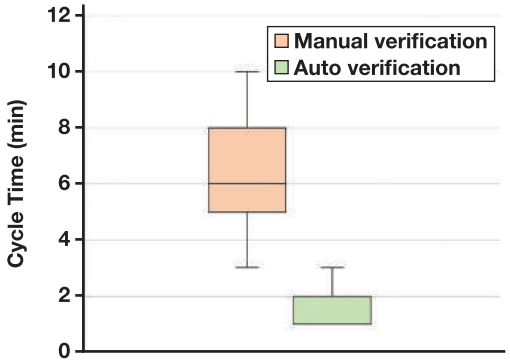

Using the LIS, we collected stat troponin T TAT data for January 2022. The average TAT for stat troponin was 35.55 min. The total number of stat troponin T samples we received in the laboratory was 1568. Out of 1568, 1499 troponin results were released within 45 min and 69 results were delayed over 45 min, a TAT compliance rate of 95%. Improved stat troponin T TAT compliance rate was calculated using the formula where the number of the stat troponin results (1499) released within 45 min was divided by the total number of stat troponin T received in the laboratory (1568), multiplied by 100. A run chart was created to display the overall improvement in the process (**FIGURE 7**).

Conclusion

Using Lean Six Sigma methodologies in the core laboratory, we successfully improved the stat troponin T TAT compliance rate from 86% to 95% by January 2022 (**FIGURE 7**). With this process improvement in the core laboratory, we were able to meet the quality indicator TAT goals for stat troponin T. Teamwork is certainly the key to the entire improvement process. We had no further complaints from healthcare professionals about the delay in troponin results. The improvement in the processing of stat samples helped to improve overall patient care as well as increasing physician satisfaction, especially in the emergency department and critical care unit. Lean Six Sigma is an approach for future consideration to improve other areas of the laboratory.

High-sensitive cardiac troponin (hs-cTn) is a novel biomarker of myocardial injury and can be used to expedite patient evaluation in the emergency department. Some hs-cTn assays have a total assay run-time of 9–11 min, whereas other contemporary troponin assays have up to 20-min assay run-time. Currently, we do not perform hs-cTn in our core laboratory and

FIGURE 7 Run chart shows an improvement in the overall stat troponin T compliance rate.

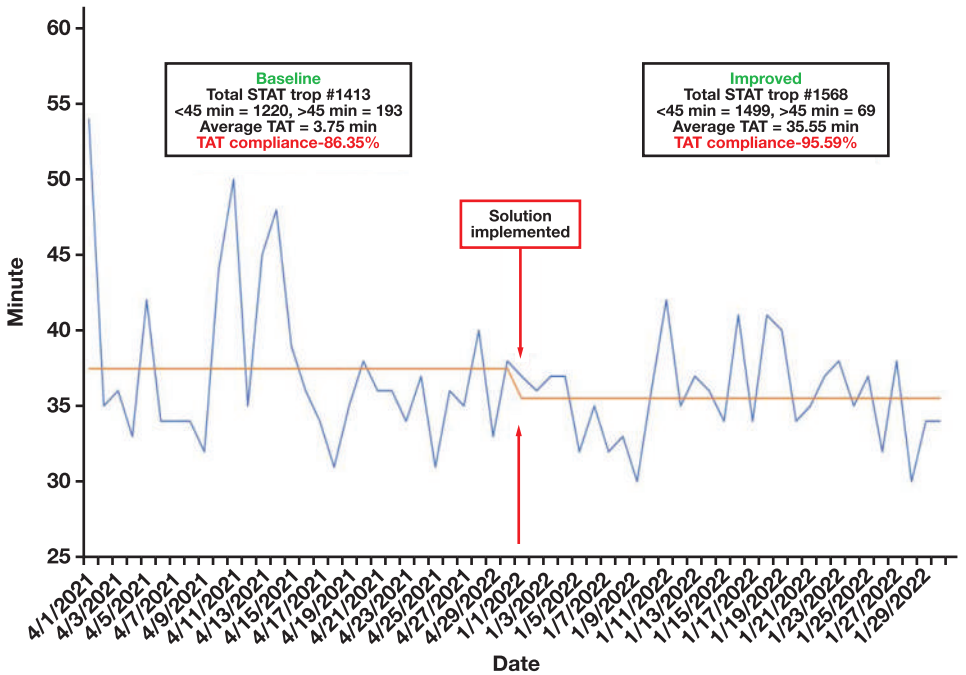

implementing hs-cTn may not be beneficial in terms of improving TAT, since our current troponin T assay also has 9 min total assay runtime on the Roche analyzer. However, considering that hscTn assays are more precise in their analytical sensitivity and can detect a lower level of cTn in the blood compared with other contemporary assays, it is a test for future consideration for expediting patient evaluation.

Acknowledgments

The authors give special thanks to Robert Wood Johnson University Hospital Somerset management.

No funding was received for conducting this study.

The authors have no conflict of interests to disclose that are relevant to the content of this article.

SCIENCE

Performance of High Throughput SARS-CoV-2 Antigen Testing Compared to Nucleic Acid Testing

Octavia Peck Palmer, PhD,[1] Joanne H Hasskamp, MS,[2] Hae-Sun La, MD,[3] Pranav Pramod Patwardhan, MD,[3] Shmyle Ghumman, MS,[3] Vandana Baloda, MD,[3] Yujung Jung, MD,[3] Sarah E Wheeler, PhD[4,]*

[1]Departments of Pathology and Critical Care Medicine, University of Pittsburgh, Pittsburgh, PA US, [2]Department of Pathology, University of Pittsburgh, Pittsburgh, PA US, [3]Department of Pathology, University of Pittsburgh Medical Center, Pittsburgh, PA US, [4]Department of Pathology, University of Pittsburgh and University of Pittsburgh Medical Center, Pittsburgh, PA US; *To whom correspondence should be addressed. wheelerse3@upmc.edu

Keywords: SARS-CoV-2, COVID-19, antigen

Abbreviations: COV2Ag, SARS-CoV-2 antigen; NAAT, nucleic acid amplification tests; Ct, cycle threshold; CI, confidence interval.

Laboratory Medicine 2023;54:e54–e57; https://doi.org/10.1093/labmed/lmac107

ABSTRACT

Objective: Independent assessment of SARS-CoV-2 antigen (COV2Ag) tests remains important as varying performance between assays is common. We assessed the performance of a new high-throughput COV2Ag test compared to SARS-CoV-2 nucleic acid amplification tests (NAAT).

Methods: A total of 347 nasopharyngeal samples collected from January to October 2021 were assessed by NAAT as part of standard-of-care testing (CDC LDT or GeneXpert System, Cepheid) and COV2Ag using the ADVIA Centaur CoV2Ag assay (Siemens Healthineers).

Results: Among NAAT positive specimens we found 82.4% agreement and in NAAT negative specimens we found 97.3% agreement (overall agreement 85.6%). In symptomatic persons, COV2Ag agreed with NAAT 90.0% (n = 291), and in asymptomatic persons, 62.5% (n = 56). Agreement between positive NAAT and COV2Ag increased at lower cycle threshold (Ct) values.

Conclusion: The COV2Ag assay exceeded the World Health Organization minimum performance requirements of ≥ 80% sensitivity and ≥ 97% specificity. The COV2Ag assay is helpful for large scale screening efforts due to high-throughput and reduced wait times.

Consistent emergence of new variants of concern in the COVID-19 pandemic requires clinical laboratories to continue SARS-CoV-2 clinical testing even in the face of widespread vaccine availability in many countries. Nucleic acid amplification tests (NAAT) remain the most sensitive testing clinically available for the detection of SARS-CoV-2 infection. The SARS-CoV-2 antigen (COV2Ag) tests are critical in supporting efforts to identify infections and control the transmission of the virus. They are generally more portable, faster, easier to perform, and tend to detect infection in people most likely to have transmittible infection.[1,2] These COV2Ag tests are an important component of a comprehensive mitigation strategy for SARS-CoV-2 spread as they offer the ability to quickly screen people participating in activities with high transmissibility risk, protect immune compromised populations, and mitigate risk in health care settings.[1–4] High-throughput COV2Ag tests allow maximization of resources for many of these risk mitigation strategies.[1,5]

Independent assessment of SARS-CoV-2 antigen tests remains important as varying sensitivity and specificity between assays is common and standard regulatory assessments have not been possible in the face of the COVID-19 pandemic.[1,2,5] Additionally, clinical laboratory-based COV2Ag tests allow for better analytic control and improved sensitivity and specificity.[5] We leveraged banked samples to assess the performance and understand the limitations of a new high-throughput COV2Ag test compared to SARS-CoV-2 nucleic acid tests in a large urban hospital system.

Materials and Methods

Cohort

Remnant nasal and nasopharyngeal swabs in viral transport media following NAAT for SARS-CoV-2 were stored at −80°C until use (the longest storage time was 1 year). The NAAT-positive samples were collected from 3 time periods representing distinct variants of SARS-CoV-2 as determined in our patient population: January 1 to 20, 2021 (pre-alpha variant predominance; n = 136; pre-alpha), April 30 to June 7, 2021 (alpha variant B.1.1.7 predominance; n = 35; alpha), and September 14 to October 24, 2021 (delta variant predominance; n = 101; delta). Negative cases were collected from December 5 to 9, 2021 (n = 75) as negative cases were not banked as part of our institutional protocol. The SARS-CoV-2 NAAT was performed as part of standard-of-care testing on the CDC LDT as previously described[6] or the GeneXpert System using either

the Xpert Xpress SARS-CoV-2 or SARS-CoV-2/Flu A/Flu B/RSV (Cepheid, Sunnyvale, CA, USA). In cases where more than 1 cycle threshold (Ct) value was produced by the NAAT, the lowest value was considered for comparison purposes.

Minimum necessary clinical variables were obtained via chart review. The electronic medical record at our institution includes a required field for SARS-CoV-2 testing purpose. This field was used to distinguish symptomatic from asymptomatic as many patients did not have sufficient documentation to further stratify by disease severity, outcomes, or specific symptomatology. Available choices for this SARS-CoV-2 testing purpose field include preprocedural, test required for facility transfer, symptomatic patient, test required prior to inpatient hospice, testing required prior to returning to work, close contact with COVID-19 patient, and unknown. Demographic and applicable disease information are summarized in **TABLE 1**. This work was performed under the auspices of the University of Pittsburgh Institutional Review Board Study #20040220.

Testing

All testing was performed in the College of American Pathologists-accredited University of Pittsburgh Medical Center Clinical Laboratories in compliance with local regulations for patient testing. Specimens were thawed, aliquoted, and neutralized per manufacturer instructions. Briefly, 1 mL of sample was incubated with 2 drops of lysis reagent for 15 minutes before storage at −20°C for 3 weeks prior to testing.

The ADVIA Centaur CoV2Ag assay is an automated sandwich immunoassay that uses mouse monoclonal antibodies to detect SARS-CoV-2 nucleocapsid antigen and provides an index value with a threshold of > 1.0 being reactive. All samples were thawed and tested on the same day. Calibration and quality control materials were within manufacturer's specifications. Precision was verified using 10 replicates of standard material at 2 levels with a resulting coefficient of variation of 30.1% (mean 0.150) for negative and 0.6% (mean 204.46) for high materials.

Analysis

Data was collected and collated using Excel (Microsoft Corporation, Redmond, WA, USA), and R Studio 2021.09.0 Build 351 with R version 4.1.1. Analyses were performed in Excel, R Studio, and GraphPad Prism 7 (GraphPad Software, San Diego, CA, USA). Subgroup comparisons were analyzed using the Mann-Whitney nonparametric rank sum test. Box-and-whisker plots are plotted using the Tukey method.

Results

We found that overall COV2Ag had 85.6% agreement with NAAT (n = 347; 95% confidence interval [CI] 81.5–89.1). Agreement between COV2Ag and NAAT among time periods sampled had overlapping CIs. Specifically, pre-alpha 82.4%(95%CI 74.9–88.3), alpha 65.7% (95%CI 47.8–80.9), and delta 88.1% (95%CI 80.2–93.7). Among NAAT positive patients we found 82.4% agreement (n = 272; 95%CI 77.3–86.7) and in NAAT negative patients, we found 97.3% agreement (n = 75; 90.7–99.7). In the 2 COV2Ag-positive and NAAT-negative specimens, the COV2Ag index values were < 1.4 (positive threshold > 0.99).

Among symptomatic subjects, COV2Ag agreed with NAAT 90.0% (n = 291; 95%CI 86.0–93.2), and among asymptomatic subjects, there was 62.5% (n = 56; 95%CI 48.5–75.1) agreement. The Ct values for NAAT positive samples were significantly different between symptomatic and asymptomatic subjects, with mean values of 22.6 (n = 232) and 31.3 (n = 40), respectively (P = 9.03E-08, **FIGURE 1A**). Agreement between positive NAAT and COV2Ag increased at lower Ct values (**FIGURE 1B**). There was 90.8% agreement for Ct values < 35 (n = 240; 95%CI 86.5–94.2), 98.1% agreement for < 30 cycles (n = 213; 95%CI 95.3–99.5), and 100% agreement for < 25 cycles (n = 177; 95%CI 97.9–100). Concordance between positive NAAT and COV2Ag was low at higher Ct values, with 25.4% agreement for Ct values > 30 cycles (n = 59, 95% CI 15.0–38.4) and 19.4% agreement for Ct values > 35 cycles (n = 31, 95% CI 7.5–37.5).

Concordance between COV2Ag and NAAT, when assessed for days from symptom onset, demonstrated insignificant variation between days with overlapping confidence intervals (**FIGURE 1C**). Median Ct values among NAAT positive symptomatic patients had little variation between days −1 (1 patient tested positive before a procedure with symptom onset the following day) and day 7. The increase after day 7 may be due to the small sample number collected after day 7, as reflected in the wide confidence interval (**FIGURE 1C**).

TABLE 1. Demographics and clinical characteristics

	Total Cohort	NAAT Positive	NAAT Negative
Total number (%)	347 (100%)	272 (78%)	75 (22%)
Female, n (%)	207 (60%)	172 (63%)	35 (47%) [a]
Male, n (%)	139 (40%)	100 (37%)	39 (52%) [a]
Age median (IQR)	51 (32–66)	47 (31–62)	64 (49–73)
Symptomatic, n (%)	291 (84%)	232 (85%)	59 (79%)
Asymptomatic, n (%)	56 (16%)	40 (15%)	16 (21%)
Transfers, n (%)	42 (12%)	31 (11%)	11 (15%)
pre-alpha, n (%)	136 (39%)	136 (50%)	NA
alpha, n (%)	35 (10%)	35 (13%)	NA
delta, n (%)	101 (29%)	101 (37%)	NA

NA, not applicable.
[a]One NAAT Negative subject was of unknown gender.

Discussion

We found that the COV2Ag assay exceeded the WHO minimum performance requirements of ≥ 80% sensitivity and ≥ 97% specificity for SARS-CoV-2 antigen assays.[7] The overlapping confidence intervals between variant collection times indicated reasonably comparable detection between variants, likely due to the multiple monoclonal antibody nature of the assay. The data also reassured us that at −80°C, the banked samples were stable for over 1 year. The alpha portion of our cohort was underrepresented with approximately one-third the sample size of the pre-alpha and delta collection time periods. This is reflected in the large confidence interval, and there may be differences in detection between these variants that our study was not sufficiently powered to observe.

As with other groups, we found that antigen assay agreement with NAAT was higher at lower Ct values.[2,4,5,8] There is ongoing debate around the use of high Ct values in SARS-COV-2 NAAT to indicate current SARS-COV-2 positivity because high Ct values can persist for months following SARS-COV-2 infection, potentially reflecting detection of viral RNA but not infectious viral particles.[9–12] We found no significant differences in percent agreement between COV2Ag and NAAT in symptomatic

FIGURE 1. Comparison of SARS-CoV-2 nucleic acid amplification test Ct values between cohort subcategories. A, NAAT positive symptomatic cases (n = 232) compared to asymptomatic cases (n = 40) Ct values. Tukey box and whisker plot. Mann-Whitney *P* < .0001. B, NAAT-positive Ct values for discordant (n = 48) and concordant (n = 224) samples between NAAT and COV2Ag. Tukey box and whisker plot. Mann-Whitney *P* < .001. C, Cohort parsed into days from symptom onset and percent agreement and NAAT median Ct values compared. Bars indicate percent agreement between NAAT and COV2Ag, left y-axis; line indicates NAAT-positive median Ct value, right y-axis. n(95%CI) for days –1 to 1 through 8 to 10, respectively: 103(84.1–95.9), 89(79.0–93.7), 61(81.9–97.3), 24(78.9–99.9), 10(34.8–93.3).

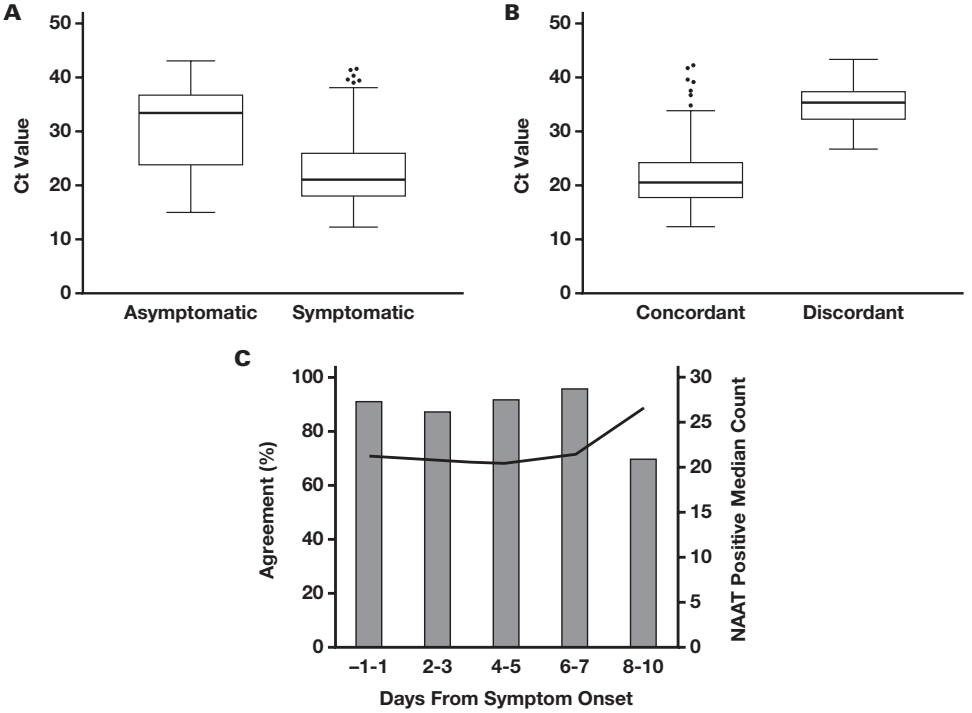

patients when assessing by days from symptom onset. This is likely a reflection of the similar median Ct values for each of these groups.

The COV2Ag assay has been considered helpful for large scale screening efforts due to high-throughput and reduced wait times as well as for procedural screening prior to patient surgery or care facility transfers, which benefit from faster turnaround times to free hospital space. For screening efforts in asymptomatic persons, it is notable that agreement with NAAT is reduced in our and other's studies,[5,13] which may reflect the higher Ct values noted in these cases (**FIGURE 1A**). Ultimate implementation with appropriate utility should be determined by local laboratory and clinical medical directors.

Acknowledgments

Donna Bush BS, MT(ASCP), Gina Pillage BS MT CHT, Melissa McCullough MLS(ASCP)^{CM}, Ashley Mays MLS(ASCP)^{CM}, Jamie Gribschaw MT(ASCP) are acknowledged for their assistance and expertise.

Funding

Siemens Healthineers provided some funding for this work.

Conflict of Interest

SW and OPP have received speaking honoraria from Siemens Healthineers.

REFERENCES

1. Peeling RW, Heymann DL, Teo YY, Garcia PJ. Diagnostics for COVID-19: moving from pandemic response to control. *Lancet.* 2022;399(10326):757–768. doi:10.1016/S0140-6736(21)02346-1.
2. Kohmer N, Toptan T, Pallas C, et al. The comparative clinical performance of four SARS-CoV-2 rapid antigen tests and their correlation to infectivity in vitro. *J Clin Med* 2021;10(2):328.
3. Bays D, Whiteley T, Pindar M, et al. Mitigating isolation: the use of rapid antigen testing to reduce the impact of self-isolation periods. *Medrxiv*. 2021;2021.12.23.21268326.
4. Schrom J, Marquez C, Pilarowski G, et al. Comparison of SARS-CoV-2 reverse transcriptase polymerase chain reaction and BinaxNOW rapid antigen tests at a community site during an omicron surge. *Ann Intern Med.* 2022;175(5):682–690.
5. Khalid MF, Selvam K, Jeffry AJN, et al. Performance of rapid antigen tests for COVID-19 diagnosis: a systematic review and meta-analysis. *Diagnostics.* 2022;12(1):110. doi:10.3390/diagnostics12010110.
6. Mitchell SL, Ventura SE. Evaluation and comparison of the hologic aptima SARS-CoV-2 assay and the CDC 2019-nCoV real-time reverse transcription-PCR diagnostic panel using a four-sample pooling approach. *J Clin Microbiol.* 2020;58(12):e02241-20.
7. World Health Organization. COVID-19 target product profiles for priority diagnostics to support response to the COVID-19 pandemic v.1.0. Target product profiles for priority diagnostics to support response to the COVID-19 pandemic. 2020 Available from: https://www.who.int/publications/m/item/covid-19-target-product-profiles-for-priority-diagnostics-to-support-response-to-the-covid-19-pandemic-v.0.1. Accessed May 13, 2022.

8. Weitzel T, Legarraga P, Iruretagoyena M, et al. Comparative evaluation of four rapid SARS-CoV-2 antigen detection tests using universal transport medium. *Travel Med Infect Dis.* 2020;39:101942.
9. Trisnawati I, Khair RE, Puspitarani DA, Fauzi AR, Gunadi. Prolonged nucleic acid conversion and false-negative RT-PCR results in patients with COVID-19: a case series. *Ann Med Surg.* 2020;59:224–228.
10. Vibholm LK, Nielsen SS, Pahus MH, et al. SARS-CoV-2 persistence is associated with antigen-specific CD8 T-cell responses. *Ebiomedicine.* 2021;64:103230. doi:10.1016/j.ebiom.2021.103230.
11. Recalde-Zamacona B, Tomás-Velázquez A, Campo A, et al. Chronic rhinosinusitis is associated with prolonged SARS-CoV-2 RNA shedding in upper respiratory tract samples: a case-control study. *J Intern Med.* 2021;289(6):921–925. doi:10.1111/joim.13237.
12. Bullard J, Dust K, Funk D, et al. Predicting infectious SARS-CoV-2 from diagnostic samples. *Clin Infect Dis*. 2020;71(10): ciaa638-.
13. Torres I, Poujois S, Albert E, Álvarez G, Colomina J, Navarro D. Point-of-care evaluation of a rapid antigen test (CLINITEST® Rapid COVID-19 Antigen Test) for diagnosis of SARS-CoV-2 infection in symptomatic and asymptomatic individuals. *J Infect.* 2021;82(5):e11–e12. doi:10.1016/j.jinf.2021.02.010.

SCIENCE

The Impact of COVID-19 on the Laboratory Professionals' Clinical Education: a Qualitative Study

Heather L Phillips, PhD, MLS(ASCP)CM, MT(AMT),[1,] Shelley R Latchem, MS, MLS(ASCP)CM,[2] Theresa Crutcher, MA, RT(R),[3] Timothy A Catalano, MA, RT(T),[4] Eleanor K. Jator, PhD, MLS(ASCP)CM[5]*

[1]Medical Laboratory Science Program, Austin Peay State University, Clarksville, Tennessee, US, [2]Department of Medical and Clinical Laboratory Sciences, Auburn University at Montgomery, Montgomery, Alabama, US, [3]Radiology Technology Program, Austin Peay State University, Clarksville, Tennessee, US, [4]Radiation Therapy Program, Austin Peay State University, Clarksville, Tennessee, US, [5]Medical Laboratory Science Program, Austin Peay State University, Clarksville, Tennessee, US. *To whom correspondence should be addressed. phillipsh@apsu.edu

Keywords: Clinical educator, preceptor, preceptor training, medical laboratory science, clinical education, COVID-19

Abbreviations: MLS, medical laboratory science; PPE, personal protective equipment,

ASCP, American Society for Clinical Pathology; CDC, Centers for Disease Control.

Laboratory Medicine 2023;54:e58–e62; https://doi.org/10.1093/labmed/lmac110

ABSTRACT

A 48-question survey was developed and disseminated to laboratory professionals. This survey sought the perspective of clinical educators on a variety of topics, including two open-ended questions on the impact COVID-19 had on student clinical rotations and the ensuing policy changes. Of 207 clinical sites that participated in the survey., Some terminated student clinical rotations without offering any other training alternative. Others employed a number of strategies such as shortening the length of clinical rotations, taking fewer students, transitioning to an online learning platform, or delaying training until a future date. Some mandated regular illness checks, symptom checks, and COVID-19 testing when available. Clinical educators expressed concern over the lack of continuity of student clinical training, policy changes related to COVID-19 and student training that were deemed to diminish the quality of the students' clinical education. With terminated, delayed or shortened clinical rotations at many sites, in combination with staff and supply shortages, clinical educators were concerned about the overall quality of clinical education the students were receiving. In addition to these concerns, the reduction of student graduates during the pandemic decreased the number of applicants for job vacancies exasperating a pre-pandemic problem.

As the COVID-19 pandemic has overwhelmed healthcare systems globally over the past 2 years, shortages of healthcare workers in every sector have reached crisis levels. Lazenby[1] notes that world trends such as an aging population, globalization, and urbanization indicate that fast-moving outbreaks of novel viruses will increase in number, and health service providers will not be able to meet the patient-care demands this portends. As educational institutions endeavor to meet the demands of the healthcare workforce by graduating qualified practitioners in medical laboratory science (MLS), respiratory therapy, radiologic technology, and nursing, the pandemic has presented many challenges. Across the spectrum of allied health training programs, hands-on practice in a suitable healthcare environment is seen as a core component of producing well-rounded practitioners in any healthcare field, as Dario and Simic[2] emphasized.

During the pandemic, clinical placements were disrupted or delayed due to many contributing factors, which negatively affected students' learning and the readiness of graduates to join the healthcare workforce. As Dewart[3] discussed, educational programs had to make difficult decisions about whether or not to continue clinical courses in consideration of student safety. Dario and Simic[2] highlighted that for other programs, the decision was forced on the educational program as clinical sites paused or cancelled student placements in clinical sites and attributed this reaction to patient load, the shortage of personal protective equipment (PPE), and concerns that students might contract and spread the virus. As the pandemic spread, educators were faced with adapting quickly to the new realities associated with the pandemic, and much of the current literature that addresses the impact of the pandemic is focused on the adaptations to the classroom learning environment, with less attention given to the impact on clinical placement and experiences. This article is focused on the challenges to clinical education from the perspective of the clinical educators and seeks to identify the sources of the challenges and the short-term and long-term effects on medical laboratory professionals.

Materials and Methods

Detailed methodology can be found in "Establishing the Need for Clinical Educator Training for Laboratory Professionals" in *Laboratory Medicine*. This is the second publication from this dataset.

Research Design

There were 48 questions developed by our research team and placed on an electronic questionnaire. The questions originated from clinical

educator and student questions and concerns as well as a literature review. The questionnaire was validated before its electronic distribution. The American Society for Clinical Pathology (ASCP) distributed the survey electronically to laboratory professionals. The survey was distributed on March 8, 2021, and was closed 6 weeks later on April 16, 2021. The data was then compiled and analyzed to find common themes and categories.

Data Analysis

Reliability of the questionnaire was determined by calculating Cronbach's alpha (0.935), which is used to measure the internal consistency among questions. Two open-ended questions were analyzed:

- What impact has the COVID-19 pandemic had on your ability to train students?
- What is your hospital's policy on accepting students for clinical training during the COVID-19 pandemic?

A thematic analysis was performed as described by Braun and Clarke[4] for the open-ended questions. Dummy codes initially assigned to the data were used to identify themes and subthemes or categories. Validity of final themes were enhanced with communication between research team members. The Institutional Review Board at Austin Peay State University approved this research under IRB # 0-066.

Results

Of the 207 participants, 110 responded to 2 open-ended questions. From these open-ended questions, 3 common themes emerged: clinical facilities' continuity of student training during the COVID-19 pandemic, policy changes that were changed or implemented for students during the COVID-19 pandemic, and concerns for the quality of the clinical education provided.

Fifty-nine clinical sites and associated MLS programs explained the greatest hindrance to a student's clinical education during COVID-19 was the termination of clinical rotations. The other 148 clinical sites worked to keep students either attending or involved in their clinical rotations. Common categories were noted by the participants who continued to work with students through the COVID-19 pandemic along with their frequencies (**FIGURE 1**).

Another theme that presented among participant responses was policy changes regarding students as a result of the COVID-19 pandemic. There were common categories noted by the responses to policy changes listed by participants. These can be found in **TABLE 1**. A majority of participants explained the main policy changes involved requiring students to adhere to infectious disease safety protocols, such as wearing a mask. Other practices implemented by policy included face shields, social distancing, daily temperature checks, and symptom questionnaires.

The last theme noted was that many clinical educators had concerns for students who attended their clinical education in person during the COVID-19 pandemic. The most frequently cited concern among clinical educators was the impact of the pandemic on the quality of training the students received due to staff shortages and limited supplies, among other things. Other clinical educators expressed concern for the shortened clinical rotations. A full list of the categories of concerns can be found in **TABLE 2**.

Discussion

Fifty-nine participants explained the greatest hindrance during the COVID-19 pandemic was that students were not allowed to attend clinical training and in these cases, participants did not provide an alternate training solution for the students. According to Lazenby,[1] some healthcare providers closed their doors to students due to overwhelming patient demand and critical shortage of personal protective equipment. One participant indicated that students were given the ability to test out of clinicals when their program was shut down. This provided an easy solution where students who had the required knowledge were exempt. The participant did not explain what happened if a student's program was shut down and the student was not able to test out of their clinical training. As explained many times by clinical educators in this survey, face-to-face training is an important part of medical laboratory professional education and outside of the COVID-19 pandemic, this would likely not be an acceptable course of action. Dario and colleagues[2] indicate that clinical experience is a core component of the healthcare curriculum. Another clinical educator stated, "students were still able to come to the [clinical laboratory] during lock down because the students were considered essential." One clinical educator indicated that their students dropped from their medical laboratory program during the COVID-19 pandemic. This is an unfortunate and extreme course of action, but perhaps for those clinical sites who still required student attendance, this may have been a request some students could not meet. This may have been due to personal fears regarding the pandemic, inability to find childcare, or the inability to afford to drive to a nonpaid clinical rotation during the pandemic. The cause was not disclosed by the clinical educator, but this is a reminder of the life-altering effects the COVID-19 pandemic had on students at the onset or during times of lockdown. Lazenby[1] expanded on another approach, that of healthcare providers hiring students to battle overwhelming staffing shortages, although none of the participants in this survey referenced that practice.

Of the 10 participants who stated that their clinical sites accepted fewer students during the COVID-19 pandemic, two participants detailed their student reduction. One participant indicated that their clinical site reduced their student intake by 75%. Another participant stated that before the pandemic, their clinical site took 3 students. After the COVID-19 pandemic began, their employer reduced this number to 1 student. Many clinical sites have several open and ready-to-fill medical laboratory professional positions. By reducing the number of students trained at their facility, ultimately the clinical site is reducing the number of graduates that could apply for those open positions. One participant reported an increase in requests to take students but provided no rationale. This is likely due to the reduced number of clinical sites willing to take students during the COVID-19 pandemic resulting in students being reassigned to sites able to continue their training.

Three participants stated that student training was delayed at their clinical site without providing additional information. Anderson[5] states that the theoretical and practical learning separation due to delays in real-world experience can adversely affect student learning and retention. However, 1 participant noted that students who tested positive for COVID-19 required a delay in clinical training until the next clinical rotation of students. This prevented the clinical educator and the MLS academic program from the need to track lost clinical training hours and coordinate make-up time. Although this was true for this clinical site, 1 participant indicated that the [clinical educators] were required to be flexible with the student's make-up hours if the student contracted

FIGURE 1. Student attendance and clinical site's pandemic return policy

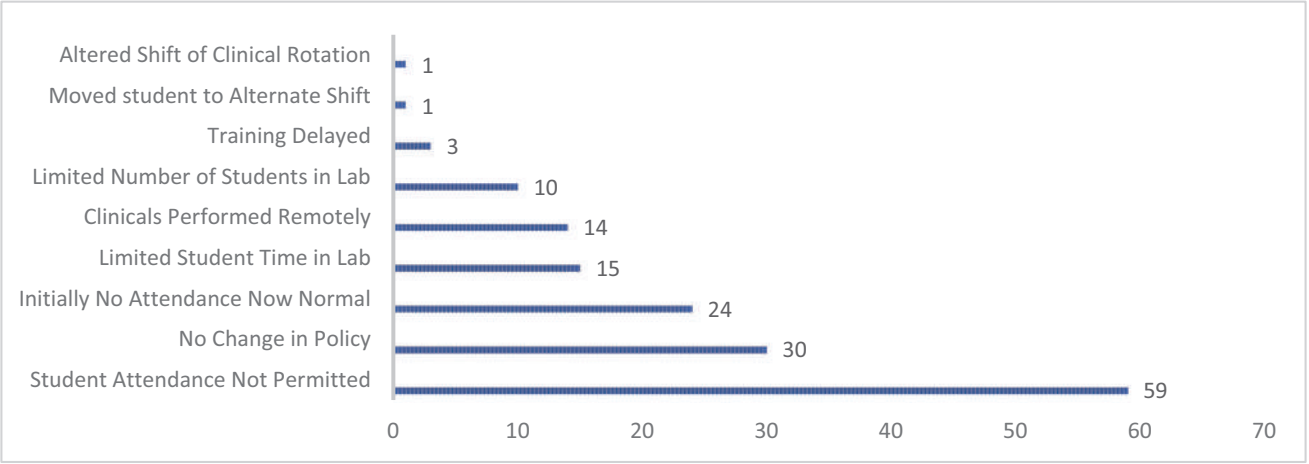

TABLE 1. Student Related Policy Changes Caused by COVID-19 Pandemic

Theme	Subthemes	Participant Response	Number of Participants
Policy changes	Illness screening • Frequency	Require daily temperature check, symptom questionnaire, etc., to attend	12
	Safety protocols • PPE • Patient contact	Require masking, eye protection or face shield, and social distancing to attend	18
		Students are no longer allowed patient contact	1
		Students are no longer afforded the ability for make-up days	1
	COVID vaccination	Require COVID-19 vaccination to attend	2
	COVID testing • Frequency	Require regularly scheduled COVID-19 testing to attend	2

TABLE 2. Clinical Educator Concerns When Students Attended During COVID-19 Pandemic

Theme	Subtheme	Participant Response	Number of Participants
Concerns about quality of education	Staff and supply shortages • Trainers • PPE • Lab supplies	Significant impacts to training quality due to staff shortages, limited supplies, and additional COVID-19 related responsibilities	9
		Not enough personal protective equipment for students	2
	Shortened rotations	Shortening student's time in clinical laboratory decreases the quality of their education	3
	COVID-19 policy-related hindrances to education • Nonverbal communication • Proximity	Mask wearing inhibits non-verbal communication with the student (Example: The mask inhibits the approving smiles from the clinical educator.)	2
		Unable to effectively adhere to social distancing policies while training	4

COVID-19. Another clinical educator had an entirely different perspective. This individual's clinical site forbade the student from making up hours, regardless of whether the absence was related to a COVID-19 illness or not.

Seven participants reported the amount of time each student trained was reduced. One participant further elaborated by explaining that before the COVID-19 pandemic, students stayed in each clinical rotation for 6 weeks. During COVID-19, rotations were reduced to 3 weeks. One clinical educator stated that student training was changed to an alternate shift. A different clinical educator reported requesting a student be moved to either second shift or a weekend shift for training. Often the idea behind moving students to an alternate shift is that the student can receive more individual attention from the assigned clinical educator. Given the desperate need for clinical laboratory staff and shortages of supplies, these problems are likely encountered on any shift. There may be some benefits to the student training on an alternate shift, but at this time no data in the literature exists.

Fourteen clinical sites transitioned to an online learning platform during the COVID-19 pandemic. This was accomplished by several modalities. Many clinical educators livestreamed their work while performing testing. Students would watch their clinical educators perform patient testing, quality control, calibration, and instrument maintenance during their daily routine. When the opportunities arose, the clinical educators would provide theoretical concepts or a detailed response to the testing they were performing. Sometimes clinical educators would record short segments of examples from patient testing they found critical to student success. Some clinical educators also created a compilation of instrument maintenance videos and procedure videos accessed using online resources. Often, these livestreams and video segments were accompanied by patient case studies. Some clinical educators were quick to point out that this type of training significantly affects the quality of education the MLS student receives and often further commented on the importance of face-to-face training. One participant stated that they only performed online clinical training for microbiology. This is likely due to the limited availability of clinical sites that have full clinical microbiology departments.

Two of the thirteen participants who indicated that there was no impact to MLS clinical education provided further evidence of their operations to maintain student attendance. One participant stated that the university the students attended required all clinical students to receive COVID-19 testing regularly. The clinical site allowed student attendance based on this COVID-19 testing schedule implemented by the university and proof of a negative test result. One participant indicated that the clinical site required regular testing of the students and further explained that students were prioritized for COVID-19 vaccination once the vaccine was made available. Implementing these policies prevented the interruption of student attendance at their clinical site during the COVID-19 pandemic.

Another challenge clinical educators encountered was lack of PPE for students. Although the students were practicing in the same environment as clinical laboratory professionals and their clinical educators, the students were not provided the same protections as clinical staff. National PPE shortages and exorbitant costs caused clinical sites to implement policies to reduce the usage of PPE. Lazenby[1] referenced the shortage of PPE and how it negatively affected clinical placement availability for nursing students. Two participants stated there was not enough PPE for students. Another participant said that students were deployed to patient floors to help prevent clinical staff from doffing PPE. Participants indicated that students took on the role of "runners and messengers." In addition to these personal protection deficiencies, 4 participants indicated that it was difficult to maintain the social distancing required by policies while attempting to train students. Although these clinical educator comments focused on concerns over protecting the students, one clinical educator explained "students did not take the infectious disease [protocols] seriously" and had concerns about his or her own wellbeing as well as the students'. A different clinical educator whose clinical site continued to take students during the COVID-19 pandemic stated, "the school prefers [students] not to go into COVID-19 rooms, but our [students] do anyway because they're not worried about [contracting COVID-19]. They know it comes with the job when they get a COVID-19 patient and the fact that we run the COVID tests, as well." Two clinical educators were not supportive of wearing masks as they felt the masks inhibited nonverbal communication with the students. In other words, students could not tell if their clinical educators were smiling in approval or simply observing their student's work. Another clinical educator said, "Observing social distance and mask wearing has made it more difficult to be 'hands-on' and ensure the student understands effectively." Students are present and handling samples in the same environment as their clinical educators. Students should be provided the same protections through either their clinical sites or through their academic institutions.

One clinical educator stated that the quality of the student was diminished. This is not seen only in medical laboratory professionals but also in multiple other levels of education and specialties. The United States Department of Education defended the return of students from online learning during the COVID-19 pandemic to brick-and-mortar learning by referencing a substantial 10-point drop in math improvement scores across the United States.[6] After the COVID-19 pandemic concludes, it is likely institutional cohort studies will reflect a similar effect caused by the rapid and unprepared transition from in-person learning to online learning. Clinical educators also pointed out the quality of clinical education students were receiving was diminished. Three clinical educators felt this was due to their clinical site's reduced time in a clinical rotation. One participant indicated this is happening because there are not enough medical laboratory professionals to train students on the bench. Two clinical educators said that being a clinical educator adds to the workload and there is not enough time to focus on the student. Nine other clinical educators stated that it is not only staffing shortages but also the limited ability to get supplies for the clinical laboratory. The COVID-19 pandemic affected supply chains and coupled with the increased demand, many materials were difficult to obtain for the laboratory. It was risky to use additional supplies for examples or to perform repeat testing while training a student because there was no guarantee that supply orders would arrive on time or at all. As 1 participant succinctly expressed, "everything" affected training a student during COVID-19.

Most participants indicated that they did not allow student attendance early in the pandemic but have recently modified their course of action to allow student attendance. Most participants who recently allowed students to attend their clinical sites further noted that students are required to be screened for COVID-19 or other illnesses before entry. Students are also required to follow the clinical site's infectious disease protocols for COVID-19. This includes wearing a mask, social distancing, and wearing goggles or eye protection.

Clinical sites varied with student expectations regarding attendance and infection control policies. It was cumbersome to keep up with constantly changing Centers for Disease Control (CDC) recommendations in an academic setting.

Limitations

Many clinical educators expressed concerns over the quality of clinical training students were receiving during the COVID-19 pandemic. Currently, there is no data that suggests the clinical education students received was poorer than the education received prior to the pandemic. Future research should correlate student ASCP scores obtained during the course of the pandemic to those scores obtained by students both before and after the pandemic. Weaker ASCP examination scores may indicate a need for a longer new employee training or orientation period for students who graduate during times when abnormally high volumes of stressors are present in the clinical laboratory, such as pandemics and extreme staffing shortages.

Another limitation was that this survey was distributed to persons who hold an ASCP membership. This survey does not take into

consideration those practicing laboratory professionals who do not hold a ASCP membership.

Conclusion

It is clear there was no consistency among clinical educators, clinical sites, or academic programs when trying to navigate the COVID-19 pandemic. Clinical sites either did not allow students to attend clinical training, reduced the number of students who went to clinicals, reduced the time students were at clinicals, or performed online clinical training. Many clinical educators believe these choices came at the expense of the students' clinical education.

Furthermore, students should be provided the same protections as their clinical educators. Students do perform patient testing in the same environment and under the same conditions as their clinical educators. Those protections should be provided by the clinical site as governmental regulations prevent entities that are not clinical in nature from purchasing PPE, such as N-95 masks, when supplies are in high demand. These regulations restricted academic institutions from purchasing supplies such as nitrile gloves and N-95 masks for academic laboratory programs. Ultimately, without changing these policies to allow academic institutions access to these materials for clinical students, students will not be able to be successfully complete their clinical internships, preventing the graduation of students in a field that is already extremely understaffed.

Most of the clinical educators who participated in this study worked at clinical sites that did not allow student attendance during the COVID-19 pandemic, limited rotation hours, or decreased the number of students in their laboratory. Many of those clinical sites also have multiple vacant laboratory professional positions. Obtaining clinical sites for students enrolled in a medical laboratory academic program where the students complete their clinical rotations is a requirement for student graduation. Decreasing the number of students training in the field ultimately decreases the number of graduated professionals able to apply for those vacant positions. As Holmes and Hogg[7] emphasized in their compilation of reflections on the pandemic, the limitations of clinical experiences for students will have a profound impact on the future supply of healthcare providers and can weaken healthcare systems in the future. Students going into the field of medicine should continue to perform clinical internships during pandemics and in times with other stressors. Clinical educators concerned about liabilities should develop a contractual agreement to release the clinical facility from responsibilities, such as infection, as opposed to not allowing students to attend their clinical rotation at the clinical site. Contracts should also state clearly the expectations for students who are completing their internship at a clinical facility during the pandemic or other clinical stressors. Contracts should state student vaccine requirements, SARS-CoV-2 testing or other testing requirements, when the student should and should not attend their clinical rotation, whether or how the student will make up hours missed, and explanations as to their role in the laboratory during their clinical rotation. Contracts can circumvent problems when expectations are clearly defined before clinicals start for students.

Part of the problem with this pandemic was limited defined expectations for students as there has not been a pandemic of this scale in decades, and there were times where regulations from the (CDC were changing daily. Expectations for students during the pandemic should be defined now to avoid reduction in students at clinical sites when the next pandemic or clinical stressor presents itself. Preventing students from completing their clinical sites exasperated preexisting staffing issues in the clinical laboratory. Reducing the number of laboratory professional graduates ultimately reduced the number of applicants for vacant positions in laboratory medicine.

Other areas of medicine, such a radiography's accrediting agency, allow clinical sites to provide students with employment opportunities during times of high demand or during stressful situations that put significant pressure on the department. Clinical sites may consider creating a student clinical/medical laboratory assistant position, where students may work 2 to 3 hours a day, in addition to their clinical hours, to relieve some of the stress from their clinical site. Although vacant phlebotomy and clinical laboratory assistant positions may exist at students' clinical sites, most require long 8-to-12-hour working times. Many students will not entertain the idea of working 8 to 12 hours in addition to their clinical rotation hourly requirements. This prevents students from applying for such positions and causes students to work in areas other than the clinical laboratory to earn wages, whereas students could be working a more manageable 2 to 3 additional hours in a working position to relieve stress on the clinical laboratory.

It is important to keep in mind that these were occurrences noted during the SARS-CoV-2 pandemic (2020 to 2021) and many clinical facilities have resumed taking students for clinical rotations, as staffing has allowed.

Acknowledgments

The authors thank Tameka Gooden, Callistus E Obunadike, Oghenetega Adogbeji, and Blessing Osadare.

REFERENCES

1. Lazenby M. et al. Clinical nursing and midwifery education in the pandemic age. *Int Nurs Rev*. 2020; 67(3): 323–325.
2. Dario A, Simic M. Innovative physiotherapy clinical education in response to the COVID-19 pandemic with a clinical research placement model. *J Physiother*. 2021; 67(4): 235–237. doi:10.1016/j.jphys.2021.08.008
3. Dewart G. et al. Nursing education in a pandemic: academic challenges in response to COVID-19. *Nurse Educ Today*. 2020; 92: 104471. doi:10.1016/j.nedt.2020.104471
4. Braun V, Clarke V. Using thematic analysis in psychology. *Qual Res Psychol*. 2006; 3(2): 77–101. 10.1191/1478088706qp063oa
5. Anderson ML. et al. Education in a crisis: the opportunity of our lives. *J Hosp Med*. 2020; 15(5): 287–289.
6. United States Depart of Education. Education in a pandemic: the desperate impact of COVID-19 of America's students. Office for Civil Rights Executive Summary. Washington, DC: United States Department of Education: Office of Civil Rights; 2021. https://www2.ed.gov/about/offices/list/ocr/docs/20210608-impacts-of-covid19.pdf
7. Holmes K, Hogg P, eds. *Reflections on the Covid-19 Pandemic*. International Society of Radiographers and Radiologic Technologists. London; 2022.

SCIENCE

Establishing the Need for Standardized Clinical Educator Training Programs for Medical Laboratory Professionals

Eleanor K. Jator, PhD, MLS(ASCP)CM,[1,] Heather L. Phillips, PhD, MLS(ASCP)CM, MT(AMT),[1] Shelley R. Latchem, MS, MLS(ASCP)CM,[2] Timothy A. Catalano, MA RT(T)[3]*

[1]Medical Technology Program, Austin Peay State University, Clarksville, Tennessee, USA, [2]Medical & Clinical Laboratory Sciences. Auburn University at Montgomery, Montgomery, Alabama, USA, [3]Duke Radiation Oncology, School of Medicine, Durham, North Carolina, USA. *To whom correspondence should be addressed: Jatore@apsu.edu.

Keywords: clinical educator, preceptor, preceptor training, medical laboratory professions, clinical instructor, clinical educator training, standardize training, clinical educator professional behavior, medical laboratory science, clinical laboratory science

Abbreviations: ASCP, American Society for Clinical Pathology; MT, Medical Technologist; MLS, Medical Laboratory Scientist.

Laboratory Medicine 2023;54:e63–e69; https://doi.org/10.1093/labmed/lmac108

ABSTRACT

Backround: There is minimal, if any, training for clinical educators in medical laboratory professions. This leads to challenges with teaching, assessment and workload/training balance. Hence, the need for standardized clinical educator training.

Method: A survey was developed, validated and deployed to medical laboratory professionals. Responses were analyzed using SPSS. Responses from two open-ended questions—is clinical educators' training important and how is this training beneficial?—were analyzed using thematic analysis.

Results: Most participants indicated that clinical educator training is important (99.4%). However, 72.4% received no formal training prior to training student. Themes from the importance of training include: Equip clinical educators, body of knowledge, standardize training and quality of training. Themes that emerged from the benefits of clinical educators training involve Training content, logistics, professional behavior and technical skills.

Conclusion: Clinical educators' training is crucial and valuable. Standardized training on pedagogy and other success strategies are warranted for successful clinical experiences.

Medical laboratory education comprises theoretical and the invaluable clinical phases. The clinical phase of a program is where students have the opportunity to apply theory, reinforce critical thinking skills, build confidence, improve competency, enhance effective communication, and refine psychomotor skills and professionalism.[1–3] Clinical education allows students to learn how to become practicing medical laboratory professionals. One of the key factors for the success of the clinical experience is skilled clinical instructors.[3,4] Typically, students in the medical laboratory professions are paired with clinical educators on a 1-to-1 ratio or 2-to-1 ratio. Clinical educators are also referred to as preceptors or clinical instructors; they may volunteer to train or be assigned students to train, often based on availability and seniority rather than competence.[5,6] These clinical educators may or may not have received any formal training or guidance on student instruction,[7] and they also train students while performing their regular bench responsibilities.

Clinical educators not only train but also serve as role models, evaluators, supervisors, confidence boosters, professional relationship builders, protectors, critical-thinking stimulators, organizers, facilitators, knowledge enhancers, experts, and positive attitude promoters.[5,8–10] They are knowledgeable and skilled at what they do, but some may be limited in their abilities to transfer or share their knowledge and skills with students[11]; hence, educating clinical educators prepares them to be better educators, assessors, evaluators, facilitators.[12] Clinical educators feel empowered that they are making an impact on the medical laboratory profession when they train students. They derive great satisfaction in seeing that they are carrying the torch to keep the profession alive,[7] but many need to be equipped for that role. According to L'Ecuyer, Hyde, and Shatto in 2018,[5] it should not be assumed that all staff are equipped to train students.

The concept of training clinical educators in different allied health programs varies. In some cases, clinical educators or preceptors receive training before training students and in others, they do not.[11] Some disciplines, such as nursing, physical therapy, and pharmacy, have structured training programs or guidelines for clinical educators. Clinical educator training is necessary and beneficial for both students and clinical educators.[5,8,13] A study that evaluated the effectiveness of a preceptor program reported that the participants not only gained more information on learning and teaching but they also enhanced their training skills, which translated to increased confidence. Participants reported that they would be able to incorporate student teaching in their work duties.[13] Another study on preceptorship also reported that clinical

educators acquired teaching and learning skills, enhanced evaluation skills, gained effective communication skills, and contributed to a conducive learning environment.[1]

A typical training program encompasses effective communication, evaluation, giving feedback, teaching, providing support and guiding students, interprofessional communication, and relationships.[14] It is no surprise that clinical educators' relationships with students affect competency building, professionalism, and learning outcomes.[1] These relationships are regarded as a very important and influential element in the learning process.[1,4,10,15,16] Preceptors want to know their trainees better to facilitate tailored training.[11]

Some national healthcare professional organizations and/or accreditation agencies for nursing, pharmacy, and physical therapy have structured preceptor training programs or guidelines that govern the requirements and qualifications of clinical educators or preceptors who train students. For example, in the Accreditation Council for Pharmacy Education Guidance for the Accreditation Standards document for PharmD programs, it is suggested that evaluations assess preceptors' competence in educating students, their interactions, how the profession is promoted.[17] American Society of Health-System Pharmacists (ASHP), an accrediting body for Pharmacy residencies, outlines preceptor responsibilities, to include among others: being able to display educator capabilities; deliver clear instruction and possess seasoned practitioner skills.

In addition, ASHP state that preceptor qualifications entail a range of effective instructing methods and skills depending on the circumstance; some of these include: tutoring, guidance, and training.[18]

The American Physical Therapy Association Guidelines and Self-Assessments for Clinical Education document states that clinical instructors demonstrate that they are proficient practitioners, of moral conduct, exhibit professionalism, exemplary teaching and management abilities, excellent assessment oversight and communication skills.[19] The American Physical Therapy Association provides a two-level voluntary, continuing education, clinical instructor training course for individuals precepting in a clinical setting.[20] Level one training is focused on learning in a clinical setting while level two focuses on developing a clinical program of study among other skills.[20]

Recognizing that clinical education requires essential skills to provide a quality clinical experience for students, health care programs such as nursing use a number of tools. For guidance and direction in developing a competency-based program, nursing educators rely on the Nurse Educator Core Competencies made available by the World Health Organization.[21] The core competencies address desired cognitive, affective, and psychomotor domains. These core competencies address aspects of knowledge of adult education, research skills, experience with program curriculum design and application, practical aspects of nursing as well as communication, professional and ethical behavior, assessment, administration and supervision.[21] The core competencies help organize and standardize clinical experience for the students while providing an organized structure for developing, directly overseeing, and evaluating the clinical experience.

The American Academy for Preceptor Advancement offers a preceptor certification at cost.[22] A 3-part precepting course covers topics such practice principles, preceptor aptitudes, pedagogy, preceptor duties, professionalism, and how to interact and collaborate effectively.[22] The certification attests to the proficiency of nurse preceptors, which prepares them for their instructional roles.

In the medical laboratory professions, there are no standardized clinical educator training or guidelines to follow. This leaves clinical affiliates with variable ways of equipping clinical educators for their students' instructional roles. Some clinical affiliates may provide minimal training to clinical educators and others do not provide any training. This leads to variability in students' clinical experiences, clinical educators' assessment of students, and training performance. It is not unusual to have recent graduates with very little work experience train students without any formal orientation, guidance, or training on pedagogy. Although many factors contribute to a successful training experience for students, clinical educators have pivotal roles when it comes to training students.

Training with clinical educators who are confident in their aptitudes and knowledge and are familiar with training expectations results in a better clinical experience. These clinical educators tend to be more willing to teach students. A study by McCullough, Maron, and Ramnanan[23] on optimizing clinical educator training programs to match motivations and concerns reported on the lack of confidence of some physicians in teaching students and others who did not teach due to lack of training. The authors recommended that experienced clinical educators and novices should participate in a faculty development program that would serve as a refresher for the experienced clinical educators or an opportunity to acquire new skills as evaluators, mentors, and teachers for the inexperienced.[23] Competence building and enhancement in clinical educators should be an ongoing process that include traits classified under attitudes, knowledge, and skills.[5] Lack of understanding of the expectations of the role of clinical educator has the potential to cause stress and feelings of unpreparedness and inadequacy[11,14] in those who train students. It can be especially daunting for the clinical educator because training students is an additional responsibility of their employment.[7] This can easily result in fatigue, frustration, and burnout[15] as well as an unsatisfactory clinical experience for students.

Very limited studies have been published on training clinical educators in the medical laboratory professions. It is highly recommended to include the art of preceptorship in guidance or orientation programs, which has the potential to enhance confidence and a sense of satisfaction in both the preceptors and students.[8] Standardizing such programs provides a framework that ensures some equivalence in training.[4]

Investing in clinical educators through training, guidance, or orientation is an effective way to maximize student learning experiences. Clinical experience does not replace formal training or guidance in clinical education[6,14] as formal training includes aspects of communication, role expectations, teaching techniques, and assessment methods. A standardized clinical educator training program, orientation, or protocol for medical laboratory professionals is nonexistent, to the best of the authors' knowledge. Not surprisingly, few if any studies on clinical educator training programs, orientation, or protocols in medical laboratory science have been published, which leads to the goal of this study. The study seeks to explore the need for clinical educator training from the perspective of laboratory professionals and makes the case to standardize training modules/programs.

Materials and Methods

Research Design

A 48-question survey was developed, validated, and distributed to laboratory personnel by the American Society for Clinical Pathology (ASCP).

The questions were developed after literature review of multiple studies on preceptorship, clinical educators and clinical education.[1,7,11] Some questions were developed from students' comments and questions asked during or after their clinical experiences. The questionnaire consists of seven sections which includes demographics, clinical educator experience, support or limitations to training students, the training methods, evaluation techniques, benefits to clinical training, and overall characteristics embodied by clinical educators. A 5-point Likert scale was utilized as well as open ended and yes/no questions. The questions were validated upon review by a mix of medical directors, laboratory managers, clinical educators, other laboratory professionals, academic faculty and non-lab individuals; changes were made based on their feedback.

A pilot study was conducted to determine the time of completion and to verify comprehension of questions. Three laboratory managers and ten laboratory professionals participated in the pilot. Data collection for this collaborative study employed the help of the American Society for Clinical Pathology (ASCP). This organization distributed the link to the self-reported survey to its members and responses were collected using Key Survey software. The survey link was emailed to potential participants using pertinent categories of medical laboratory professionals within ASCP's membership database. These categories included Clinical Laboratory Assistant/Medical Laboratory Assistant, Medical Laboratory Technician /Clinical Laboratory Technician, Medical Technologist (MT)/Medical Laboratory Scientist (MLS)/Clinical Laboratory Scientist, Molecular Biologist, Phlebotomist, and Specialist in Blood Banking.

The survey link was accessible for 6 consecutive weeks from March 8 to April 16, 2021. A reminder email to complete the survey was sent periodically. To avoid duplication, a statement in the informed consent asked participants to respond only to the first invitation and not to take the survey more than once. The survey was discontinued if participants had never trained students. Participants who are currently training students or who had trained students in the past were allowed to complete the survey. This paper is 1 of many using the same dataset. The Institutional Review Board of Austin Peay State University approved this research (IRB # 0-066).

Data Analysis

Responses were analyzed using the Statistical Package for the Social Sciences (SPSS 16.0). Reliability was determined by calculating Cronbach's alpha, which is used to measure internal consistency (0.935). Descriptive statistics and χ^2 analysis were performed with the *P*-value set at 0.05. Two open-ended questions were analyzed in this study: why is clinical educator training important and how is the training that you received beneficial? For the open-ended questions, thematic analysis was used as described by Braun and Clarke.[24] Thematic analysis involves familiarity with data, initial data coding, searching data for themes, reviewing themes, defining and naming themes, and reporting findings. Initial codes were assigned to the data after which themes, subthemes, and categories were developed. Final themes, subthemes, and categories were then compared between 3 research team members to enhance validity.

Results

The survey had a response rate of 6.33% (n = 207). A total of 5675 individuals opened the email they received from ASCP. A total of 359 individuals clicked on the survey link, although not all of these clicks resulted in a completed survey. Participants were asked if they believed it is important to train clinical educators. Nearly all, 99.4%, responded in the affirmative. Those responding in the affirmative were asked a follow-up question regarding why they thought clinical educator training is important. Four themes were identified from the 34% of participants who provided open-ended responses (**TABLE 1**). These 4 themes include (i) equip clinical educators (63%); (ii) enhance body of knowledge and emerging technologies (20%); (iii) provide standardized training (14%); and (iv) improve quality of training (3%). Examples of participant responses can be seen in **TABLE 1**. Three percent of participants felt providing students with a high-quality clinical training experience was best accomplished by training the clinical educators. Sixty-three percent of participants felt clinical educator training was a great opportunity to equip clinical educators. This is to ensure that only appropriately trained and credentialed professionals train students.

Most participants (72.4%) reported no education, training, orientation, or clinical instruction prior to becoming a clinical educator. For those reporting no prior training, a follow-up question asked if they would appreciate receiving formal clinical educator training. The vast majority of participants without prior training, 82.1%, indicated that they would appreciate clinical educator training. When all participants (those with prior training and those without), were asked if they would appreciate a formalized training process or protocol to follow while training students, 79.5% answered in the affirmative.

Of the 27.6% of clinical educators who had received clinical training prior to becoming a clinical educator, 92.6% valued the training they received. Participants were then asked, in an open-ended format, to explain how the clinical education they received before training students was beneficial. The responses to this question varied greatly. Comments regarding the benefits of clinical educator training from those who had received training (27.6%) could be grouped into 4 themes (**TABLE 2**). Those clinical educators who found their training beneficial remarked favorably about the training content covered regarding curriculum development and organization and objective writing in a clinical laboratory setting. Logistical matters such as creating schedules for students and setting appropriate entry-level goals and guidance on how to evaluate student performance were also considered helpful topics. Clinical educators also benefited from clinical educator training that emphasized their role as professional role model. Soft skills and aspects of professional deportment were commented on by participants as well. Clinical educator training was also beneficial because it refined technical skills and offered laboratory technique best practices. The most common themes can be seen in **TABLE 2**.

Participants were also asked which type of facility they were employed at as a clinical educator. The percentage of participants at each facility type is shown in **FIGURE 1**. Most participants worked at critical/acute care hospitals (43%) or privately owned/not for profit hospitals (both at 32.4%). A χ^2 analysis was performed using participants' responses for the facility type they worked at as a clinical educator and whether they had received clinical educator training. The results indicated a lack of clinical educator training for all facility types. No association ($P > .05$) was found between the type of facility and the likelihood of clinical educator training.

Participants were asked about their training methods and evaluation techniques. Comparing students, when done properly, can be used as an evaluation tool. When the clinical educators were asked

TABLE 1. Why Clinical Educator Training Is Important

Themes	Subthemes and Categories	Selected Participant Responses	Participant %
		"Students need experienced techs to help them develop not only technical skills but empirical thinking skills so they understand how our jobs impact patient outcomes."(participant AQ189)	
		"Training is not just performing the job while a student observes, but requires the clinical educator to connect with the subject matter and provide opportunities for problem solving and decision making."(participant AQ169)	
Equip clinical educators	Pedagogy • Teaching skills • Critical thinking skills • Assessment • Feedback/Communication • Learning styles	"We all should know how to best relate to our students, be updated with new issues, and be able to access training on how to be effective educators. Like how teachers are trained, lab educators should also be trained." (participant AQ175)	63%
		"They also should be educating in the methods of education delivery."(participant AQ196)	
		Clinical educator training teaches soft skills, understanding learning styles . . ."(participant AQ 98)	
		"Also, learning how to teach, write exam questions, . . ."(participant AQ59)	
		"The person who is educating new employees or students must be someone who has more knowledge about the topic than your average MT who has just been assigned to do the task." (participant AQ196)	
Body of knowledge/emerging technologies	Professional development • Enhanced knowledge on new technology/techniques • Knowledge on developing laboratory issues	".... be updated with new issues . . ." (AQ175)	20%
		"It may have given me some added information to present to the students while I am training them on the lab procedures." (participant AQ188)	
		". . . and time to really learn the material in depth would be highly advantageous."(participant AQ59)	
Standardized training	Variability in training • Lack of consistency • Lack of structure	"I recall some of my rotations as a student many years ago. Some of them weren't very good. Others were great. However, there was too much inconsistency. If individuals were trained, perhaps this would be remedied." (participant AQ210)	14%
		". . . teaching how to provide structured training." (participant AQ98)	
		"How to be an effective educator is a skill —- while some people may have these skills as a natural ability, most do not. Providing some training about how to do this helps ensure the clinical experience is beneficial." (participant AQ90)	
Quality of training	Training abilities of clinical educators • Attributes of clinical educators • Training/work responsibilities of clinical educators	"If just anybody trains, it can make it harder for the student later on if they start off with a bad trainer who is teaching them wrong, or isn't making it interesting or exciting. It is probably the students first hands on experience of the lab, and you don't want them to be turned off from the start." (participant AQ117)	3%
		"In a hospital setting, it is difficult for an instructor to manage her responsibilities to her patients and her students. These priorities are often conflicting. Any training that may be available would be beneficial."(participant AQ59)	

This table contains themes, subthemes, and categories that emerged from the open-ended responses of participants who indicated that clinical educator training is important.

whether they found themselves comparing current students to previous students, 61% of participants stated "yes." Clinical educators were also asked whether they changed their approach to teaching based on their students' performance. Eighty-two percent of clinical educators explained they did change their approach. Ninety-six percent of clinical educators stated that student mistakes and errors are used as a teaching tool. Ninety-nine percent of clinical educators indicated that they give verbal instructions when demonstrating procedures and 97% state they explain the theory or principles behind what they are demonstrating. Clinical educators were then asked whether they provided a comprehensive picture of diseases processes by integrating laboratory results from other departments. Thirty percent of clinical educators stated they always did this. Fifty-nine percent stated they sometimes do this and 10% state they never did this.

Discussion

The results of this study agree with other studies in confirming that most clinical educators or preceptors do not receive formal training or guidance before training students or that the training received is inadequate.[25,26] Clinical educators who participated in this survey indicated they would appreciate training prior to training students. Clinical educator training in other allied health science programs address topics relevant to and necessary for an optimal clinical training experience for the student such as assessments, communication, feedback, teaching, and learning skills.[25] Although years of clinical experience translate to increase in knowledge and skills, it is still beneficial to provide training to clinical educators. Wong et al[14] stated that clinical educator training has been shown to enhance the perception of desired clinical teaching behaviors among preceptors. The study participants who, having been made aware of their roles as role models, were conscious of their behavior, which affected the learning process. They also highlighted the importance of the appropriate use of soft skills when training students.[14] Clinical educator training has an enormous impact on the educator's confidence and abilities,[5,8,13] which aligns with the current findings in which participants who received training prior to training students indicated that their knowledge on developing the curriculum, teaching abilities, grading, technical skills were enhanced. They also stated

TABLE 2. Benefits to Clinical Educator Training.

Themes	Subthemes and Categories	Selected Participant Responses	Participant %
	Curriculum development • Organize and prepare materials	"Helped to organize information and look at best ways to impart this information to students."(participant AY54)	
		"Practicing . . . to develop instructional materials."(participant AY27)	
		"I have been through train the trainer programs, orientation for onsite f147151aculty for MLS programs, and preceptor trainings, each with a different scope. Most beneficial take away is to be organized, understand that each person is unique and will learn at a different speed and rate. There are multiple different learning styles and can take patience when training if someone is struggling. Check in regularly with the trainee, closed loop feedback is ideal with the trainee to ensure that they are retaining the information."(participant AY140)	
Training content	Objective writing	"Showed me how to plan and group learning objectives. Helped with learning how to make 'test' patients for students to work with . . . ." (participant AY81)	56%
		"I learned about objectives, curriculum, and different domains of learning - more structured approach." (participant AY95)	
		"It taught me . . . how to first list the learning objectives for better presentations. It also taught me about individual learning styles." (participant AY98)	
		"I learned how to develop objectives and what pedagogy is best suited for different clinical environments."(participant AY123)	
		"I studied education as part of my master's degree program. We learned the important of behavioral objectives and their role in the process of assessing student achievement." (participant AY147)	
		"It allowed me to understand . . . the best way to present the lecture material using objectives." (participant AY151)	
		"It helped me to develop a lesson plan, objectives, and measure effectiveness of the training." (participant AY177)	
	Teaching skills	"I learn best by watching and listening to demonstrations before trying the skill myself. The most beneficial thing I got from my trainers was their experience with events and circumstances that I might have to handle in the future. This one-on-one time in a guided practical experience is the most valuable thing you can share with your learners." (participant AY191)	
		"I find hands on experience to be the best way to test learned knowledge." (participant AY135)	
		"It showed me different ways to teach things as all people learn differently." (participant AY3)	
		"Helped to become a better educator. Also qualified for preceptor pay." (participant AY65)	
		"It made me a better educator. I believe in hands on training." (participant AY28)	
		"I feel that training how increases your confidence and that leads to better teaching." (participant AY176)	
		"It helps me to train my students in real world situations that I experienced in the field."(participant AY25)	
		"Trained you to adapt to different learning preferences." (participant AY154)	
		"Training helps you see the big picture. You need to set goals, and training gives you the tools to set those goals in place and how to measure outcomes to see if the goals were reached."(participant AY82)	
		"It allowed me to understand how to put together a clinical rotation . . ." (participant AY151)	
Logistics	Scheduling and goal setting	"To be able to determine a schedule and focus on goals that the student should have accomplished in a certain time frame. A guide for ways to help with certain learning situations and for dealing with different learning strategies." (participant AY171)	9%
	Evaluating • Grading rubric	"Instruction on how to grade students. Helped to standardize process."(AY106)	
	Modeling	"I was made aware of how positive role-modeling and good training can affect students, so I try to apply that each time I am with a student or new hire."(participant AY175)	
Professional behavior	Attitude/soft skills	".... reminded me that when you are just starting out it can be overwhelming and that keeps you humble and more understanding to new trainees." (participant AY81)	3%
		"It taught me about soft skills . . ." (participant AY98)	
Enhanced techniques	Technical skills	"When a tech senses that the student is receptive to learning, they pass on their work efficiency skills/techniques that they themselves have learned through experience. One tech taught me how to prevent the forceps from getting contaminated by bacteria growing on an agar plate when performing a biochemical paper disc test." (participant AY116)	9%
		"Yes it was the work shop, and learn some or all the factors with storing blood and why is it to separate red blood cell from serum, hematoma when drawing how significant drawing blood is so important in so many ways." (participant AY211)	
		"Understanding in-depth an instrument is paramount to teaching others."(participant AY190)	
Other			23%

This table contains themes, subthemes, and categories that emerged from the open-ended responses of participants who indicated that they had received clinical educator training and found the training beneficial. Selected participant responses to the open-ended question can be seen in the table.

FIGURE 1. Facility Types.

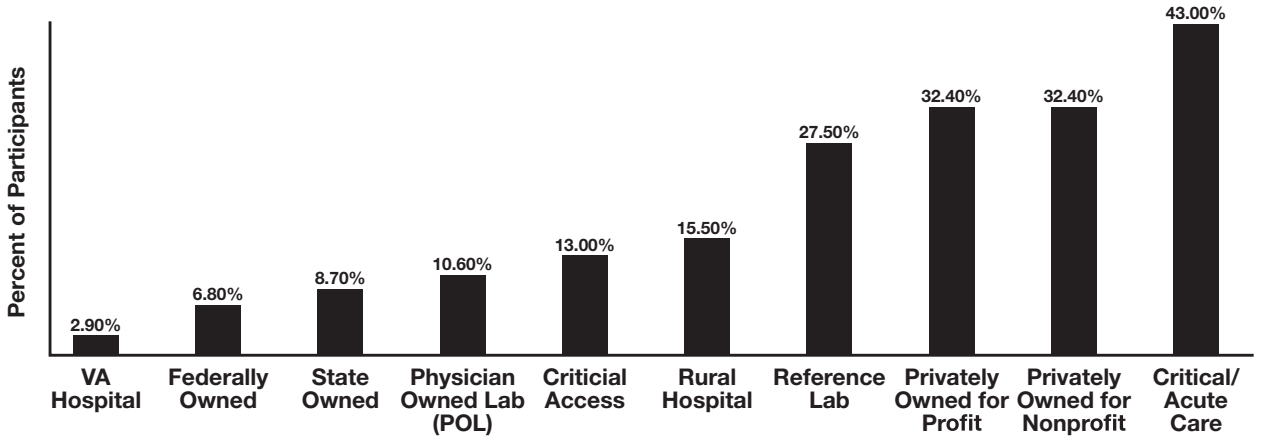

that they are more aware, patient and understanding, especially when students are struggling and are overwhelmed.

A study by McSharry and Lathlean[16] on clinical teaching and learning within a preceptorship model in an acute care hospital in Ireland called for preceptors to undergo preceptor educational preparation to equip them with pedagogical skills, which are required to foster learning. Multiples studies have reported that preceptors who participated in preparatory programs indicated increased teaching abilities, willingness to train, and self confidence, among other attributes.[1,13,23] Similarly, this study's participants who received training prior to training students stated that they learned how to develop objectives and adjust teaching style to match students' learning styles. Participants also indicated that they learned to be more organized and provide timely feedback to foster learning. This reiterates the debatable assumption that practicing clinicians need lessons on pedagogy.

Having a blueprint for training clinical educators has its benefits. Variability in the content of training programs and subjectivity among clinical educators would be reduced, resulting in more pleasant clinical experiences. When asked why clinical educator training is important, study participants who had not received training prior to training students indicated that the inconsistency in training made some clinical rotations unpleasant and they stated that having standard training protocols would lessen these occurrences. Participants also indicated that clinical educator training would help to facilitate examination writing, assessments, teaching styles, and delivery modalities. In addition, educators would enhance critical thinking and communication skills, keep abreast of emerging issues, and increase their knowledge of certain laboratory techniques and how to balance daily workload and still provide quality training. Interestingly, these elements are typical components of preceptor and clinical educator training programs. A typical program or module includes communication, prioritizing, teaching techniques, critical thinking, learning styles, teamwork, conflict management, assessment, giving feedback, and familiarity with roles and responsibilities.[11,15] These elements are comparable to those wanted by this study's participants.

This study indicated a lack of standardization in the clinical training and evaluations of students in laboratory medicine. This could be seen in the assessment of responses to questions about training methods and evaluation techniques. Results indicated less than one-third of participants provided students with a comprehensive picture of disease processes by integrating laboratory results obtained from other departments. This prevents students from obtaining a complete diagnostic picture of a patient. Training provided to clinical educators should equip them with the tools to provide a comprehensive picture of a patient's laboratory results. Almost 20% of clinical educators stated they did not change their approach to training based on student performance. Educator training should provide strategies to implement change based on a student's performance, supply methods to measure a student's performance, and provide information for interpreting the results of performance measures.[4] Questions revolving around student performance measurement tools and performance result interpretation were not asked by this survey. Future studies focusing on clinical educators should consider this as focus for further research.

Few responses to questions regarding technique and evaluation provided greater than 90% favorable responses. It is clear that clinical educators use errors made by students as a teaching tool. They indicated that they explain the theories and principles behind the testing performed and provide clear instructions when they were demonstrating procedures and techniques. However, currently there is no tool used to evaluate clinical educators in their ability to communicate information. Future research should focus on the student's perception of their clinical instructor's ability to deliver such information. Comparisons of students not done in such a way to reduce confidence but to appreciate success can be used as a guide for future students.

Ultimately, the goal of clinical education is to allow students to acquire and enhance skills to become competent practitioners. To make this experience a positive one, the clinical educator or preceptor needs to have adequate abilities and attributes to successfully serve as a bridge between academics and professional practice.[10]

Limitations

The low response rate to the survey may be due to the exclusive use of the ASCP's membership database to distribute the survey. This implies that some laboratory professionals who are not members of the ASCP have not been included. This survey was also distributed approximately 1 year into the COVID-19 pandemic, which may have influenced the level of responses received.

Conclusion

This study sought to establish the need for standardized medical laboratory professional clinical educator training programs. Overwhelmingly, study participants agreed that having some formal training would be beneficial prior to training students. We note that some survey

participants with prior training in education found it easier to train students because of their background. This demonstrates that there is a need for clinical educators to receive some training in aspects of pedagogy for a successful clinical experience. To provide students with an excellent and consistent clinical experience, clinical educators need to be equipped for the role. An organized clinical educator training program, workshop, or orientation is needed to support clinical education. Various modalities can be used to train clinical educators, including face-to-face, online, or hybrid formats.[6] Blueprints for training modules can be developed by national professional organizations for academic units and clinical affiliates to build on, thereby equipping clinical educators.

As McSharry and Lathlean[16] called for the development of national competency-based standards for preceptor preparation, we recommend the formation of a task force by professional and/or accrediting organizations such as the ASCP, the American Society for Clinical Laboratory Science, and the National Accrediting Agency for Clinical Laboratory Sciences to consider the development of a standardized approach to clinical educator training. Medical laboratory professional organizations underscore the importance of quality clinical training, but the guidance for clinical educator training is not as structured as those of some healthcare professions.

Acknowledgments

The authors thank Edna Garcia, MPH, American Society for Clinical Pathology; Iman Kundu, MPH, American Society for Clinical Pathology; Tameka Gooden, MS, MLS(ASCP)^{CM}, Baptist Health Sciences University; Callistus E. Obunadike, Austin Peay State University; Oghenetega Adogbeji, Austin Peay State University; and Blessing Osadare, Austin Peay State University.

REFERENCES

1. Ernstzen DV. Roles and attributes of physiotherapy clinical educators: is there agreement between educators and students? *Afr J Health Prof Educ.* 2013;5(2):91–94. doi:10.7196/ajhpe.252.
2. Kamolo E, Vernon R, Toffoli L. A critical review of preceptor development for nurses working with undergraduate nursing students. *Int J Caring Sci.* 2017;10(2):1089–1100.
3. Chipchase LS, Buttrum PJ, Dunwoodie R, et al. Characteristics of student preparedness for clinical learning: clinical educator perspectives using the Delphi approach. *BMC Med Educ.* 2012;12:112. doi:10.1186/1472-6920-12-112.
4. Perram A, Hills C, Johnston C, et al. Characteristics of an ideal practice educator: perspectives from undergraduate students in diagnostic radiography, nuclear medicine, nutrition and dietetics, occupational therapy, physiotherapy and radiation therapy. *Radiography.* 2016;22(4):295–305. doi:10.1016/j.radi.2016.04.007.
5. L'Ecuyer KM, Hyde MJ, Shatto BJ. Preceptors' perception of role competency. *J Contin Educ Nurs.* 2018;49(5):233–240. doi:10.3928/00220124-20180417-09.
6. Rodger S, Webb G, Devitt L, et al. A clinical education and practice placements in the allied health professions: an international perspective. *J Allied Health.* 2008;37(1):53–62.
7. Miller W. Developing a theory of clinical instructor identity using the experiences of medical laboratory science practitioners. *Clin Lab Sci.* 2014;27(2):97–104.
8. Ward A, McComb S. Precepting: a literature review. *J Prof Nurs.* 2017;33(5):314–325. doi:10.1016/j.profnurs.2017.07.007.
9. Baltimore JJ. The hospital clinical preceptor: essential preparation for success. *J continuing education in nursing.* 2004;35(3):133–140.
10. Shinners JS, Franqueiro T. Preceptor skills and characteristics: considerations for preceptor education. *J Contin Educ Nurs.* 2015;46(5):233–236. doi:10.3928/00220124-20150420-04.
11. Chan HY, So WK, Aboo G, et al. Understanding the needs of nurse preceptors in acute hospital care setting: a mixed-method study. *Nurse Educ Pract.* 2019;38:112–119. doi:10.1016/j.nepr.2019.06.013.
12. Omer TA, Suliman WA, Moola S. Roles and responsibilities of nurse preceptors: perception of preceptors and preceptees. *Nurse Educ Pract.* 2016;16(1):54–59. doi:10.1016/j.nepr.2015.07.005.
13. Smedley A, Morey P, Race P. Enhancing the knowledge, attitudes, and skills of preceptors: an Australian perspective. *J Contin Educ Nurs.* 2010;41(10):451–461. doi:10.3928/00220124-20100601-08.
14. Wong CSY, Chan HYL, Aboo G, et al. Associations of preceptors' training needs with clinical teaching experience and training received. *J Contin Educ Nurs.* 2022;53(4):165–170. doi:10.3928/00220124-20220311-06.
15. Frankenberger WD, Roberts KE, Hutchins L, et al. Experience of burnout among pediatric inpatient nurse preceptors. *Nurse Educ Today.* 2021;100:104862. doi:10.1016/j.nedt.2021.104862.
16. McSharry E, Lathlean J. Clinical teaching and learning within a preceptorship model in an acute care hospital in Ireland; a qualitative study. *Nurse Educ Today.* 2017;51:73–80. doi:10.1016/j.nedt.2017.01.007.
17. Accreditation Council for Pharmacy Education. Guidance for the Accreditation Standards and Key Elements for the Professional Program in Pharmacy Leading to the Doctor of Pharmacy Degree. PharmD Guidance For Standards 2016.pdf Accessed February 24, 2022.
18. American Society of Health-System Pharmacists website. Guidance document for the ASHP accreditation standard for postgraduate year two (pgy2) pharmacy residency programs. https://www.ashp.org/-/media/assets/professional-development/residencies/docs/pgy2-guidance-document.pdf.March 2021. Accessed March 4, 2022.
19. American Physical Therapy Association. Guidelines and self-assessments for clinical education. https://www.apta.org/contentassets/7736d47f2ec642a3962276d9b02503d2/guidelinesandselfassessmentsforclined.pdf Accessed February 24, 2022.
20. American Physical Therapy Association website. Credentialed clinical instructor program (CCIP). https://www.apta.org/for-educators/clinical-education-development Accessed February 24, 2022.
21. World Health Organization. Nursing Educator Core Competencies. Retrieved from https://www.who.int/publications/i/item/nurse-educator-core-competencies accessed February 24, 2022.
22. American Academy for Preceptor Advancement website. https://preceptoracademy.org/certifications/ Accessed March 3, 2022.
23. McCullough B, Marton GE, Ramnanan CJ. How can clinician-educator training programs be optimized to match clinician motivations and concerns? *Adv Med Educ Pract.* 2015;6:45–54. doi:10.2147/AMEP.S70139.
24. Braun V, Clarke V. Using thematic analysis in psychology. *Qual Res Psychol*. 2006;3(2):77–101. doi:10.1191/1478088706qp063oa
25. Luhanga FL, McCrystal S, Domm E. Evaluating preceptor perception of role development and support initiatives in a collaborative bachelor of science in nursing program. *Qual Adv Nurs Educ - Avancées en formation infirmière*: 2020;6:(3) doi:10.17483/2368-6669.1241
26. Panzavecchia L, Pearce R. Are preceptors adequately prepared for their role in supporting newly qualified staff? *Nurse Educ Today.* 2014;34(7):1119–1124. doi:10.1016/j.nedt.2014.03.001.

On labmedicine.com

Several articles featuring practical information are now available on labmedicine.com.

This month, the website features a paper by Vasani et al detailing Six Sigma methodologies to reduce troponin turnaround times. In "The Impact of COVID-19 on the Laboratory Professionals' Clinical Education: A Qualitative Study," Phillips et al discuss clinical laboratory science education during the COVID-19 pandemic. Jator et al continue the conversation in "Establishing the Need for Standardized Clinical Educator Training Programs for Medical Laboratory Professionals." In addition, several online-only papers discussing SARS-CoV-2 diagnostics are listed in this month's table of contents.

Check out these articles and more on labmedicine.com.

Lablogatory

Recent contributions to the blog for medical laboratory professionals include case studies and laboratory safety. To see why over half a million readers visit Lablogatory each year, visit labmedicineblog.com.

ASCP STRONGERTOGETHER

Advance Your Career and Improve Your Skills with the ASCP Certificate Programs Sale!

Pathologists, Laboratory Professionals, Residents—ASCP offers *you* a broad selection of online certificate programs developed to support *your* ongoing professional needs!

All certificate programs on sale through March 15, 2023.

Comprehensive and Inclusive Leadership Training for the Laboratory Medicine Team

Hone your leadership skills at your own pace with 18 on-demand courses offering CME/CMLE credit! This program teaches participants to adapt their behavior, communication skills, and leadership styles to be effective in a variety of workplace situations through an advanced self-assessment program.

Use promo code **LI23JA** to save $50.

ASCP LEADERSHIP INSTITUTE®

The Most Complete Pathology Informatics Education Program You Will Find

Take the lead to improve lab productivity and move your lab to the next level with this unique self-paced online certificate program. The program is designed for individuals participating in laboratory informatics initiatives to enhance quality diagnosis, throughput and patient safety.

Use promo code **UPI23JA** to save $100.

UNIVERSITY OF PATHOLOGY INFORMATICS
A joint collaboration between API and ASCP

The Best Training Resource in Laboratory Management Today

LMU is a customizable program for pathologists, laboratory professions and residents planning on moving into management positions or seeking to advance their management skills. With this comprehensive education resource you can achieve your career goals and improve the performance of your lab.

Use promo code **LMU23JA** to save $150.

LAB MANAGEMENT UNIVERSITY
A JOINT COLLABORATION BETWEEN ASCP AND APF

ASCP Continuous Quality Improvement (CQI): Assuring Patient and Laboratory Team Safety

ASCP CQI aids laboratory teams to assess their practice operations and improve performance, with the objective of increasing both patient and laboratory team member safety. This guided curriculum includes on-demand courses split between five modules, including a suite of downloadable tools for use in the lab.

Use promo code **CQI23JA** to save $100.

ASCP CQI
CONTINUOUS QUALITY IMPROVEMENT

Visit www.ascp.org/cert-programs to enroll today!